PhD Programme in Neuroscience

Characterization of gustatory second-order neurons in the *Drosophila melanogaster* brain

Rubén Mollá Albaladejo

Thesis Director

Dr. Juan Antonio Sánchez Alcañiz

Neuroscience Institute UMH-CSIC

Miguel Hernández University of Elche

- 2024 -

The image presented in the previous page has been made by myself by using the software Flywire. Thus, it is not protected by any copyright issue.

This Doctoral Thesis, entitled “Characterization of gustatory second-order neurons in the *Drosophila melanogaster* brain” is submitted under the format of Thesis by compendium of the following publication:

Mollá-Albaladejo, R., & Sánchez-Alcañiz, J. A. (2021). Behavior Individuality: A Focus on Drosophila melanogaster. Frontiers in Physiology, 12, 719038. https://doi.org/10.3389/fphys.2021.719038

INSTITUTO DE NEUROCIENCIAS

UNIVERSITAS Miguel Hernández

EXCELENCIA SEVERO OCHOA 2014 - 2027

REPORT OF THE DIRECTOR

Sant Joan d'Alacant, 13th May 2024

Dr. Juan Antonio Sánchez Alcañiz, Director of the Doctoral Thesis entitled "Characterization of gustatory second-order neurons in the *Drosophila melanogaster* brain"

CERTIFIES:

That Mr. Rubén Mollá Albaladejo has carried out under my supervision the work entitled "Characterization of gustatory second-order neurons in the *Drosophila melanogaster* brain" in accordance with the terms and conditions defined in his Research Plan and in accordance with the Code of Good Practice of the Miguel Hernández University of Elche, satisfactorily fulfilling the objectives foreseen for its public defence as a doctoral Thesis.

I sign for appropriate purposes, at Sant Joan d'Alacant to 13th from May from 2024

Thesis supervisor

Dr. Juan Antonio Sánchez Alcañiz

INSTITUTO DE NEUROCIENCIAS

UNIVERSITAS Miguel Hernández

EXCELENCIA SEVERO OCHOA 2014 - 2027

REPORT OF THE DOCTORAL PROGRAMME COORDINATOR

Sant Joan d'Alacant, 13th May 2024

Dra. Cruz Morenilla Palao, Coordinator of the Neurosciences PhD programme at the Institute of Neurosciences in Alicante, a joint centre of the Miguel Hernández University (UMH) and the Spanish National Research Council (CSIC),

INFORMS:

That Mr. Rubén Mollá Albaladejo has carried out under the supervision of our PhD Programme the work entitled "Characterization of gustatory second-order neurons in the *Drosophila melanogaster* brain" in accordance with the terms and conditions defined in its Research Plan and in accordance with the Code of Good Practice of the University Miguel Hernández de Elche, fulfilling the objectives satisfactorily for its public defence as a doctoral Thesis.

Which I sign for the appropriate purposes, at Sant Joan d'Alacant to 13th from May from 2024.

And for the record, for all due purposes, I sign this certificate.

Dra. Cruz Morenilla Palao

Coordinator of the PhD Programme in Neurosciences

E-mail: elvirap@umh.es
www.in.umh.es

Tel: +34 965 919533
Fax: +34 965 919549

Av Ramón y Cajal s/n
SANT JOAN CAMPUS
03550 SANT JOAN D'ALACANT- SPAIN

FUNDING

During my studies, to carry out my PhD Thesis entitled “Characterization of gustatory second-order neurons in the *Drosophila melanogaster* brain”, I received funding from the next sources:

- Subvenciones para la contratación de investigadoras e investigadores doctorales de excelencia para desarrollar un proyecto de I+D+I en la Comunidad Valenciana (CIDEGENT 2018), ref: CIDEGENT/2018/035, para el proyecto de tesis “Bases neuronales de la integración sensorial”.
- Ayudas Ramón y Cajal 2019, ref: RYC-2019-026747-I, para la realización de la tesis doctoral “Bases neuronales de la integración sensorial”.
- Proyectos de I+D+i en el marco de los programas estatales de generación de conocimiento y fortalecimiento científico y tecnológico del sistema de I+D+i a los retos de la sociedad 2019, ref: PID2019-105839GA-100, para la realización de la tesis doctoral “Bases neuronales de la integración sensorial”.

AGRADECIMIENTOS

Son muchas las emociones encontradas al enfrentarme a esta sección en blanco. Realizar una tesis doctoral no es tarea fácil, pero sin duda el equipo humano que me ha acompañado en este camino ha hecho que este sea más liviano. A todas esas personas que se me vienen a la cabeza, y a las que sintiéndolo mucho se me escapan ahora mismo, con las que he compartido cualquier momento, por pequeño que sea, de apoyo, consejos, lágrimas, risas, y un largo etc., GRACIAS.

Me gustaría empezar esta sección pasando por lo profesional, que sin quererlo ha pasado a ser también parte de lo personal. Agradecer al Dr. Juan Antonio Sánchez Alcañiz, Juan para mí, no solo por haber sido mi director de tesis sino por haber sido un pilar fundamental todo este proceso, sin ti esto no hubiera sido posible. Todavía recuerdo la entrevista que tuvimos a finales de 2019, con tu laboratorio todavía vacío por tu reciente reincorporación al INA como Investigador Principal. Todavía sigo preguntándome que vistes en mí, con la entrevista algo desastrosa que hice, para darme el honor de ser tu primer estudiante de doctorado, pero es algo de lo que te estaré eternamente agradecido por la significancia profesional y personal que suponía poder estar cerca de casa estos años. Sé que no he sido el predoctorando modelo, y que mis circunstancias personales han hecho que no siempre estuviese a la altura de lo esperado, pero tu comprensión y apoyo (a veces incluso dejando de lado tus intereses por respetar los míos) han hecho que no tirase la toalla y hoy esté aquí escribiendo estas líneas. Gracias por subirte a mi carro en estos últimos meses y remar en mi dirección para poder terminar la tesis a tiempo. No solo por tu extensa vocación y madurez científica, sino en particular por tu calidad humana, haces que crea que la ciencia de este país merece la pena. Continuando con el grupo de laboratorio paso a nombrar a mis compañeros predocs: Chema y Manuel. Contigo Chema empezó la tesis, y también acaba, gracias por tu calidad humana y los buenos momentos que hemos pasado en el lab. Manuel, gracias por tu espíritu sevillano (más bien bético) que nos ha traído miles de risas y por ser abanderado del “dulsesito” postcomida. No me cansaré de recordarte el claro ejemplo de esfuerzo y superación que representas para mí. Espero poder seguir viendo cómo creces como persona y científico, y que nuestra amistad perdure en el tiempo. María, la técnico, gracias por tu ayuda, los pequeños momentos de tertulia que a veces hemos tenido, y por ver las cosas siempre de forma positiva. Pasando a antiguos miembros del lab, no podía olvidarme de Pol, quien dejó huella en el laboratorio, y no solo por el increíble trabajo que hizo. Gracias por tus consejos, tus risas y tu afán por hacer las cosas con mimo (gracias por ser el pionero del INA en el FACS con *Drosophila*) y delicadez, aunque te enrolles como las persianas. No pongo en duda que tu profesionalidad y humanidad harán que dejes huella allá donde vayas.

Gracias también a todos los laboratorios de *Drosophila* del INA. Al lab de la Dra. María Domínguez, Dr. Javier Morante, Dr. Jose Carlos Pastor, Dr. Paco Tejedor, Dra. Ana Carmena, Dr. Luis García Alonso, a cada uno de vosotros y vuestro equipo, gracias por vuestra ayuda durante estos años, y por siempre tener el laboratorio abierto a cualquier duda o problema científico que he tenido. También a Irene y Sergio, gracias por tenerlo todo siempre a punto y recibirnos siempre con una sonrisa. Dentro de este párrafo, agradecer encarecidamente a Fran por su ayuda, sus cafés, sus charlas y sobre todo por su trompeta de cada mañana. A Alicia por haberme ayudado siempre con una sonrisa. A los predocs Dani, Ernesto, Juan Carranza y Juan Ramón Guirado, gracias por todos los momentos que hemos compartido entre risas y algún que otro llanto.

Pasando al personal técnico del instituto, gracias a todos, y en especial a Antonio Caler y Pep. Vuestra alegría hacía que bajar a Ómicas fuera como un respiro de aire fresco en los largos días de experimentos. Gracias también al personal de gerencia y administración del INA, en especial a Maria José, quien en el último año me ayudó siempre con una sonrisa ante mis interminables preguntas.

Siguiendo con el INA, pero pasando al lado más social, gracias en especial a dos personas que me ha regalado la tesis: Pablo y Lucía. Pablo, gracias por ser como eres y haberte convertido en un gran amigo. Tu vocación y esfuerzo hacen de ti un gran científico, pero no olvides que tu persona brilla aun más por tu humildad y generosidad con los demás, no cambies, amigo (canallita). Lucía, gracias por ser la dramas que eres, y porque poco a poco has pasado a ser una persona en la que poder apoyarme. De ti me quedo con la facilidad que tienes para verlo todo alegremente, y por supuesto con nuestra bonita amistad. También me gustaría hacer homenaje a otras personas que aun habiendo pasado menos momentos con ellas han hecho de esta etapa final más bonita: Sergio[2], Alerie, Vicky, Álex, Álvaro (contigo empezó y también esta etapa), etc, GRACIAS.

Me gustaría finalizar esta primera parte agradeciendo a todos aquellos científicos que he conocido en congresos, y a los que no he tenido la suerte de conocer, que me han precedido, sin los que no habría sido posible hacer nada de lo que he hecho.

Ahora es momento de pasar a mi lado más personal, el cual ha fraguado de manera más indirecta al doctorado pero de forma indispensable sobre mí para la consecución de esta tesis. Aquí me gustaría nombrar a Bea, mi estupenda psicóloga desde hace un par de años. Gracias por dejar de lado los prejuicios y hacerme entender tantísimas cosas para poder tener una buena salud mental, y hacerme cuidar de ella.

A nivel local, los Pirañicas y Lusilus, gracias por vuestros momentos de apoyo. Gracias Rafa por ser la persona que eres, no dudo de la fenomenal persona que eres y el gran apoyo que has supuesto estos largos años. Gracias también a lo que yo considero los reales Farrus, por seguir sumando risas y momentos de amistad a pesar de la distancia, y que estos nunca acaben. Riki, gracias por ser quien eres y por a pesar de la dureza de la vida, tanto personal como profesional, no guardarte nunca una risa o lágrima de complicidad conmigo. A Sheila, un pilar fundamental en la carrera y que, después de tantos años, aun sigue siéndolo. A otra parte fundamental en mi vida, los Mantequinhas. Álex, Marcos y Víctor, gracias por ser como sois y demostrar el valor de la amistad a lo largo de ya tantos años. A todos vosotros, gracias por dejarme llevaros en mi corazón día tras día.

A la familia Durá-Herrera no solo por acogerme como un igual, sino por mostrarme su apoyo y cobijo todos estos años, gracias Rafa, Estela, Érika, Cristina e Iñaki. Gracias también al pequeño Ian, Iansillo para mí, porque pasar ratos contigo es sinónimo de olvidarse de los malos momentos y disfrutar del privilegio de ser tu tío. Espero verte crecer y ayudarte en todo lo que necesites.

Ara es moment de dedicar unes paraules en la meua llengua als que m'han acompanyat des que vaig conèixer el mon, la meua família. Gràcies al meu pare i a la meua mare, Jaime i Rafaela. Gràcies papà per donar-me la capacitat de l'esforç i de no rendir-me a pesar dels obstacles. Per a tu no demane altra cosa que no fora temps per poder gaudir d'aquelles coses que, per veure'ns a nosaltres amb tot el que necessitàvem, no has pogut disfrutar: la teua família, en la qual s'inclou des de fa poc la teua neta. Gràcies mamà per ser un pilar fonamental tota la meua vida i lluitar sempre per la meua felicitat i els meus objectius. El teu sacrifici i valentia han demostrat de tu ser una persona imbatible. A Vanesa, la meua germana major, "tata" quan m'agafa carinyós. A tu gràcies per des que vaig nàixer haver sigut un pilar fonamental amb l'únic objectiu de donar-me suport i protegir-me. Sé tota la càrrega d'autoexigència que has tingut i que has exercit de la millor manera que has sabut. Per tot això, i per infinites coses més, GRÀCIES. Passe a parlar d'altra de les persones més importants de la meua vida, Gabriela, "la nena" per a mi. No solament has sigut un respir d'aire fresc i alegria per a tota la família des que vas nàixer fa poc més de dos anys, per a mi eres un lloc on poder tornar la ment en blanc i disfrutar de l'amor d'un oncle (el tio per a tu) enamorat de la seua nebodeta. Espere poder ser per a tu tota la vida un lloc segur on poder refugiar-te sempre que ho necessites. Tampoc podia oblidar-me dels meus cosins, Los Primos, de la meua tia Carmen, ni de Raul, qui en tot aquest temps han suposat un pilar de suport per a mi i tota la família.

Pasando al castellano de nuevo, me gustaría poder agradecer encarecidamente no solo esta tesis (contigo empezó y contigo acaba) sino toda una vida a una persona que ante todo sigue estando a mi lado, Ana (y no diré las innumerables formas en las que te llamo jejej). Todas las palabras hacia ti son pocas, pues tú has sido quien ha vivido más de cerca no solo todo este proceso, sino toda la parafernalia de locuras en las que he estado inmerso estos años mientras hacía la tesis y ha hecho que mi tiempo contigo se redujese al mínimo: un máster, una oposición, trabajar de profesor, etc. Infinita gratitud hacia ti por haberme hecho la vida más fácil, incluso cuando ni yo mismo he podido estar ni física ni mentalmente. Supones un ejemplo para mí de humildad, generosidad, vocación por ayudar a los demás y de amor (y un largo etc.), y solo espero poder seguir aprendiendo de tu calidad humana toda la vida pues ante cualquier circunstancia siempre me enseñas algo nuevo. Solo me queda agradecerte todo ello con la cosa más preciada que tenemos, nuestro tiempo.

Por último, me gustaría agradecer a todas las personas (incluso a mí mismo) cualquier muestra de apoyo que han tenido conmigo durante todos estos años. Sin duda estos años me han marcado en lo profesional, pero aún más en lo personal.

A todos vosotros y vosotras, gracias por haberme dejado ser quien soy.

Eternamente agradecido.

INDEX

ABBREVIATIONS

5-HT	5-hydroxytryptamine or serotonin
Ab	Antibody
ABLK	Abdominal leucokinin neurons
AKH	Adipokinetic hormone
AKHR	AKH receptor
AL	Antenal lobe
APCs	AKH-producing Cells
asRNA	antisense RNA
AstA	Allostatine A
BAcTrace	Botulinum Activated Tracer
BoNT/A	Clostridium botulinum neurotoxin A1 ligand/protease
BP	Biological process
BSA	Bovine serum albumin
CB	Central brain
CC	Cellular compartment
cDNA	complementary DNA
ChAT	Choline acetyltransferase
CNS	Central nervous system
CRG	Centre for Genomic Regulation
Crz	Corazonin
D. melanogaster	*Drosophila melanogaster*
DAN	Dopaminergic neuron
DAPI	4',6-diamidino-2-phenylindole
DCSO	Dorsal cibarial sense organ
Ddc	Dopa decarboxylase
DenMark	Dendritic Marker
DGRP	*Drosophila* Genetic Reference Panel
Dh31	Diuretic hormone 31
Dh44	Diuretic hormone 44
DILP	*Drosophila* insulin-like peptide
Dop1R2	Dopamine 1-like receptor 2
Dop2R	Dopamine 2-like receptor
DopEcR	Dopamine/ecdysteroid receptor
DPBS	Dulbecco's phosphate buffered saline
DSK	Drosulfakinin
dTrpA1	*Drosophila* transient receptor potential A1
EB	Ellipsoid body
EC_{50}	Half maximal effective concentration
EcR	Ecdyson receptor
EM	Electron microscopy
FACS	Fluorescence-activated cell sorting
FAFB	Full Adult Fly Brain
Fdg	Feeding neuron
FDR	False discovery rate
FlyPAD	Fly Proboscis and Activity Detector
FSC-A	Forward scatter area
FSB	Fan-shaped body

GABA	Gamma-aminobutyric acid
GABA-BR2	metabotropic GABA-B receptor subtype 2
GABA-BR3	metabotropic GABA-B receptor subtype 3
GABAT	γ-aminobutyric acid transaminase
Gad1	Glutamic acid decarboxylase 1
Gapdh2	Glyceraldehyde 3 phosphate dehydrogenase 2
GFP	Green fluorescent protein
GNG	Gnathal ganglia neuron
GO	Gene ontology
GPCR	G protein-coupled receptors
GR	Gustatory receptor
GRASP	GFP Reconstruction Across Synaptic Partners
GRN	Gustatory receptor neuron
GSEA	Gene set enrichment analysis
GSON	Gustatory second-order neuron
Hug	Hugin
I	Intermediate
IA-2	IA-2 protein tyrosine phosphatase
IPC	Insulin-producing cell
IQR	Interquartil range
IR	Ionotropic receptor
ISN	Interoceptive SEZ Neuron
ITP	Ion transport peptides
KC	Kenyon cell
Kir2,1	Inwardly rectifying potassium channel 2.1
L	Long
Lar	Leukocyte-antigen-related-like
LH	Lateral horn
LHLK	Lateral horn leucokinin neurons
Lk	Leucokinin
Lkr	Leucokinin receptor
lncRNA	long non-coding RNA
LSO	Labral sense organ
MB	Mushroom body
md-L	Labellum multi-dendritic neurons
MF	Molecular function
MN9	Motor neuron 9
mRNA	messenger RNA
mtdTomato	membrane targeted Tomato
nAChRbeta1	nicotinic Acetylcholine Receptor beta 1
NGS	Normal goad serum
NompC	No mechanoreceptor potential C
NPF	Neuropeptide F
NPY	Neuropeptide Y
OA-VL	Octopaminergic/tyraminergic interneurons
OBP49a	Odorant binding protein 49a
OL	Optic lobe

OR	Olfactory receptor
OSN	Olfactory sensory neuron
PANGEA	Pathway, Network and Gene-set Enrichment Analysis
PBS	Phosphate buffer saline
PBT	PB with Triton X-100
PC	Principal component
PCA	Principal component analysis
PER	Proboscis extension response
PFA	Paraformaldehyde
PI	Preference index
PN	Projection neuron
PPK	Pickpocket channels
qPCR	quantitative Polimerase Change Reaction
RNAi	RNA interference
RNAseq	RNA sequencing
ROI	Region of interest
S	Short
scRNAseq	single-cell RNA sequencing
SELK	Subesophageal zone leucokinin neurons
SEM	Standard error of the mean
SerT	Serotonine transporter
SEZ	Subesophageal zone
sGPNs	sweet Gustatory Projection Neurons
sNPF	short Neuropeptide F
sNPF-R	short Neuropeptide F receptor
SSC-A	Side scatter area
syt	synaptotagmin
Tdc2	Tyrosine decarboxylase 2
TEV	Tobacco etch virus
TH	Tyrosine hydroxylase
TNT	Tetanus toxin
TNT^{IMP}	Tetanus toxin impaired
TPM	Transcripts per million
TPN	Taste projecton neuron
TRACT	TRAnsneuronal Control of Transcription
Trh	Tryptophan hydroxylase
TRP	Transient receptor protein
UAS	Upstream activated sequence
VCSO	Ventral cibarian sense organ
VFB	Virtual Fly Brain
VGAT	Vesicular GABA transporter
VGlut	Vesicular glutamate transporter
VNC	Ventral nerve cord

ABSTRACT / RESUMEN

Animals, including the fly *Drosophila melanogaster*, continuously receive and process sensory information from the surrounding environment via different sensory systems, which ultimately direct appropriate behavioral responses. Among those behaviors, feeding is essential as it is how animals get all the needed nutrients to support their lives. In order to discriminate between nutritious and potentially toxic food, a set of specialized neurons, gustatory receptor neurons (GRNs), housed in gustatory sensilla along the body, express a combination of chemosensory receptors for the detection of food chemicals. These GRNs project their axons to the subesophageal zone (SEZ), the primary taste center in the brain, where gustatory information is integrated primarily by the gustatory second-order neurons (GSON). While much is known regarding the gustatory receptors and the role of GRNs, it is not yet clear how GSONs process the gustatory information conveyed by GRNs to the SEZ.

This Thesis aims to understand how GSONs integrate gustatory information in the central brain and how the metabolic state of the flies can modulate this process. Using *trans*-Tango and fluorescence-activated cell sorting (FACS), we separated the GSONs receiving direct input from sweet, bitter and mechanosensory GRNs in fed and starved conditions to characterize them molecularly by RNA sequencing. Gene analysis expression reveled that GSONs receiving input from sweet, bitter, and mechanosensory neurons segregate molecularly and that their molecular profile varies with the metabolic state of the fly (fed vs. starved). Furthermore, GSONs express a complex combination of neurotransmitters and neuropeptides, indicating that those neurons are not homogenous even when receiving information from the same taste quality.

Of all genes analyzed, we found that the neuropeptide Leucokinin (*Lk*) was highly expressed during starvation by two single neurons located in the SEZ (SELK neurons). Our results revealed that both SELK neurons receive information from sweet and bitter GRNs, validated using different molecular strategies and the recently published Full Adult Fly Brain (FAFB) connectome with Flywire. We consider that those results show for the first time that a neuron in the SEZ directly collects information of opposing valence, sweet and bitter (attractive and repulsive).

We tested the functionality of those SELK neurons during feeding behavior in two paradigms: feeding initiation with the Proboscis Extension Response (PER) and feeding two-choice assay with flyPAD. While the expression of tetanus toxin in all Lk neurons does not alter apparently feeding behavior in free-moving flies, our results suggest that SELK neurons are involved in integrating bitter and sweet tastants to tolerate bitter compounds during starvation during feeding initiation.

To the best of our knowledge, our work reveals for the first time the molecular transcriptomic profile from two metabolic states of three different taste GSONs populations, highlighting behaviorally the essential role of SELK neurons in directly integrating the sweet and bitter taste information.

Los animales, incluyendo a la mosca *Drosophila melanogaster*, constantemente reciben y procesan información sensorial proveniente del ambiente que les rodea a través de diferentes sistemas sensoriales, para finalmente producir el comportamiento apropiado. Entre todos los comportamientos que los animales pueden mostrar, la alimentación es particularmente esencial, ya que es la forma con la que los animales se abastecen de los nutrientes necesarios para sustentar sus vidas. Para discriminar entre comida nutritiva y potencialmente tóxica, un grupo de neuronas especializadas, neuronas gustativas sensoriales (*GRNs*, en inglés), localizadas en sensilas gustativas por todo el cuerpo, expresan una combinación de receptores quimiosensitivos que detectan los diferentes compuestos químicos en la comida. Estas GRNs proyectan sus axones a la región subesofágica (*SEZ*, en inglés), el centro primario para el gusto en el cerebro, donde la información gustativa se integra en las neuronas gustativas de segundo orden (*GSON*, en inglés). En estos momentos tenemos un conocimiento detallado de los receptores gustativos y acerca de la función de las GRNs, sin embargo sabemos muy poco cómo las GSONs procesan la información gustativa recibida por las GRNs en el SEZ.

Esta tesis pretende entender cómo las GSONs integran la información gustativa en el cerebro central y cómo el estado metabólico de las moscas puede modular este proceso. Empleando *trans*-Tango y la separación de células activadas por fluorescencia (*FACS*, en inglés), separamos las GSONs que recibían señal directa de GRNs dulces, amargas y mecanosensitivas en condiciones de saciado y ayuno para caracterizarlas molecularmente mediante secuenciación de ARN (*RNAseq*, en inglés). El análisis del RNAseq reveló que las GSONs que recibían señal de GRNs dulces, amargas y mecanosensitivas se segregaban molecularmente y su perfil molecular variaba en función del estado metabólico de la mosca (saciado y ayuno). Además, las GSONs expresan una compleja combinación de neurotransmisores y neuropéptidos, indicando que esas neuronas no son homogéneas aun recibiendo información de la misma modalidad de sabor.

De todos los genes analizados, encontramos que el neuropeptido Leucokinin (Lk) estaba altamente expresado durante el ayuno por dos neuronas localizadas en el SEZ (neuronas SELK). Nuestros resultados revelaron que ambas neuronas SELK recibían información de GRNs dulces y amargas. Estos resultados fueron validados usando diferentes estrategias moleculares y el reciente publicado conectoma del Full Adult Fly Brain (FAFB) con Flywire. Consideramos que estos resultados muestran por primera vez que una neurona en el SEZ colecta directamente información de diferente valencia, dulce y amarga (atractiva y repulsiva).

Igualmente estudiamos la funcionalidad de estas neuronas SELK durante el la alimentación de la mosca en dos situaciones: inicio de la alimentación con el ensayo de Respuesta de Extension de la Probóscide (*PER*, en inglés) y el ensayo de elección de alimentación con flyPAD. Mientras que el silenciamiento de todas las neuronas Lk no altera el comportamiento de alimentación en moscas con movimiento libre, nuestros resultados sugieren que las neuronas SELK están involucradas en integrar el sabor dulce y amargo para tolerar compuestos amargos en ayuno durante el inicio de la alimentación.

Consideramos que nuestro trabajo muestra por primera vez el perfil molecular transcriptómico de dos estados metabólicos en tres poblaciones diferentes de GSONs, destacando el papel esencial durante el comportamiento de las neuronas SELK integrando la información para el sabor dulce y salado.

INTRODUCTION

1. Decision-making mechanisms under competing demands

Animals constantly receive and process massive amounts of sensory information that must integrate with internal demands to ensure their survival (Bell, 2024). For example, among these demands could be the defense from predators, protect the progeny to ensure reproduction, the formation of social communities to promote protection, or even the decision of what to eat to supply the caloric demands of the body in specific internal and environmental conditions (Kristan, 2008; Pearson et al., 2014). Therefore, to respond correctly to those demands, it is crucial to integrate as much information as possible to face decision-making processes that orchestrate which behavior to perform in a given moment while others are suppressed.

Generally, decision-making is often thought of as a high-level cognitive process that leads to choices by weighing the different options and their expected outcomes, often over long periods. Many animals with apparently little cognition, like invertebrates, make choices of what to do (whether to eat or to escape, for example) depending on both external and internal factors (**Figure 1**) (Palmer & Kristan, 2011).

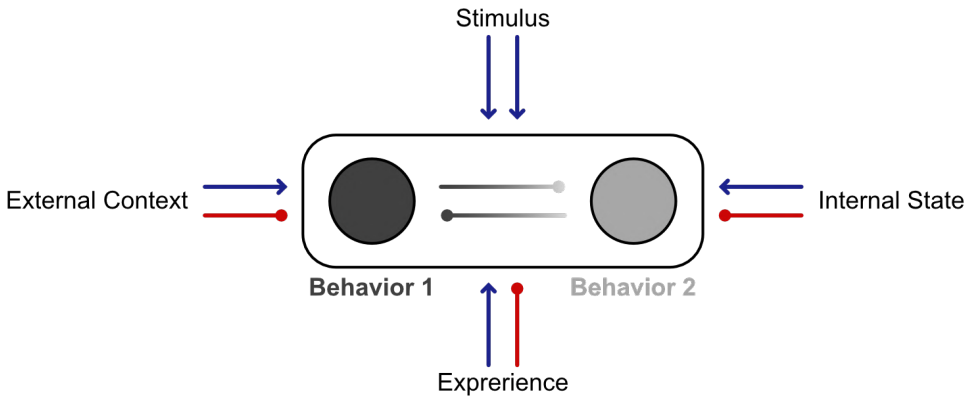

Figure 1: Schematic representation of decision-making processes. Animals make decisions of how to behave in front of specific stimuli by considering the environmental context and internal state, and also modulated by their previous experience. Arrows represent promoting and circles suppression.

The problem of selecting a behavior, given the use of overlapping neural networks and effector systems to resolve competing demands, is a key feature of behavior (Pearson et al., 2014). Therefore, nervous systems need mechanisms in place to successfully implement these competitive interactions (Koyama & Pujala, 2018). Therefore, studying how animals can sense and perceive internal and external specific states and scenarios and how all this information is integrated may be the first approach to understand how decision-making processes take place.

During this Thesis, I aim to understand how sensory information is integrated into the central nervous system (CNS) to produce final behaviors and how animals' internal demands can modulate this process.

1.1. Feeding as an essential behavior in animals

Feeding constitutes a fundamental behavior for all animals, from invertebrates to vertebrates, serving as the primary mechanism for acquiring essential nutrients to supply their caloric needs. Therefore, animals are constantly weighing their internal nutrient needs against external nutrient availability, which is partially modulated by environmental cues. However, animals need to distinguish which specific nutrients are in deficit to manage competing needs and, most importantly, distinguish between healthy food sources and those that are toxic. Thus, feeding is an essential behavior that needs to be carefully regulated in order to manage correct decisions.

The ability of animals to locate food, assess its quality, and make decisions regarding ingestion is influenced by various internal factors, including the reproductive state and starvation levels. In *Drosophila melanogaster* (*D. melanogaster*), for example, reproductive status influences food preferences, with mated flies displaying a preference for protein-rich diets (Steck et al., 2018). Additionally, starvation induces heightened food-seeking behavior, increased food intake, and a greater tolerance for toxic compounds in the food (LeDue et al., 2016). Therefore, hormone signals, circulating nutrients, and chemicals in the food, among other internal and external cues, are critical factors that complex endocrine pathways and neuronal circuits need to be sensed and processed to drive proper feeding behavior (Itskov & Ribeiro, 2013). However, the neurogenetic factors modulating this intricate process are not totally understood.

Overall, feeding is perfect for studying the genetic and neuronal basis controlling sensory and metabolic information integration, as this behavior is well-stereotyped and easy to measure, and we have many genetic and neuronal tools available.

2. *Drosophila melanogaster* as a model to study the neurogenetic bases of behavior

Studying the genetic and neural mechanisms controlling behavior can be challenging in complex nervous systems. Model systems with compact and numerically small CNS are more amenable to detailed characterization of the neural circuit mechanisms involved in competitive interactions (Jovanic, 2020).

D. melanogaster is the perfect model system for studying the neural and genetic basis of sensory integration and processing for several reasons (Amrein & Thorne, 2005). It has been used as a classic system to study genetics and development, providing endless information regarding the organization of the *Drosophila* genome and anatomy (Venken, Simpson, et al., 2011). The short life cycle of *D. melanogaster* is advantageous compared with other more complex animal models. While experiments in flies commonly take days, weeks, or a few months at most, the same experiments in mice last several months or years. Flies are grown for around 10 days at 25ºC to generate adults that live for a maximum of 10 weeks. The growth temperature can be modified to take more days of development, for example, 21 days at 18ºC (Yamaguchi & Yoshida, 2018). Thus, it is possible to dispose of large quantities of animals in short periods of time with low resources due to their small size and breeding.

This section describes some of the main genetic and behavioral tools available in *D. melanogaster* for dissecting neural circuits molecularly, functionally, and behaviorally.

2.1. Tools available to genetically manipulate neurons

In addition to its fully sequenced genome (Adams et al., 2000), it has extensive collections of genetic reagents that can be used to label and manipulate most cell types, including neurons. To further facilitate its study, the whole brain of *D. melanogaster* has approximately only 200,000 neurons controlling various sophisticated behaviors (Raji & Potter, 2021). Thus, the relative simplicity of the nervous system and rich genetic reagents to manipulate neurons provide the feasibility of understanding how neural circuits control behaviors (Venken, Simpson, et al., 2011).

D. melanogaster counts with a significant collection of mutant, deficient, and transgenic lines and more recently incorporated complex genomic editing techniques such as CRISPR/Cas9 (Bosch et al., 2021; Ma et al., 2014) that can be used to inspect the role of particular neurons or genes. Of all the genetic tools available, one of the most broadly used is the yeast-derived Gal4/UAS binary system, which revolutionized *Drosophila* research (Brand & Perrimon, 1993; Venken, Schulze, et al., 2011). Briefly, the Gal4 transcription factor is expressed via specific promoters that bind to the upstream activated sequence (UAS) site to activate the transcription of the downstream responder to UAS. Virtually any promoter can control the expression of Gal4 and mimic the expression of a gene of interest to some extent. There are large collections with thousands of Gal4 lines (Jenett et al., 2012), split-Gal4 collections (Dionne et al., 2018),

or databases for searchable neurons (Meissner et al., 2023) that facilitate the screening and genetic manipulation of neurons.

Specific promoters can control the expression of Gal4 to drive the expression of specific transgenes downstream of the UAS sequence: for example, the reporters GFP (green fluorescent protein) and mtdTomato (membrane targeted Tomato), or dTrpA1 (*Drosophila* transient receptor potential A1) (Hamada et al., 2008) and Kir2.1 (inwardly rectifying potassium channel 2.1) (Baines et al., 2001) to artificially depolarize (activate) or hyperpolarize (silence) neurons respectively, or to block the synaptic transmission by expressing the tetanus toxin (TNT) (Sweeney et al., 1995). Over the years, other specific binary systems have been developed like LexA/LexAop (Pfeiffer et al., 2010) and QF/QUAS (Potter & Luo, 2011), whose function is similar to the Gal4/UAS system. The possibility to combine multiple binary expression systems allowed not only the labeling of multiple neurons with different fluorescent markers simultaneously but also the development of tools much more sophisticated, like transsynaptic tools to label pre- and postsynaptic neurons, as well as synaptic connections. For example, *trans*-Tango (Talay et al., 2017) and *retro*-Tango (Sorkaç et al., 2023), developed by the same laboratory, allow the anterograde and retrograde transsynaptic tracing, respectively, by combining the Tango assay with the expression of two reporters by two the Gal4/UAS and QF/QUAS binary systems. Further, TRACT (TRAnsneuronal Control of Transcription) (Huang et al., 2017) and BAcTrace (Botulinum Activated Tracer) (Cachero et al., 2020) can also label anterograde and retrograde, respectively, transsynaptic neurons based on ligand-induced intramembrane proteolysis. On the other hand, GRASP (GFP Reconstruction Across Synaptic Partners) (Feinberg et al., 2008) makes use of the trans-cellular complementation of split GFP parts (spGFP1-10 and spGFP11), expressed by the Gal4/UAS and LexA/LexAop binary systems, to detect the membrane proximity of two cells.

Studying functional neuronal interconnectivity by manipulating one neuron and monitoring the other is also possible. The most precise method to date uses paired electrophysiological recording electrodes from two neurons. Alternatively, optogenetic and chemogenetic techniques can also activate neurons using light or chemicals like CsChrimson (Lima & Miesenböck, 2005) and ReaChR (Watanabe et al., 2017) or P2X2 (Yao et al., 2012), respectively. Further, the GCaMP fluorescent sensor to intracellular calcium concentration allows us to measure neuron depolarization upon stimulation (Streit et al., 2016). All these approaches unveil direct and indirect functional connections between neurons.

In addition to all molecular tools available to manipulate and trace neurons, the development of whole-brain wiring diagrams, achieved by aligning thousands of stochastically labeled single neurons into a standardized brain, offers a framework for assessing brain organization and neuronal connectivity (Chiang et al., 2011). For example, NBLAST allows the identification of neurons that can be fitted to a reference brain and obtain hits regarding their connectivity and morphology (Costa et al., 2016). Moreover, the recently published connectome of the Full Adult Fly Brain (FAFB) carried out by electron microscopy (EM) with synaptic resolution shed light on the possibility of tracing neuronal circuits *in silico* to produce hypotheses at the circuit level that can be cross-validated with results obtained *in vivo*, saving time, money and animal usage (Zheng et al., 2018).

The disposition of all those tools suggests that *D. melanogaster* is an outstanding animal model for manipulating neurons and studying how neural circuits process sensory information.

2.2. How to study behavior in *Drosophila melanogaster*

D. melanogaster has emerged as an excellent model for several reasons to study how neuronal circuits evoke final behaviors. Their small size and short breeding time allow testing large quantities of animals in a high-throughput manner, reducing time and providing large samples to analyze statistically. For that reason, in combination with all genetic tools available (described in the previous paragraphs), *D. melanogaster* has been used over recent years to study the underlying mechanisms of multisensory processing (Sánchez-Alcañiz & Benton, 2017), motor control (Zhou et al., 2019), behavioral choice (Yu et al., 2023; Shao et al., 2017; Münch et al., 2022) and learning and memory (Boto et al., 2020).

There is a large list of hardware and software tools to trace behaviors, from individual to collective behavior, in a high-throughput manner thanks to the development of machine learning and computer capacity (Mollá-Albaladejo & Sánchez-Alcañiz, 2021). For example, *Honegger et al*. built a paradigm arena where individual flies could choose between two odors emanating from opposing ends of a corridor (K. S. Honegger et al., 2020). Also, the Buridian paradigm arenas are highly used to test object orientation responses using video tracking of individuals or groups (Linneweber et al., 2020). Another example is flyPAD (fly Proboscis and Activity Detector), an automated high-throughput method to study fly ingestion in individual flies when they choose between two types of foods (Itskov et al., 2014). However, despite most of the mentioned methods being focused on analyzing individual flies, the study of collective behaviors raised the

possibility of comparing the performance of the group with the individual. To do that, there are several specialized softwares to analyze the interactions of individual flies within a group like CTrax (Branson et al., 2009) or *idtracker.ai* (Romero-Ferrero et al., 2019).

So far, the large quantity of animals tested enables us to analyze further the huge variability that emerges from behavior. Variation is the interindividual differences within a population resulting from the interplay between genetic and non-genetic factors (Casillas & Barbadilla, 2017; Ayroles et al., 2015). However, even in highly controlled experimental conditions, high levels of variability can be observed (K. Honegger & De Bivort, 2018). With the disposition of large collections of inbred lines such as the *Drosophila* Genetic Reference Panel (DGRP), which is a set of >200 fly strains derived from subsequent inbred generations with sequenced genomes and all their polymorphisms annotated (Mackay et al., 2012). With them it is possible to test that variation in behavior to later search for the genetic bases responsible for such behavior. For example, by using the DGRP lines it has been described how variability in locomotor handedness might be determined by genetic cues, highlighting Tenascin-a as a candidate involved in the observed behavior heterogeneity (Ayroles et al., 2015; Buchanan et al., 2015). Others have used the DGRP lines to study the genetic variation in different behaviors such as mating (Ruedi & Hughes, 2008).

Altogether, it highlights *D. melanogaster* as a model for studying sensory integration in the nervous system and how this influences final behavior. Thus, in this Thesis, I took all the advantages of the fruit fly *D. melanogaster* to study the molecular and neural basis of taste coding and how it can modulate feeding behavior.

3. Anatomical organization of the gustatory system in the adult *Drosophila melanogaster*

The decision by *D. melanogaster* to consume food depends on the direct contact with volatile and non-volatile compounds. The gustatory system carries out this capacity, whose function is to sense chemosensory cues (mostly non-volatiles) from food and substrate, which is essential not only for feeding but also for mating and oviposition and possibly in the formation of social networks (Amrein & Thorne, 2005). It is one of the most studied sensory systems in the fruit fly, and it is composed of a set of taste organs distributed in different parts of the body in the adult where they contact the different environmental chemosensory stimuli, which are finally decoded in CNS (Stocker, 1994;

Vosshall & Stocker, 2007). These taste organs can be external which include the anterior wing margin (**Figure 2A**), distal segments of the legs (**Figure 2B**), and the labellum, or internal taste organs like the three pharyngeal taste organs located internally in the proboscis: labral sense organ (LSO), ventral cibarian sense organ (VCSO), and dorsal cibarial sense organ (DCSO) (**Figure 2**).

The location of taste organs is not random, as they comprise specific functions in each body part. While the role of the margin wings may be involved in the exploration of ecological niches, the presence of taste organs in the ovipositor system of females triggers the decision to lay eggs in one substrate or another, enhancing the probability of surviving the progeny after larval growth in a suitable source of food (Raad et al., 2016). Further, the internal position of the three pharyngeal taste organs may be suggested to act as a final gate to promote ingestion or repulsion to food sources (LeDue et al., 2015; Chen & Dahanukar, 2017).

However, despite the different locations of each taste organ, all of them share a basic common morphological and functional structure responsible for chemosensory detection, the taste sensilla. Gustatory sensilla are responsible for detecting taste, and each comprises multiple gustatory receptor neurons (GRN) housed within a cuticular hair-like structure, and in most of the sensilla types, also a mechanosensory neuron (MSN) (S. et al., 2001; Chen & Dahanukar, 2020). These GRNs are bipolar cells with a cell body that lies beneath the surface of the cuticle and includes a single dendrite that extends to the tip of the sensilla and one axon that projects to the CNS, specifically to regions specialized in gustatory processing (Chen & Dahanukar, 2020). Therefore, each of these taste hairs has a single pore at the tip of the sensilla, which allows tastants to enter and make contact with the GRNs within them. These GRNs project their axons to specific regions of the CNS where gustatory information is processed.

The proboscis, the main feeding organ of *D. melanogaster*, is the equivalent of the mammalian mouth (Yarmolinsky et al., 2009). It comprises external and internal taste organs. The internal part is the pharynx (**Figure 2C**), and it serves as the final gatekeeper, allowing the fly to decide whether to expel the food or proceed to its ingestion. The external taste organ consists of two labellar lobes forming the labellum on the most external part of the proboscis (**Figure 2D**). In each half of the labellum, 31 hairs can be further divided into morphological subtypes based on the length of the hairs: L (long), I (intermediate), and S (short) (**Figure 2E**). The L- and S-type sensilla each houses four GRNs plus one MSN, while the I-type sensilla contains two GRNs plus one MSN (**Figure 2F**) (Montell, 2013). Furthermore, in the internal part of the labellum, there

are ~30-40 taste pegs, a type of hairless sensilla that houses just one GRN and one MSN (**Figures 2E** and **2G**). These taste pegs are specifically located between rows of pseudotrachea, so they only access the food when the flies open their labial palps during feeding. Internally, in the pharynx, sensilla are organized in a pharyngeal hairless sensillum that usually lacks MSN (except for the #8 and #9 LSO), and the number of GRNs varies from 1-8 (**Figures 2C** and **2H**).

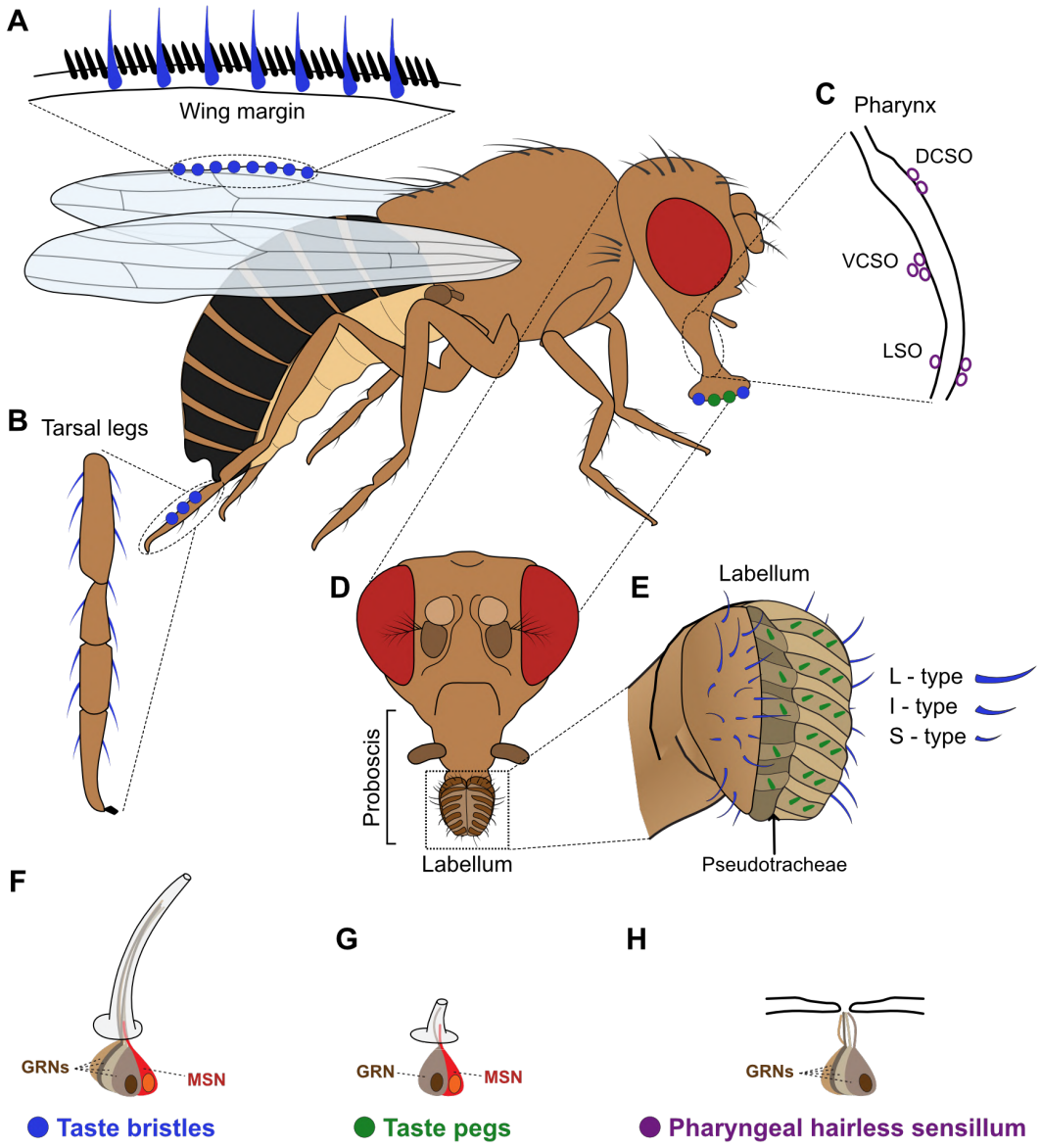

Figure 2: Organization of the adult *Drosophila melanogaster* gustatory system. The gustatory system of *D. melanogaster* comprises different taste organs spread all over the body and involved in different processes. These taste organs share a common structural and functional structure, the sensilla. There are three types of taste sensillum in the different taste organs: taste bristles (in blue), taste pegs (in green), and pharyngeal hairless sensillum (in purple). Taste bristles are distributed in the anterior wing margins (**A**), the distal segment of the legs (**B**), and the labellum (**D-E**). The hairless sensilla are located in the three internal pharyngeal taste organs: LSO, VCSO and DCSO (**C**). Taste pegs are located between pseudotrachea in the labellum (**E**). (**F-H**) Schematic diagrams showing the structures of three types of taste sensillum. All of them have a terminal pore (arrows) that allows tastants to contact the taste neurons in each sensillum.

The taste bristle has 2–4 GRNs (4 GRNs in this schematic example) whose dendrites extend up to the tip of the taste sensillum (**F**). The taste peg has one GRN (**G**). Both taste bristles and taste pegs have one MSN at the base of each sensillum (**F** and **G**). The pharyngeal hairless sensillum usually lacks MSN, except for the #8 and #9 LSO sensillum. The number of GRNs in the pharyngeal hairless sensillum can vary from 1–8 (4 GRNs in this schematic example) (**H**).

In addition to the sensilla that fruit flies presented in the proboscis mentioned above, each leg contains at least 30 taste bristles, and the anterior wing margin of each wing has an additional 40 such bristles (He et al., 2019; Raad et al., 2016). This wide distribution of taste cells throughout the fly's body underscores the critical role that chemosensory stimuli represent in the fly's world. However, sexual dimorphism has been noted in the number of taste sensilla. On the forelegs, males have, on average, 50, whereas females have about 37 (Chen & Dahanukar, 2020). Interestingly, the male taps the female's abdomen extensively during courtship, presumably to sample pheromone chemicals secreted from specialized cells in this body part by female taste bristles and promote courtship behavior (Bray & Amrein, 2003; Hall, 1994; Thistle et al., 2012). Further, males have more labellar taste bristles than females (Bray & Amrein, 2003; Stocker, 1994). On the contrary, females have more taste pegs in their labellum than males (S. et al., 2001). This sexual dimorphism in the number of taste sensilla indicates how the gustatory system has adapted to sex-specific behaviors, arising the evolutionary effect of adaptation in taste detection. Hence, the total number of taste sensilla that *D. melanogaster* has spread in all gustatory organs is about 260 (Raad et al., 2016).

3.1. Taste detection by gustatory receptor neurons

Similar to humans, flies can discern five taste qualities (sweet, bitter, salty, sour and umami) through different populations of neurons tuned to each of these qualities (Yarmolinsky et al., 2009). To detect and respond to the different peripheral compounds, flies have adapted the properties of their GRNs to detect most of the food chemicals found in nature selectively. For example, GRNs located in legs tarsi (**Figure 2B**) respond selectively to sugar and bitter compounds, water, and low salt and may participate in pheromone detection in combination with other chemosensory neurons on the legs (Bray & Amrein, 2003).

Generally, GRNs fall into five classes (A-E) based on their response profile. These include 'A' GRNs (formerly sugar GRNs), which respond to attractive compounds such as low salt, sugars, glycerol, fatty acids, and carboxylic acids, 'B' GRNs (formerly bitter GRNs) which are activated by high Na^+, bitter compounds, acids, polyamines, tryptophan, and L-canavanine, 'C' GRNs respond to water, 'D' GRNs detect high levels of cations such as Na^+, K^+ and Ca^{2+}, and 'E' GRNs sense low Na^+ levels (Montell, 2009; Montell, 2021). However, GRNs are popularly classified depending on their response to

tastants, such as water, sweet, salt, and bitter-sensing (Montell, 2009). Single GRNs respond to compounds of the same valence, for example, attractive stimuli, such as low salt or sugars, or aversive compounds, including high salt and bitter compounds, but not to stimuli of different valence (Montell, 2009). Nevertheless, the precise degree to which each group of taste neurons is specifically attuned to various tastants is still uncertain. Several research indicates that certain taste neurons may exhibit the capability to react to compounds spanning different taste categories (Hiroi et al., 2004; Charlu et al., 2013; Ahn et al., 2017). This implies the potential existence of multimodal taste detection attributes within the taste neurons of insects (Chen & Dahanukar, 2020). Generally, the four GRNs in L-type sensilla are most sensitive to attractive stimuli and respond weakly to aversive stimuli (Hiroi et al., 2002). Nevertheless, molecular, calcium-imaging, and electrophysiological studies have identified that each of the four GRNs is tuned to different stimuli: one is strongly responsive to low salt, another is strongly responsive to sugars, a third is weakly responsive to high salt and bitter, and the fourth is moderately responsive to water (Amrein & Thorne, 2005; Chen & Dahanukar, 2020). In contrast, the four GRNs in S-type sensilla are most sensitive to bitter compounds and high salt, and respond only weakly to low salt and sugars (Freeman & Dahanukar, 2015). The I-type sensilla includes two GRNs, one excited by a narrow group of bitter compounds and aversive high levels of salt and the other activated by sugars and low levels of salt that are attractive (Hiroi et al., 2004; Weiss et al., 2011).

So far, activation of different GRNs drives different behaviors, suggesting that there are innate pathways from taste detection to behavior. For example, expressing the capsaicin-gated cation channel in the sweet GRNs attracts the flies to capsaicin, but if expressed in the bitter GRNs, flies avoid capsaicin (Marella et al., 2006). The same happened when the light-gated channel CsChrimon was expressed in the sweet GRNs where flies extended their proboscis to initiate feeding upon light stimulation (Gordon & Scott, 2009). These show how activation of GRNs drives innate behaviors in front of appetitive or aversive compounds. Nevertheless, sensory perception can rapidly adapt to environmental changes, such as in the case of the german cockroach in which glucose activates both sweet and bitter GRNs, leading to avoiding the glucose present in toxic baits (Wada-Katsumata et al., 2013). This suggests that the huge plasticity of the gustatory sensory system is necessary to adapt to environmental features.

On the other hand, not only is taste information sensed by the sensillum to drive feeding, but mechanosensory information is also processed in the periphery to drive final feeding behavior. The physical property of food is essential for animals to access the palatability of the food source, as well as gustation is essential for taste sensing, and has

a direct impact on feeding or egg-laying behavior to promote survival (Jeong et al., 2016). Food that is too soft or viscous could be indicative of over-ripen or contamination, while too difficult to swallow indicates that the food is unripe (Stensmyr et al., 2012). As previously mentioned, the sensilla located in the labellum house a set of GRNs but also one MSN (**Figures 2E** and **2F**) that expresses the NompC mechanosensory ion channel (No mechanoreceptor potential C), a TRP-family mechanosensory channel required for food texture discrimination (Sánchez-Alcañiz et al., 2017). Among these MSNs, the labellum multi-dendritic neurons (md-L) innervate most of the sensilla to sense the hardness or viscosity of food so as to suppress feeding (Zhang et al., 2016; Wu et al., 2019). Other sets of neurons, the sd-L neurons, are located in the junction of the labellum and the haustellum to sense the deformation of the proboscis during feeding and finally promote ingestion by the indirect activation of sweet GRNs and motor neurons (J. Yu et al., 2023). All these, allow flies to integrate the food texture with taste sensing in order to choose the correct food source with an intermediate stiffness and great taste properties.

In summary, GRNs are tuned to sense different types of chemicals, which cover most of the substances present in food. In addition, mechanosensation by MSNs plays a fundamental role in feeding behavior. This allows animals to discriminate between toxic and nutritious sources of food and drive the appropriate decision during feeding, among other behaviors, to promote their survival.

3.2. Molecular organization of gustatory receptor neurons

GRNs express a large variety of receptors that define their selectivity and tuning properties for gustatory perception. Among them, there are four major families of receptors expressed in the *Drosophila* gustatory system: gustatory receptors (GRs), ionotropic receptors (IRs), transient receptor proteins (TRPs), and pickpocket channels (PPKs) (Montell, 2021; Scott, 2018). Many of these receptors are expressed in GRNs in a combinational fashion, and are responsible for detecting most of the chemicals in the food (Chen & Dahanukar, 2020).

60 genes in the *D. melanogaster* genome encode the entire 68 GRs family by alternative splicing (Clyne et al., 2000). Most of them are clustered (groups of 2-6 GRs genes) in small regions of the chromosomes, indicating that GRs may undergo an ancient gene duplication and divergence (Freeman et al., 2014; Robertson et al., 2003). GRs are seven-transmembrane proteins that initially were thought to be G-protein coupled receptors (GPCRs) but soon was demonstrated that their topology was inverted with an extracellular C-terminus and an intracellular N-terminus, opposite to GPCRs (Dunipace et al., 2001; Robertson et al., 2003; Scott et al., 2001; D. Ma et al., 2024).

Those results suggested that GRs might act as tetrameric ion channels, as, in fact, has been shown recently through heterologous expression and Cryo-EM of some GRs (D. Ma et al., 2024).

GRs are expressed in the GRNs according to their taste modality. For example, Gr5a and Gr66a are each found in different populations of gustatory neurons that respond to sweet and bitter compounds, respectively (Marella et al., 2006; Thorne et al., 2004; Z. Wang et al., 2004). However, the number of GRs that respond to either sweet or bitter is large. For example, there are 8 GRs (Gr5a, Gr61a, and Gr64a-f) that respond to sweet compounds and are co-expressed in the sweet GRNs (Dahanukar et al., 2007; Fujii et al., 2015; Jiao et al., 2007, 2008). There are other GRs expressed in bitter GRNs, like Gr66a, Gr33a, and Gr93a, that are necessary for the detection of bitter compounds (Dunipace et al., 2001; Y. Lee et al., 2009; Moon et al., 2006). Nevertheless, multiple GRs and other receptors with overlapping expression contribute to normal responses to sweet and bitter compounds. For example, 33 GRs are expressed in subsets of bitter GRNs to mediate bitter-taste detection (Weiss et al., 2011). However, despite the recent structure knowledge advances, detailed functional studies of GRs need to be elucidated to characterize the possible implications of this heterologous expression.

Regarding the IR family, 66 IRs were identified in *D. melanogaster* and showed different functions and expression patterns (Benton et al., 2009). They contain an extracellular N-terminus, a two-lobed ligand-binding domain, 3 transmembrane domains, and an intracellular C-terminus. They participate in different sensory modalities. Only 16 IRs are expressed in the fly antenna, in a set of olfactory neurons that do not express olfactory receptors (ORs), some acting as odorant receptors for amines and acids (Ai et al., 2010, 2013; Croset et al., 2010) and others participating in thermosensation and hygrosensation (Enjin et al., 2016; Knecht et al., 2016; Ni et al., 2016). At least 16 IRs are presumably expressed in the adult taste system, including taste bristles, labellar taste pegs, and pharyngeal taste organs (Koh et al., 2014; Sánchez-Alcañiz et al., 2018). The role of some of those IRs has been described. For example, *Ir25a* and *Ir76b* are broadly co-expressed in the proboscis GRNs, where they might serve as co-receptors (Ganguly et al., 2017; Hussain et al., 2016; Sánchez-Alcañiz et al., 2018; Zhang et al., 2013). Ir56d is involved in carbonation and hexanoic acid-sensing (Sánchez-Alcañiz et al., 2018), while *Ir52c* and *Ir52d* are expressed in GRNs located in the legs tarses involved in pheromone sensing (Koh et al., 2014).

Finally, the other two ion channel families that participate in gustatory detection in *D. melanogaster* are the PPK family (epithelial sodium channel/degenerin family) and

the TRP family, with only a few members of each family involved in gustatory detection. There are 31 PPKs in *D. melanogaster*, and only a few have been shown to have a role in chemosensory detection. The *ppk28* is exclusively expressed in water-sensing gustatory neurons and is necessary for cellular and behavioral responses to water (Cameron et al., 2010; Chen et al., 2010). Moreover, exogenous expression of *ppk28* confers low osmolarity responsiveness to other fly gustatory neurons or heterologous cells, suggesting that it is a direct osmosensor (Cameron et al., 2010). Three other PPKs (*ppk23, ppk25*, and *ppk29*) are expressed in GRNs on the legs that participate in the detection of male and female pheromones (Liu et al., 2012; Thistle et al., 2012). One member of the TRP family, dTRPA1, is expressed in bitter GRNs on the proboscis, where it is involved in the aversion to electrophiles such as allylisothiocyanate found in wasabi, and also it depolarizes in response to increased temperature (>30◦C) (Kang et al., 2012). Another essential TRP channel is the NompC, which is expressed in all mechanosensory neurons as it detects food texture (Sánchez-Alcañiz et al., 2017).

In summary, a huge range of receptors are expressed in GRNs and may define their chemosensory modality. However, some GRNs respond to different taste modalities because they co-express different types of receptors, limiting taste discrimination by the activity pattern of the GRN itself and elucidating a complex taste recognition strategy.

4. Gustatory processing in the *Drosophila melanogaster* central brain

Gustatory information is sensed by peripheral taste organs, specifically by their GRNs, which contact food and substrate directly. These GRNs extend their axons directly to the CNS, where this information is integrated and processed in combination with other internal cues to drive final behavioral outputs. Thus, to understand the organization of the CNS, it is crucial to study how and where this gustatory information is processed.

4.1. The central nervous system of *Drosophila melanogaster*

The CNS of *D. melanogaster* is composed of three main regions: the ventral nerve cord (VNC), which is analogous to the spinal cord in vertebrates; the central brain (CB), where the main processing features take place; and the optic lobes (OLs) which process visual information (**Figure 3**) (Nériec & Desplan, 2016).

The VNC contains around ~20,000 neurons, and it is divided into several segmental neuromeres (**Figure 3A**). It is the place that receives and integrates sensory information such as mechanosensation and is involved in generating most of the locomotor actions that underlie fly behaviors such as walking, grooming, jumping, flying, courtship, and copulation (Card & Dickinson, 2008; Crickmore & Vosshall, 2013; Dickinson & Muijres, 2016; Mamiya et al., 2018; Seeds et al., 2014). The VNC is, however, not a passive executive center receiving descending signals from the CB; it also sends significant major ascending projections to it (Tsubouchi et al., 2017).

As previously mentioned, the main processing center of information in *D. melanogaster* is the CB*,* which is analogous to the telencephalon in mammals and comprises around 100,000 neurons (Raji & Potter, 2021). The CB receives input from the VNC via the ascendant neurons that go through the neck area and connect to the CB. Besides, the CB sends processed information to other regions of the body via descending neurons that connect the CB with the VNC and then via the peripheral nerves to the final organ. The CB (**Figure 3B**) is compartmentalized into specialized regions that comprise most of the CNS functions like memory, learning, sensory integration, and behavioral coordination. The mushroom bodies (MB), which are located in the upper part of the CB and comprise an intricate network of kenyon cells (KCs), play a pivotal role in associative learning and memory formation (Aso & Rubin, 2016). Adjacent to the MB, the central complex comprises distinct substructures, including the fan-shaped body (FSB), ellipsoid body (EB), and noduli, which are involved in spatial orientation, motor control, navigational behaviors, circadian rhythms and sleep. Further, other regions of the central brain receive and process sensory inputs from various modalities, such as olfaction and gustation. The olfactory information is initially processed in the antennal lobes (ALs), which comprise a set of organized glomeruli of olfactory sensory neurons (OSNs) that express a huge arrange of ORs involved in the detection of volatile chemicals (Fishilevich & Vosshall, 2005). This olfactory sensory information is mainly sent to the MB via the projection neurons (PNs), where the information is integrated to produce specific behaviors and memory formation (Jeanne et al., 2018; Masse et al., 2009). Also, the lateral horns (LHs) participate in olfactory and learning processing and other functions like innate behavioral responses by encoding biological valence to novel stimuli (Schultzhaus et al., 2017). Gustation is mainly integrated into the subesophageal zone (SEZ), located below the esophagus opening and containing ~4,000 neurons (Amrein & Thorne, 2005; Scott, 2005). The SEZ is not a region compartmentalized like the AL, where information is segregated in glomeruli. However, a certain level of organization can be appreciated in how sensory information arrives at the SEZ and is related

to how SEZ neurons respond to stimuli, even though no anatomical structure is visible (Münch et al., 2022).

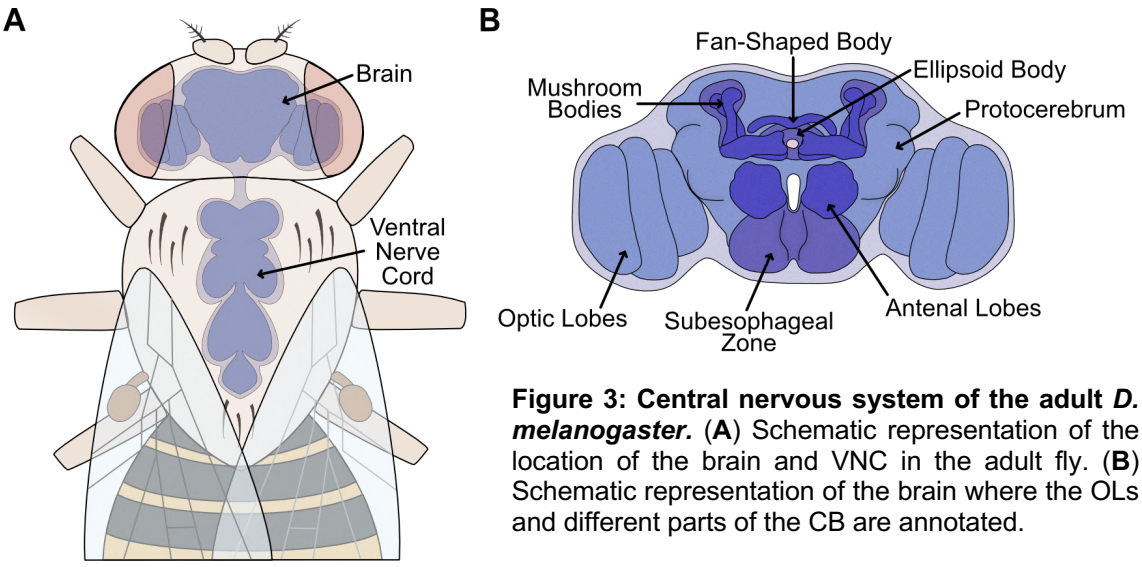

Figure 3: Central nervous system of the adult *D. melanogaster.* (**A**) Schematic representation of the location of the brain and VNC in the adult fly. (**B**) Schematic representation of the brain where the OLs and different parts of the CB are annotated.

In the next section, I will describe in detail what is currently known about the SEZ and how it integrates peripheral sensory information and the internal state of the fly to be jointly processed in order to elucidate complex feeding behaviors.

4.2. Taste pathways in the central nervous system impact final behavior

As mentioned previously, the main gustatory processing center in the CB of fruit flies where GRNs project their axons is the SEZ. GRNs located in the legs, wing margins, and ovipositor organ project to the VNC to be redirected to the SEZ by ascending neurons. GRNs located in the labellum send the gustatory information directly to the SEZ through the labial nerve, and the mouthpart neurons project along the pharyngeal and accessory pharyngeal nerve (Scott, 2018) (**Figure 4**). GRN axons derived from different taste organs are spatially segregated in the SEZ. Mouthpart neurons terminate in the dorsal anterior SEZ, proboscis axons terminate in the medial SEZ, and leg axons terminate in the dorsal posterior SEZ (Z. Wang et al., 2004). We are specifically focused on understanding how gustatory information detected by the proboscis, the main feeding organ, is integrated and processed in the SEZ to drive final feeding behavior.

All GRNs send their axons segregated to SEZ by taste modality. While bitter GRNs converge in the medial ring, the sweet GRNs and water-sensing GRNs remain ipsilateral and terminate as two bundles near the bitter GRNs axonal terminals (**Figure 4A**) (Thorne et al., 2004). This suggests that different taste modalities might activate separate pathways in the brain, with sugar-responsive circuits that drive taste

acceptance and bitter-responsive circuits that drive avoidance. Whole brain *in vivo* calcium imaging has reported only a few neurons in SEZ responding to both sweet and bitter tastants, reinforcing the hypothesis of a segregated circuitry beyond the GRNs (Harris et al., 2015). Similar results have been obtained in electrophysiological studies carried out in the moths *Manduca sexta* and *Heliothis virescens*, which found that there are few interneurons that receive gustatory information from different GRNs and that they are interconnected, leading to elaborately structured patterns (Reiter et al., 2015).

Results in mammals point in the same direction as they have found that gustatory information is kept segregated not only in the geniculate ganglion neurons but in the gustatory cortex, only to be partially integrated into the amygdala (Barretto et al., 2015; Chen et al., 2011; Jin et al., 2021; Sugita & Shiba, 2005). The results from both models support the label line hypothesis, where taste modalities are integrated through different pathways in the CB, contrary to the across-neuron hypothesis, where different taste modalities converge into common neuronal circuits to drive final feeding behaviors (Scott, 2018).

Contrary to the olfactory system, where a system of glomeruli in the ALs shows the rationale of olfactory processing (Jeanne et al., 2018), no anatomical structure is appreciated in the SEZ. So far, as mentioned earlier, we are only certain that information seems to arrive and may be processed separately (**Figure 4B**). Which interneurons in the SEZ process gustatory information? Which interneurons control the initiation of termination of feeding? And how do those neurons integrate sensory information with the internal state? Our current knowledge about the interneurons in SEZ is poor, and only some neurons have been identified to play some roles in the questions mentioned earlier. Our lack of knowledge regarding their molecular nature has impeded studying them in detail and developing genetic tools to manipulate them. Most of the work done to identify the role of some of the SEZ interneurons has been based on electrophysiological studies, *in vivo* calcium imaging (mentioned earlier), and the screening of large collections of Gal4 lines. The latter approach has identified a handful of key neurons but at the expense of complicated and arduous experiments. In the next paragraphs, I will briefly describe what is known about the identified interneurons populating the SEZ and their possible roles.

Chu et al. found that some GABA (Gamma-aminobutyric acid) neurons in the SEZ receive direct input from bitter GRNs to inhibit presynaptically sweet GRNs, acting as regulators of contradictory information (Chu et al., 2014). These GABAergic processing mechanisms are well studied in the olfactory system, where GABAergic

neurons widely give feedback to olfactory inputs regulating olfactory information (Olsen & Wilson, 2008). In another work, after a massive visual screening of more than 8000 images, a set of three taste projection neurons (TPNs) were identified to collect separately sweet and bitter taste information from other taste organs like legs, so their activations or inhibition implies the extension or not of the proboscis (Kim et al., 2017). Within the SEZ, one neuron involved in this process is the motor neuron 9 (MN9), which contracts the rostrum protractor muscle to extend the proboscis and is required for feeding initiation (McKellar et al., 2020; Schwarz et al., 2017). Other neurons like the second-order sweet gustatory projection neurons (sGPNs) are implicated in processing sweet taste detection from the proboscis and drive the final proboscis extension, suggesting that they may be connected with the neuronal motor program (Kain & Dahanukar, 2015). Further, by screening a large number of driver lines, *Flood et al.* described a single neuron in the SEZ named the Feeding neuron (Fdg) that, despite it is not directly connected to GRNs, is sufficient to drive the proboscis extension upon sucrose stimulation (Flood et al., 2013). Also, *Bohra et al.*, by using a similar functional screening approach of driver lines with the proboscis extension response (PER) assay, described a single pair of interneurons implicated in the proboscis extension inhibition in response to bitter tastants (Bohra et al., 2018). All those data are invaluable, but they only provide information about some scattered neurons within the SEZ, without explaining how the information flows and gets integrated.

Similar to OSNs, GRNs contact a first layer of neurons in the SEZ termed gustatory second-order neurons (GSON), which act as a first relay of gustatory information (**Figure 4B**). We do not know how GSONs are organized, meaning we do not know whether they collect information from different tastes or are segregated as the GRN axons are. We neither know much about their molecular nature due to the complete absence of tools to label them specifically. A recently published transsynaptic tool, *trans*-Tango (Talay et al., 2017), can label any postsynaptic neuron to any neuron of interest. It has been described that at least sugar-sensing GRNs expressing *Gr64f* make synapsis with a significant number of GSONs. Although this tool is a great advancement in the field, it cannot label GSONs permanently, and initially, only immunohistochemical analysis can be done.

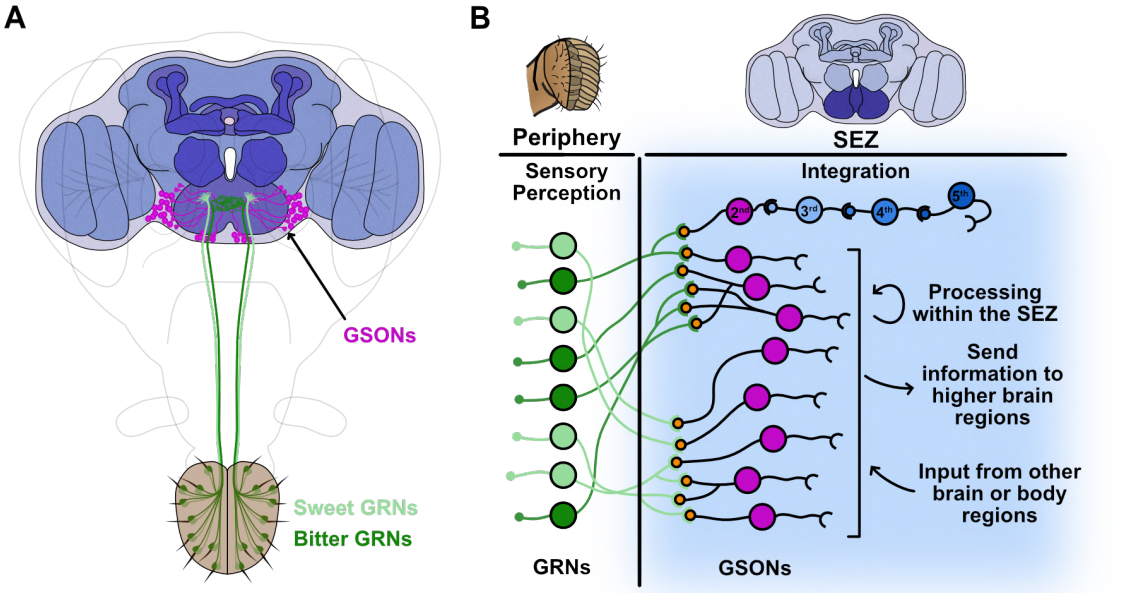

Figure 4: Schematic representation of gustatory information integration in the SEZ. (**A**) Taste stimuli are sensed through GRNs located in the taste organs (**Figure 2**), and the taste information sensed by the GRNs located in the labellum is directly sent to the SEZ where taste information segregates according to taste modality (sweet in light green and bitter in dark green) and synapses with GSONs. (**B**) Once gustatory information arrives into the SEZ from the periphery; it is integrated firstly by GSONs, which drive the gustatory information within the SEZ, send the gustatory information to other brain regions to be processed, or receive input from other brain and body regions to process both information, gustatory and other type.

I consider that to understand the rationale of gustatory information processing and integration, we need to characterize the GSONs as they are the first layer of neurons collecting this information. Understanding their molecular nature, whether they receive information segregated like the geniculate ganglion in mammals, or if some of them already integrate information for different tastants, is of paramount importance to describe gustatory processing in the *D. melanogaster* brain. Thus, in this Thesis, we performed RNA sequencing (RNAseq) from three different GSON populations, collecting different taste modalities: sweet, bitter, and mechanosensory information, to characterize molecularly those GSONs and understand how peripheral gustatory information is integrated first place within the CNS.

4.3. Regulation of feeding behavior in *Drosophila melanogaster* through the interplay of gustation, physiology and neuromodulation

External sensory inputs, along with internal physiological cues, convey the nutritional status of the body to the CNS in order to modulate the feeding behavior by orchestrating the activity of various neuronal circuits. The decision-making regarding food intake is managed through the intricate communication between chemicals present in the food (sensed by GRNs) and the internal metabolic signals. The metabolic state of

D. melanogaster is mainly regulated by the fat body (an endocrine organ that combines the adipose tissue and liver function in vertebrates) and corpora cardiaca, which sense changes in the physiological state and account for those to the brain for proper feeding behavior (Arrese & Soulages, 2010). A complex network of neuropeptide-expressing neurons, some of which are located in the SEZ, are involved in the evaluation of internal energy levels to control feeding. It is important to notice that it is not known if some of those neurons could be GSONs.

While certain neuropeptides promote food ingestion, another group counteracts these effects and hinders the feeding process. Hugin (Hug) is the homologous to the mammalian neuromedin U, and is released by the hug neurons, which arborize the SEZ and interconnect the GRNs with the pharyngeal muscles, possibly mediating the tolerance to aversive compounds via connection to bitter GRNs (Melcher & Pankratz, 2005; Schlegel et al., 2016; Thorne et al., 2004). Also, these hug neurons might be integrating the nutritional state of the fly as their axons arborize in the ring gland and the crop, two organs involved in growth and metabolisms, so finally, they are modulating food ingestion by integrating the taste of food source and the metabolic state of the fly resulting into behavioral outputs (Bader et al., 2007).

Similarly, the *Drosophila* neuropeptide F (dNPF), analogous to the human neuropeptide Y (NPY), is expressed by neurosecretory cells in the brain that integrate the starvation state of flies by detecting circulating glucose and it is also released in the midgut (Yoshinari et al., 2021). These dNPF-producing neurons act upstream of dopaminergic neurons to finally stimulate food intake by activating the sweet GRNs, also determining the formation of taste memory and subsequent appetitive behavior (Feng et al., 2021; Krashes et al., 2009). Likely, the short neuropeptide F (sNPF) promotes food intake and might serve as a communication crosstalk between the sNPF neurons and the insulin-producing cells (IPCs) (K.-S. Lee et al., 2004; Oh et al., 2019). These IPCs are located in the upper part of the protocerebrum and release *Drosophila* insulin-like peptides (DILPs), which are homologous from the mammalian insulin, as well as the drosulfakinin (DSK) which can be realized by other neurons in the brain, to drive satiation and attenuate feeding motivation finally (Hergarden et al., 2012; Shao et al., 2017; Y. Yu et al., 2016).

A study carried out by *Inagaki et al*. showed that over-expression of *dNPF* in the CNS enhanced sugar sensitivity, but not to bitter, as if flies were starved, while over-expression of *sNPF* led to a loss of bitter sensitivity during starvation via GABAergic neuron inhibition of bitter GRNs (Inagaki et al., 2014). These results highlight the

important role of dNPF and sNPF in promoting feeding and tolerating avoiding compounds in starved conditions. On the contrary, the neuropeptide allostatin A (AstA) neurons inhibit feeding by integrating the satiated state (Hergarden et al., 2012).

The adipokinetic hormone (AKH), analogous to the mammalian glucagon, is secreted from the corpora cardiaca by the AKH-producing cells (APCs) in starved conditions due to the low levels of circulating glucose (Hughson, 2021). Sweet GRNs express the AKH receptor (AKHR), so the AKH induce attractive feeding behavior (Bharucha et al., 2008; Kubrak et al., 2022; Lee et al., 2004; Yu et al., 2016). This AKH signaling pathway activates the interoceptive SEZ neuron (ISNs) upon starvation to induce sugar consumption. However, ISNs are inhibited by DILPs to control food satiety and electron microscopy studies reveled that these ISNs act upstream to IPCs, so ISNs represent a convergence node in the fly brain where hunger and thirst motivations compete for behavioral expression (González-Segarra et al., 2023; Jourjine et al., 2016).

Similarly, the neuropeptide corazonin (Crz), a homologue of AKH that is expressed in salivary gland and fat body, also promotes food consumption upon starvation (Lin et al., 2019). Further, AKH secretion also integrate the reproductive state of flies as it is by the dNPF/AstC signaling pathway when flies are fed, changing the preference of mated females from sugar-rich food into protein-rich food, necessary for egg production (Corrales-Carvajal et al., 2016; Malita et al., 2022). These suggest that the metabolic state of the fly, which is regulated mainly in the corpora cardiaca, midgut and fat body, is integrated in the brain in order to orchestrate food choice during feeding behavior.

Other neuropeptide involved in regulating feeding during starvation is the diuretic hormone 44 (Dh44), which is expressed by 6 neurons in the brain and regulate sugar and amino acids consumption, and activate downstream neurons to extend the proboscis upon starvation (Cannell et al., 2016; Schlegel et al., 2016). However, these Dh44-secreting neurons also express the hugin receptor, suggesting that Hug also play a role in modulating Dh44 releasing (Yang et al., 2018).

Also, neurotransmitters along with endocrine signals regulate the feeding behavior in response to the inner and outer nutritional state. For example, the enhance response of sweet GRNs upon starvation requires the presence of the dopamine/ecdysteroid receptor (DopEcR) which receive input from a single dopaminergic neuron, the TH-VUM neuron. This suggests that the TH-VUM neuron is activated during starvation via NPF signaling and drive the sweet GRNs excitability to promote the feeding initiation (Inagaki et al., 2012, 2014; Marella et al., 2012). Also,

downstream of AKH, octopamine and octopaminergic neurons have been shown to be both necessary and sufficient for starvation-induced food seeking (Yang et al., 2015).

On the other hand, despite of the decreased response of bitter GRNs upon starvation via the sNPF signaling pathway reported above, two pairs of SEZ-innervating octopamine/tiramynergic (OA)-ventrolateral (VL) neurons release octopamine and tyrame to directly potentiate bitter GRNs in fed flies to prevent feeding from avoiding compounds (LeDue et al., 2016). This bitter GRNs desensitization could be modulated by GABAergic neurons that integrate the AKH/sNPF signal (Inagaki et al., 2014).

In summary, a huge range of neuropeptides and neurotransmitters integrate gustatory and metabolic state information via different neuronal circuits to drive the appropriate feeding behaviors. These complex mechanisms highlight the importance of studying the molecular and neural bases of gustatory processing to understand how hunger-driven behaviors arise. Thus, in addition to the analysis of the molecular nature from three different GSON populations collecting different taste modalities by RNAseq, we performed this analysis by collecting those populations in two different metabolic states: fed and starved. Altogether, we were able to analyze the GSONs molecular profile changes upon starvation from totally different taste modalities, presumably to adapt gustatory processing to the physiological state of the fly and finally modulate feeding behavior.

OBJECTIVES

The main objective of my Thesis was to elucidate how peripheral gustatory sensory information is integrated and processed in the central nervous system to drive feeding behavior. To this end we focused in these specific objectives:

1. To label with *trans*-Tango the gustatory second-order neurons that receive input from sweet, bitter, and mechanosensory gustatory receptor neurons and isolate them by fluorescent-activated cell sorting.

2. To characterize molecularly the nature of those gustatory second-order neurons collecting taste information from different modalities in two metabolic states: fed and starved.

3. To find neuromodulators and neurotransmitters differentially expressed in the gustatory second-order neurons that may be involved in gustatory processing upon starvation.

4. To characterize the role of candidate neuropeptides and neuromodulators that could be involved in the integration of gustatory information and the metabolic state during feeding behavior

MATERIALS AND METHODS

1. ***Drosophila melanogaster*** **husbandry**

D. melanogaster strains were reared and maintained under a 12 h light:12 h dark cycle at 25ºC in standard Iberian fly food. A copy of each stock was stored at 18ºC. w^{1118} and *Oregon-R* fly lines were used as a mutant and wild-type strain controls unless otherwise indicated. All *D. melanogaster* strains used in this Thesis are listed in **Table 1**.

Table 1. *Drosophila melanogaster* strains.

***Drosophila* strains**	**Source**	**Identifier**
ChAT-Gal4	Bloomington *Drosophila* Stock Center	BDSC 84618
Ddc-Gal4	Bloomington *Drosophila* Stock Center	BDSC 7010
Dop1R2-Gal4	Bloomington *Drosophila* Stock Center	BDSC 84711
Dop2R-Gal4	Bloomington *Drosophila* Stock Center	BDSC 84628
GABA-B-R2-Gal4	Bloomington *Drosophila* Stock Center	BDSC 84634
GABA-B-R3-Gal4	Bloomington *Drosophila* Stock Center	BDSC 84635
Gad1-Gal4	Bloomington *Drosophila* Stock Center	BDSC 51630
Gr64f-Gal4	Kindly donated by Prof. Richard Benton	NA
Gr64f-LexA	Kindly donated by Prof. Richard Benton	NA
Gr66a-Gal4	Bloomington Drosophila Stock Center	BDSC 57670
Gr66a-LexA; LexAop-rCD2:GFP	Kindly donated by Prof. Richard Benton	NA
LexAop-mCD8::GFP	Bloomington *Drosophila* Stock Center	BDSC 32203
Lk-Gal4	Bloomington *Drosophila* Stock Center	BDSC 51993
NompC-GAl4	Bloomington *Drosophila* Stock Center	BDSC 36361
NompC-LexA	Bloomington Drosophila Stock Center	BDSC 52240
Oregon-R (wild type)	Kindly donated by Prof. Richard Benton	NA
QUAS-mtdTomato; retro-Tango; UAS-retro-Tango-GFP (*retro*-Tango)	Bloomington *Drosophila* Stock Center	BDSC 99661
SerT-LexA	Bloomington *Drosophila* Stock Center	BDSC 84434
Tdc2-Gal4	Bloomington *Drosophila* Stock Center	BDSC 9313
TH-Gal4	Kindly donated by Prof. Richard Benton	NA
Trh-Gal4	Bloomington *Drosophila* Stock Center	BDSC 38389
UAS-DenMarK	Bloomington *Drosophila* Stock Center	BDSC 33062
UAS-CD8::myrGFP	Bloomington *Drosophila* Stock Center	BDSC 32186
UAS-myrGFP, QUAS-mtdTomato; trans-Tango (*trans*-Tango)	Bloomington *Drosophila* Stock Center	BDSC 77124
UAS-TNT	Bloomington *Drosophila* Stock Center	BDSC 28837
UAS-TNTimp	Bloomington *Drosophila* Stock Center	BDSC 28839
VGlut-Gal4	Bloomington *Drosophila* Stock Center	BDSC 24635
UAS-CD4-spGFP1-10, lexAop-CD4-spGFP11 (GRASP)	Bloomington *Drosophila* Stock Center	BDSC 58755
LexAop-GFP, LexAop-QF; UAS-B3RT, QUAS-mtdTomato (BAcTrace)	Bloomington *Drosophila* Stock Center	BDSC 90826
w^{1118} (mutant control)	Kindly donated by Prof. Francisco Tejedor	NA

1.1. Starvation protocol

Starvation was induced by transferring flies into vials containing a solid medium formed with a piece of paper (Kimberly-Clark Kimtech, ref. 7552) soaked with 2,5 ml tap water. The number of starved flies in the same vial was controlled to avoid any effect induced by the population density. Additionally, the number of males and females, otherwise indicated, was controlled to be the same in the vial.

2. Immunohistochemistry and image analysis

2.1. Immunohistochemistry procedure

Brains and proboscis were dissected in cold phosphate buffer (PB) and fixed for 25 minutes in 4% paraformaldehyde (PFA) in PB at room temperature. After that, brains and proboscis were washed 5 times for 10 minutes (min) with PB + 0.3% Triton X-100 (PBT) and blocked for 1 hour in PBT + 5% normal goad serum (NGS) (Abcam, ref. ab7481). Later, primary and secondary antibodies (**Table 2** and **3**, respectively) were incubated for 48 h each in PBT + 5% NGS at 4ºC in constant agitation. Finally, after 5 washes of 10 min, brains and proboscis were equilibrated and mounted in Vectashield Antifade Mounting Medium with DAPI (4',6-diamidino-2-phenylindole) (Vector Laboratories, ref. H-1200-10), maintaining their 3D structure.

Table 2. Primary antibodies.

Antigen	Host Specie	Reference	Working dilution
Green Fluorescent Protein (GFP)	Chicken	Abcam (ab13970)	1:500
Red Fluorescent Protein (RFP)	Rabbit	Abcam (ab62341)	1:500
nc82 Bruchpilot	Mouse	DSHB	1:50
GFP reconstructed GRASP	Mouse	Sigma-Aldrich (G6539)	1:500
Leucokinin	Rat	Kindly donated by Prof. Pilar Herrero (de Haro et al., 2010)	1:100

Table 3. Secondary antibodies.

Antigen	Fluorophore	Reference	Working dilution
Chicken	Alexa 488	Abcam (ab150169)	1:500
Rabbit	Cy3	Jackson Immunoresearch (111-165-144)	1:500
Mouse	Cy5	Jackson Immunoresearch (115-175-146)	1:500
Mouse	Alexa 488	Jackson Immunoresearch (115-545-003)	1:500
Rat	Alexa 647	Jackson Immunoresearch (112-605-167)	1:500
Mouse	Cy3	Jackson Immunoresearch (112-165-166)	1:500
Rat	Cy3	Jackson Immunoresearch (112-165-167)	1:500

2.2 Microscopy image capture and processing

Images were acquired using a Leica SPEII laser scanning confocal microscope. Routinely, images of dimensions 512x512 pixels were acquired using an oil immersion 20x objective in stacks of 1-2 µm. Files were saved in *.tiff* format and processed with ImageJ (Fiji) open-source image-processing software (Schindelin et al., 2012). For fluorescence quantification, the fluorescent intensity from the Region Of Interest (ROI) area was analyzed by using the ROI Manager from ImageJ, and data is presented as mean ± standard error of the mean (SEM) and was statistically analyzed using two-tailed Student's *t*-test, considering *p*-value < 0,05 to be statistically significant.

3. Isolation of the neuron population of interest

3.1 Tissue dissociation into individual cells

CBs or SEZs were dissected in cold Calcium- and Magnesium-free 1X Dulbecco's phosphate buffered saline (DPBS) (ThermoFischer, ref. 14190094) and transferred to a protein LowBind (Eppendorf, ref. 0030108116) tube containing DPBS 0.01% bovine serum albumin (BSA) (Invitrogen, ref. AM2616). After centrifuge for 4 min at 3000 rpm, the supernatant was replaced by 500 µl of DPBS with an enzymatic digestion solution of papain and collagenase (Sigma-Aldrich, ref. P4762 and C2674, respectively) at 1 mg/ml. Then, the tissue digestion mix was incubated for 30 minutes at room temperature with continuous shaking at 400 rpm. After enzymatic digestion, to reinforce dissociation, with pre-wet low bind P1000 tips (Rainin, ref. 30389220) brains or SEZs were pipetted up and down 10 times every 2 min for three times, always keeping samples on ice. Finally, tissue dissociated solution was filtered through a 20 µm filter (pluriSelect, ref. SKU 43-10020-40) into 300 µl DPBS BSA 0.01% in a protein LowBind tube, ensuring that all liquid flowed through the filter, and samples were kept at -80ºC or even directly sorted by fluorescent-activated cell sorting (FACS).

3.2. Fluorescence-activated cell sorting

After the tissue was dissociated into single cells, they were sorted using the FACS Aria™ III. Different filters were applied. Firstly, plotting events in the side scatter area (SSC-A) and the forward scatter area (FSC-A) allowed the discard of any debris and dead cells, as well as clustered cells, from the population (P1) of interest. Then, SSC width versus height excluded cells by complexity, isolating a second single-cell population (P2). Next, FSC width versus height discard cells by size to separate a third single-cell population (P3). A filter for DAPI fluorescence was applied to discard all dead

cells. To do that, cells containing DAPI in their nuclei were previously sorted to delimitate the area where live cells fall into, so all single cells from P3 that fall there constituted a fourth live single-cell population (P4). Then, cells were sorted by their fluorescence with different fluorescent lasers.

To sort the GSONs labeled by *trans*-Tango from P4, the 561 nm laser was applied to the P4 in combination with an RFP PE-Texas Red A filter to discard non-fluorescent cells from the red fluorescent population (P5). In addition, to differentiate that autofluorescence (far red, λ > 670 nm) from actual mtdTomato *trans*-Tango signal from GSONs (λ = 615 nm), extra filtering was applied with a PE-Cy7-A filter consecutively to only conserve those mtdTomato fluorescent single cells for PE-Texas Red-A filter and not for PE-Cy7-A filter (P6). On the other hand, to sort the Lk GFP^+ neurons from P4, the 488 nm laser was used to sort only GFP^+ fluorescent cells (P5) by applying the FITC-A filter.

All fluorescent cell populations were sorted into protein LowBind RNase-free tubes containing 15 µl of lysis buffer for RNA extraction (extraction buffer from Thermo Fisher PicoArcturus Kit, ref 12204-01) and finally stored at -80ºC until RNA extraction.

4. RNA extraction, retrotranscription and quantitative PCR

4.1 RNA extraction

To isolate mRNA from FACS populations, due to the relatively low amount of cells sorted, RNA was extracted using the PicoArcturus RNA isolation kit (ThermoFisher, ref. 12204-01), whose extraction yield is so accurate. RNA extraction was performed according to manufacturer standards protocol. Prior to column RNA retention, samples with the corresponding number of isolated cells were lysed for 30 min at 42ºC while shaking at 500 rpm in the standard lysis buffer solution provided in the kit. Then, after mixing the lysate with ethanol 70%, a sequence of centrifugations was applied according to manufacturer instructions. An RNase-Free DNase (Qiagen, ref. 79254) treatment was applied to eliminate the remaining DNA. Final RNA was eluded in 15 µl of elution buffer and stored at -80ºC until use.

4.2. Total mRNA quantification and quality determination

The spectrophotometer NanoDrop® ND-1000 was used for samples estimated to contain higher amounts of total mRNA extracted, in the range of 100-3.000 ng/µl.

Additionally, to obtain the exact concentration and to test the quality of the mRNA, total mRNA was measured by using the 2100 Bioanalyzer (Agilent Technologies). 50 to 5.000 pg/µl range was measured using chips from the RNA 6.000 Pico Kit (Agilent Technologies).

4.3. Retrotranscription for qPCR: cDNA synthesis

Due to the low amount of mRNA extracted, total mRNA was retrotranscribed to cDNA with SuperScript III Reverse Transcriptase (Invitrogen, ref. 18080-044) and Oligo dT Primers (Invitrogen, ref. 18418020) incubated for 60 min at 50ºC, and a final step of 15 min at 70ºC. Then, a deoxynucleotide mix (Sigma-Aldrich, ref. D7295) and an RNaseOUT ribonuclease inhibitor (Invitrogen, ref. 10777-019) were added to the mix to elongate the cDNA and to to avoid external RNA digestion, respectively.

4.4. Quantitative PCR: qPCR

Standard real-time quantitative PCR (qPCR) was performed with 2 ng of template cDNA, PowerUp SYBR Green PCR Master Mix (Applied Biosystems, ref. A25742) and gene-specific primers (**Table 4**) read on QuantStudio 3 Real-Time PCR System (Applied Biosystems, ref. A28567) with a standard cycling mode: 2 min at 50ºC and another 2 minutes at 95ºC followed by 40x cycles of 15 seconds at 95ºC and 1 min at 60ºC. *Gapdh2* (Glyceraldehyde 3 phosphate dehydrogenase 2) of *D. melanogaster* protein expression levels, was used as a housekeeping gene to normalize the results. Triplicate samples per each condition, as well as technical triplicates, were performed, and the relative gene expression was normalized by ΔCt analysis. Data is presented as mean ± SEM, and was statistically analyzed using two-tailed Student's *t*-test, considering *p*-value < 0,05 to be statistically significant.

Table 4. Primers pairs for qPCR.

Gene	Forward sequence (5' to 3')	Reverse sequence (5' to 3')	Source
LK	GCCTTTGGCCGTCAAGTCTA	TGAACCTGCGGTACTTGGAG	(Zandawala, Yurgel, et al., 2018)
Gapdh2	CTACCTGTTCAAGTTCGATTCGAC	AGTGGACTCCACGATGTATTC	(Uchizono et al., 2017)

5. Bulk RNA sequencing

After RNA extraction from FACS-sorted GSON populations, samples were sequenced at the Genomics Unit of the Centre for Genomic Regulation (CRG) of Barcelona, Spain. Three independent replicas per condition were sequenced for each

biological replica. As the total amount of RNA extracted of each sample was so low (0'58 ng to up to 1 ng), libraries were prepared by the GRC using an ultra-low RNA input protocol. This kit allowed the use of the total RNA to prepare the cDNA, and then a second amplification was performed to increase the cDNA concentration. Then, samples were sequenced using 50 bp single reads on an *Illumina HiSeq2500* (for fed condition) and *Illumina NextSEq2000* (for starved condition) sequencers.

5.1. Bulk RNA sequencing analysis

Reads were quality-checked with MultiQC v1.0 software using the tool FastQC v0.11.9. RNAseq output reads were aligned to the *D. melanogaster* reference genome from the Ensemble Project database (EMBL-EBI, Cambridge, UK) using STAR v2.7.9a (Spliced Transcripts Alignment to a Reference) (Dobin et al., 2013). Differential gene expression analysis was performed using DESeq2 v1.28.1 (Love et al., 2014) with the free *R* programming language (GNU project) software *RStudio* v4.2. Also, the reads within the gene were transformed by this tool to a total of counts per gene. Transcripts per million (TPM) were calculated using Salmon 1.10.2 (Roberts et al., 2011). A combination of packages (or libraries) from CRAN and Bioconductor v3.14 (Gentleman et al., 2004; Huber et al., 2015) open-source projects were used for data processing and plotting.

5.2. Gene Ontology analysis

The Gene Ontology (GO) analysis was performed using the open-source interface PANGEA (Pathway, Network and Gene-set Enrichment Analysis; https://www.flyrnai.org/tools/pangea/) (Hu et al., 2023), specifically the *Drosophila* GO subsets terms at the online platform. Only those genes significantly up-regulated or significantly down-regulated in the differential gene expression analysis were included in the GO analysis. Each of the GSONs differential expressed genes were analyzed separately, and then, only those GO terms of interest were plotted in one single graph.

Additionally, other GO analysis interfaces and tools such as g::Profiler (https://biit.cs.ut.ee/gprofiler/gost), AmiGO2 (https://amigo.geneontology.org/amigo) (Ashburner et al., 2000; The Gene Ontology Consortium, 2017) were used to validate the results of PANGEA. Finally, gene set enrichment analysis (GSEA) was represented using *R*Studio v4.2 software.

6. Electron microscopy neural reconstructions and connectivity

Candidate neurons were reconstructed in a serial section transmission electron volume (Zheng et al., 2018) using Flywire (https://flywire.ai/) (Dorkenwald et al., 2022; Schlegel et al., 2023). To do that, from the open-source interface of Virtual Fly Brain (VFB) (Milyaev et al., 2012), several sweet and bitter GRNs skeletons (*.swc* format) described previously were downloaded (Engert et al., 2022). All skeletons were aligned to Flywire dataset (Dorkenwald et al., 2022) by using the Flywire Gateway tool, taking as a reference the JRC2018U reference brain (Bogovic et al., 2020). All Flywire IDs for the sweet and bitter GRNs analyzed were identified from this skeleton alignment.

To identify synaptic partners to the Flywire IDs identified, the open-source BrainCircuits interface (https://braincircuits.io/app?p=fruitfly_fafb_flywire_public) was used by uploading the Flywire IDs in the "Connectivity" tool space. Those IDs with synaptic points with sweet and bitter GRNs were selected as candidates. Then, according to previous morphological immunohistochemistry experiments, manual and visual criteria were applied to identify the neurons of interest. The Flywire Codex platform was used to find morphological similar neurons to those identified. On the other hand, for other applications, only upstream and downstream IDs with ≥10 synaptic sites were selected as presynaptic and postsynaptic candidates.

Final FAFB reconstructions were done using Flywire Sandbox and virtual reconstructed neuron images were taken by online screenshots.

7. Behavior experiments

7.1. Proboscis extension response

PER to labellar stimulation was assessed following a standard protocol (Shiraiwa & Carlson, 2007). Flies were anesthetized on ice and individually immobilized on P200 tips, whose narrow end was cut so that only the fly's head could protrude from the opening, leaving the rest of the body, including legs, constrained inside the tip. After flies were recovered in a humidified chamber for 20 min, flies were water-satiated before testing *ad libitum*, discarding those that, after 5 min, continued extending their proboscis in response to water. Tastants were delivered using a small piece of paper (Kimberly-Clark Kimtech, ref. 7552) and touching very gently the labellum for 2 s maximum, leaving a gap of 1 min between stimulations. To do the tastants stocks of 1 M sucrose (Sigma Aldrich, ref. 102174662) and 75 mM caffeine (Sigma-Aldrich, ref. 102143502) were diluted in miliQ sterile water in the appropriate proportions.

Up to ten flies were prepared simultaneously, and thetants were randomly distributed across trials. PER was manually recorded: only full proboscis extensions were counted as PER and registered as 1, considering partial or absent proboscis extension as 0. Finally, flies were tested at the end of the experiment with water as the negative control and 1 M of sucrose as the positive control. Only flies that showed negative PER for water and positive PER for 1 M of sucrose were included in the analysis.

7.2. FlyPAD

FlyPAD assays were performed to study the feeding microstructure in a two-choice feeding paradigm as described previously (Itskov et al., 2014), and several feeding parameters were measured individually in a high throughput manner. Individual flies were placed in individual arenas with two different food sources in independent well electrodes. The flyPAD hardware used was composed of 56 individual chambers divided into two independent pieces of hardware, each consisting of 28 chambers connected to an independent computer.

All tastants used were solved in water 1% low melt agarose (Lonza, ref. 50100) and stored in one-use aliquots at -20ºC until use. Before the experiment, tastants were hot in the heating block until 45ºC and delivered very carefully to each of the well electrodes with an automatic P200 pipette in small 7 µl drops inside each well. After 5 min, all tastants were a solid substrate.

To transfer flies to each chamber, flies were anesthetized in ice for 5 min and individually placed in the arena by mouth aspiration according its sex and genotype. All the experiments began once all flies woke up and were active. Flies were allowed to feed at 25ºC for 60 min. After time ended, dead flies were annotated, and all electrodes and chambers were carefully cleaned with 70% ethanol and distilled water to avoid cross-contamination between experiments.

FlyPAD data were acquired using the Bonsai framework, and analyzed in MATLAB using custom-written software delivered by *Itskov et al., 2014* (Itskov et al., 2014). Then, specific *R* software scripts developed by the lab were applied to analyze the bulk of flyPAD experiment data. Only those flies that permormed more than 2 bouts and 25 sips were included in the analysis.

8. Statistical analysis and illustration

The sample size was determined based on preliminary experiments. Data were analyzed using *R* software v4.1.0 (R Foundation for Statistical Computing, Vienna, Austria, 2005; https://www.r-project.org) (code available upon request) and plotted using *R* or *Graphpad Prisms 6*. For each of the plots, the statistical test is determined in the figure legend. When *p*-value correction for multiple comparisons was required, the Bonferroni method was used. Except for PER and flyPAD experiments, quantitative data are represented showing their distribution by superimposing a boxplot. For the boxplots the whiskers are calculated as follows: the upper whisker equals the third quartile plus 1.5× the interquartile range (IQR) and the lower whisker equals the first quartile minus 1.5× the IQR. Any data points above the superior or below the inferior whisker values are considered outliers. The outliers were included in the statistical comparisons as we performed non-parametric rank tests.

For PER experiments, data were analyzed using a logistic regression set to a binomial distribution model (function glm() in *R* software) and error bars represent the standard error of the proportion ($\sqrt{\mathrm{p}(1-\mathrm{p})/\mathrm{n}}$). For flyPAD experiments, a set of *R* software scrips developed by the lab was used to analyze the feeding microstructure behavior, which employs different statistical tests depending on the final goal of the analysis. The preference index is calculated as follows:

$$\text{Preference Index (PI)} = \frac{\mathrm{N_A} - \mathrm{N_B}}{\mathrm{N_{TOTAL}}}$$

The statistical test is determined in the figure legend for each plot. The Bonferroni method was used when *p-value* correction for multiple comparisons was required.

All the illustrations and drawings presented during the Thesis have been made with *Affinity Designer* v1.6 software.

RESULTS

1. Molecular characterization of gustatory second-order neurons

1.1. Labeling of gustatory second-order neurons by *trans*-Tango

GRNs are responsible for sensing gustatory information and sending it to the CNS to be processed (**Figure 4**). However, although great effort has been made to elucidate the molecular and cellular mechanisms involved in taste perception in the periphery (Cameron et al., 2010; Dweck et al., 2022; Dweck & Carlson, 2023; Montell, 2013; Shim et al., 2015), we still do not understand how such massive amount of gustatory information is integrated and modulated in the CNS to drive final feeding behavior.

During my Thesis, I was particularly interested in understanding how flies deal with the integration of sensory information. While sweet tastants elicit feeding (Brown et al., 2021; Marella et al., 2006; Tauber et al., 2017; Thorne et al., 2004), bitter compounds induce food rejection (Weiss et al., 2011) and mechanosensory information modulates how flies detect sweet compounds (Sánchez-Alcañiz et al., 2017). I consider that the selection of sweet, bitter and mechanosensory GRNs is an excellent strategy to understand how flies integrate gustatory information and deal with decision-making processes during feeding behavior, as we cover most of the GRNs located in the labellum and the information that produces opposite valence (sweet and bitter) and modulatory (mechanosentation).

By using the *Gr64f-Gal4*, *Gr66a-Gal4* and *NompC-Gal4* driver lines, we were able to label most of the sweet, bitter and mechanosensory GRNs ($Gr64f^{GRN}$, $Gr66a^{GRN}$ and $NompC^{GRN}$, respectively) (Dahanukar et al., 2007; Z. Wang et al., 2004; Weiss et al., 2011). We used *Gr64f-Gal4* and *Gr66a-Gal4* instead of *Gr5a-Gal4* (for sweet GRNs) and *Gr33-Gal4* or *Gr93a-Gal4* (for bitter GRNs) as these are more broadly expressed, including other types of gustatory neurons. Moreover, mutants for *Gr64f* and *Gr66a* genes have ablated their ability to sense sweet and bitter compounds (Moon et al., 2006). Besides, with the *NompC-Gal4* driver line we selected, we were able to label only the mechanosensory neurons located in the gustatory sensilla but not the mechanosensory neurons that project to the antenna mechanosensory center (Sánchez-Alcañiz et al., 2017; Shearin et al., 2013).

The GRNs expressing the aforementioned drivers project their axons to the SEZ, the main gustatory processing center of gustatory information in the CB (Gordon & Scott, 2009; Scott et al., 2001; Z. Wang et al., 2004). GRN axons that transduce sweet (**Figure 5A**), bitter (**Figure 5B**) and mechanosensory (**Figure 5C**) information segregate in the SEZ in a non-overlapping fashion. Apart from the proboscis, these drivers are also

expressed in different GRNs located in other parts of the body as the wings margins, legs or the ovipositor organ (**Figure 2**) (He et al., 2019; Ling et al., 2014), and project their axons to the VNC ganglions or the SEZ.

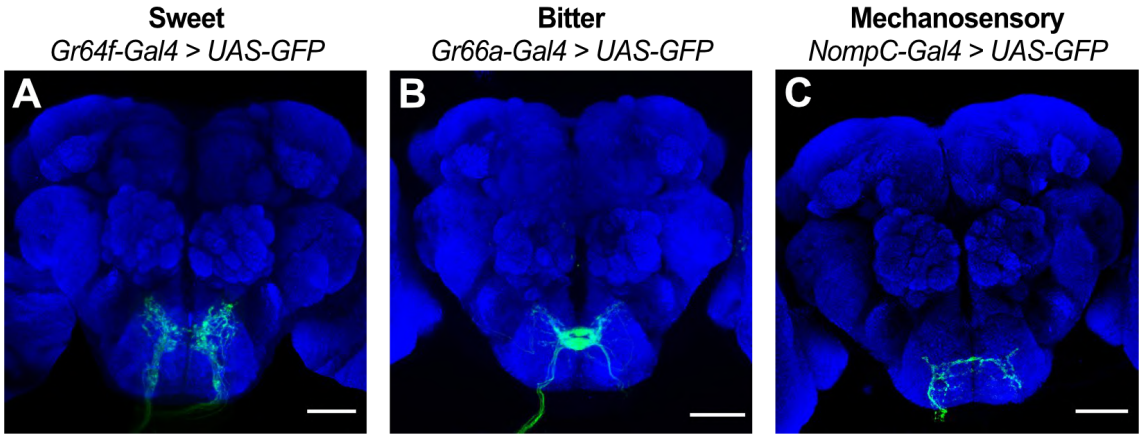

Figure 5: Gustatory receptor neuron axonal terminals in the central brain. Sweet (**A**), bitter (**B**) and mechanosensory (**C**) neuronal axonal projections into the SEZ labeled with anti-GFP (green) by expressing the *UAS-GD8::GFP* by the *Gr64f-Gal4* (**A**), *Gr66a-Gal4* (**B**) and *NompC-Gal4* (**C**) driver lines, respectively. Brain structure (blue) was labeled with anti-nc82. Scale bars: 50 µm.

Our main objective is to study how gustatory information is integrated in the CB. As most of the SEZ neurons are uncharacterized, no genetic tools can help us differentiate subpopulations receiving and integrating GRNs information due to their genetic heterogeneity. We focused on the neurons that receive direct sensory input from the GRNs located in the peripheral organs, the GSONs. Those neurons constitute the first layer of neurons collecting sensory information. As mentioned earlier, GSONs are not genetically accessible, so to start their characterization, we used a transsynaptic tool, *trans*-Tango (Talay et al., 2017), to label GSONs synaptically connected to each of the GRNs mentioned above, allowing us to label a large number of GSONs. This system is based on Tango, a cellular assay for recording the activation of specific receptors by their ligand (Barnea et al., 2008). Basically, it allows the expression panneurally of three components of the signaling pathway. The first one is a glucagon receptor, a GPCR, bound at its cytoplasmatic tail to the transcriptional activator QF via a linker containing the cleavage site for the highly specific N1a protease from the tobacco etch virus (TEV). The second component is a fusion between TEV and human β-arrestin2, a protein recruited to activate the GPCRs. The third component is the reporter mtdTomato under the transcriptional control of QUAS (*QUAS-mtdTomato*). Only in the neurons that are postsynaptic to those that express a membrane-tethered (by a Gal4 driver) form of glucagon at the presynaptic terminals will activate the pathway (Barnea et al., 2008) and express the mtdTomato reporter. Additionally, the Gal4 driver will activate the expression

of a *UAS-myrGFP* transgene. To summarize, the presynaptic neuron will be labeled with GFP and the postsynaptic with mtdTomato (Talay et al., 2017).

The initial work describing *trans*-Tango showed that the system requires time to accumulate the reporter mtdTomato in the postsynaptic neuron. Each driver line (*Gr64f-Gal4*, *Gr66a-Gal4*, and *NompC-Gal4*) was crossed with the *trans*-Tango transgenic line, and adults were raised for 21 days at 18ºC after pupation before dissection (Talay et al., 2017). The GSONs labeled were located surrounding the SEZ, with dendrites and axons projecting to the entire SEZ (**Figure 6**). It was possible to observe GSON arborizations innervating the upper part of the CB, near the LH. That region could be involved in water sensing when flies are starved, as shown with a modified version of *trans*-Tango flies that express the calcium sensor GCaMP6 in the postsynaptic neurons instead of mtdTomato (Snell et al., 2022). *trans*-Tango labels with good resolution the somas of the GSONs, allowing the quantification of the sweet ($Gr64f^{GSON}$) (**Figure 6B**), bitter ($Gr66a^{GSON}$) (**Figure 6D**) and mechanosensory ($NompC^{GSON}$) (**Figure 6F**) GSON populations. Between 60 and 100 GSONs could be quantified for each population, with the $Gr64f^{GSON}$ as the largest population.

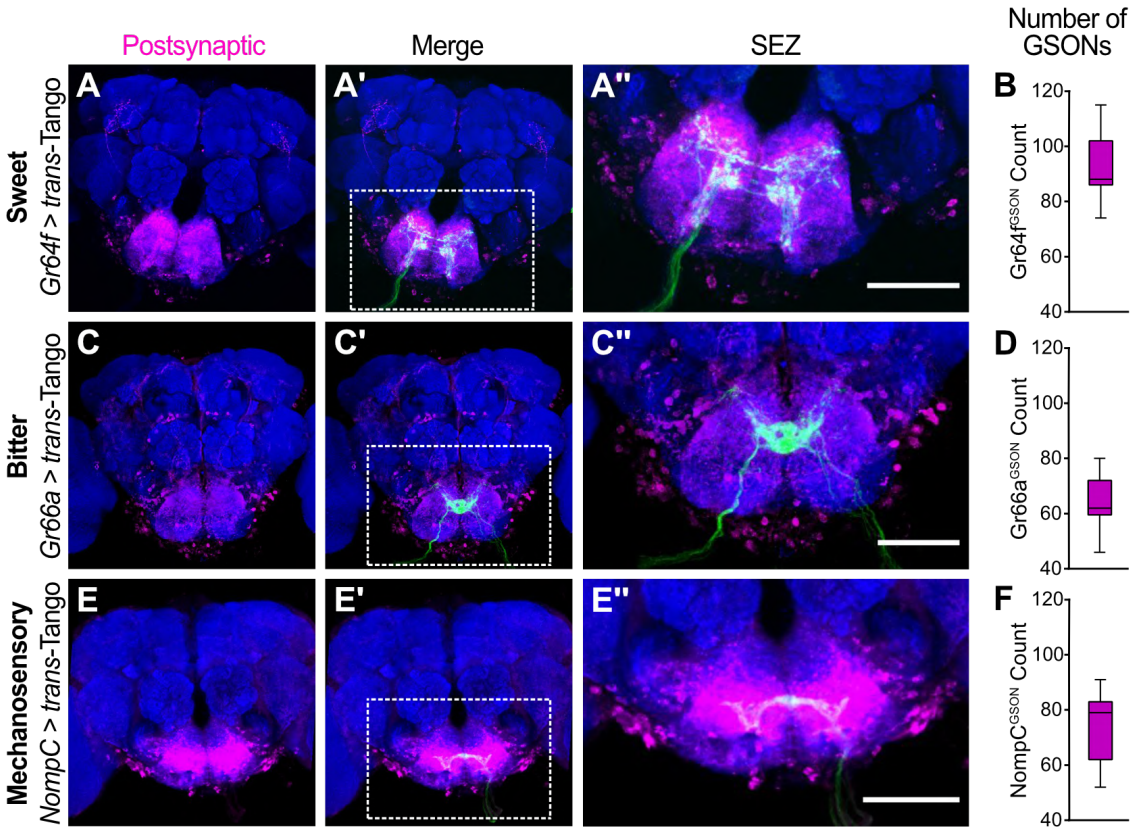

Figure 6: Gustatory second-order neurons labeled with *trans*-Tango. Expression of *trans*-Tango (labeled with anti-RFP (magenta)) driven by the sweet (**A**), bitter (**C**), and mechanosensory (**E**) Gal4 driver lines (labeled with anti-GFP (green)) in the CB (**A'**, **C'** and **E**, respectively). *Zoom in* was done to see the GSONs surrounding the SEZ (**A''**, **C''** and **E''**, respectively) and to count manually the number of sweet (**B**), bitter (**D**) and mechanosensory (**F**)

GSONs labeled with *trans*-Tango (n=9-11 brains/genotype). Brain structure (blue) was labeled with anti-nc82. Scale bars: 50 μm.

Recent studies have shown neurons of ectothermal animals like *D. melanogaster* connect synaptically to non-canonical partners if grown at 18ºC (Kiral et al., 2021). Accordingly, two different growth conditions were applied to the *trans*-Tango experiments: raising flies at 25ºC and 18ºC (**Figure 7A**). Besides, as many neurons connected to GRNs are involved in regulating feeding upon starvation (Shiu et al., 2022; Snell et al., 2022), a third extra condition was applied to check if there was any variation in the number of GSONs labeled by *trans*-Tango: 24h starvation. For all three GSON populations, the number of neurons labeled increased significantly when flies were grown at 18ºC (**Figures 7C-C''**). On the other hand, the number of GSONs labeled when flies were raised at 25ºC (**Figures 7B-B''**) was significantly lower. Further, the number of labeled GSONs in the starved condition (**Figures 7D-D''**) was lower than the standard condition in the $Gr66a^{GSON}$ but higher in the $Gr64f^{GSON}$ (**Figure 7E**). It is important to note that there was significant variability between replicates, indicating that *trans*-Tango varies among replicates. Finally, we decided to proceed with the rest of the experiments using flies grown until pupation at 25ºC and three more weeks as adults at 18ºC before dissection, as these were the conditions used in the original publication.

A recent study analyzing in detail the GRN projections to the SEZ has used the reconstructed FAFB dataset to show that GRNs receive synaptic inputs from many other GRNs (Engert et al., 2022). To test the possible cross synaptic connectivity among GRNs and check if *trans*-Tango could capture this connectivity, we decided to analyze if we could find any signal in the proboscis of the *Gr64f-Gal4* (**Figure 8A**)*, Gr66a-Gal4* (**Figure 8B**) and *NompC-Gal4* (**Figure 8C**) >*trans*-Tango flies. No *trans*-Tango signal was found in the labellum of any *GRN*>*trans*-Tango fly. These results indicate that if GRNs synapse onto other GRNs, *trans*-Tango could not capture this connectivity as we found no evidence of other GRNs labeled with mtdTomato.

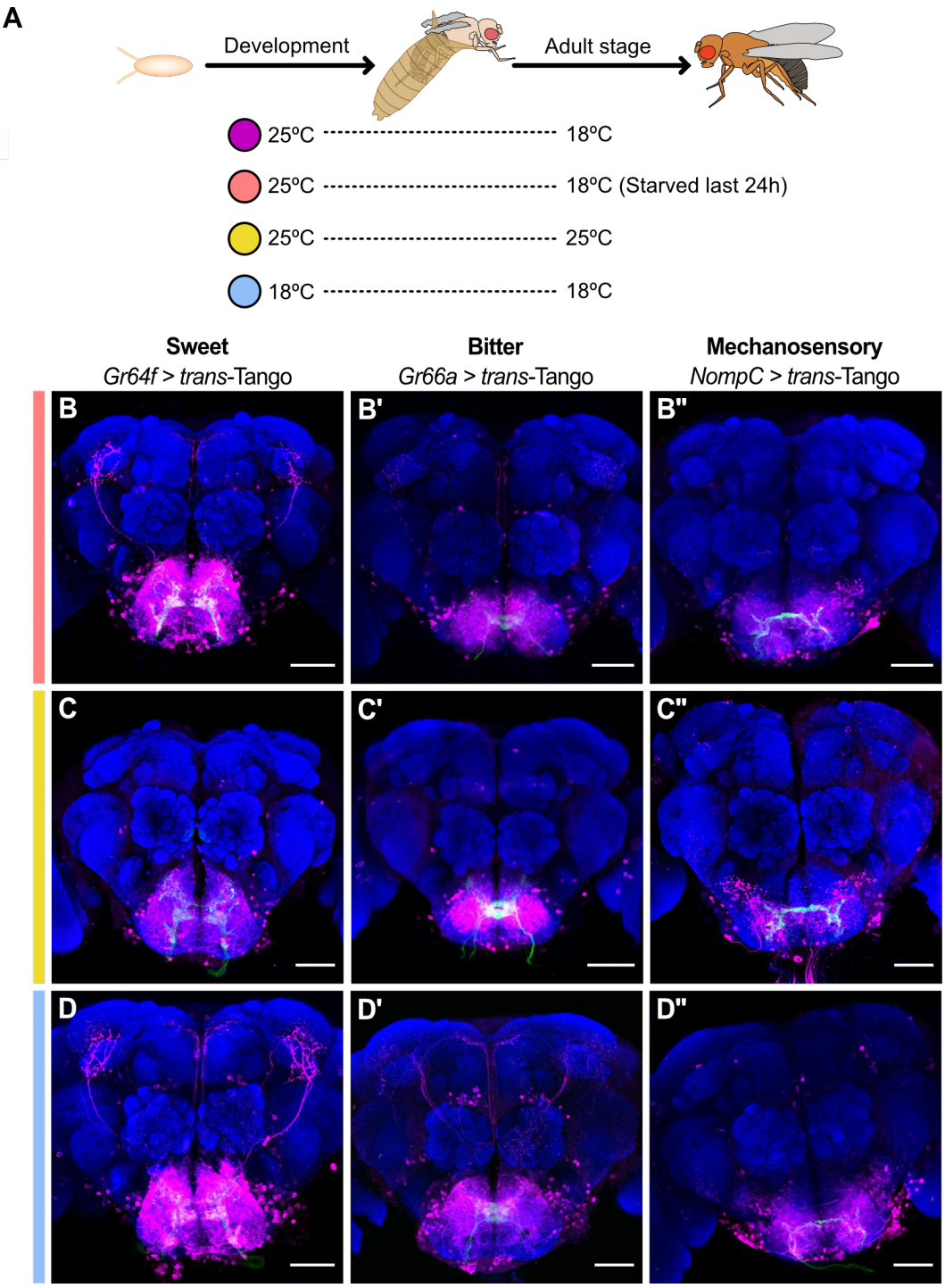
A
Development
Adult stage
25ºC ---------- 18ºC
25ºC ---------- 18ºC (Starved last 24h)
25ºC ---------- 25ºC
18ºC ---------- 18ºC
Sweet
Gr64f > trans-Tango
Bitter
Gr66a > trans-Tango
Mechanosensory
NompC > trans-Tango
B
B'
B"
C
C'
C"
D
D'
D"
E
GSONs Count
200
150
100
50
0
*
****
ns
**
**
**
ns
****
*
Gr64f GSON
Gr66a GSON
NompC GSON

Figure 7: Gustatory second-order neurons labeled with *trans*-Tango using different raising protocols. (**A**) Schematic representation of the protocol was used to raise transgenic flies before dissection at 18-21 days post-eclosion. (**B-D**) Anatomy of the presynaptic GRNs labeled with anti-GFP (green) connected synaptically with its postsynaptic GSONs labeled with anti-RFP (magenta) by *trans*-Tango technique in the 3 different growth protocols. Brain structure (blue) was labeled with anti-nc82. (**C**) GSONs count for all the conditions (n=8-11 brains/genotype/condition). Statistical analysis: *t*-test against standard protocol (magenta). ns: non-significant, **p<0.05, **p<0,01, ****p<0,001*. Scale bars: 50 µm.

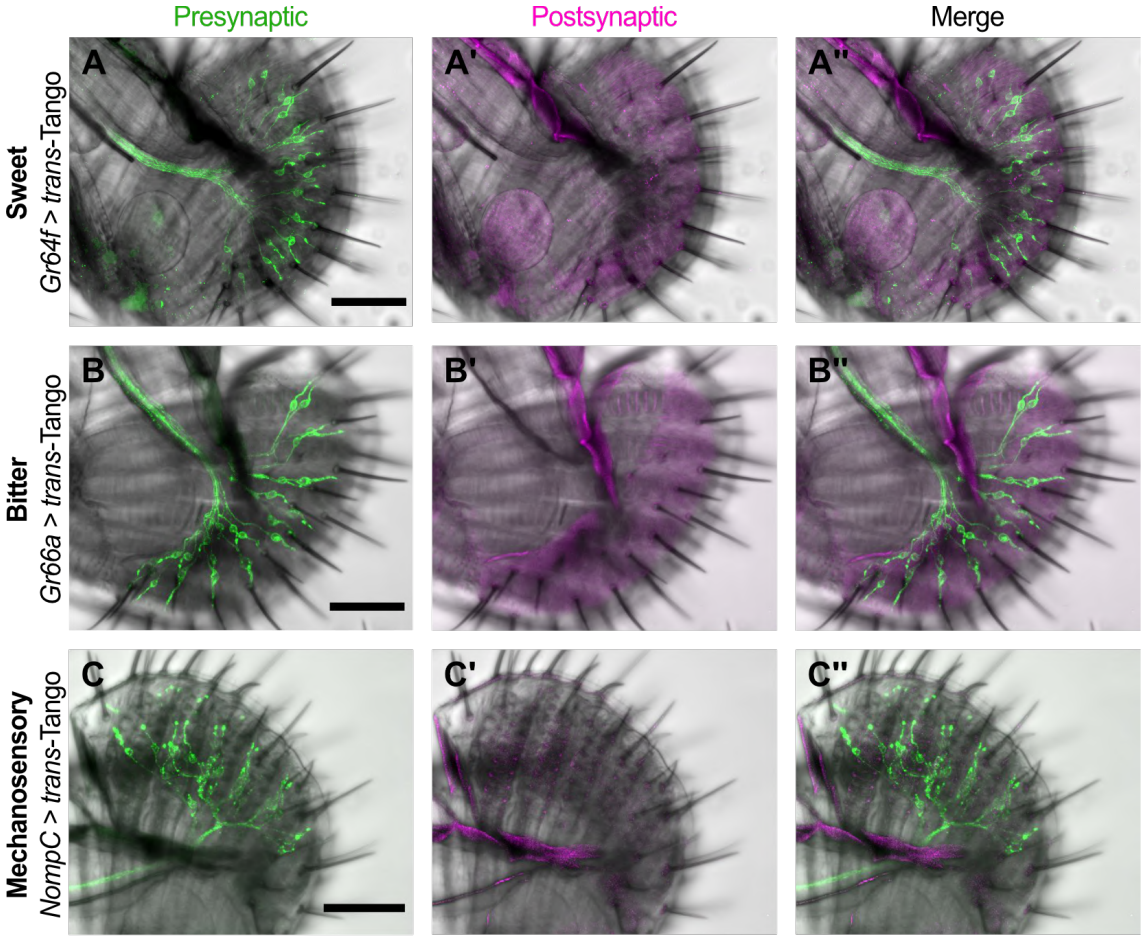

Figure 8: Gustatory second-order neurons labeled with *trans*-Tango in the proboscis. Anatomy and distributions of the sweet (**A**), bitter (**B**) and mechanosensory (**C**) GRNs located in the sensilla of the labellum labeled with anti-GFP (green). mtdTomato (labeled with anti-RFP (magenta)) from *trans*-Tango transgene was expressed by using the Gal4 driver transgenic lines to see the possible presence of sweet (**A'**), bitter (**B'**) and mechanosensory (**C'**) GSONs in the labellum. **A''**, **B''** and **C''** show merge images. Scale bars: 50 µm.

1.2. Fluorescent cell sorting of gustatory second-order neurons for transcriptomic analysis

Our main objective was to analyze the molecular nature of each GSON population (Gr64f^{GSON}, Gr66a^{GSON}, and NompC^{GSON}) labeled with *trans*-Tango by performing a transcriptomic analysis. Furthermore, we want to analyze how those neurons modulate their transcriptomic profile when integrating the metabolic state of flies. To do that, we took advantage of the *trans*-Tango mtdTomato fluorescence and

isolated each GSON population by FACS in two different metabolic states: fed and starved 24h. As mentioned in the materials and methods section, this technique consisted of the enzymatic and mechanical dissociation of tissue into single cells, followed by a computational fluorescent cell sorting to isolate the cells of interest (Harzer et al., 2013). Thus, the first step was to decide which part of the CNS to collect, as there were many GSONs dispersed in the CB (**Figure 6**) and the VNC, as previously reported (Talay et al., 2017). Moreover, we decided only to sort the SEZ, discarding any extra tissue from the CB or OLs and the VNC (**Figure 9**). Tissues were incubated with an enzymatic mix (Papain and Collagenase I) and mechanically disaggregated by continuous agitation. To avoid any saturation from the enzymatic mix and ensure the maximum number of single cells disaggregated from the tissue, we included a maximum of 40 SEZs per disaggregation.

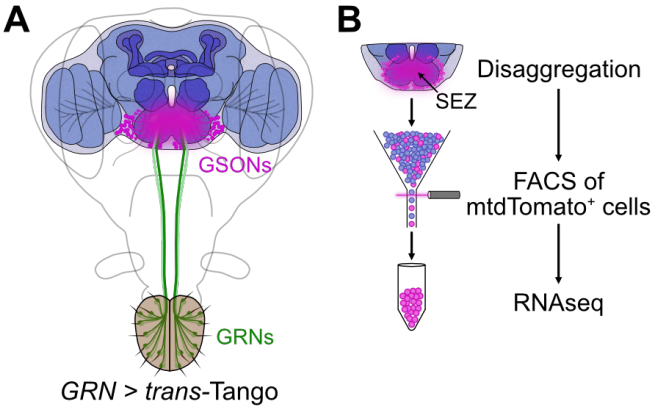

Figure 9: Schematic representation of the protocol used to FACS gustatory second-order neuron populations. (**A**) The scheme of *trans*-Tango shows the presynaptic GRNs from the labellum connected to the GSONs in the SEZ. (**B**) Diagram of the FACS methodology followed to collect GSONs surrounding the SEZ for the RNAseq experiments.

To correctly FACS only the mtdTomato^{+} cells and not other events, we performed a series of pilot experiments to set different parameters and standardize a stringent FACS protocol that ensured the proper sorting of GSONs (**Figure 10A**). As a quality control of the procedure, part of the collected cells were checked in the fluorescence microscope to ensure that single GSONs were properly FACS sorted. Once debris by size (**Figure 10B**), dead cells by DAPI approach (**Figure 10C**) or clusters (**Figures 10D-E**), and dying cells were removed by morphology and complexity, the living single cells were ready to be separated by fluorescence (**Figure 10F**). Any autofluorescence signal overlapping was discarded by far red filtering (**Figure 10G**). Simultaneously, the number of brains dissected was adjusted to optimize time, disaggregation, and FACS technique.

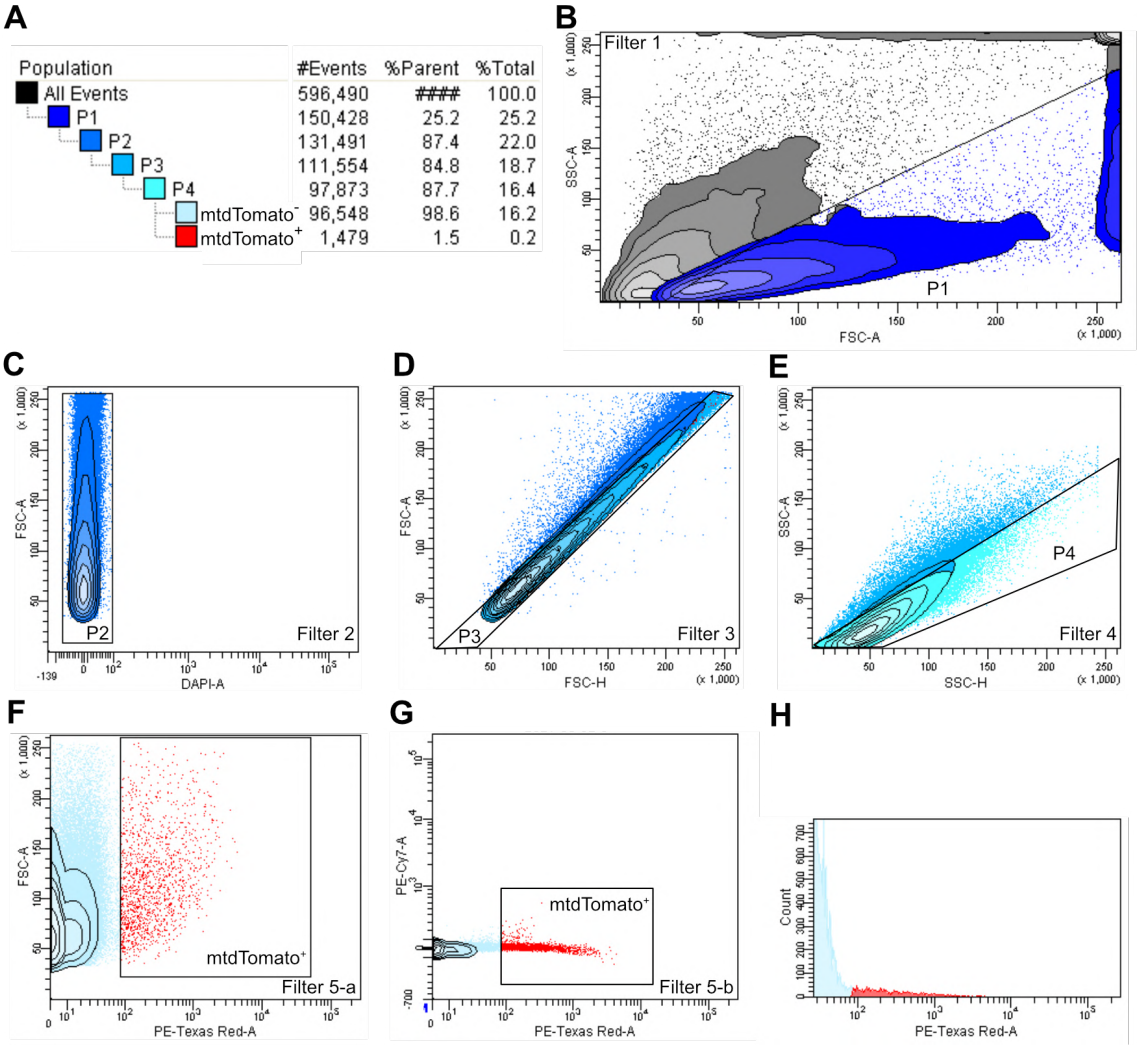

Figure 10: FACS sorting of sweet, bitter and mechanosensory gustatory second-order neurons. Fluorescent cell sorting for which the sweet (*Gr64f-Gal4*), bitter (*Gr66a-Gal4*) and mechanosensory (*NompC-Gal4*) promoters are driving fluorescent expression of mtdTomato by *trans*-Tango technique. Gating of SEZ disaggregated cells (**A**) from debris (**B**), dead cells using a DAPI labeling approach (**C**) and clustering single cells by morphology (**D**) and complexity (**E**) to finally separate the GSON populations according to its red fluorescence (**F**) and discarding the autofluorescense cells (**G-H**).

After all parameters were optimized, samples of 40 SEZs were dissected, disaggregated and FACS sorted into LowBind tubes (see materials and methods). The final percentage of mtdTomato$^+$ fluorescent cells (0,3-0,5%) revealed that at least 60-80 cells were isolated from each *trans*-Tango SEZ (**Figure 10A**).

To maximize the efficiency of the FACS and the posterior RNA extraction, we collected several FACS from the same GSON into the same LowBind tube. In this way, we ensured that the minimum quantity of cells was lost by pipetting during the RNA extraction protocol. This was possible by sorting the same day enough samples from a particular GSON population. Finally, each GSON replicate comprised 21000-27000 GSONs (**Figures S1A** for fed and **S2A** for starved). After finishing FACS sorting and

obtaining all replicates from the three GSON populations, the next step was to extract the cells' mRNA with extraction kits as indicated in the materials and methods section.

Interestingly, unlike in other eukaryotes, the integrity of *D. melanogaster* RNA cannot be evaluated using the conventional ratio for integrity. When fly RNA is run on electrophoresis gels, the ribosomal RNA 28S band splits into two bands of similar molecular weight (around 2000 nt), which migrate similarly to the 18S RNA, resulting in the appearance of one unique band (**Figures S1B** and **S2B**). Thus, the common ratio for integrity, RIN (28S:18S), is unsuitable for giving the integrity value even though the fragment is intact. For this reason and also due to the low amount of RNA obtained for each GSON population, the quality and quantity of RNA for all FACS replicates were validated with RNA chips of the Bioanalyzer systems before proceeding to the RNAseq. The RNA concentration for each replicate can be seen in **Figures S1C-E** for the fed condition and **Figures S2C-E** for the starved condition.

It is important to note that the FACS sorting of the fed and starved conditions was performed separately. While all RNA samples for fed conditions were being sequenced at the CRG of Barcelona, starved replicates for all GSON populations were done.

1.3. Gustatory second-order neurons transcriptome sequencing and bioinformatics analysis of gene expression

Transcriptome analysis requires high-quality samples. Our samples included two different metabolic conditions to know how each GSON population ($Gr64f^{GSON}$, $Gr66a^{GSON,}$ and $NompC^{GSON}$) integrate gustatory information in fed and starved states. Three biological replicates were analyzed for each condition, and only those samples with enough concentration (despite being very low) and quality were evaluated (**Figures S1** and **S2**). The RNAseq was performed at the CRG of Barcelona, and the bioinformatics analysis was carried out in our laboratory.

First, it is essential to note that the methodology followed to sequence the transcriptome was based on a total RNA ultra-low input. This means that all RNA extracted from each sample was used for sequencing, and a specific extra amplification of the cDNA was carried out before sequencing the transcriptome.

A detailed understanding of differential gene expression over time requires careful high-throughput data management. *R* software v4.1.0 was used as the principal informatics tool to face this part of the bioinformatics analysis. *R* is a free software environment for statistics and plotting from the GNU project. We run the user interface *R* Studio, which allows tracking scripts, managing *R* packages, and viewing datasets all

in one interface. The packages of functions were provided by the projects CRAN and Bioconductor (Gentleman et al., 2004; Huber et al., 2015). After converting reads into counts (Huber et al., 2015), the differential gene expression between samples was analyzed with DESeq2 (Love et al., 2014) based on the negative binomial distribution. Firstly, we normalized counts with the sequencing depth because long genes can have more counts but low expression, and thus, normalizing helps to stabilize the variance through the mean.

A sample-to-sample distance representation helps to visualize overall similarities between samples. We plotted each replicate with a principal component analysis (PCA). The PCA is a dimensionality reduction technique that simplifies complex datasets while preserving important information. It consists of finding the first and the second components (PC1 and PC2) that explain most differences between samples. Thus, the samples are projected into a bi-dimensional plane when those components are plotted on each graph axis. The PC1 explains 40% of the variance within our samples, and the PC2 the 25%. This suggested that both principal components refer to the GSON population and the metabolic state condition. The graph also shows that triplicates are nicely clustered while the different conditions are far apart (**Figure 11**). It allowed us to conclude that the three GSON populations (Gr64f^{GSON}, Gr66a^{GSON} and NompC^{GSON}) are molecularly different (PC1) and also that metabolic state (fed and starved) (PC2) dictates gene expression in each GSON population. In summary, we could differentiate each replicate according to their GSON population and metabolic state. These results suggested that the neurons that collect sensory information from the periphery within the CB (GSONs) were already differentiated by the metabolic state of the fly, meaning that the posterior processing of information is affected by the metabolic state.

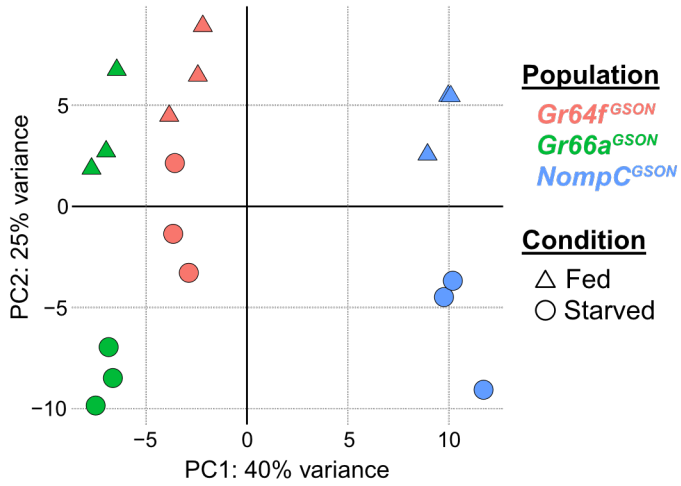

Figure 11: Principal component analysis. The PCA graph separates the samples into the two most dissimilar components. The x-axis represents the direction along which samples differ the most (PC1) while the y-axis is the second most (PC2): on both are notated the percentage of the

variance is. Color differentiates the GSON population and forms the metabolic state of the flies when GSONs are collected.

Once the RNAseq data was verified as reliable, different approaches could be realized to handle this step. The first method used was comparing the gene expression for each of the GSON populations between the metabolic states. This allowed us to plot how starvation was affecting the gene expression profile. To do this, we decided to represent in the same volcano plot the significant gene expression change (up-regulated or down-regulated to fed condition) in two different colors and simultaneously represent the TPM mean, which is related to the number of counts to that gene. Each axis in the graph represents the estimated *log2* fold change (x-axis) and the *p*-value. However, a multiple testing correction was needed to overcome the false positive that results from calculating the *p*-value even when *p*-value<0,01. This correction is named the Benjamini-Hochberg adjustment and calculates an adjusted *p*-value (*p*-adjusted) for each gene, which takes into account the false discovery rate (FDR). Then, a probability of *p*-adjusted<0,1 was considered acceptable. Thus, the *p*-value represented in the y-axis is presented as $-\log_{10}(p\text{-value})$.

Figure 12 shows that we obtained several genes that were either up-regulated or down-regulated in fed conditions compared to starvation for each GSON comparison test. Among these genes, many of them were uncharacterized genes, which means that their role or importance had not been characterized. We identified 21 in $Gr64f^{GSON}$, 103 in $Gr66a^{GSON}$ and 79 in $NompC^{GSON}$ genes that were up-regulated in fed conditions. Otherwise, we identified 4 in $Gr64f^{GSON}$, 64 in $Gr66a^{GSON}$ and 45 in $NompC^{GSON}$ genes that were down-regulated in fed conditions. We assumed so be significant only genes with *p*-adjusted>$-\log_{10}(0,05)$ and a $\log_2$(fold change) larger or smaller than $\log_2$ or $-\log_2$ respectively. Some of those genes were common in all comparisons, but most were significantly changed in one of the GSON populations (**Figure 12D**). For example, *tweek* was up-regulated in the $Gr66a^{GSON}$ and $NompC^{GSON}$ comparisons, which is involved in the endocytosis of synaptic vesicles (Verstreken et al., 2009). Also, *Non1* was down-regulated in the $Gr66a^{GSON}$ and $NompC^{GSON}$ comparisons, which is involved in assembling the mitotic spindles (Moutinho-Pereira et al., 2013).

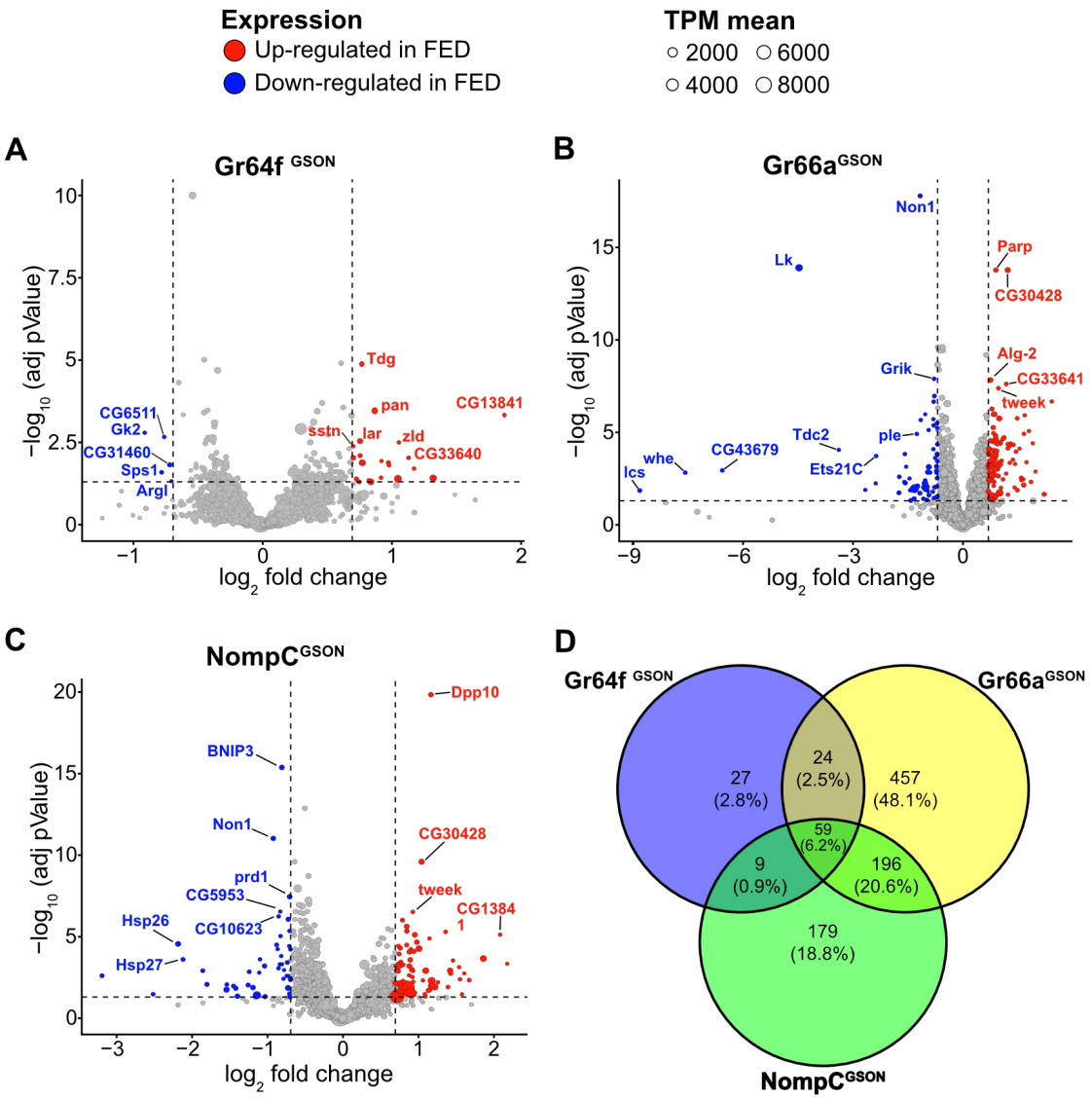

Figure 12: Differential gene expression analysis comparing fed versus starved conditions. Volcano plots of log_2 average fold change in the sweet (**A**), bitter (**B**) and mechanosensory (**C**) GSON populations for all genes. The y-axis represents the p-*adjusted* from the Bonferroni-Hochberg correction statistical test. Genes are represented according to TPM mean expression (size) and differential expression against fed condition (color). Only those genes much significantly changed were annotated.

Regarding the large number of genes that were up and down-regulated for each comparison, it was essential to perform a gene ontology analysis to interpret RNAseq data better, shedding light on the biological significance of gene expression changes. By categorizing genes into hierarchical ontologies based on biological processes (BP), molecular functions (MF), and cellular components (CC), the GSEA reveals the functional context underlying gene expression patterns. This allowed the identification of overrepresented functional categories within differentially expressed gene sets, providing valuable insights into the biological mechanisms to uncover key biological pathways, cellular processes, and molecular functions associated with the metabolic states of those GSON populations. We used PANGEA (Hu et al., 2023), a novel GO

software based on the characterization of GSEA in *D. melanogaster*. We only included those genes that significantly changed to reduce noise for this analysis. As the number of GO terms obtained in the comparisons was so large, we decided to manually select those GO terms that were more relevant in our analysis, focusing primarily on those that were related to neuronal circuits assembly and physiology and with processing and response to sensory stimuli (**Figure 13**). Otherwise, in more detail, all GO terms can be seen in **Figure S3**. All GSEA graphics illustrate the fold enrichment in a heatmap legend and the number of genes included for each GO term by size for all GSON populations and metabolic states analyzed. As we can see, we found several genes involved in DNA transcription and organization, as well as cell differentiation, indicating a significant number of transcriptional changes occurred in the nucleus as flies adapt to food-deprived conditions (**Figure 13**). Furthermore, several genes were involved in nervous system development and synapse organization, highlighting the possible importance of synapse remodeling during adaptation to starvation. Besides, there were some GO terms related to response to sensory stimuli and stress response, as starvation may induce molecular stress in flies. Finally, some genes related to signaling GO terms indicated that some neurotransmitter and neuropeptide signaling processes might be affected during starvation, carrying up specific adaptations in the neuronal circuits where the GSON could be involved.

Next, we decided to focus on the expression of neurotransmitters, neuropeptides, and their respective receptors as it has been shown they are involved in modulating feeding behavior, olfaction, or sleep, and act as integrators controlling many different behaviors (González Segarra et al., 2023; Jourjine et al., 2016). For example, glutamate inhibits olfaction (W. W. Liu & Wilson, 2013); starvation enhances behavioral sugar-sensitivity via increased dopamine release onto sweet GRNs, indirectly decreasing sensitivity to bitter tastants (Inagaki et al., 2012); or NPF modulates taste perception in starved flies by increasing sensitivity to sugar, and decreasing to bitter by promoting GABAergic inhibition onto bitter GRNs (Inagaki et al., 2014). Neuropeptides and neurotransmitters are exciting candidates to look for genes involved in integrating the metabolic state at the level of GSONs.

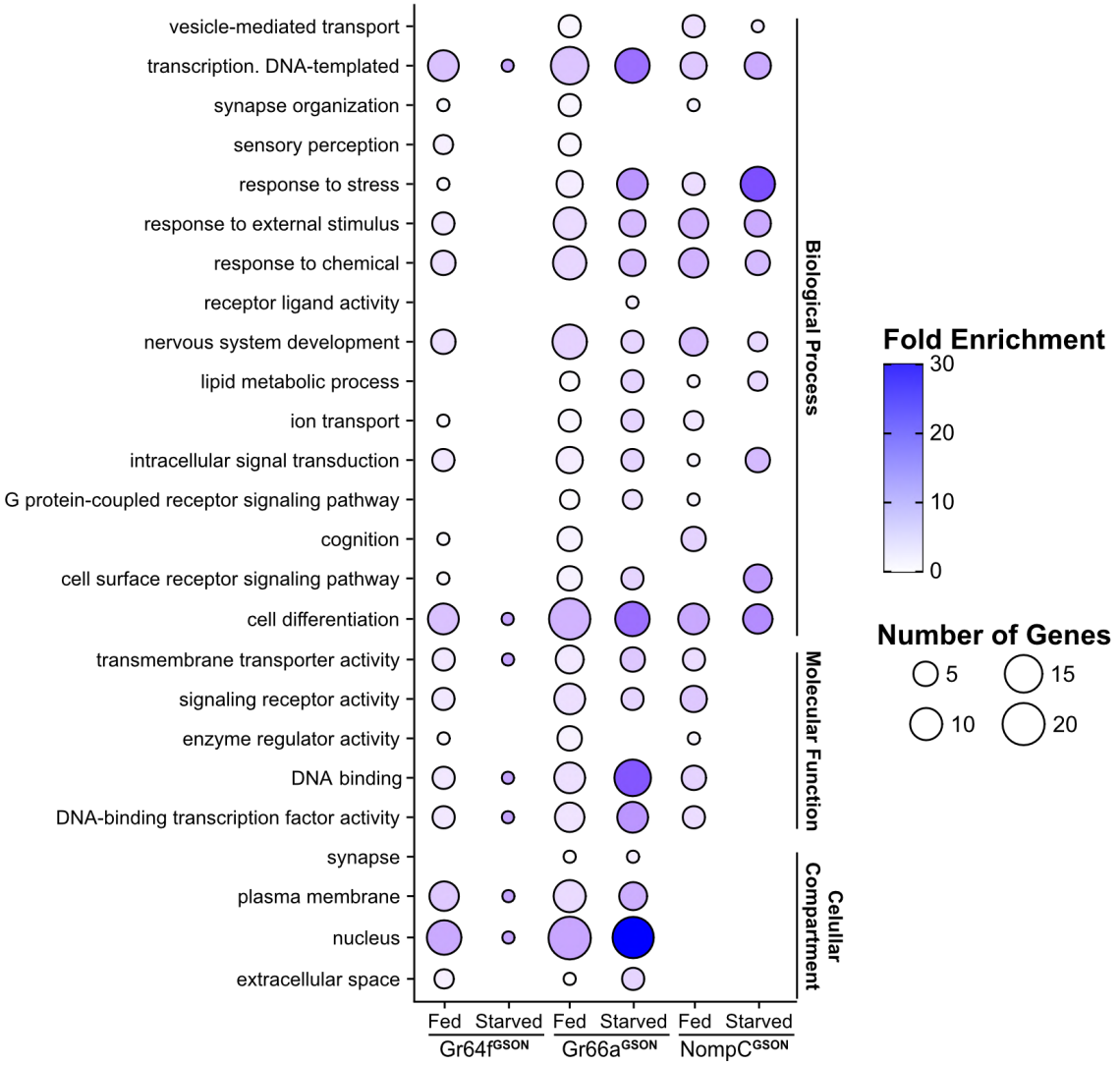

Figure 13: Gene set enrichment analysis. Graphical representation of the GO terms obtained from the GSEA, grouped by the GO category. The data represent the fold enrichment with a heatmap and the number of genes included in each GO term by size for all GSONs and metabolic states analyzed.

Our RNAseq data revealed that among all neurotransmitter receptors, we found that the most prominent receptor was *nAChRbeta1* (nicotinic Acetylcholine Receptor Beta 1) (**Figure 14A**). This is consistent with previously published results showing that GRNs are mostly cholinergic (Jaeger et al., 2018). Other acetylcholine receptors were expressed in GSONs, including receptors for other neurotransmitters, showing that although GSONs receive significant information from GRNs, a complex network of other neurons using different neurotransmitters send information to the GSONs. Regarding the expression levels of all neurotransmitter analyzed, *Gad1* (Glutamic acid decarboxylase 1) and *Ddc* (Dopa decarboxylase), two essential enzymes involved in the synthesis of GABA and dopamine, respectively, were highly expressed in all populations and both metabolic states (**Figure 14B**). Other enzymes involved in the GABA pathway, like *VGAT* (vesicular GABA transporter) or *GABAT* (γ-aminobutyric acid transaminase), were also

expressed, but at lower levels than *Gad1*. Similarly, other enzymes or transporters related to other neurotransmitters, like glutamate (Glu) or serotonin (5-HT), were present but at lower levels. The analysis of the neurotransmitter expression revealed that most GSONs were either GABAergic or dopaminergic and that the starvation level did not affect the expression of any of the neurotransmitters analyzed. Similar to the neurotransmitters, we found no variation in expression level in the neurotransmitter receptors.

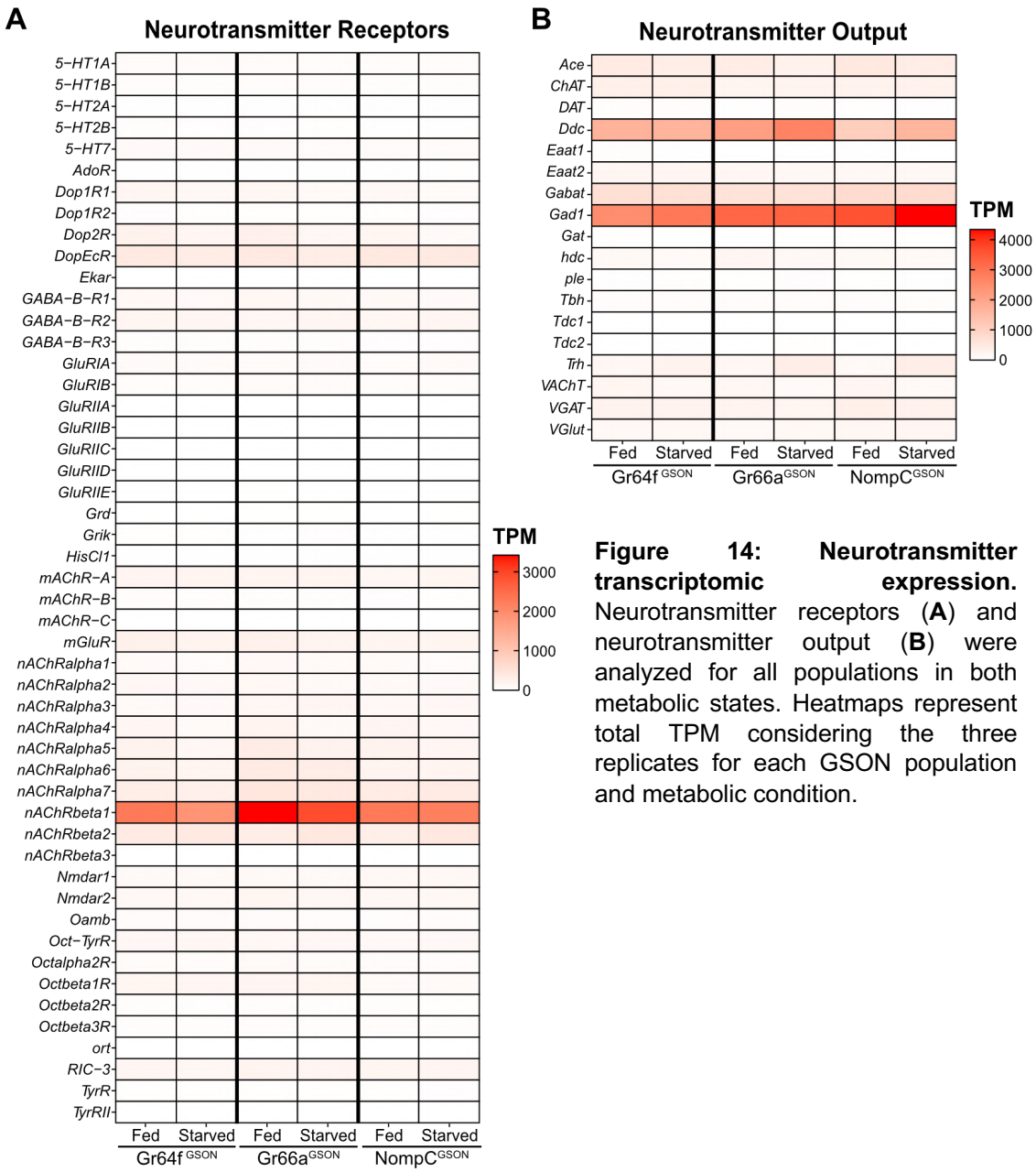

Figure 14: Neurotransmitter transcriptomic expression. Neurotransmitter receptors (**A**) and neurotransmitter output (**B**) were analyzed for all populations in both metabolic states. Heatmaps represent total TPM considering the three replicates for each GSON population and metabolic condition.

We later focused on the neuropeptide and its receptor expression (**Figure 15**). Regarding the neuropeptide receptors, we saw many receptors expressed in all GSON populations with fluctuating expression level dynamics (**Figure 15A**). For example, the *EcR* (Ecdyson Receptor) showed a decrease in expression in all three populations in the starved condition, pointing to a possible role in the adaption to food deprivation. Also, the *sNPF-R* was highly expressed with similar expression patterns as its ligand *sNPF*, raising the importance of sNPF and its signaling pathway in regulating starvation and feeding (K.-S. Lee et al., 2004; Q. Wu et al., 2003; Yoshinari et al., 2021). Regarding neuropeptides, many showed either low expression or no changes in expression level, with some showing high expression and particular expression patterns (**Figure 15B**). For example, the *sNPF* was highly expressed in all GSONs, particularly in the $Gr66a^{GSON}$ population, without change associated with the metabolic state. sNPF production is related to circulating sucrose levels impacting food intake by integrating sweet and bitter information in food-deprived flies (Inagaki et al., 2014). This evidences the role of sNPF and its receptor (sNPF-R) in regulating the feeding behavior according to metabolic state, as it is secreted in the midgut and by neurosecretory cells in the brain (K.-S. Lee et al., 2004; Yoshinari et al., 2021). Also, *Dh31* (diuretic hormone 31) and *Dh44* showed a notable expression in all GSON populations, as they are involved in desiccation tolerance and starvation adaptation (Cannell et al., 2016). *Nplp1*, involved in synaptic organization in the nervous system and water balance (Nässel & Zandawala, 2019), was also expressed in all GSONs but particularly increased in the starved state. The most striking neuropeptide was Leucokinin (Lk), showing an increased expression in the $Gr66a^{GSON}$ population in starved conditions, with nearly absent expression in the other GSONs neither in fed nor starved conditions. This particular expression pattern might indicate that Lk could participate in bitter information processing in starved conditions.

In summary, there was a considerable variety in the expression of neuropeptide receptors among all GSON populations and metabolic states, pointing to the importance of neuropeptides in the gustatory sensory perception in the GRNs and signaling.

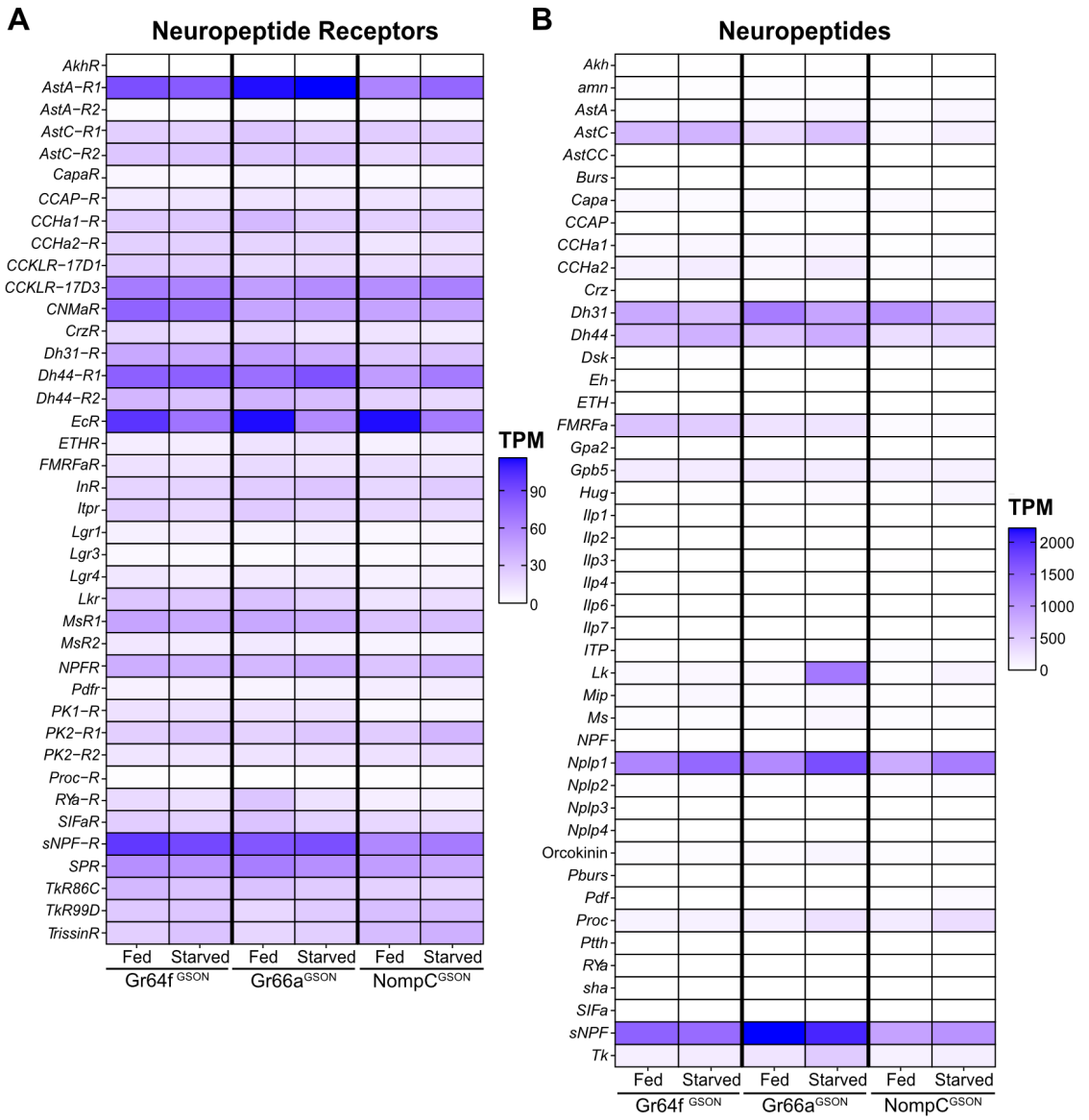

Figure 15: Neuropeptide transcriptomic expression. Several neuropeptide receptors (**A**) and neuropeptide output (**B**) were analyzed for all populations in both metabolic states. Heatmaps represent total TPM considering the three replicates for each GSON population and metabolic condition.

Altogether, these results illustrate the vast range of neurotransmitters and neuropeptides and their receptors expressed for each GSON population and how they are modulated by starvation. This raises the possibility of peptidergic neurons within the GSON that integrate the gustatory information by modulating its processing upon starvation.

2. Leucokinin is highly expressed in food-deprived conditions

Of all neuropeptides (**Figure 15B**), one showed a striking change in expression pattern. *Lk* showed an increase in expression in the Gr66a^{GSON} when flies were starved for 24h but not an increase in other GSON populations, indicating that the expression levels of *Lk* in some neurons from the bitter GSON population might reflect the starvation level of the fly. Lk is a neuropeptide that participates in the neuroendocrine system by modulating complex behavioral and physiological processes in several insects (Nässel & Wu, 2021). In *D. melanogaster,* three different groups of Lk neurons are located in the CNS (de Haro et al., 2010). These neurons also have their counterparts in the larval CNS. In the VNC, there are approximately 20 Lk neurons (ABLKs) (Zandawala, Marley, et al., 2018), while in the CB there are four Lk neurons (**Figure 16A**): two located in the LH (LHLK) (**Figure 16A'**) and another two located in the SEZ (SELK) (**Figure 16A''**).

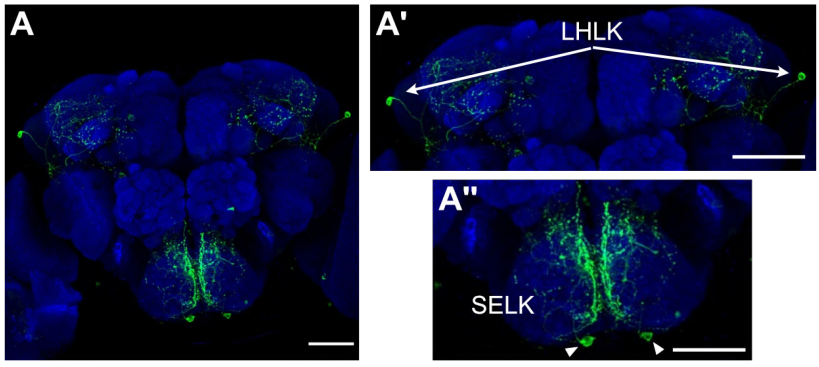

Figure 16: Anatomy of the Lk-producing neurons in the central brain. There are two leucokinin-producing neurons located in the LH (LHLK neurons) (**A** and **A'**) and two leucokinin-producing neurons located at the ventral part of the SEZ (SELK neurons) (**A** and **A''**). *UAS-CD8::GFP* was expressed in the LHLK and SELK neurons by using the *Lk-Gal4* driver. They were labeled with anti-GFP (green). Brain structure (blue) was labeled with anti-nc82. Scale bars: 50 µm.

There is mounting evidence that the ABLKs use Lk as a hormonal signal that targets peripheral tissues, including the renal tubules (Zandawala, Marley, et al., 2018), and that the brain Lk neurons act in neuronal circuits within the CNS (Al-Anzi et al., 2010; Cavey et al., 2016; Murakami et al., 2016). This fact sheds light on the importance of ABLK neurons in the regulation of water and ion homeostasis in response to desiccation, starvation, and ion stress, as Lk regulates fluid secretion in the Malpighian (renal) tubules (Cavey et al., 2016; Zandawala, Marley, et al., 2018). This is also correlated with the dispersed expression of the *Lk* receptor (*Lkr*) along the renal tubules and intestine cells, including the water-regulating rectal pads, as well as the IPCs which secrete DILPs to affect feeding, metabolism, sleep, activity, and stress responses (Broughton et al., 2005; Crocker et al., 2010; Nässel & Broeck, 2016; Rulifson et al., 2002; Zandawala, Yurgel,

et al., 2018). *Lkr* is also expressed by another set of brain neurosecretory cells (IPC-1/IPC-2a) known to regulate stress responses using three co-expressed neuropeptides (Kahsai et al., 2010). On the other hand, the LHLK neurons are part of the output circuitry of the circadian clock in regulation of locomotor activity and sleep suppression induced by starvation (Al-Anzi et al., 2010; Murakami et al., 2016; Murphy et al., 2016). SELK neurons may regulate feeding as possible synaptic partners to the premotor feeding program. Functional imaging revealed that LHLK neurons, not SELK neurons, were required to suppress sleeping during starvation (Yurgel et al., 2019). This is consistent with the fact that LHLK are possible synaptic partners of the IPCs, which regulate sleep and metabolism by integrating the metabolic state of the fly (Crocker et al., 2010; Erion et al., 2012; Yurgel et al., 2019). Further, a loss in Lk signaling results in an increase in postprandial sleep (Murphy et al., 2016), impaired locomotor activity (Cavey et al., 2016), and diminished feeding initiation as well as increased resistance to starvation and desiccation (Zandawala, Yurgel, et al., 2018).

In summary, Lk is an essential neuropeptide in regulating water retention, survival responses to desiccation and starvation, subtle regulation of food intake, and chemosensory responses (Liu et al., 2015; Zandawala, Yurgel, et al., 2018). While the role of ABLK and LHLK neurons has been described extensively, the role of SELK neurons in feeding behavior is unclear. The increase in *Lk* expression in the Gr66a^{GSON} that we have found in our RNAseq analysis (**Figure 15B**), which will correspond to SELK neurons during starvation, points to a clear role of Lk in feeding regulation.

We only captured SELK neurons and not the LHLK during the dissection procedure for the RNAseq analysis (**Figure 9**). To confirm that starvation induces changes in the expression of the *Lk* gene, we performed a gene expression analysis by qPCR under both fed and starved conditions. As there are only 4 Lk neurons in the *D. melanogaster* CB (out of approximately 100.000 neurons, excluding glial cells (Raji & Potter, 2021), we decided to FACS the Lk neurons by using a GFP reporter to enrich the RNA from Lk neurons. We used the same *Lk-Gal4>UAS-mCD8:GFP* flies as in **Figure 16** and followed the same stringent protocol for FACS sorting (**Figure 17A**) as with the GSON FACS labeling with *trans*-Tango ((**Figure 10**), see materials and methods for more detail). Briefly, once debris by size (**Figure S4B**), dead cells by DAPI approach (**Figure S4C**) or clusters (**Figures S4D** and **S4E**), and dying cells were removed by morphology and complexity, the living single cells were separated by GFP fluorescence (FITC-A filter) (**Figures S4F** and **S4G**), sorting finally the GFP^{+} Lk cells into LowBind tubes.

As the final number of GFP⁺ fluorescent Lk neurons was low compared to the total number of events sorted (around ~60 GFP⁺ Lk neurons from ~250.000 events for 30 CBs) (**Figure S4A**), each replicate was supplemented with weak GFP⁺ events from P5 to obtain replicates of ~3000 cells. It is important to note that the yield of disaggregation and sorting was low (~60 GFP⁺ Lk neurons from 120 GFP⁺ Lk neurons expected) due to the variability of the enzymatic process and sorting procedure. This was made to avoid errors due to the low number of starting cells during the RNA extraction and cDNA synthesis steps before the qPCR. Finally, the total amount of mRNA extracted from each FACS replicates was used to synthesize the cDNA.

To compare the gene expression levels of the SELK with the LHLK neurons in fed and starved conditions, we decided to perform two dissecting strategies in parallel: dissect the SEZ region, where we could FACS only the SELK neurons, and dissect the total CB (without OLs) to FACS the SELK and LHLK in the same pull of cells. Each replicate included 60 SEZs (for SELK samples) and 30 CBs (for SELK + LHLK samples).

Our qPCR experiments revealed that the gene expression levels of *Lk* were significantly higher in 24h starved conditions compared to fed conditions in the CB (SELK + LHLK neurons) and SEZ (SELK neurons) samples, with a slight increase in expression of the *Lk* gene in the SELK neurons (**Figure 17B**). This result supported our RNAseq finding, indicating that *Lk* expression is modulated by the internal metabolic state.

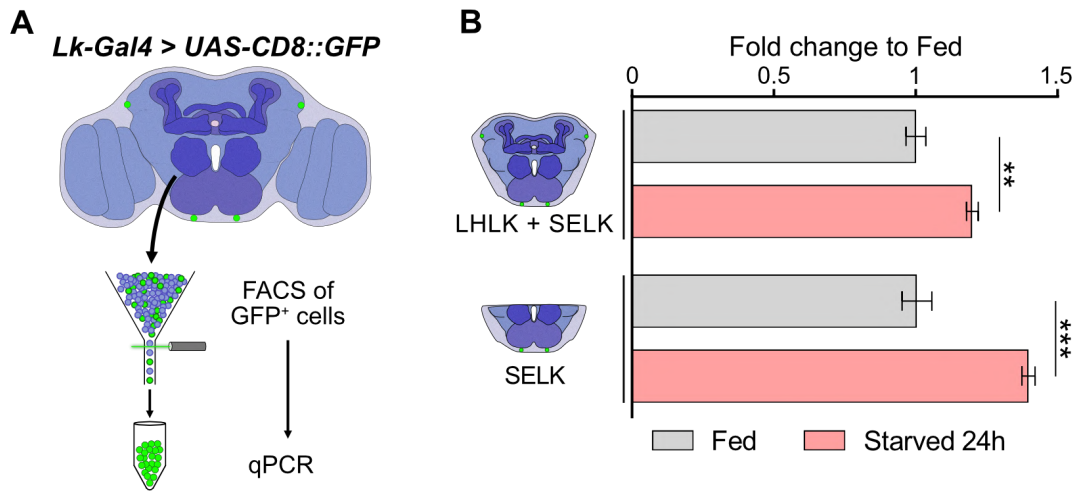

Figure 17: Gene expression levels of *Lk* by qPCR. (**A**) Schematic representation of the protocol followed to sort Lk GFP⁺ neurons (green) to quantify the levels of Lk gene expression by qPCR. (**B**) Quantitative PCR for Lk gene expression in LHLK and SELK neurons from fed and starved *Lk-Gal4>UAS-CD8::GFP* flies. mRNA levels were normalized to the fed condition. Statistical analysis: *t*-test. ***p<0,01, ***p<0,001*.

To support the RNAseq and qPCR findings and further confirm that the increase in *Lk* expression levels (**Figures 15B** and **17B**) was transduced to an increase in protein

translation, we performed immunohistochemistry using a specific anti-LK antibody (de Haro et al., 2010) that labels both SELK and LHLK neurons (**Figure 18**). We quantified the fluorescence intensity of the Lk neurons (arborizations and somas) in wild-type Oregon-R CBs in both fed and starved conditions. To quantify the SELK fluorescence intensity, we used a specific ROI area in ImageJ that covers all of the SELK neurons (**Figures 18A-B** and **18E-F**). To quantify the LHLK's fluorescence intensity, each LHLK (right and left) was measured with one independent ROI area to avoid any extra fluorescence in the middle of the CB, and the mean between the right and left LHLK neurons was calculated (**Figures 18C-D** and **18G-H**). Only those brains with both SELK or LHLK somas visible were measured, discarding those with any of them ablated due to dissecting or immunohistochemistry failure. As the RNAseq and qPCR data showed, the fluorescence intensity of the Lk neurons was significantly higher in starved conditions compared with fed conditions in the SELK and LHLK neurons (**Figure 18I**). Interestingly, the SELK neurons' fluorescence was slightly higher than the LHLK neurons. Still, the fact that the measurement procedure is different does not allow us to compare them statistically.

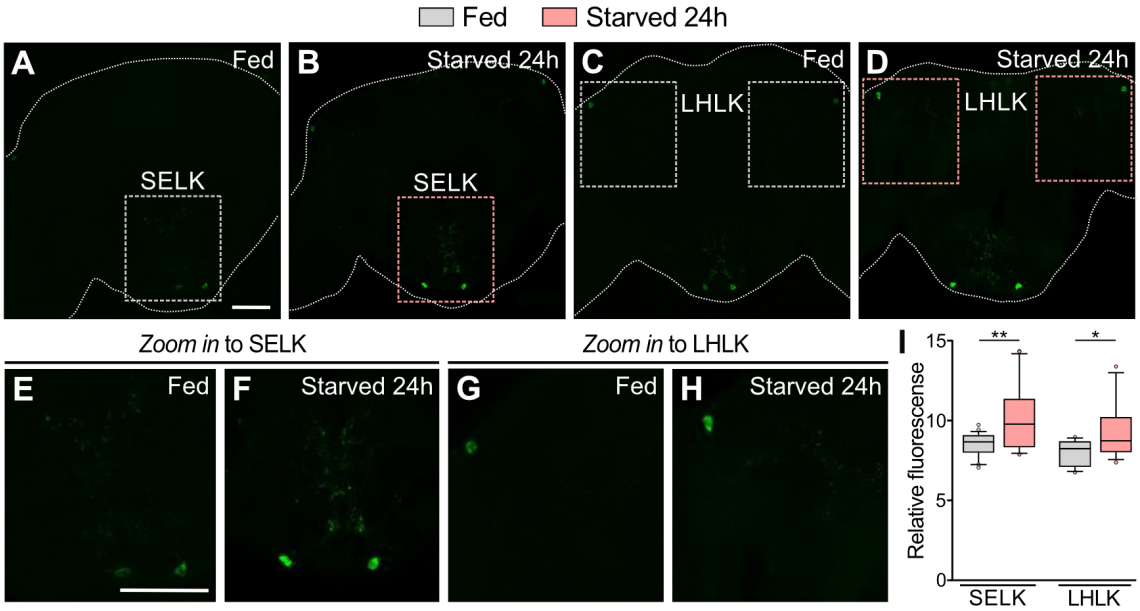

Figure 18: Leucokinin fluorescence quantification in fed and starved conditions. Both SELK (**A-B** and **E-F**) and LHLK (**C-D** and **G-H**) neurons were labeled with anti-LK antibody (green) in Oregon-R flies in fed and starved conditions. Brains perimeters were delimited manually. (**I**) Their fluorescence was quantified by using the same ROI area (square indicated above) to compare the change in fluorescence in the fed condition (grey) versus the starved condition (pink). n=12-20 brains/condition. Statistical analysis: *t*-test. **p<0,05, **p<0,01*. Scale bars: 50 µm.

Altogether, the qPCR and the anti-LK fluorescence intensity quantification showed an increase in *Lk* expression in the SELK neurons compared to those starved and fed, similar to the expression differences found in the RNAseq data. Thus, the

expression of the *Lk* gene depends on the metabolic state of the fly, leading to an increase of Lk neuropeptide disposition in the cell during starvation.

3. Leucokinin neurons are gustatory second-order neurons to gustatory receptor neurons

3.1. Molecular validation of SELK neurons as postsynaptic partners to bitter gustatory receptor neurons

The RNAseq data presented above showed increased *Lk* gene expression in starved conditions, specifically in the $Gr66a^{GSON}$ population and not in the $Gr64f^{GSON}$ or $NompC^{GSON}$ (**Figure 17B**). We hypothesized that Lk neurons, specifically the SELK neurons, might receive direct input from the $Gr66a^{GRN}$ located in the labellum.

As SELK neurons have a large arborization (**Figure 16**) and innervate a significant portion of the SEZ, we wanted to analyze the location of the dendrites and axons within the SEZ. To do so, we employed a Dendritic Marker (DenMark) technique (Nicolaï et al., 2010). Briefly, DenMark uses the combination of a neuroanatomical marker to label the entire morphology of a neuron. The axons are specifically labeled with synaptotagmin::GFP (syt::GFP), a presynaptic genetically encoded marker. The dendrites are targeted via ICAM5 (Denmark) fusion, an intracellular adhesion molecule that specifically targets dendrites in the mammalian brain telencephalon (Oka et al., 1990). We saw that SELK neuron arborization (**Figures 19A-A'**) and dendrites (**Figures 19B-B'**) overlap significantly through the middle and dorsal regions of the SEZ (**Figures 19C-C'**), where GRNs send gustatory sensory information, and other neurons like IPCs innervate the SEZ (Nässel et al., 2013). That could indicate that SELK neurons receive input from GRNs and integrate information related to the IPCs. IPCs express the *Lkr*, making those neurons strong candidates for postsynaptic neurons to Lk neurons (Zandawala, Yurgel, et al., 2018).

Many genetic techniques can be used to test if two neurons are synaptically connected (Ni, 2021). We have used *trans*-Tango combined with immunohistochemistry for Lk (Talay et al., 2017), GRASP (Feinberg et al., 2008), and BAcTrace (Cachero et al., 2020), to validate that LK^{GSON} neurons are postsynaptic partners to $Gr66a^{GRN}$.

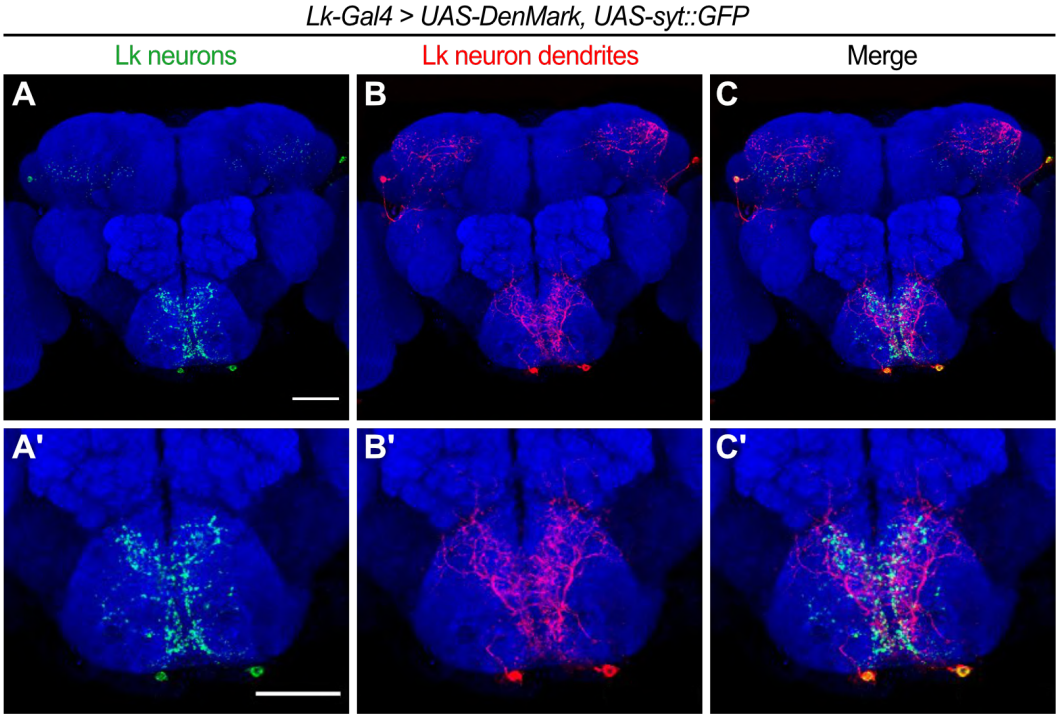

Figure 19: Dendritic arborization of SELK neurons labeled by DenMark technique. The SELK neurons were labeled with anti-GFP (green) via *syt::GFP* (**A** and **A'**), and their dendritic arborization with mCherry (red) via DenMark (**B** and **B'**). (**C** and **C'**) Merge of both channels, GFP and mCherry signal, and *Zoom in* where co-localization from both reporters are seen, especially in the SELK neuron somas. Brain structure (blue) was labeled with anti-nc82. Scale bars: 50 µm.

First, to test if Lk neurons were indeed part of the Gr66a^{GSON} and not Gr64f^{GSON} nor NompC^{GSON}, we decided to label Lk neurons using an anti-LK antibody (de Haro et al., 2010) in GRNs>*trans*-Tango flies. According to our RNAseq hypothesis, we should only find Lk-positive neurons labeled with mtdTomato in *Gr66a>trans*-Tango flies but not in *Gr64f>trans*-Tango nor *NompC>trans*-Tango. To better appreciate the co-localization of the anti-LK signal with the *trans*-Tango, it was crucial to represent the confocal stacks where the anti-LK signal falls in. Besides, it was essential to visualize these confocal stacks by navigating between them in a *.tiff* composite format in ImageJ to confirm the results. As expected for the *Gr66a>trans*-Tango brains, there was co-localization (purple) between the anti-LK signal (in blue) and the *trans*-Tango labeled neurons (Gr66a^{GSON}, in magenta) (**Figures 20B-B'''**). To our surprise, we found co-localization between anti-LK signal and *Gr64f>trans*-Tango (Gr64f^{GSON}) (**Figures 20A-A'''**), indicating that SELK neurons might also be postsynaptic to Gr64f^{GRN}. We found no co-localization between the anti-LK antibody and the *NompC>trans*-Tango signal (**Figures 20C-C'''**). Initially, this data contradicts our RNAseq data, which suggested SELK as postsynaptic only to Gr66a^{GRN}, not Gr64f^{GRN} or NompC^{GRN}.

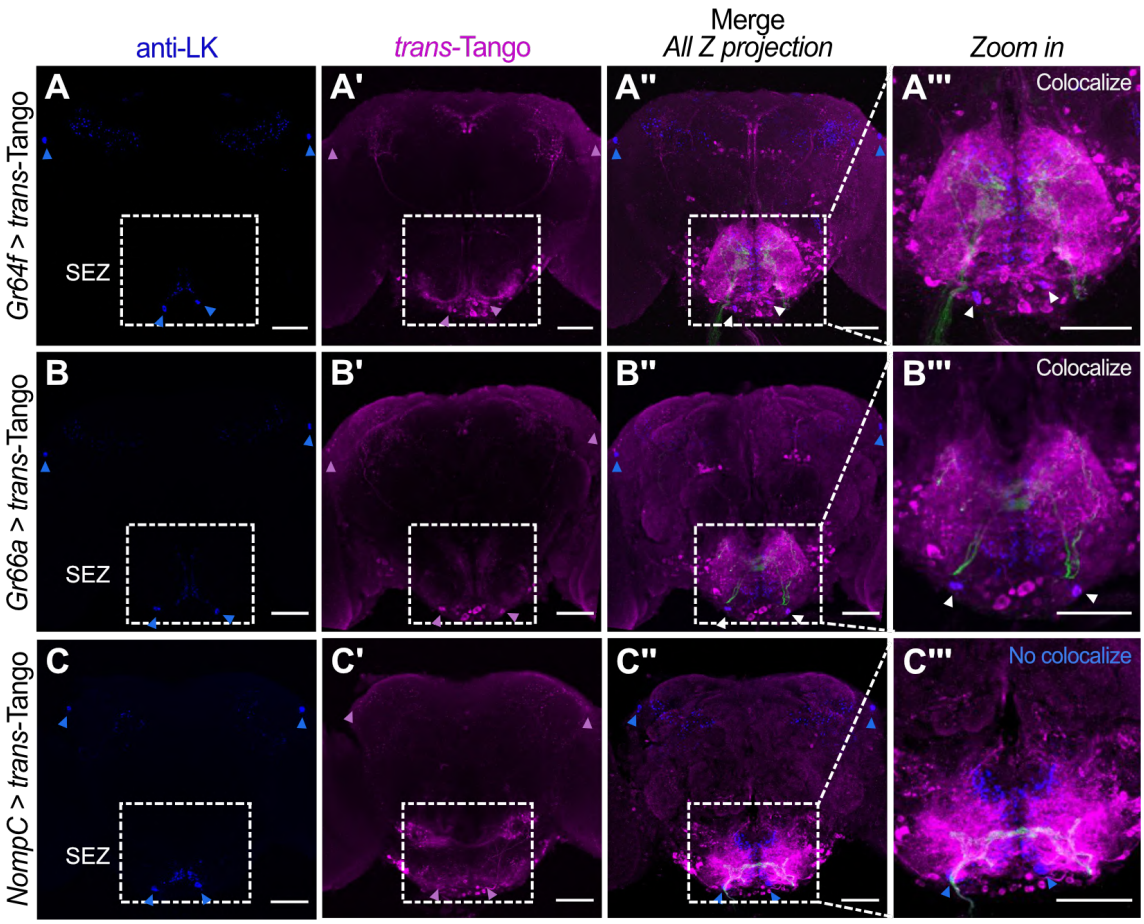

Figure 20: Anti-Leucokinin antibody co-localization with the *trans*-Tango signal. Each *GRN>trans-Tango* transgenic line was tested for the co-localization of the SELK neurons with the *trans*-Tango signal, which labels the GSONs. The SELK and LHLK neurons (blue arrows) were labeled with the anti-LK antibody (blue) donated by Pilar Herreros lab (de Haro et al., 2010), (**A**, **B** and **C**). (**A'**, **B'** and **C'**) *trans*-Tango signal from mtdTomato reporter (labeled with anti-RFP (magenta)) from the stack where the SELK and LHLK neurons may fall in (magenta arrows). (**A''**, **B''** and **C''**) Merge of all stacks from the anti-LK antibody labeling the LHLK and SELK neurons (blue) with the *trans*-Tango signal (magenta) and the GRN axonal terminals labeled with anti-GFP (green) showed the possible co-localization of anti-LK antibody signal with the *trans*-Tango signal (white arrows when colocalize and blue arrows when not colocalize) which may indicate that SELK neurons are GSONs to the GRNs analyzed. (**A'''**, **B'''** and **C'''**) *Zoom in* to the SEZ to focus on the SELK neurons to confirm that Gr64f^{GRN} and Gr66a^{GRN}, but not NompC^{GRN}, are presynaptic neurons to SELK neurons, which showed co-localization (white arrows). Scale bars: 50 µm.

We used another genetic technique to test our hypothesis further: GRASP (Feinberg et al., 2008). Briefly, GRASP is based on two GFP complementary fragments (*spGFP11 and spGFP1-10*) expressed in two candidate neurons, which are exposed to the extracellular space via transmembrane carrier proteins. When both neurons are synaptically connected, the complete GFP protein is reconstructed, and fluorescence can be detected. To properly reveal the reconstruction of the GFP protein, we have used an antibody that detects only the complete GFP protein to avoid the possible detection of fragments. GRASP results indicate that, effectively, there were synaptic connections between Gr66a^{GRN} and Gr64f^{GRN} with the SELK neurons (**Figures 21A-A'** and **21B-B'**)

but no GRASP signal between NompC^{GRN} and SELK neurons (**Figures 21C-C'**). These results support the hypothesis that maybe SELK neurons receive input not only from Gr66a^{GRN} but also from Gr64f^{GRN}.

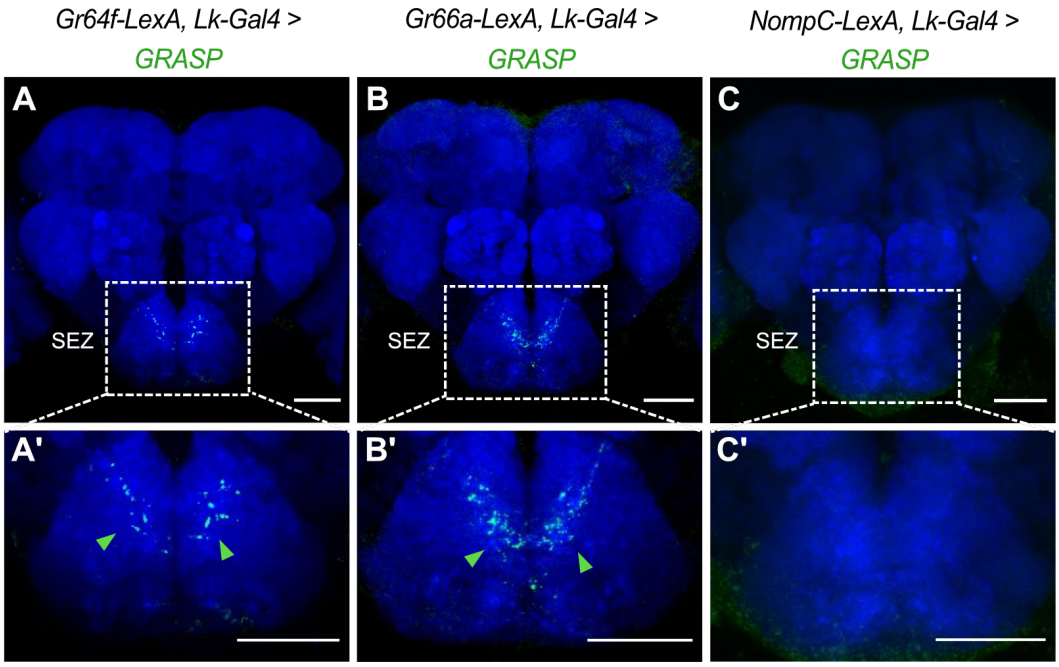

Figure 21: GFP reconstitution across synaptic partners (GRASP) for the SELK neurons with the sweet, bitter and mechanosensory GRNs. GRASP signal (labeled with anti-GRASP/GFP (green)) between sweet (**A**), bitter (**B**) and mechanosensory (**C**) GRNs, and SELK neurons and *Zoom in* to the SEZ (**A'**, **B'** and **C'**, respectively). The *GRN-LexA* expressed the *lexAop-nSyb-spGFP1-10* portion, while *Lk-Gal4* expressed the *UAS-CD4-spGFP11* portion. Green arrows indicate the presence of GRASP signal. Brain structure (blue) was labeled with anti-nc82. Scale bars: 50 µm.

However, one particularity of the GRASP technique is that it does not reveal the direction of the connection and which of the candidate neurons is the presynaptic or postsynaptic. Another particularity is that the proximity in the axon terminals from the bitter and sweet GRNs to the SELK arborization (**Figures 5A-B** and **19**) in the SEZ could induce the formation of false positive GRASP signals (Feinberg et al., 2008). For that reason, to further validate the connection between Gr66a^{GRN} and Gr64f ^{GRN} to SELK neurons in the correct direction (from GRNs to SELK neurons) we used a third technique: BAcTrace (Cachero et al., 2020). BAcTrace is a retrograde tracing system based on the *Clostridium botulinum* neurotoxin A1 ligand/protease (BoNT/A). Basically, the presynaptic candidate neuron expresses via LexA/LexAop binary system a receptor linked with synaptobrevin to a GFP (first reporter), and in the postsynaptic candidate neuron expresses via Gal4/UAS binary system a BoNT/A ligand/protease linked to a GFP antibody. When both candidate neurons are synaptically connected, the BoNT/A ligand/protease binds to the presynaptic receptor via GFP-antiGFP, and a QF

transcription factor is translocated from the postsynaptic neuron to the presynaptic neuron, which drives the expression of mtdTomato (second reporter) under the control of QUAS. The presynaptic candidate neurons (sweet and bitter GRNs in our case) will express GFP via *Gr64f-LexA* and *Gr66a-LexA,* respectively, and only when the postsynaptic candidate *Lk-Gal4* is synaptically connected, the presynaptic candidate neuron will also express mtdTomato. As **Figure S5** shows, we found that the GFP reporter signal (presynaptic neurons) from the *Gr64f-LexA* and *Gr66a-LexA* expression (**Figures S5A** and **S5B**, respectively), and the mtdTomato reporter signal **Figures S5A'** and **S5B'**, respectively) were co-localizing (**Figures S5A''** and **S5B''**, respectively), indicating that both Gr64f^{GRN} and Gr66a^{GRN} are presynaptic neurons from SELK neurons. These results confirm the results obtained with the anti-LK antibody combined with *GRN >trans*-Tango (**Figure 20**) and GRASP (**Figure 21**).

These results indicate that SELK neurons receive presynaptic input from Gr66a^{GRN} and Gr64f^{GRN} but not from NompC^{GRN}. This is the first time a GSON is identified as collecting information from two populations of GRNs that transduce sensory information of different valence, sweet-attractive and bitter-repulsive. However, how SELK neurons integrate this information is still unknown.

3.2. Computational characterization of SELK neurons

We validated molecularly using three different techniques (anti-LK antibody combined with *trans*-Tango*,* GRASP, and BAcTrace) that Gr66a^{GRN} and Gr64f^{GRN}*,* but not NompC^{GRN}, are presynaptic neurons to SELK neurons (**Figures 20, 21** and **S5**, respectively), indicating that SELK neurons are transducing sensory information of totally different valence, sweet-attractive and bitter-repulsive. To properly understand the role of Lk neurons in gustatory information processing, we need to know all their presynaptic and postsynaptic partners, something that the techniques we used cannot reveal. The connectome of the *D. melanogaster* adult brain has been reconstructed since a few years ago (Bates et al., 2020; Galili et al., 2022; F. Li et al., 2020; Scheffer et al., 2020; Winding et al., 2023), allowing us to search *in silico* which of the neurons in the connectome that correspond to the Lk neuron and later possibly find pre- and postsynaptic partners. For that purpose, we employed the FAFB volume. This whole-brain EM volume provides synaptic resolution of all neurons in the fly brain to find which identified neurons correspond to the Lk neurons (Zheng et al., 2018).

A recent work published by *Engert et al*. (Engert et al., 2022), has characterized with synaptic resolution using the FAFB, the connectivity in the SEZ of some subsets of GRNs, including *Gr64f* and *Gr66a* expressing ones. As Lk neurons receive presynaptic

inputs from Gr64f^{GRN} and Gr66a^{GRN} neurons, we reasoned that we could use the VFB dataset (Court et al., 2023) to obtain the different labellar Gr64f^{GRN} and Gr66a^{GRN} skeletons from the right hemisphere in the SEZ, described by *Engert et al*. (Engert et al., 2022), and then find which neurons receive input from both populations. We should find the Lk neurons within those neurons. 4 GRN groups were considered according to *Engert et al*. results for NBLAST Gr64f^{GRN} and Gr66a^{GRN} morphology. A total of 52 GRN skeletons were downloaded from the VFB dataset in *.swc* format and aligned to the FAFB by using the JRC2018U reference brain as a template (Bogovic et al., 2020; Costa et al., 2016; Zheng et al., 2018). From these, 19 GRNs were bitter sensing (12 from group 1 (**Figures 22A-A'**) and 7 from group 2 (**Figures 22B-B'**)), and 33 GRNs were sweet sensing (17 from group 4 (**Figures 22C-C'**) and 16 from group 5 (**Figures 22D-D'**)). Only Gr64f^{GRN} and Gr66a^{GRN} of the right hemisphere were used in this analysis as the dataset is more precise. All these GRN skeletons were aligned to the recently released Flywire dataset, a dense, machine learning-based reconstruction of more than 80,000 FAFB neurons (Dorkenwald et al., 2022; Eckstein et al., 2023) (for more detail, see materials and methods). By using the Flywire Gateway tool, each of the sweet and bitter GRNs analyzed was aligned and reconstructed to the EM dataset (**Figures 22E-F''**) in the Flywire toolbox, where a brain mesh template was used to represent the morphology of the tracing aligned (**Figures 22G-L**) and the IDs annotated.

Once we obtained all IDs for the GRNs analyzed, by using the BrainCirctuits online software from Flywire Consortium, a platform for comparative connectomics (https://braincircuits.io/), we were able to find synaptic segments for each of the sweet and bitter GRNs, differentiating those that are presynaptic (upstream) from those postsynaptic (downstream). Using *R* software, only those downstream segments that presented synapses sites with either Gr64f^{GRN} or Gr66a^{GRN} were considered postsynaptic solid candidates for GRNs to be the SELK neurons. After collecting all SELK candidates postsynaptic to Gr64f^{GRN} and Gr66a^{GRN}, a manual comparison was made in *R* software to identify downstream segment IDs common for both GRN. A total of 334 downstream segment IDs were identified to be connected to Gr64f^{GRN} and Gr66a^{GRN}, and 17 downstream segment IDs were visually classified as strong candidates to be SELK neurons. After visual comparison between the SELK neuron candidates and the SELK arborization (**Figures 16** and **19**), one downstream ID segment (720575940623529610 ID (or 720575940632524559 ID as both labels the same neuron)) was identified as a strong candidate to be the left SELK neuron (**Figure 23, magenta**). As can be seen, this candidate SELK neuron has a significant arborization that covers the upper part of the SEZ, as DenMark's previous experiment showed

(**Figure 19**). Additionally, the position of the candidate left SELK soma at the bottom of the SEZ is consistent with the position of the SELK somas previously described molecularly (**Figure 16**) (de Haro et al., 2010). Further, by using the Flywire Codex online software tool (https://codex.flywire.ai/), we were able to identify the left SELK neuron as the GNG.276 (gnathal ganglia neuron 276), and classified as a possible GABAergic neuron, based on previous annotation and proofreading by the Flywire community (Eckstein et al., 2023; Schlegel et al., 2023).

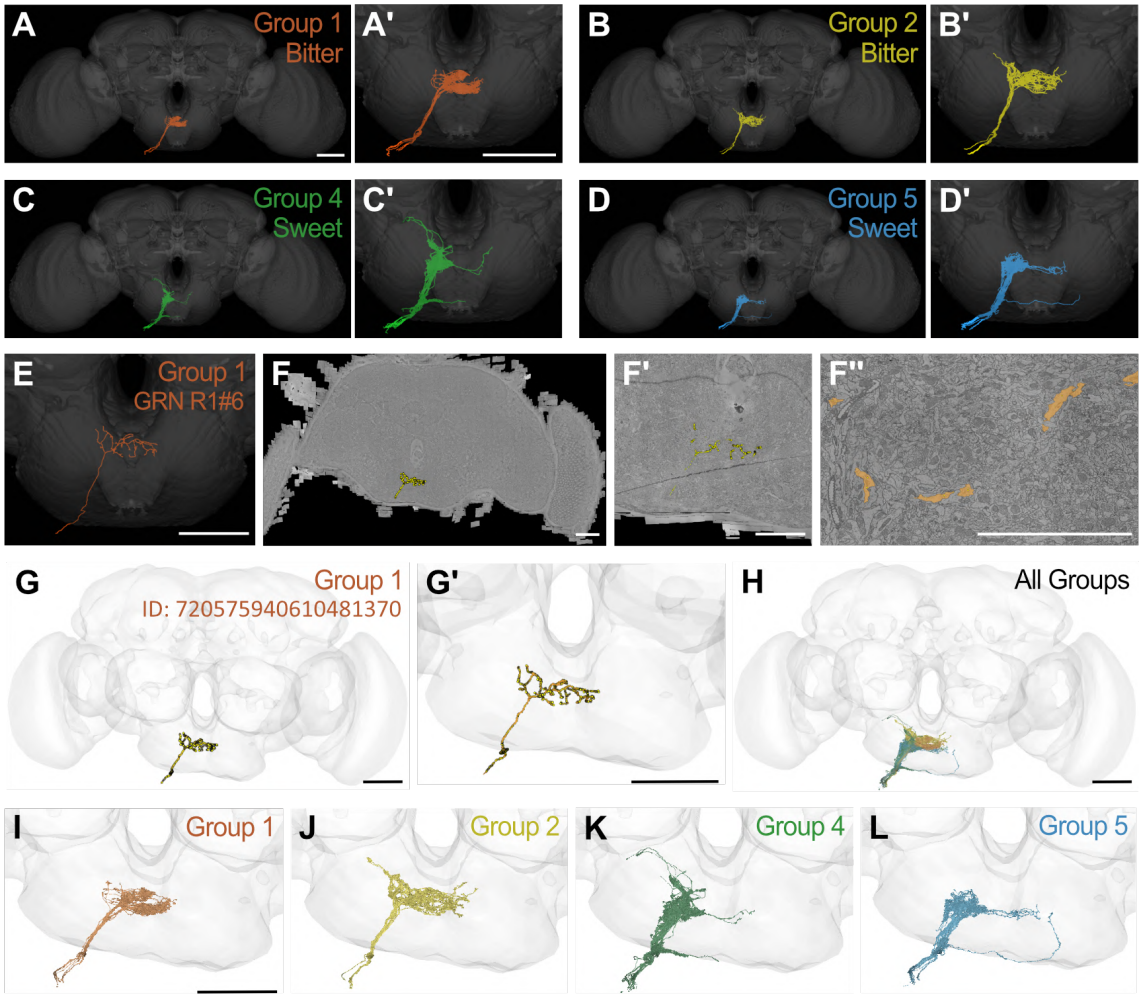

Figure 22: Electron microscopy-based reconstructions of gustatory receptor neurons. (**A-D**) VFB skeleton reconstruction frontal view from bitter (groups 1 and 2) and sweet (groups 4 and 5) GRNs in the right hemisphere and *Zoom in* to the SEZ region on the right of each group image (**A'-D'**). (**E**) Bitter GRN skeletons from Group 1 in the VFB template, which was reconstructed via Flywire Gateway in the EM dataset of the Flywire Sandbox (**F**) and *Zoom in* (**F'** and **F''**) of the area aligned in orange. (**G** and **G'**) Reconstructed GRN R1#6 in the Flywire Sandbox brainmesh template with the Flywire ID720575940610481370. (**H-L**) Reconstruction representation in Flywire from all groups of GRNs analyzed (**H**) and its *Zoom in* to the SEZ region for all the groups individually (**I-L**). Scale bars: 50 µm.

The next step was to identify strong candidates for the right SELK neuron. To do this, we used the online morphology NBLAST from Flywire Codex to find neurons with

similar arborization to GNG.276 but in the right hemisphere. One strong candidate was the GNG.246 with 720575940632407826 ID (**Figure 23, cian**). This right SELK candidate neuron has similar arborization to the left SELK candidate neuron, as it also has identical arborization found in the immunohistochemistry images (**Figure 16**). Furthermore, this GNG.246 neuron is also classified as a possible GABAergic neuron, lighting the possibility that both neurons are SELK neurons.

To confirm that these SELK candidate neurons effectively receive input from the analyzed GRNs, we looked for which GRNs were presynaptic to SELK neurons. We found that only one bitter (GRN R2#5) and one sweet (GRN R4#17) GRNs were presynaptic to GNG.276 (right SELK neuron), and that only one sweet GRN (R4#14) was presynaptic to GNG.246 (left SELK neuron). The fact that only so few presynaptic neurons were found indicates that SELK proofreading is still required for a much more precise assembly and annotation of the FAFB dataset, which is currently underway.

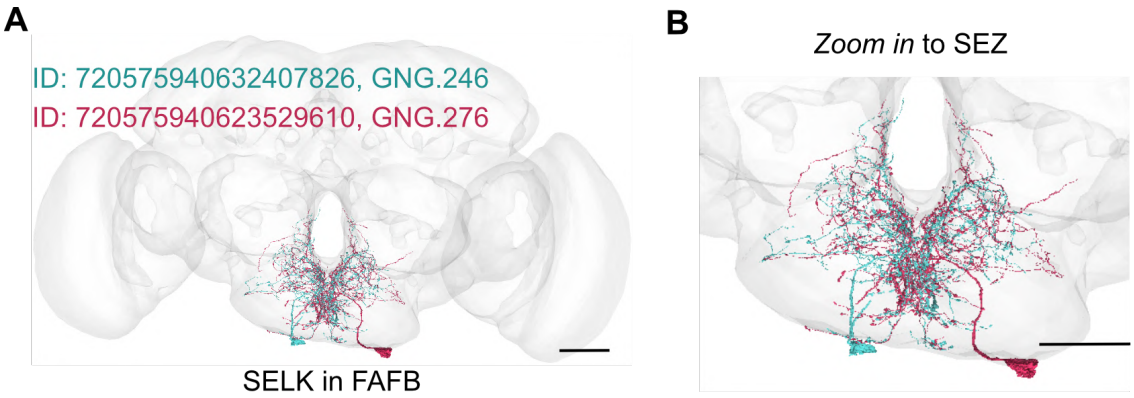

Figure 23: SELK neurons EM-reconstruction using Flywire. (**A**) Anatomy of the SELK neurons (right in cian and left in magenta) reconstructed in the FAFB brainmesh template in Flywire, and *Zoom in* to the SEZ (**B**). IDs from Flywire are indicated: 720575940632407826 ID for the right SELK (GNG.246) and 720575940623529610 for the left SELK (GNG.276). Scale bars: 50 µm.

We wondered about the upstream and downstream neurons connected to the SELK neurons, so with BrainCircuits, we computationally characterized both pre- and postsynaptic neurons as SELK neurons. Moreover, we compared this analysis with the molecular *retro*-Tango and *trans*-Tango methods. However, we never tried to find the possible identities of the LHLK neurons in the FAFB as they are not the focus of the present study, so all this computational comparative analysis will focus exclusively in the SELK located in the SEZ. Thus, some differences between both methods, molecular and computational, were expected as we could not differentiate the signal from LHLK or SELK neurons in the *retro*-Tango and *trans*-Tango experiments.

To look for the upstream (presynaptic) neurons to SELK neurons we used the molecular transsynaptic tool *retro*-Tango (Sorkaç et al., 2023) (**Figure 24A**), a retrograde transsynaptic technique that employs similar transsynaptic mechanisms as *trans*-Tango but in the retrograde direction, and computationally with BrainCircuits (**Figure 24B**). We only considered those presynaptic partners with ≥10 synaptic connections (84 presynaptic candidate neurons in total) to discard any signal from segments close to SELK arborizations but without any real connection. We need to consider that presynaptic SELK candidate neurons need to be proofread by the Flywire community to have a more consistent result. Moreover, we could not detect *retro*-Tango signal in the proboscis, so we did not see the $Gr64f^{GRN}$ and $Gr66a^{GRN}$ labeled with mtdTomato (**Figure S6**).

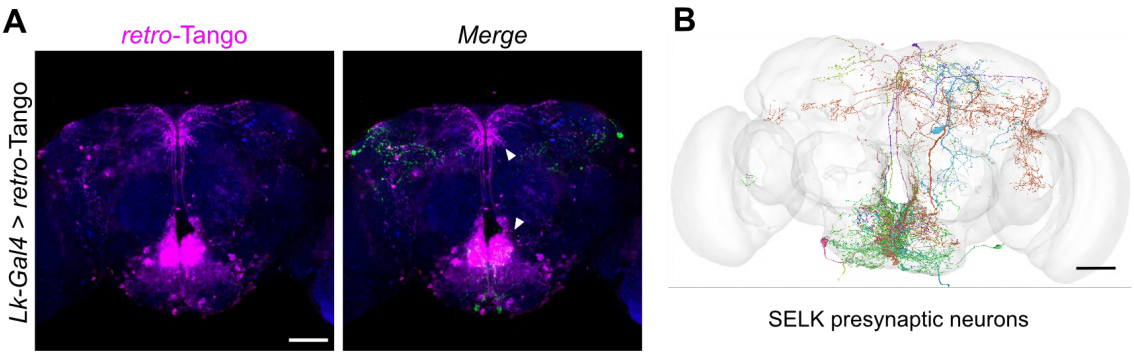

Figure 24: Presynaptic neurons to SELK. (**A**) Anatomy of the Lk neurons (SELK and LHLK) labeled with anti-GFP (green) connected synaptically with their presynaptic neurons labeled with anti-RFP (magenta) by *retro*-Tango technique. Brain structure (blue) was labeled with anti-nc82. (**B**) SELK presynaptic candidate neurons reconstructed in the FAFB brainmesh template in Flywire. Only presynaptic candidate neurons with ≥10 synaptic points with SELK neurons are shown (84 presynaptic candidate neurons). Scale bars: 50 µm.

Regarding the postsynaptic output from SELK neurons, we compare the BrainCircuits downstream candidates' output with the *trans*-Tango signal. The majority of the postsynaptic partners of SELK neurons localize in the SEZ, with some projections to the dorso-medial region of the CB. This region contains IPC neurons that project to the tritocerebrum in the SEZ, where a significant concentration of fibers can be appreciated in the *trans*-Tango immunohistochemistry (**Figure 25A**). Those results coincide with previous observations suggesting Lk neurons as IPC neurons' presynaptic partners (Zandawala, Yurgel, et al., 2018). It is essential to notice that the number of postsynaptic partners of Lk neurons is much larger when looking at the FAFB-derived results (174 postsynaptic candidate neurons with ≥10 synaptic connections) (**Figure 25B**) compared to *trans*-Tango. Besides, SELK neurons could be connected to the premotor feeding program as they seem to integrate both bitter and sweet information as well as the metabolic state of the fly (Al-Anzi et al., 2010).

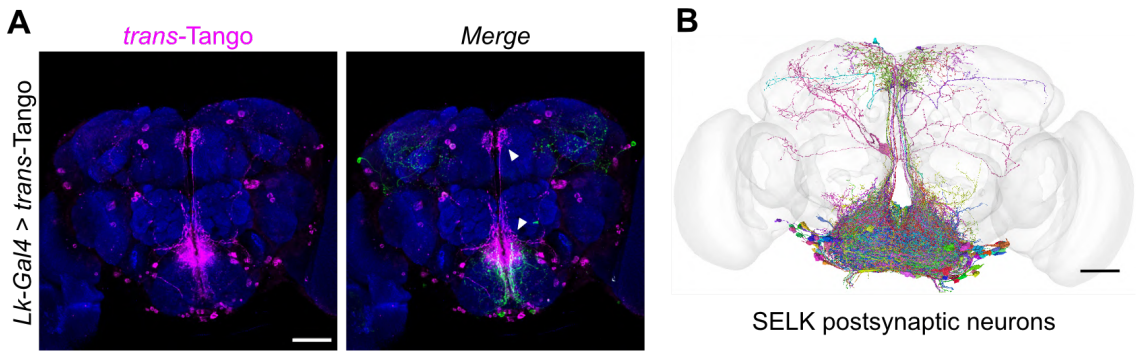

Figure 25: Postsynaptic neurons to SELK. (**A**) Anatomy of the Lk neurons (SELK and LHLK) labeled with anti-GFP (green) connected synaptically with their postsynaptic neurons labeled with anti-RFP (magenta) by *trans*-Tango technique. Brain structure (blue) was labeled with anti-nc82. (**B**) SELK postsynaptic candidate neurons reconstructed in the FAFB brainmesh template in Flywire. Only postsynaptic candidate neurons with ≥10 synaptic points with SELK neurons are shown (174 postsynaptic candidate neurons). Scale bars: 50 µm.

In summary, we found two central SELK candidate neurons with the Flywire software, including the FAFB dataset's EM. Although we consider our results solid (identifying the SELK candidates in the FAFB) we cannot yet prove definitively that those neurons are in fact Lk neurons. The differences between the Braincircuits analysis and *trans*- and *retro*-Tango are due to different factors. First, both *trans*- and *retro*-Tango label only the pre- and postsynaptic partners to a certain level, so they only capture a fraction of their partners. Regarding Braincircuits, although the FAFB is done, only a fraction of the neurons are annotated and proofread, so we are missing many pre- and postsynaptic partners. However, the identification of the SELK in Braincircuits, will give us access to possible split Gal4 lines that could label specifically SELK neurons and not LHLK or ABLK, so we could test the role of those neurons in feeding behavior independently of the others.

4. Leucokinin neurons modulate feeding behavior

We have shown that SELK neurons are postsynaptic neurons to Gr64f^{GRN} and Gr66a^{GRN} (**Figures 20, 21** and **S5**), indicating their apparent role as integrators of contradictory information. Gr64f^{GRN} neurons collect sweet information that initiates feeding, while Gr66a^{GRN} neurons transduce bitter information that inhibits feeding (Dweck & Carlson, 2020; Weiss et al., 2011). All animals must evaluate the food's quality and integrate it with their metabolic needs. While bitter tastants typically induce rejection, depending on the context, food laced with low amounts of bitter compounds can appeal if starvation or sucrose concentrations are high. Previous studies have demonstrated interactions between sweet and bitter taste modalities at the level of sensory neurons,

pointing to the existing interaction between those neurons to regulate feeding (French et al., 2015; Hiroi et al., 2004). For example, some GABAergic neurons collecting bitter information from GRNs inhibit sweet GRNs to avoid feeding (Chu et al., 2014). At the level of the sensilla, the odorant binding protein 49a (OBP49a), which is expressed in accessory cells, binds bitter tastants to regulate sweet responses (Jeong et al., 2013). Regarding how starvation modulates sweet-bitter interaction, there are inhibitory mechanisms to decrease the activity of two octopaminergic-tyraminergic interneurons (OA-VL neurons) that integrate bitter information from GRNs when flies are starved, promoting bitter acceptance (LeDue et al., 2016). Also, in mammals, it has been reported that a local inhibitory circuit for bitter-sweet integration exists (Jin et al., 2021). Other studies have elucidated the role of different gustatory interneurons that participate in processing bitter and sweet tastes to drive the activation or not of premotor neurons in the sensorimotor program (Inagaki et al., 2014; Shiu et al., 2022). Altogether, those results highlight the evolutionary importance of balancing the hunger state with the attractiveness of sweet tastes against the aversion to bitter tastes to decide whether to feed finally. However, the precise mechanisms downstream neurons modulate appetitive feeding behaviors in response to sweet and bitter taste detection remains unclear.

SELK neurons are located at the caudal part of the SEZ (**Figures 16** and **23**). As they are postsynaptic neurons to $Gr64f^{GRN}$ and $Gr66a^{GRN}$, we hypothesize that SELK neurons might participate in feeding behavior by integrating different value information when flies are exposed to sweet and bitter stimuli. To address this possibility, we decided to silence the activity of SELK neurons and test the effect on feeding behavior using TNT to block the function of the Lk neurons. The tetanous toxin cleaves the synaptic vesicle protein synaptobrevin, a protein involved in the formation of vesicles during exocytosis, so those neurons expressing TNT are not able to release neurotransmitter vesicles into the synapse cleavage (Sweeney et al., 1995). As a control, we used a mutated version of TNT, the tetanus toxin impaired (TNT^{IMP}), that does not cause any defect in synaptic transmission in the neurons. We used the *Lk-Gal4* driver to express *UAS-TNT* or *UAS-*TNT^{IMP} transgenes, to silence all Lk neurons, including the SELK neurons. With both transgenes, we could compare the effect of nonfunctional SELK neurons with functional ones in the feeding paradigm and test how SELK neurons integrate sweet and bitter information simultaneously. However, we must consider that those transgenes expressed the Gal4 in all Lk neurons (SELK, LHLK, and ABLK neurons), so any difference between both groups was carefully analyzed. In addition, as the metabolic state of the flies modulates the gene expression profile of the GSONs (**Figures 11** and **12**), including *Lk* gene expression in the SELK neurons (**Figures 15B, 17** and **18**), and

that hunger state modulates Gr64f^{GRN} and Gr66a^{GRN} activity (Inagaki et al., 2012; Weiss et al., 2011), starvation was used not only as a strategy to motivate flies to feed but to study the function of the SELK neurons in both metabolic paradigms, fed and starved (Yurgel et al., 2019).

4.1. Modulation of the feeding initiation behavior in response to sweet and bitter stimuli

Animals evaluate internal nutritive state and food quality to decide whether to initiate feeding (Trisal et al., 2023). To investigate how food quality alters feeding initiation, we examined how the detection of bitter compounds is integrated with sugar taste information in the feeding initiation circuit using the PER assay upon proboscis stimulation. Briefly, PER measures the total extension or not of the proboscis in response to a stimulus. Extension of the proboscis is associated with an attractive behavior. For example, flies showed higher PER responses when exposed to higher concentrations of sucrose and significant starvation times (Trisal et al., 2023; Yapici et al., 2016). However, flies showed lower PER response when exposed to bitter tastants as they are related to toxic compounds in nature (Inagaki et al., 2014). The strategy to use PER upon proboscis stimulation assured us that only the two SELK neurons, and not other Lk neurons, were receiving this sensory information from stimulating Gr64f^{GRN} and Gr66a^{GRN} in the labellum, as these GRNs project to the SEZ and not other regions where LHLK neurons, or the ABLK neurons, arborize (de Haro et al., 2010; Scott, 2018; Z. Wang et al., 2004).

We decided to use sucrose to activate Gr64f^{GRN} and caffeine to activate Gr66a^{GRN} (Jiao et al., 2007; Y. Lee et al., 2009). Before the analysis of the behavior of *Lk-Gal4>UAS-TNT* and *Lk-Gal4>UAS-TNT^{IMP}* transgenic flies, we decided to analyze the response of *w^{1118}* flies to sucrose and caffeine to set the appropriate concentrations of the tastants (**Figure 26**). All tastants used during the Thesis were diluted in miliQ water to avoid any repulsion or attraction effect from tap water composition. For all PER experiments, flies were immobilized in P200 tips, and water was provided ad libitum before the test (see materials and methods for more detail).

We performed a PER dose-response curve of starved *w^{1118}* flies to increasing concentrations of sucrose, from 6.25 mM to 800 mM (**Figure 26A**). The PER to sucrose exhibited a proportional increase from 6.25 mM to 100 mM. Notably, at 100 mM sucrose, the flies demonstrated a complete PER response, indicative of saturation, plateauing with subsequent concentrations (ranging from 200 mM to 800 mM), yielding saturated PER responses. Once the response to sucrose in our flies was established, the next step

would be to find the right concentration of sucrose so we could test the response to caffeine.

To select the right sucrose concentration, it was imperative to avoid saturating the PER response while ensuring a sufficient range to discern any decrease in PER when combined with varied concentrations of caffeine. Given that the EC_{50} (half maximal effective concentration, the theoretical concentration eliciting a response in 50% of the tested flies) for w^{1118} flies, derived from the sucrose PER response curve (**Figure 26A**), was determined to be 25.04 mM of sucrose via non-linear regression modeling, it was decided that concentrations of 30 mM and 50 mM of sucrose would best serve our objectives. These concentrations, exceeding the calculated EC_{50}, afford a suitable range to observe the effects of caffeine on PER response without inducing saturation from sucrose PER. Thus, they were deemed optimal for subsequent PER assays involving the combination of sucrose and caffeine.

In the same way, to establish the appropriate concentration of caffeine, various concentrations (1, 5, 10, 20, and 50 mM) were combined with 30 mM and 50 mM of sucrose. As anticipated, the PER was notably higher in starved flies tested with the 50 mM sucrose mixtures than those tested with the 30 mM sucrose mixtures (**Figure 26B**). Specifically, statistically significant differences were observed between them in the 20 mM and 50 mM caffeine mixtures. Based on these results, we concluded that employing a concentration of 50 mM sucrose would be optimal, rather than 30 mM, because it provided the necessary dynamic range in response when combined with various concentrations of caffeine.

To test that the hunger state also modulates the PER response to sweet and bitter stimuli with our methodology, w^{1118} flies were tested in three metabolic states: fed, 12h starved, and 24h starved. We decided to test only four mixtures: 50 mM of sucrose alone and 50 mM of sucrose mixed with 5, 10, and 20 mM of caffeine. These mixtures gave us the possibility to compare not only between metabolic states but also among sweet-bitter value coding. Flies starved for 24h showed the highest PER for all mixtures, and the fed condition showed the lowest PER, the 12h starvation PER response between them (**Figure 26C**). Even though only the 10 mM and 20 mM caffeine mixtures were significant, the tendency was that the hunger state of the fly impacted PER proportionally for all mixtures. Furthermore, it is essential to note that for the fed state there was a non-PER saturation for the 10 mM and 20 mM caffeine mixtures which indicated that bitter stimuli at concentrations higher than 10 mM of caffeine suppressed PER.

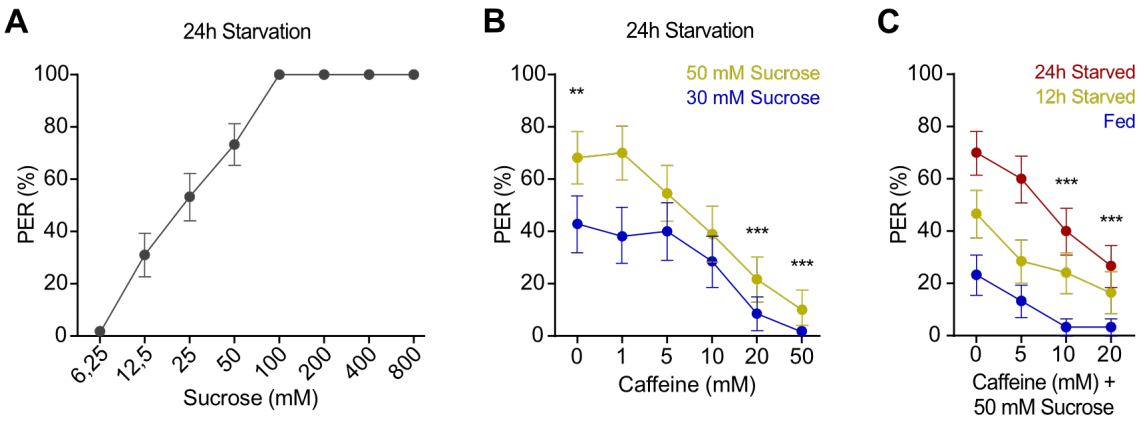

Figure 26: Proboscis extension response assay in *w*^{1118} flies. (**A**) PER to increased concentrations of sucrose in *w*^{1118} flies that have been starved for 24 hours. (**B**) PER to increased concentrations of caffeine mixed with 50 mM (yellow) and 30 mM (blue) of sucrose in *w*^{1118} flies that have been starved for 24 hours. (**C**) PER to increased concentrations of caffeine mixed with 50 mM of sucrose in *w*^{1118} flies in three different metabolic states: fed (blue), starved for 12 hours (yellow) and starved for 24 hours (red). All x-axis represents the concentrations of mixtures delivered in the PER and the y-axis the percentage (%) of flies that showed PER. n=30 for all concentrations and metabolic states tested. The statistical test was a binomial regression model; error bars represent the standard error of the proportion; only significant differences are shown: ****p<0,001*.

Considering these results, the final mixtures chosen (50 mM sucrose alone and 50 mM sucrose with 5, 10, and 20 mM caffeine) for experiments involving Lk transgenic flies were deemed suitable for comparing metabolic stages and identifying potential deficiencies in PER due to the absence of *Lk* gene expression in the fed condition. Additionally, 50 mM sucrose with 1 mM caffeine was added to the mixtures to reference the PER with a diluted bitter mixture.

4.2. SELK neurons are involved in the feeding initiation behavior

We have tested that sucrose enhances PER response as concentration increases (**Figure 26**). A bitter compound such as caffeine elicits a reduction in the PER elicited by a sweet compound, indicating the existence of a value coding behavior in feeding initiation as previously reported (Inagaki et al., 2014). To test the function of the SELK neurons in the feeding initiation behavior, *Lk-Gal4>UAS-TNT* and *Lk-Gal4>UAS-TNT*^{IMP} transgenic flies were assayed with labellar stimulation PER only to measure the SELK role and not other Lk neuron implication, as previously explained.

Previous studies reported that mutant flies for the Lk gene induced a decrease in PER response to sucrose by labellar stimulation (Zandawala, Yurgel, et al., 2018). This may indicate that SELK neurons are involved in the response to sucrose. To evaluate this possibility, we assayed the *Lk-Gal4>UAS-TNT* and *Lk-Gal4>UAS-TNT*^{IMP} transgenic flies with the same sucrose concentrations as **Figure 26**. We did not see differences between *Lk-Gal4>UAS-TNT* or *Lk-Gal4>UAS-TNT*^{IMP} in their capability to respond to

sucrose at all concentrations tested, indicating that, in our hands, Lk neurons do not modulate per se the response to sucrose at the concentrations tested (**Figure 27**). Consistent with the results obtained with *w*^{1118} flies, at 50mM sucrose approximately 50% of the flies responded to sucrose, both control (*Lk-Gal4>UAS-TNT*^{IMP}) and experimental (*Lk-Gal4>UAS-TNT*) conditions, indicating that this was an appropriate sucrose concentration to test flies with the different concentrations of caffeine previously established.

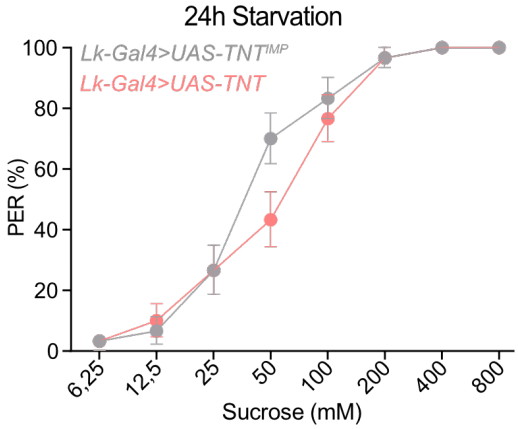

Figure 27: Role of SELK neuron during proboscis extension response to sucrose. PER to increased concentrations of sucrose of flies in which TNT is expressed under the control of *Lk* promoter (in pink). Comparisons are made with control animals expressing and impaired version of this toxin (TNT^{IMP}) (in grey). All flies were starved for 24 hours. n=30 for all concentrations and transgenic lines tested. The statistical test applied was a binomial linear regression model; error bars represent the standard error of the proportion; no significant differences were obtained.

The addition of caffeine to sucrose decreases the PER in a concentration-dependent manner (**Figure 26B**). We found that silencing of Lk neurons with TNT decreased the ability of the flies to respond to sucrose + caffeine, making this effect more dramatic with longer starvation times (**Figure 28**). In detail, we found that when flies are fed, the response of control and experimental conditions was similar to the different mixtures, indicating that the reduction in *Lk* gene expression by SELK neurons, according to data shown above (**Figure 28A**), makes that neuron noncapable to participate in the sensory integration of bitter and sweet information.

Contrarily, when *Lk-Gal4>UAS-TNT* and *Lk-Gal4>UAS-TNT*^{IMP} flies undergo a 12-hour period of starvation, we hypothesized that *Lk* gene expression increases and may alter how sweet and bitter information is processed. Our findings suggest that while blocking synaptic transmission of SELK neurons with TNT did not affect the PER response to sucrose alone and with low concentrations of caffeine, silencing the SELK neurons with TNT decreased the PER response at higher concentrations of caffeine compared to control TNT^{IMP} at 12h starvation (**Figure 28B**). This observation implies that SELK neurons might modulate the attractiveness of stimuli based on the metabolic state

and the intensity of bitter stimuli. However, when SELK neurons were blocked with TNT, they appeared to lose this ability to encode combinatory sweet-bitter information, thus potentially devaluing the hunger state by reducing the PER response at higher concentrations of caffeine.

When flies were subjected to a 24-hour starvation period, the levels of *Lk* gene expression increased compared to fed and 12-hour starved flies (**Figure 28C**). This resulted in higher differences in PER responses between control flies and the experimental condition across all mixtures of sucrose and caffeine, unlike the response observed with 50 mM sucrose alone in previous experiments (**Figure 27**). Our analysis revealed that the differences between control and experimental conditions were statistically significant at 5, 10 and 20 mM of caffeine with 50 mM sucrose (**Figure 28C**). Moreover, these differences increased gradually in proportion to the concentration of caffeine. This observation suggests that as the bitterness of the stimuli increases, the positive value coding mediated by *Lk-Gal4>UAS-TNT* flies diminishes, as evidenced by lower PER response levels.

These findings suggest that SELK neurons are critical in integrating sweet and bitter sensory information. The ability to respond to a mixture of sucrose and caffeine was reduced when the Lk neurons were silenced. This effect was particularly significant when flies were under conditions of increased starvation. This implies that the activity of SELK neurons is essential for processing and responding to combined sweet and bitter stimuli, especially in situations where food availability is limited.

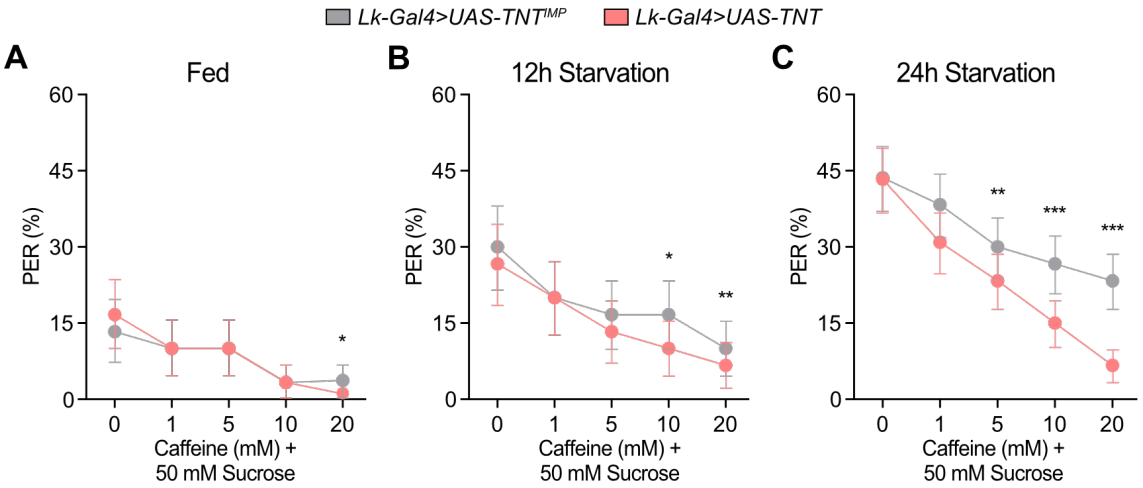

Figure 28: Role of SELK neurons in proboscis extension response to sweet and bitter tastants for three different metabolic states. PER to increased concentrations of caffeine mixed with 50 mM of sucrose of flies in which TNT is expressed under the control of *Lk* promoter (in pink) for three different metabolic states: fed (**A**), starved for 12 hours (**B**) and starved for 24 hours (**C**). Comparisons are made with control animals expressing and impaired version of this toxin (TNT^{IMP}) (in grey). All flies were starved for 24 hours. n=30 for all concentrations, metabolic

states and transgenic lines tested. The statistical test was a binomial regression model; error bars represent the standard error of the proportion; only significant differences are shown: **p<0,05, ***p<0,01, ***p<0,001*.

Despite the differences found between the control and experimental conditions for all metabolic states tested, all results were analyzed with both sexes mixed, so we did not know clearly if these differences might be the effect of males and females or maybe only one of them. Several studies support the idea that males and females differ in integrating gustatory information. First, the gustatory receptor neurons' distribution is sexually dimorphic (S. et al., 2001). This may suggest the different feeding needs between both sexes. For example, males prefer feeding rather than courting upon starvation (Cheriyamkunnel et al., 2021). Females prefer to feed on protein sources rather than sweet or fatty acid food, compared to males (Steck et al., 2018). These differences may reflect the nutrient demands of females from egg production according to their reproductive state.

To see if the SELK effect found in the PER experiments resulted from male or female behavior, we analyzed the PER responses to the mixtures in both sexes when they were starved for 24 hours. We saw that the differences between control and experimental conditions were maintained in males and females (**Figure 29**). If we focus on males (**Figure 29A**), we can see that there is a tendency in PER response similar to both sexes mixed (**Figure 28C**). The ability to respond to mixtures with higher concentrations of caffeine decreases in the *Lk-Gal4>UAS-TNT* flies. This is also seen if we focus on the PER response for mated females (**Figure 29B**), especially for 10 mM and 20 mM caffeine mixtures. It is important to note that there were visual differences between males and females. Despite both results are not statistically compared to each other, we saw that females showed less PER response compared to males in both control and experimental conditions (**Figures 29A** and **29B**). This is also consistent with previous results, which indicate that females are less sensitive to sweetness due to the metabolic differences associated with mated status (Münch et al., 2022).

On the other hand, the mating status of females is a crucial factor that modulates decision-making processes by altering the chemosensory processing of food stimuli and influencing nutrient-specific appetites (Münch et al., 2022). For instance, while male and non-mated female flies typically prefer sugar over yeast, mated females exhibit a shift towards preferring yeast (Kahsai et al., 2010; Ribeiro & Dickson, 2010). Moreover, low protein intake in mated females triggers a compensatory appetite for yeast, mediated by direct neuronal nutrient sensing mechanisms that enhance taste perception (Henriques et al., 2020). These findings suggest that the brain integrates internal states, such as

mating status, to assess the value of external sensory information from potential food sources. Ultimately, this guides food choice and maintains nutrient and energy homeostasis (Carvalho-Santos et al., 2020). Building upon this, it was hypothesized that the mating status of females could impact the normal function of SELK neurons, potentially leading to variations in the perception of bitter and sweet information as observed in the PER assay (**Figure 28**).

To assess this, we tested 7-day-old non-mated females (virgin females) that were raised separately from males to avoid copulation and that were starved for 24h. We saw that PER response from control and experimental conditions were similar except when there was a large concentration of caffeine (20 mM caffeine) (**Figure 29C**). This may reflect that SELK neurons are probably integrating also indirect information from the reproductive state of the fly, leading to a general decrease in the ability to sense sucrose and caffeine. Furthermore, non-mated females seem to show less PER response for 50 mM sucrose. This is consistent with previous studies that found a lack in the sweet perception of non-mated females compared with mated ones (Münch et al., 2022). Non-mated females presented a milder slope in the curve across all sucrose + caffeine mixtures, indicating that they presented more tolerance to bitter than mated females (**Figure 29B** and **29C**).

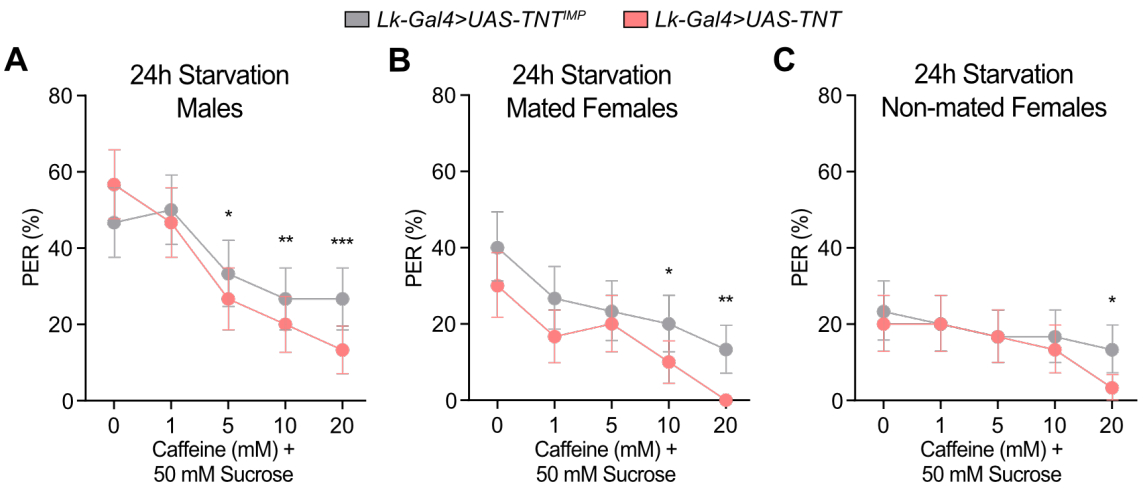

Figure 29: The role of SELK neurons in proboscis extension response to sweet and bitter tastants during starvation is dependent on sex and reproductive state. PER to increased concentrations of caffeine mixed with 50 mM of sucrose of flies in which *UAS-TNT* is expressed under the control of *Lk* promoter (*Lk-Gal4*) (in pink) for three different sex and reproductive states: males (**A**), mated females (**B**) and non-mated females (**C**). Comparisons are made with control animals expressing an impaired version of this toxin (*UAS-TNT^{IMP}*) (in grey). All flies were starved for 24 hours. n=30 for all concentrations and transgenic lines tested. The statistical test was a binomial regression model; error bars represent the standard error of the proportion; only significant differences are shown: **p<0,05, ***p<0,01, ***p<0,001*.

In summary, all these results suggest that Lk may be involved in the sensory processing of labellar sweet and bitter information via SELK neurons. These SELK neurons integrate this combined gustatory information to finally initiate or not feed according to the food source's bitterness and hunger state.

4.3. Role of Leucokinin neurons during two-choice feeding decisions

We have tested the role of SELK neurons in the initiation of feeding when flies are exposed to sweet and bitter tastants in different metabolic states with the PER assay (**Figure 28**). These PER experiments revealed that blocking the synaptic transmission of SELK neurons with TNT led to a loss of tolerance to bitter compounds when flies were food-deprived. Still, we did not see any effect in the initiation of feeding when flies were exposed to only sucrose (**Figure 27**).

A free-moving and feeding assay is necessary to test the role of Lk neurons in a more natural paradigm. To achieve that, we decided to perform a set of flyPAD experiments. In this feeding assay, we were able to measure different feeding parameters in free-moving flies when exposed to two food sources, each connected to one electrode that registers all fly interactions (**Figure 30A**). These experiments have the difficulty that there are so many variants that may affect the feeding behavior as flies can touch the food sources with the leg tarsi, explore the entire arena without interacting with the food drop, or just be influenced by any odor or pheromone, even though all arenas and electrodes are carefully cleaned with alcohol and sterile water. Moreover, by using the *Lk-Gal4* driver, we were silencing all Lk neurons and not only the SELK neurons, so with this flyPAD experiments, we could not differentiate the effect of just blocking SELK neurons among all Lk neurons effect because flies could contact food with other taste organs apart from the proboscis.

For the two-choice feeding assay, we decided to test flies' ability with silenced Lk neurons with two different experiments (**Figure 30B**). The first one (Experiment 1), to choose between two concentrations of sucrose: 20 mM versus 100 mM of just sucrose. The second one (Experiment 2), to test their ability to choose between a source of sucrose (20 mM Sucrose) versus a high concentration of sucrose with caffeine (100 mM sucrose + 50 mM caffeine). By analyzing the total number of sips between both control (*Lk-Gal4>UAS-TNT*^{IMP}) and experimental (*Lk-Gal4>UAS-TNT*) transgenic lines, no differences were detected for any of the two experiments (**Figure 30C**). However, the total number of sips done in Experiment 1 was slightly higher than in Experiment 2. This fact may reflect the avoiding effect of bitter (caffeine) when mixed with sweet (sucrose). When analyzing the preference index for both experiments, in Experiment 1 there was a

preference to feed from the higher concentration of sucrose (100 mM sucrose) compared to the lower (20 mM sucrose), showing that the experimental flies (*Lk-Gal4>UAS-TNT*) were significantly more attracted to 100 mM sucrose than control flies (*Lk-Gal4>UAS-TNT*^{IMP}) (**Figure 30D left**). This difference disappeared when caffeine was added to the highest concentration of sucrose (100 mM sucrose + 50 mM caffeine), flies with Lk neurons silenced (*Lk-Gal4>UAS-TNT*) felt as repelled by the combination of sucrose plus caffeine as controls (*Lk-Gal4>UAS-TNT*^{IMP}), without showing any clear tendency to feed from any source of food (**Figure 30D right**).

Altogether, those data indicate that SELK neurons may be involved in integrating sweet and bitter information to initiate feeding upon starvation, but when flies were exposed to a free-moving feeding test we could not attribute any role to the SELK neurons as more taste organs could direct or indirectly communicate with other implicated Lk neurons.

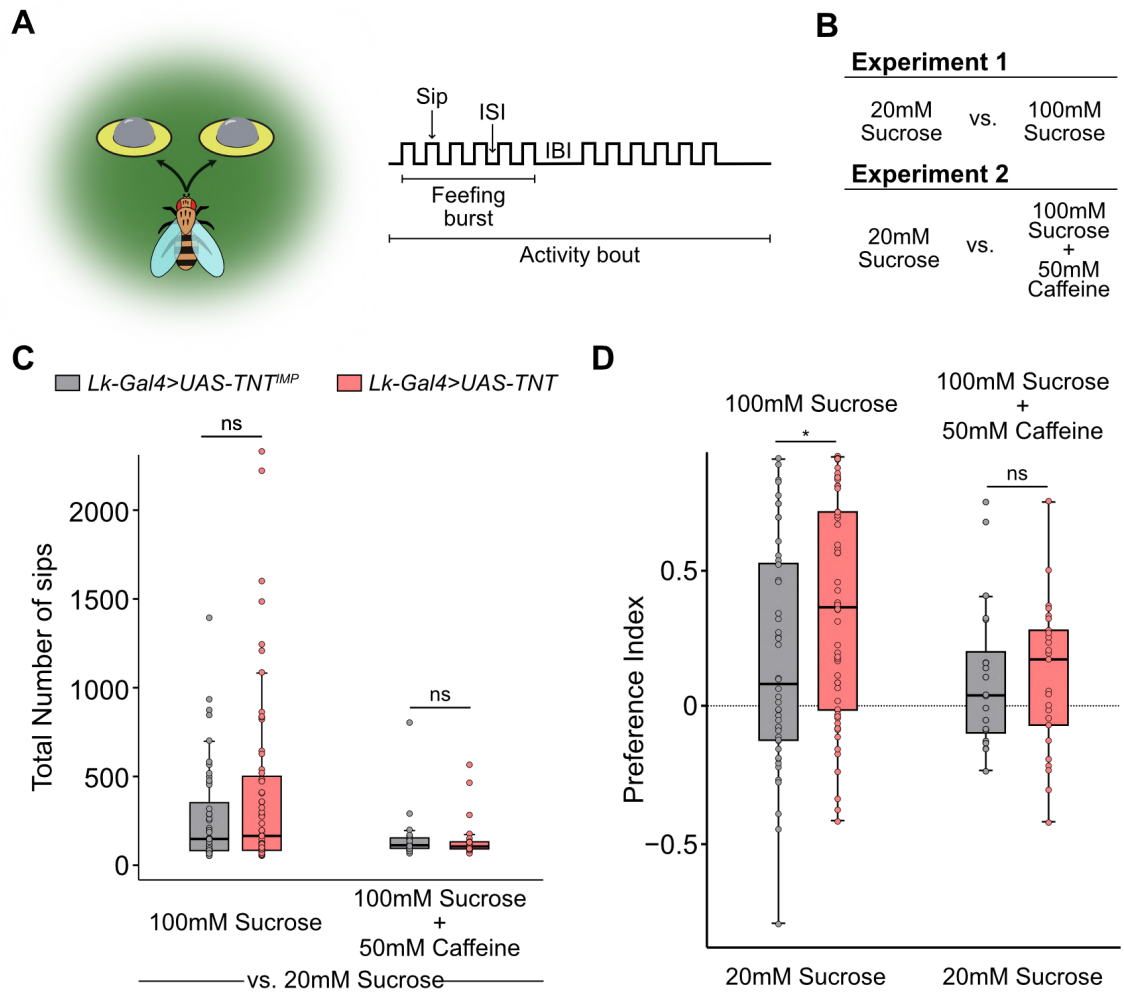

Figure 30: Role of Lk neurons during feeding behavior in two-choice flyPAD assay. (**A**) Schematic representation of the two-choice flyPAD assay, where free-moving flies can choose between two sources of food connected to electrodes and the feeding microstructure parameters

that can be measured (adapted from *Itskov et al., 2014*). (**B**) Mixture of tastants delivered to each electrode for each of the flyPAD experiments carried out; Experiment 1: 20 mM of sucrose versus 100mM sucrose, Experiment 2: 20 mM of sucrose versus 100 mM sucrose with 50mM caffeine. (**C**) Total number of sips for *Lk-Gal4>UAS-TNT*^{IMP} (grey, control condition) and *Lk-Gal4>UAS-TNT* (pink, experimental condition) flies. (**D**) Preference index for 100 mM sucrose (Experiment 1) and 100 mM sucrose with 50 mM caffeine (Experiment 2) versus 20 mM sucrose. All flies were starved for 24 hours. Only flies with >2 bouts and >25 sips were included in the analysis (Experiment 1: *Lk-Gal4>UAS-TNT*^{IMP} (n=48) and *Lk-Gal4>UAS-TNT* (n=59); Experiment 2: *Lk-Gal4>UAS-TNT*^{IMP} (n=20) and *Lk-Gal4>UAS-TNT* (n=25)). The statistical test applied was a Wilcoxon rank sum test; ns: not significant, **p<0,05*.

5. SELK neurons express other neurotransmitters

Leucokinin is expressed in four neurons in the CB: two of them are located in the LH (LHLK) and the other two are located at the ventral part of the SEZ (SELK) (**Figure 16**). These SELK neurons are postsynaptic neurons to sweet and bitter GRNs (**Figures 20, 21** and **S5**), so these are Gr64f^{GSON} and Gr66a^{GSON} even though Lk was only seen to be highly expressed in the Gr66a^{GSON} when flies were food deprived (**Figure 15B**).

As **Figure 14** and **Figure 15** show, there are several neurotransmitters and neuropeptides and their receptors that are also highly expressed in the Gr64f ^{GSON} and Gr66a^{GSON} populations. For example, *Gad1* and *Ddc* were highly expressed in GSON populations for both metabolic states, indicating that gustatory information may be integrated by GABAergic and dopaminergic circuits (**Figure 14B**). For example, dopaminergic neurons are required for increased sucrose taste sensitivity by glutamine diet and in the induction of PER (S.-S. Li et al., 2024; Marella et al., 2012). Further, GABAergic neurons convey, upstream to the motor neurons, an inhibitory tone on ingestive behavior required to regulate taste quality and satiety state (Cheung & Scott, 2017; Pool et al., 2014; Zhao et al., 2022). Other neurotransmitters like 5-HT are involved in feeding behavior through serotonergic pathways that integrate bitter information to initiate gastric motility and induce insulin release via IPC neurons to limit sugar consumption (Yao & Scott, 2022). Also, the dopaminergic neurons interact with the insulin-producing neurons to enhance sweet taste sensitivity (Q.-P. Wang et al., 2020).

In summary, many neurotransmitters and neuronal pathways are involved in gustatory integration and feeding behavior. Several studies have focused on finding Lk co-expression with other neuropeptides in the LHLK and ABLK neurons. Still, little is known about the molecular nature of the SELK neurons that could be modulating their role during gustation (Nässel & Wu, 2021). To further characterize how gustatory information is processed in the CNS, and more specifically, how GSONs may be integrating this information, we wondered if some of the neurotransmitters and receptors

analyzed in the RNAseq (**Figure 14**) could also be expressed in the SELK neurons. We focused on some neurotransmitters, especially: GABA, dopamine, glutamate, acetylcholine, serotonine, octopamine and tyrosine. First, we performed immunohistochemistry of some driver lines for them (**Figure 31**) to test how many neurons in the CB may be expressing each of the neurotransmitters and, more specifically, if most of these neurons were surrounding the SEZ, where the GSONs populations analyzed (**Figure 6**) fall in. We saw the same labeling patterns as previously described (Deng et al., 2019) for each of the neurotransmitters tested (**Figure 31**). Some of these neurons labeled fallen within the SEZ, where SELK neurons are located, suggesting that some of those neurons could be GSONs analyzed in the RNAseq.

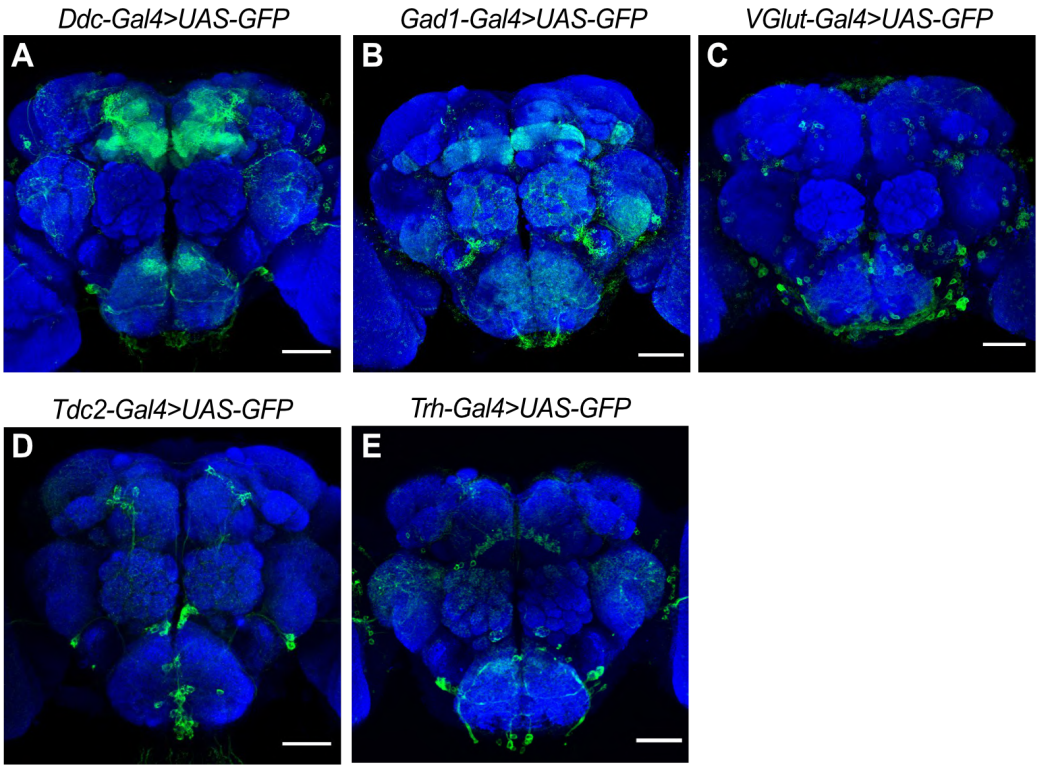

Figure 31: Neurotransmitter expression pattern in the central brain. Anatomy of the different neurotransmitter expression patterns by expressing *UAS-CD8::GFP* (labeled with anti-GFP (green)) via different *Gal4* promoters: *Ddc-Gal4* (dopaminergic neurons) (**A**), *Gad1-Gal4* (gabaergic neurons) (**B**), *VGlut-Gal4* (glutamatergic neurons) (**C**), *Tdc2-Gal4* (octopaminergic and tyraminergic neurons) (**D**) and *Trh-Gal4* (serotoninergic neurons) (**E**). Brain structure (blue) was labeled with anti-nc82. Scale bars: 50 µm.

As we wanted to focus on analyzing which is the expression pattern of the SELK neurons, we focused our effort on trying to find neurotransmitters, or their receptors, expression in the SELK neurons by co-localizing the signal of the anti-LK antibody with the expression of GFP under the control of different neurotransmitters and neurotransmitter receptors promoters (**Figures 32** and **33**, respectively). As we can see in **Figure 32**, for the six sets of neurons tested with the promoters *VGlut* (Vesicular glutamate transporter) for glutamatergic neurons (**Figures 32A-A'**), *SerT* (Serotonine

transporter) and *Trh* (tryptophan hydroxylase) for serotonergic neurons (**Figures 32B-B'** and **C-C'**), *Gad1* for GABAergic neurons (**Figures 32D-D'**), *TH* (Tyrosine hydroxylase) and *Tdc2* (Tyrosine decarboxylase 2) for dopaminergic neurons (**Figures 32E-E'** and **F-F'**), and *ChAT* (Choline cetyltransferase) for acetylcholinergic neurons (**Figures 32G-G'**), we only saw co-localization with the SELK neurons for the *ChAT* promoter (**Figures 32G-G'**), indicating that SELK neurons may also be cholinergic neurons. Nevertheless, the expression pattern of *ChAT* in the central brain is so dispersed that confirmation with another Gal4 line for cholinergic neurons may be necessary. Moreover, further GABA driver lines should be tested as the FAFB dataset indicated that both SELK candidate neurons are potential GABAergic neurons.

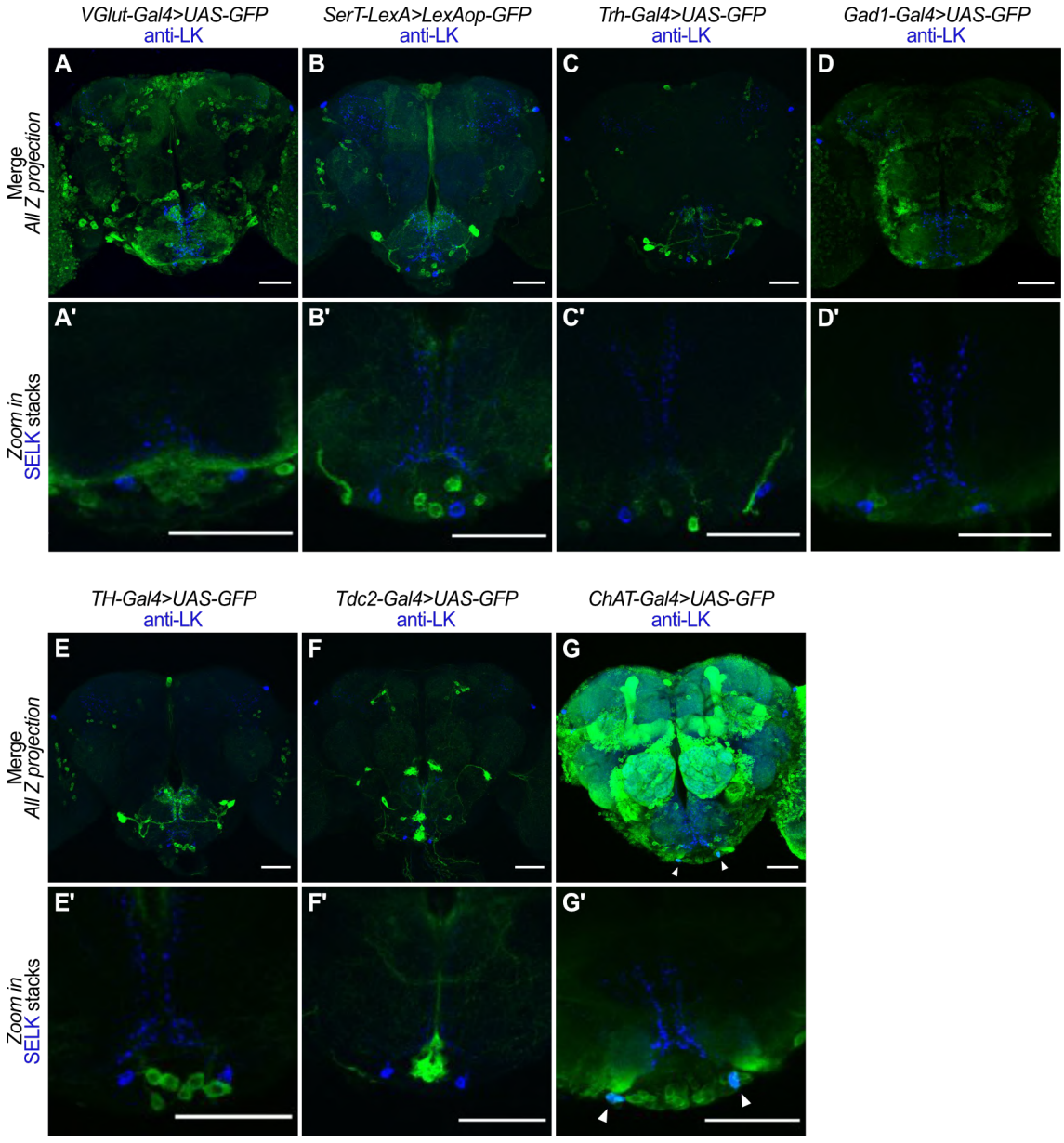

Figure 32: Co-localization between SELK neurons and several neurotransmitters tested. Colozalization of the SELK neurons labeled with anti-LK antibody (blue) with the anatomy of the different neurotransmitter expression patterns studied by expressing *UAS-CD8::GFP* (by Gal4

drivers) or *LexAop-mCD8::GFP* (by LexA drivers) (labeled with anti-GFP (green)) via different driver lines: *VGlut-Gal4* (glutamatergic neurons) (**A** and **A'**), *SerT-LexA* (serotorinergic neurons) (**B** and **B'**), *Trh-Gal4* (serotoninergic neurons) (**C** and **C'**), *Gad1-Gal4* (GABAergic neurons) (**D** and **D'**), *TH-Gal4* (dopaminergic neurons) (**E** and **E'**), *Tdc2-Gal4* (dopaminergic neurons) (**F** and **F'**) and *ChAT-Gal4* (acetylcholinergic neurons) (**G** and **G'**). White arrows indicate co-localization between anti-LK signal and GFP. Scale bars: 50 µm.

Focusing on the expression of some neurotransmitter receptors in SELK neurons (**Figure 33**), we decided to test some Dopamine and GABA receptors using the *Dop2R-Gal4* (**Figures 33A-A'**), *Dop1R2-Gal4* (**Figures 33B-B'**), *GABA-BR2-Gal4* (**Figures 33C-C'**) and *GABA-BR3-Gal4* (**Figures 33D-D'**) promoters. For these four driver lines tested, we did not see any co-localization between their expression pattern and the SELK neurons labeling with anti-LK antibody. Anyway, further *Gal4* promoter lines for GABA and dopamine receptors should be tested in order to see any possible co-localization to them with the SELK neurons.

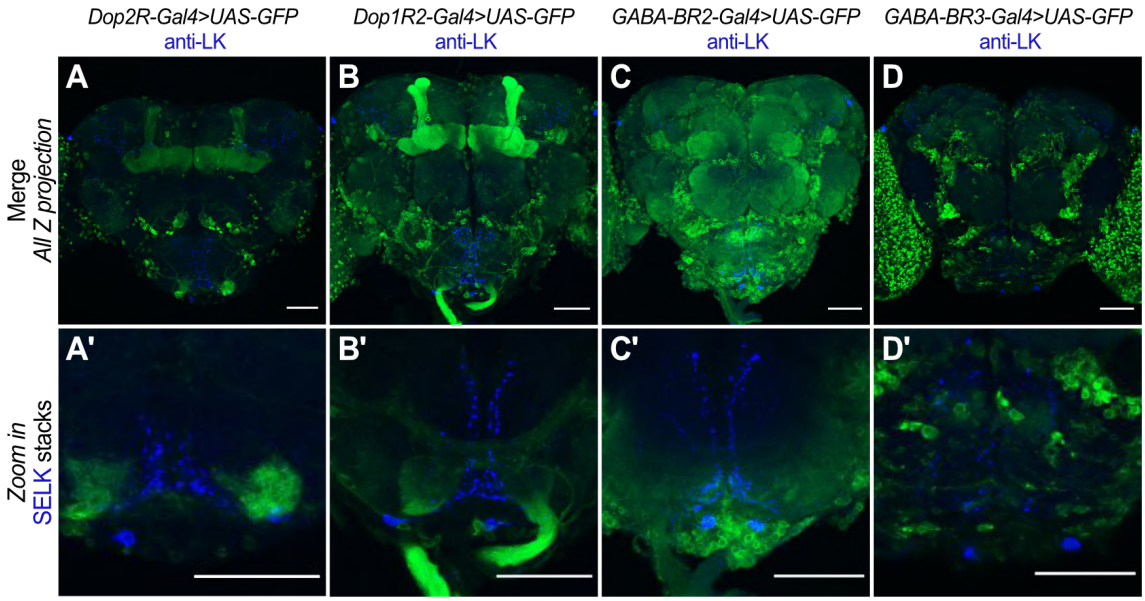

Figure 33: Co-localization between SELK neurons and the dopamine and GABA receptors. Co-localization of the SELK neurons labeled with anti-LK antibody (blue) with the anatomy of the different neurotransmitter expression patterns studied by expressing *UAS-CD8::GFP* (labeled with anti-GFP (green)) via different *Gal4* promoters: *Dop2R-Gal4* (**A** and **A'**), *Dop1R2-Gal4* (**B** and **B'**), *GABA-BR2-Gal4* (**C** and **C'**) and *GABA-BR3-Gal4* (**D** and **D'**). Scale bars: 50 µm.

All these results suggest a possible co-expression of *Lk* and *ChAT* in the SELK neurons, indicating that the integration of gustatory information, specifically sweet and bitter, may also be processed by acetylcholinergic circuits. Anyway, further characterization of the expression of SELK neurons for neurotransmitters and its receptors may be done with other Gal4 drivers and by browsing big datasets as the single cell dataset *Scope* (H. Li et al., 2022). These genomic datasets, in combination with the novel electron microscopy reconstruction of the FAFB, will facilitate the research not only in neuroscience but in all scientific fields.

DISCUSSION

Animals constantly process massive amounts of sensory information to drive appropriate behavioral responses to ensure their survival. Thus, it is essential to integrate the information they sense from the environment and the animal's internal state to drive the correct decisions.

In this Thesis, I have contributed to understanding how gustatory and metabolic information are integrated into the central brain of *D. melanogaster*. By using novel transsynaptic labeling techniques like *trans*-Tango, we were able to label most of the GSONs within the SEZ that receive direct input from sweet, bitter, and mechanosensory GRNs, and by FACS isolate each of them. By analyzing the transcriptomic profile of three GSONs population in two different metabolic states, fed and starved using RNAseq, we have found that each of the GSONs is molecularly different according to the taste modality they receive and that starvation significantly alters the gene expression levels for each of the GSONs populations. Moreover, we have found specific transcriptomic patterns for several neuropeptides and neurotransmitters and their receptors that might be involved in the hunger and gustatory integration within the SEZ. One of the most characteristic transcript patterns was leucokinin, which showed higher expression for the bitter $Gr66a^{GSON}$ in starvation. Previously, it was reported that the Lk-producing neurons in the central brain (SELK and LHLK neurons) regulated flies' physiologic state, which finally impacts feeding behavior, sleep activity, and stress responses (Nässel & Wu, 2021; Yurgel et al., 2019; Zandawala, Yurgel, et al., 2018). Consistent with this notion, we wonder if SELK neurons collected bitter information and could be involved in bitter tolerance in starved conditions.

One of the most intriguing discoveries of this Thesis is that, after performing molecular and computational validation of the connectivity of the SELK neurons with the GRNs, SELK neurons are receiving direct input from sweet and bitter GRNs ($Gr64f^{GRN}$ and $Gr66a^{GRN}$). This is the first time we demonstrate that single neurons collect taste information of opposite valences, sweet and bitter. According to that, we tested the functionality of these SELK neurons during feeding initiation behavior by PER and two-choice feeding behavior in free-moving flies by flyPAD with different taste stimuli and metabolic states. Altogether, our results suggest that SELK neurons are involved in the tolerance of bitter taste during starvation, but we did not see any differences in sweet taste behavior. To the best of our knowledge, our work reveals the molecular transcriptomic profile from two metabolic states of three different taste GSON populations for the first time, highlighting behaviorally the essential role of SELK neurons in directly integrating the sweet and bitter taste information.

1. Labeling of the gustatory second-order neurons by *trans*-Tango and FACS technique

The decision to use the *Gr64f-Gal4*, *Gr66a-Gal4*, and *NompC-Gal4* driver transgenic lines to label all the sweet, bitter, and mechanosensory GRNs was crucial to label the correct GSONs populations of interest further. We did not use other taste modalities because we were interested in using two opposite taste modalities (sweet as attractive and bitter as repulsive) and another that modulated the feeding behavior. By using others like salt or fatty acid sensing, we could not obtain such simple stereotyped behaviors because the complexity of their taste detection would have hindered the study of gustatory integration (Ahn et al., 2017; Jaeger et al., 2018; Zhang et al., 2013). We used the *Gr64f-Gal4* and *Gr66a-Gal4* driver lines for sweet and bitter GRNs, respectively, instead of *Gr5a-Gal4* (driver line for sweet GRNs) or *Gr33a-Gal4* and *Gr93a-Gal4* (driver lines for bitter GRNs) because these last ones could be broadly expressed in other gustatory neurons and are less used by the community (Scott, 2018). Moreover, *NompC-Gal4* transgenic line labels specifically mechanosensory neurons in the gustatory sensilla, projecting their axons to the SEZ (Sánchez-Alcañiz et al., 2017; Shearin et al., 2013). Altogether, using these Gal4 drivers we could see the axonal terminals into the SEZ segregating by taste modality.

The ability to label synaptically connected neurons using novel genetic tools has provided fundamental advances in how neurons process information. Our *trans*-Tango experiments allowed us to label most GSONs for each taste modality tested: sweet, bitter, and mechanosensory. However, the *trans*-Tango technique may have some limitations. The number of synaptic connections needed to induce the expression of the second reporter in the postsynaptic neuron is unclear. Similar novel transynaptic techniques like *retro*-Tango, developed by the same laboratory as *trans*-Tango, could not label presynaptic neurons with less than 17 synaptic connections (Sorkaç et al., 2023). Further, our results showed some GSONs in which the soma is dispersed in other regions of the CB, but we were not sure about the possible implication of these GSONs in gustatory processing. We decided to focus our efforts on studying interneurons located in the SEZ as this is the main gustatory processing center (Amrein & Thorne, 2005; Scott, 2005). Another issue to take care of was the growth temperature of the *trans*-Tango flies, as it was critical for the number of GSONs labeled. Previous experiments reported that higher temperatures (25ºC) decrease the number of postsynaptic neurons labeled compared to lower temperatures (18ºC). Still, at low temperatures (18ºC), the possibility of labeling false-positive postsynaptic neurons increases (Talay et al., 2017). Because of that, and to the fact that the formation of synapses increases at lower temperatures

but the final adult behavioral activity remains relatively stable (Kiral et al., 2021), we decided to use only 18ºC in the adult stage to raise the *trans*-Tango flies (and 25ºC in the larval stage) and collect only those GSONs from the SEZ area (**Figures 6** and **7**).

To do the FACS of the GSONs surrounding the SEZ and avoid any false-positive neurons with very low fluorescence, we applied several stringent filters to the GSONs according to their morphology and mtdTomato fluorescence. First, before the FACS procedure, the dissection and disaggregation were restricted only to the SEZ tissue, and any GSONs from other regions of the CB were manually discarded. In that process, the amount of tissue used for each enzymatic digestion was critical as an over-saturation of the enzymes might be reflected in a low yield in the GSON sorting. So far, after testing several preparations and comparing the number of GSONs registered by immunohistochemistry (**Figure 7**) to those sorted, we decided to prepare samples of just 40 SEZs, considering the dissection time. Second, we only sorted those GSONs whose fluorescence fell in the far red area of the filtering (**Figure 10**). This strategy was applied after noticing that some cells could be sorted by their autofluorescence, so this filter allowed us only to sort GSONs and not other cells. Finally, to maximize the yield of the posterior RNA isolation for the RNAseq, we sorted several FACS experiments of the same GSON population in the same tube and directly to the lysis buffer to avoid any GSON loss while pipetting.

Finally, isolating the mRNA to sequence was critical as the total amount of mRNA obtained for each replicate was low. For the fed condition samples, we used a total of approximately 21,000 GSONs in each replicate (**Figure S1**). Still, the number of SEZs dissected was not the same because of the variability efficiency of the digestion before FACS. On the other hand, for the starved condition, we sorted 23,000-27,000 neurons for each replicate (**Figure S2**). These differences in the number of neurons collected per replicate were due to the better experience in the protocol after performing the fed condition and to ensuring that we had enough neurons to isolate sufficient mRNA for the sequencing. Nevertheless, the low amount of mRNA isolated, but with a high-quality range, was enough to perform a normalized ultra-low input RNAseq with $40x10^6$ reads.

In summary, labeling and sorting the different GSON populations allowed us to obtain low, but high-quality, mRNA of those GSON populations.

2. Transcriptional analysis of the gustatory second-order neurons in two different metabolic states

Our results suggest that each of the GSONs analyzed is molecularly different. By considering the PCA, we saw that all replicates clustered by taste modality and metabolic state (**Figure 11**), which indicated that GSONs are integrating the hunger state of flies to modulate how gustatory information is processed. This, in relationship with the previous characterization of some groups of secreting neurons like the Hug-producing neurons or the NPF-producing neurons that surround the SEZ and participate in the regulation of starvation and feeding, could raise the possibility that these neurons pertain to the GSONs analyzed (Feng et al., 2021; Krashes et al., 2009; Melcher & Pankratz, 2005; Schlegel et al., 2016; Thorne et al., 2004). However, the fact that we analyzed the total population of GSONs from each taste modality by bulk RNAseq and not by single-cell RNA sequencing (scRNAseq) does not allow us to establish a direct relationship as to whether any of those secreting neurons could pertain to the GSONs populations analyzed. Thus, a scRNAseq analysis could be done to determine, more specifically, the nature of each of the GSONs that receive direct input from GRNs, but this is much more time-consuming and expensive.

We saw many genes up and downregulated by analyzing the gene differential expression between fed and starved for each GSON population (**Figure 12**). In particular, the expression of some genes changed in all GSON populations during starvation (**Figure 34**). Several were involved in DNA transcription or nervous system development, such as the Leukocyte-antigen-related-like (*Lar*), which is involved in embryonic motor axon guidance and also sleep (Agrawal & Hardin, 2016; Hakeda-Suzuki et al., 2017). However, most were uncharacterized genes, so their role is unknown. Further, some long non-coding RNAs (lncRNAs) showed a change in expression for all the populations. Still, their specific function remains unknown. lncRNAs have been implicated in various biological processes and diseases as critical regulators of gene expression at the epigenetic, transcriptional, and post-transcriptional levels (K. Li et al., 2019). For example, the antisense RNA (asRNA) *asRNA:CR46486* has the opposite matching sequence to the IA-2 protein tyrosine phosphatase (IA-2) gene, which encodes a protein involved in DILP secretion, so it could be involved in facing starvation by modulating the DILP release by IPCs (Harrison et al., 2021; J. Kim et al., 2008). Moreover, to our surprise, other highlighting lncRNA was the *lncRNA:CR44834*, located in the same locus as the *Lk* gene. Despite its transcriptomic profile being not particular, when we saw its expression pattern carefully (**Figure S7**), we realized an increased expression for the fed condition compared to starvation for all GSON populations. So far,

we have not been able to relate any clear role of lncRNA and asRNA to the GSONs during starvation. Their implication in neurodevelopment, disease and behavior need further study. However, their study in our GSONs context may open an exciting research line to elucidate how not only neuromodulators process gustatory sensory information but also those non-coding RNA species integrate both gustatory information and metabolic state to manipulate the functionality of neural circuits.

Our RNAseq analyses revealed many neurotransmitters, neuropeptides, and their receptors, whose gene expression levels were changed upon starvation (**Figures 14** and **15**). Although it was impossible to directly associate our GSONs to any neuromodulatory set of neurons previously described, the screening of neurotransmitters and neuropeptides allowed us further to characterize the nature of each of the GSONs analyzed. Regarding the expression of neurotransmitter receptors, all the populations highly expressed the *nAChRbeta1*, indicating that GSONs receive acetylcholine input. This is consistent with previous results that characterized the GRNs as acetylcholinergic, so its receptor in the GSONs validated that the RNAseq analysis was correct (Jaeger et al., 2018). However, we cannot confirm that all GSONs express the *nAChRbeta1* as these analyses are from a bulk RNAseq. Similarly, the expression of *Ddc* and *Gad1* suggested the interplay of dopaminergic and GABAergic signaling during gustatory processing, and probably some GSONs are involved in the indirect inhibition of sweet GRNs by bitter compounds (Chu et al., 2014; Harris et al., 2015; LeDue et al., 2016). The same happens with the expression patterns for neuropeptides, which indicate that within the GSON populations, an extensive range of neurons that express *sNPF, EcR, Dh44, Nplp1, or AstA-R1*, among others, are involved in the neuromodulation of feeding upon starvation. These insights showed a possible connection between presynaptic GRNs and postsynaptic NPF-producing neurons to integrate gustatory information and potentiate sweet sensitivity upon starvation (Feng et al., 2021; Krashes et al., 2009).

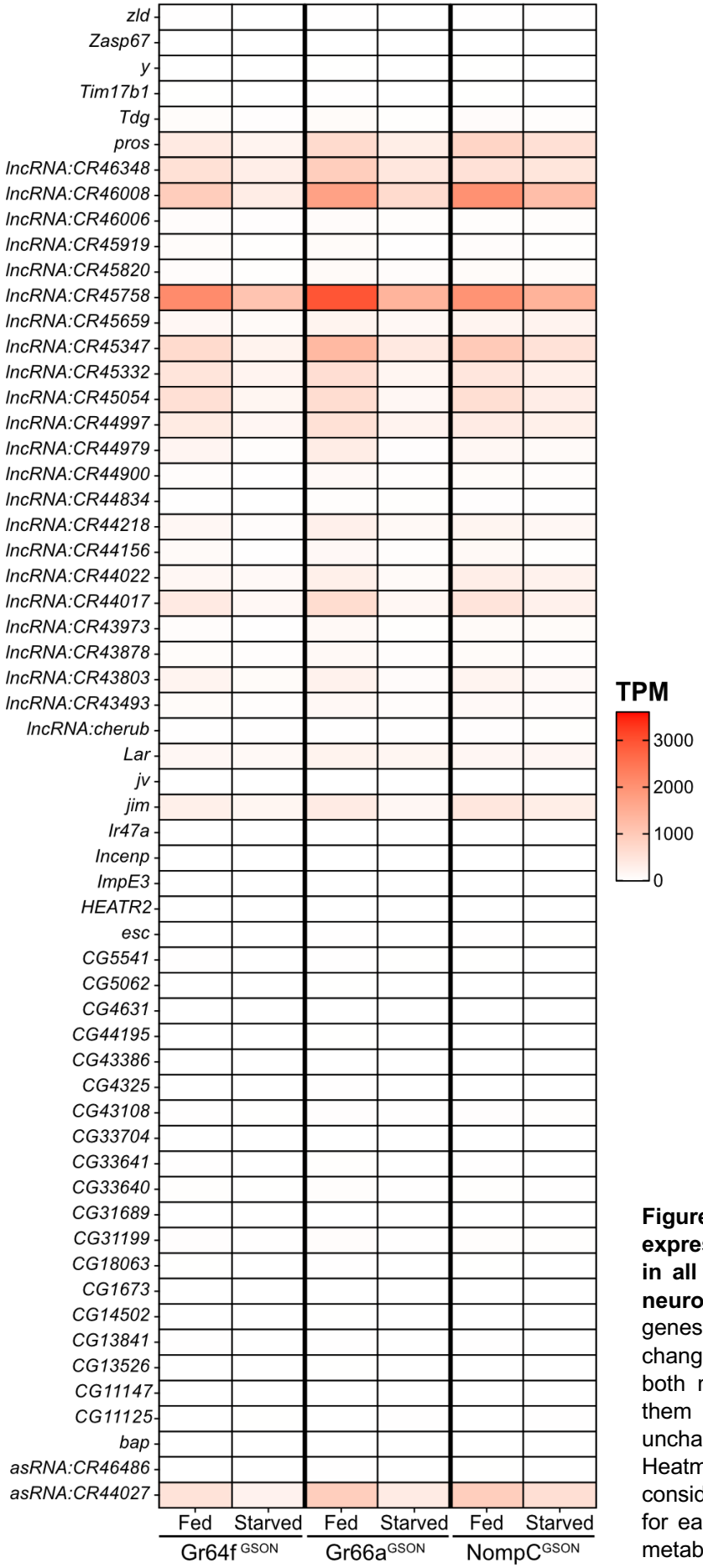

Figure 34: Transcriptomic expression for changed genes in all gustatory second-order neuron populations. Many genes were significantly changed in all populations and both metabolic states. Most of them are lncRNAs and uncharacterized genes. Heatmaps represent total TPM considering the three replicates for each GSON population and metabolic condition.

3. SELK neurons overexpress *Lk* upon starvation and collect gustatory information of opposite valence

Our RNAseq data indicated that *Lk* was only upregulated in starved conditions in the Gr66a^{GSON}. The fact that *Lk* was upregulated upon starvation was also validated by qPCR from FACS-sorted GFP^{+} Lk-producing neurons and by anti-LK fluorescence intensity. Our gained experience with FACS and RNA isolation from *trans*-Tango experiments for the RNAseq allowed us to perform a qPCR from only the SELK and LHLK neurons. Both analyses, from all CB (SELK and LHLK neurons) and SEZ (only SELK neurons), revealed that *Lk* is upregulated in starved conditions (**Figure 17**). This was also validated by the higher fluorescent signal of anti-LK upon starvation of SELK and LHLK (**Figure 18**).

However, despite our predictions being validated, when we further analyzed the co-localization of anti-LK signal with *trans*-Tango labeling, we saw that SELK neurons were labelled by anti-LK antibody and *trans*-Tango from *Gr64f-Gal4* and *Gr66a-Gal4* driver lines, indicating that SELK neurons were Gr64f^{GSON} and Gr66a^{GSON} at the same time (**Figure 20**). This result was validated by GRASP and BAcTrace experiments. With GRASP, we saw that both Gr64f^{GRN} and Gr66a^{GRN} were synaptically connected to SELK neurons (**Figure 21**). This result could be attributed to GRASP employing two candidates to express each portion of the GFP molecule but does not discriminate which neuron may be the pre- and the postsynaptic (Feinberg et al., 2008). On the other hand, BAcTrace concluded that effectively SELK neurons were receiving direct input from Gr64f^{GRN} and Gr66a^{GRN} (**Figure S5**). The question now is why we could not see the upregulation of *Lk* in the Gr64f^{GSON} in our RNAseq analysis. A possible explanation for this question might derive from the capacity of *trans*-Tango to label all postsynaptic neurons to a particular presynaptic neuron, as happens with *retro*-Tango, indicating that possibly the number of synaptic connections between Gr64f^{GRN} and SELK neurons is not large enough. This could be justified by the number of GFP dots labeled by GRASP, which is possibly higher for the Gr66a^{GRN} with SELK than for Gr64f^{GRN} with SELK neurons (**Figure 21**), but this is not conclusive as other experiments with specific synapse markers must be done. Moreover, the presence of GFP signal with GRASP does not mean functionality. Other experiments with an active version of GRASP, which is only reconstructed in active synapses, could be done to find functional synapses between GRNs and SELK neurons (Macpherson et al., 2015).

The fact that the number of putative synapsis from a particular neuron is temperature-dependent in ectothermic animals like *D. melanogaster* could have altered

the *trans*-Tango labeling from Gr64f^{GRN} to SELK neurons by our growth protocol for the RNAseq (Kiral et al., 2021). Nevertheless, we compared the number of neurons labeled by *trans*-Tango in flies raised at different temperatures, and we found that indeed, the number of neurons labeled varied; our protocol labeled the most number of neurons (**Figure 7**). The last reason we wondered was that the FACS protocol used was quite stringent. We only sorted those events filtered within the high red fluorescence group, discarding those with low fluorescence intensity (**Figure 10**). Despite that, we balanced the stringency of the protocol, and it was better to lose GSON fluorescent outliers instead of sequence neurons that did not pertain to the GSON population.

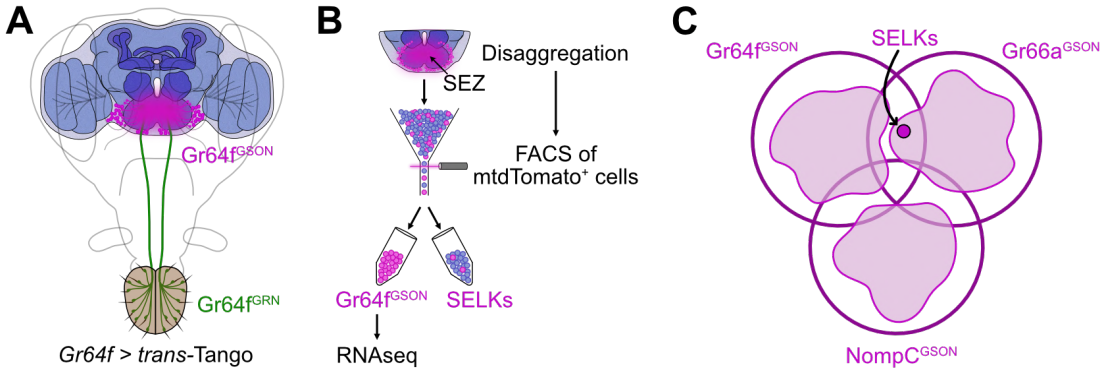

Figure 35: Schematic representation of sweet gustatory second-order neurons FACS sorting. Sweet GSONs labeled by *trans*-Tango (**A**) within the SEZ were FACS sorted by applying a stringent sorting protocol for mtdTomato^{+} cells (**B**). This stringency discarded some mtdTomato^{+} cells like SELKs possibly due to their low fluorescence, only being sorted within the Gr66a^{GSON} population for the RNAseq (**C**).

To further validate that SELK neurons receive direct input from Gr64f^{GRN} and Gr66a^{GRN}, we employed the recently published FAFB connectome with Flywire. Even though we only screened the postsynaptic candidates to sweet and bitter GRNs of the right hemisphere, we could find the left SELK candidate neuron by visual comparisons. Then, we found the right SELK neuron using the Flywire Codex, which morphologically compared both SELK neurons. This right SELK neuron has synaptic connections with the sweet GRNs. Each of them only has 2-3 synaptic connections with the Gr64f^{GRN} and Gr66a^{GRN} analyzed, so it is necessary to perform proofreading of those neurons to characterize them better computationally, as probably more synaptic connections can be traced. However, this proofreading needs to have polished computational skills to avoid errors.

Altogether, we considered that the discrepancy between our RNAseq data and the connectivity analysis points to an imbalance in the number of synaptic inputs onto Lk neurons from Gr64f^{GRN} and Gr66a^{GRN}. Possibly, SELK neurons receive more synaptic input from Gr66a^{GRN} than from Gr64f^{GRN}, indicating that the connectivity of bitter GRNs

is much more robust to Lk neurons than that of the sweet GRNs. So far, our model suggests that SELK neurons are collecting information directly from sweet and bitter GRNs, which is the first time a single neuron in the SEZ is directly collecting information of opposite valence, sweet (attractive) and bitter (repulsive), at the same time (**Figure 36**).

4. SELK neurons integrate gustatory information and the metabolic state to modulate feeding behavior

Our results suggest that SELK neurons integrate gustatory information by their connection with the sweet and bitter GRNs as well as the metabolic state of the fly by overexpressing *Lk* upon starvation. Previously, different studies showed that peptidergic neurons were involved in integrating the metabolic state and the modulation of taste processing. For example, NPF neurons were implicated in the modulation of sweet and bitter sensing in hungry flies to enhance feeding (Feng et al., 2021; Inagaki et al., 2014; Krashes et al., 2009). Similarly, Hug neurons mediated the tolerance to aversive compounds upon starvation by their connection to bitter GRNs (Melcher & Pankratz, 2005; Schlegel et al., 2016; Thorne et al., 2004). Thus, we wondered about the possible role of SELK neurons in regulating sweet and bitter taste processing by integrating the hunger state of flies differently.

Previous studies in other species, such as the cockroach *Leucophaea maderae*, reported many Lk-expressing cells, suggesting a wide range of functions for this peptidergic system (Winther et al., 1996). In *D. melanogaster*, Lk regulates water retention, desiccation, sleep, starvation, and food intake (Y. Liu et al., 2015; Nässel & Wu, 2021). Their role in facing starvation and restoring homeostasis may be due, in part, to their connectivity with the IPCs and ion transport peptides (ITP) neurons (Crocker et al., 2010; Erion et al., 2012; Gáliková et al., 2018; Gáliková & Klepsatel, 2022; Yurgel et al., 2019). The *trans*-Tango and FAFB reconstruction experiments reinforced the possible postsynaptic connectivity from SELK neurons to IPCs and ITPs neurons by comparing the localization of both sets of neurosecretory neurons with the position of postsynaptic neurons to SELK neurons (**Figure 25**). This hypothesis is reinforced by the fact that both neurosecretory cells express the *Lkr* (Yurgel et al., 2019; Zandawala, Yurgel, et al., 2018). However, to confirm that SELK neurons are integrating the metabolic state of the fly via the IPCs and ITPs requires the functional characterization of those connections.

Next, we hypothesized that SELK neurons could regulate the tolerance to bitter compounds when flies are starved. To confirm this, we decided to test behaviorally the role of SELK neurons during feeding behavior. The main problem in testing their role during feeding behavior is that there was not any driver line specifically for the SELK neurons, as we used the *Lk-Gal4,* which drove the expression of *UAS-TNT* and *UAS-TNT^{IMP}* in all Lk neurons (SELK, LHLK and ABLK neurons). However, we decided to use the PER assay in which we only tested the role of SELK neurons by stimulating only the GRNs from the labellum that only connect to SELK and not other Lk neurons.

Similar experiments previously reported that a lack of SELK activity reduced PER to sucrose (Zandawala, Yurgel, et al., 2018). We did not observe any defect in the sensitivity to sucrose when SELK neurons were silenced with TNT (**Figure 27**). These discrepancies could arise from the different PER protocols used, as we only stimulated flies with one single touch instead of three to avoid any extra PER from habituation. Further, we used ice instead of CO_2 to anesthetize flies as CO_2 toxicity could impact flies' behavior (Bartholomew et al., 2015; Verspoor et al., 2015). Then, using 50 mM of sucrose with different concentrations of caffeine allowed us to activate the sweet GRNs with increasing levels of bitter GRNs activation. Our observations showed that differences between the experimental condition (*Lk-Gal4>UAS-TNT*) and the control (*Lk-Gal4>UAS-TNT^{IMP}*) only appeared when flies were starved, and those flies that lost the SELK neurons activity showed decreased PER to higher concentrations of caffeine (**Figure 28**). We wondered if this effect might result from SELK neurons modulating the avoidance of bitter compounds, so when flies are starved, they tolerate better bitter tastants. This insight is in correlation with previous studies of peptidergic neurons that modulate the bitter tastant processing upon starvation to promote feeding (Bader et al., 2007; Melcher & Pankratz, 2005; Thorne et al., 2004). So far, we do not know how sweet and bitter gustatory information modulates the activity of SELK neurons, as we only reported that Lk levels increase upon starvation (**Figures 17**, **18** and **36**). However, other studies reported that starvation does not seem to affect SELK neuron activity, contrary to the LHLK neurons, which are more active during starvation due to the loss of circulating glucose (Yurgel et al., 2019). Thus, further experiments might be required to test the functionality of SELK neurons upon activation of sweet and bitter GRNs by different tastants during starvation. In that line, our laboratory is working on standardizing an *in vivo* calcium imaging protocol that allows us to see both SELK neurons *in vivo* while stimulating GRNs from the labellum with different tastant mixtures. Currently, we have tried it by expressing the *UAS-GCaMP7* in the SELK neurons with the *Lk-Gal4*. Still, its fluorescence was not stable as the SELK somas were not always labeled, and the

location of the SELK neurons in the ventral part of the SEZ, while stimulating the proboscis, was difficult to register.

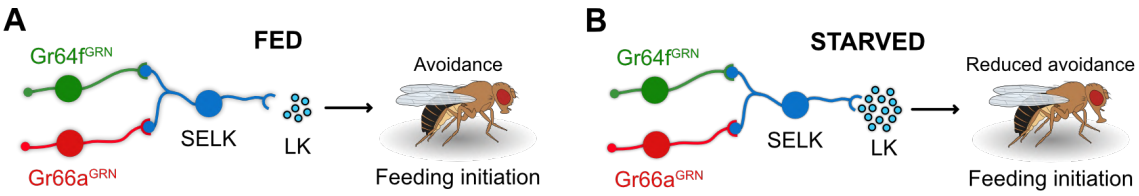

Figure 36: SELK neurons integrate sweet and bitter gustatory information to promote feeding initiation upon starvation. Feeding initiation is modulated by sweet-bitter taste integration via *Lk* expression by SELK neurons. When flies are fed, they are not attracted to bitter compounds, so they avoid them (**A**). However, when flies are starved, SELK neurons overexpress *Lk*, which is related to higher tolerance to bitter compounds and initiation of feeding (**B**).

On the other hand, we decided to test SELK transgenic flies in a two-choice assay. The internal state of flies is integrated into SEZ-specific regions to shape feeding decision-making behaviors (Münch et al., 2022). Regarding this, we wondered if the activity of SELK neurons when flies need to choose between two food sources in a free-moving arena like flyPAD is enough to drive decisions. For this porpoise, we employed a mix of sweet and bitter sources. However, as flies could move freely in the arena, tastants were sensed by different GRNs spread in the legs and proboscis and the ovipositor system in females. We did not see any effect from inhibiting Lk neurons with TNT. This could be because, during decision-making processes in that paradigm, the other Lk-producing neurons (LHLK and ABLK) and other neurons may be involved and could buffer the SELK inhibition effect. To further test the possible role in free-moving flies, optogenetic activation or inhibition of SELK neurons by expressing CsChrimson or GtACR2 in Lk neurons could be an excellent strategy to test feeding behavior changes when flies touch with the proboscis, the food source in the optoPAD (Moreira et al., 2019).

5. Are SELK neurons expressing other neurotransmitters?

Our RNAseq analysis revealed that a wide range of neurotransmitters, neuropeptides, and receptors were expressed in the GSONs. This suggested that neurons of diverse natures could be involved in different pathways among those populations, highlighting the complexity of gustatory processing.

One of the main disadvantages of our bulk RNAseq analysis was that we could not attribute the molecular nature to a small group of neurons, as each GSON population was composed of at least 70-80 neurons. A scRNAseq analysis would have provided a

more detailed characterization of the individual molecular nature of those GSONs. We found two single neurons that receive integrated sweet and bitter gustatory information from GRNs and overexpress *Lk* during starvation. Further, these SELK neurons participate in bitter tolerance during feeding upon starvation (**Figure 36**). Despite the described role of SELK neurons during feeding upon starvation, it was necessary to note that our strategy was based on eliminating synaptic transmission with TNT, which inactivates the hole SELK neurons and not only the *Lk* expression and release. Thus, testing their implication in feeding behaviorally by inhibiting *Lk* expression with specific Lk^{RNAi} could demonstrate precisely which could be the role of Lk in the SELK neurons. So far, we could understand if some other neuromodulators are necessary for the SELK's normal function.

Notably, many GSONs were either GABAergic or dopaminergic (**Figure 14**), so we wondered about the possible nature of SELK neurons to express those neurotransmitters or even their receptors. Moreover, according to previous morphology comparisons, the Flywire community classified the SELK neurons as strong GABAergic candidates (Eckstein et al., 2023; Schlegel et al., 2023). The relatively recently published Fly Cell Atlas has provided a massive transcriptomic dataset of the adult fruit fly from distinct tissues (H. Li et al., 2022). It is accessible with the software *Scope*, where we found cells expressing *Lk* and compared them to those expressing GABA or dopamine and their receptors. This strategy was also used by *Zandawalla et al.* (Zandawala, Yurgel, et al., 2018). However, although some cells could be co-expressing *Lk* with some neuromodulators (dopamine receptors (*Dop2R* and *Dop2R1*)), knowing which cells expressing *Lk* represented the SELK or even the LHLK neurons was impossible. Further, we employed the same strategy as done previously with the anti-LK antibody to compare the anti-LK labelling with the expression of GFP reporter by different Gal4 drivers for neurotransmitters and receptors. We did not see co-localization between anti-LK labeling and *Gad1-Gal4>UAS-CD8::GFP*, so this result suggests that SELK neurons are not GABAergic (**Figure 32**). However, the *Gad1-Gal4* driver line used for GABAergic neurons is not enough conclusive as it labels so many dispersed neurons in the brain and other Gal4 lines for GABAergic neurons should be analyzed. We saw only a weak co-localization of the anti-LK signal with the *ChAT-Gal4>UAS-CD8::GFP* reporter signal, indicating that SELK neurons probably express acetylcholine. GSONs express the acetylcholine receptor *nAChRbeta1* (**Figure 14**) as GRNs were characterized as cholinergic (Jaeger et al., 2018), so possibly the SELK neurons are also presynaptic neurons to some GSONs analyzed as several SELK postsynaptic neurons were surrounding the SEZ (**Figure 25**). This hypothesis raises a model where local processing

of gustatory information may occur. However, it is so risky to think about a possible model where SELK neurons could be part of some previous simple models of local depotentiation of bitter taste processing to tolerate further avoiding compound upon starvation (Chu et al., 2014; Harris et al., 2015; LeDue et al., 2016). Moreover, although we know that gustatory information derived from sweet and bitter-sensing GRNs arrives segregated to the SEZ, the SEZ does not show any particular anatomical structure that might indicate its possible function or integration hinders this task. It remains to be explored how gustatory information is integrated and processed in the central brain, what is more complex and sophisticated, and how external sensory information and internal state deal with each other to face proper feeding decision-making processes.

CONCLUSIONS / CONCLUSIONES

1. Gustatory second-order neurons located in the SEZ collecting different type of gustatory sensory information (sweet, bitter and mechanosensory) can be differenciated molecularly according to their gene expression profile.

2. Gustatory second-order neurons integrate the metabolic state of the fly by modulating their transcriptomic profile upon starvation.

3. Lk neurons located in the SEZ (SELK neurons) express *Lk* in a metabolic-dependent manner, and it is more expressed when flies are starved.

4. SELK neurons are gustatory second-order neurons that collect sweet and bitter information from sweet and bitter gustatory receptor neurons located in the labellum, respectively.

5. SELK neurons are involved in integrating sweet and bitter taste in a metabolic-dependent manner to modulate the tolerance to bitter compounds in the feeding initiation behavior.

6. SELK neurons might co-express other neurotransmitters, and acetylcholine is a strong candidate for co-expression.

1. Las neuronas gustativas de segundo orden localizadas en el SEZ que colectan información gustativa de diferente tipo (dulce, amarga y mecanosensitiva) pueden diferenciarse molecularmente de acuerdo a su perfil de expresión génica.

2. Las neruonas gustativas de segundo orden integran el estado metabólico de la mosca a través de la modulación de su perfil transcriptómico frente al ayuno.

3. Las neuronas Lk localizadas en el SEZ (neuronas SELK) expresan *Lk* en función de su estado metabólico, siendo este más expresado cuando las moscas están en ayuno.

4. Las neuronas SELK son neuronas gustativas de segundo orden que colectan información dulce y amarga proveniente de las neuronas gustativas sensoriales dulces y amargas localizadas en el labellum, respectivamente.

5. Las neuronas SELK estan involucradas en integrar el saber dulce y amargo en función del estado metabólico para modular la tolerancia a compuestos amargos en el comportamiento de inicio de la alimentación.

6. Las neuronas SELK pueden estar coexpresando otros neurotransmisores, siendo acetilcolina un fuerte candidato.

REFERENCES

Adams, M. D., Celniker, S. E., Holt, R. A., Evans, C. A., Gocayne, J. D., Amanatides, P. G., Scherer, S. E., Li, P. W., Hoskins, R. A., Galle, R. F., George, R. A., Lewis, S. E., Richards, S., Ashburner, M., Henderson, S. N., Sutton, G. G., Wortman, J. R., Yandell, M. D., Zhang, Q., … Venter, J. C. (2000). The Genome Sequence of *Drosophila melanogaster*. *Science*, *287*(5461), 2185–2195. https://doi.org/10.1126/science.287.5461.2185

Agrawal, P., & Hardin, P. E. (2016). The *Drosophila* Receptor Protein Tyrosine Phosphatase LAR Is Required for Development of Circadian Pacemaker Neuron Processes That Support Rhythmic Activity in Constant Darkness But Not during Light/Dark Cycles. *The Journal of Neuroscience*, *36*(13), 3860–3870. https://doi.org/10.1523/JNEUROSCI.4523-15.2016

Ahn, J.-E., Chen, Y., & Amrein, H. (2017). Molecular basis of fatty acid taste in Drosophila. *eLife*, *6*, e30115. https://doi.org/10.7554/eLife.30115

Ai, M., Blais, S., Park, J.-Y., Min, S., Neubert, T. A., & Suh, G. S. B. (2013). Ionotropic Glutamate Receptors IR64a and IR8a Form a Functional Odorant Receptor Complex In Vivo in Drosophila. *Journal of Neuroscience*, *33*(26), 10741–10749. https://doi.org/10.1523/JNEUROSCI.5419-12.2013

Ai, M., Min, S., Grosjean, Y., Leblanc, C., Bell, R., Benton, R., & Suh, G. S. B. (2010). Acid sensing by the Drosophila olfactory system. *Nature*, *468*(7324), 691–695. https://doi.org/10.1038/nature09537

Al-Anzi, B., Armand, E., Nagamei, P., Olszewski, M., Sapin, V., Waters, C., Zinn, K., Wyman, R. J., & Benzer, S. (2010). The Leucokinin Pathway and Its Neurons Regulate Meal Size in Drosophila. *Current Biology*, *20*(11), 969–978. https://doi.org/10.1016/j.cub.2010.04.039

Amrein, H., & Thorne, N. (2005). Gustatory Perception and Behavior in Drosophila melanogaster. *Current Biology*, *15*(17), R673–R684. https://doi.org/10.1016/j.cub.2005.08.021

Arrese, E. L., & Soulages, J. L. (2010). Insect Fat Body: Energy, Metabolism, and Regulation. *Annual Review of Entomology*, *55*(1), 207–225. https://doi.org/10.1146/annurev-ento-112408-085356

Ashburner, M., Ball, C. A., Blake, J. A., Botstein, D., Butler, H., Cherry, J. M., Davis, A. P., Dolinski, K., Dwight, S. S., Eppig, J. T., Harris, M. A., Hill, D. P., Issel-Tarver, L., Kasarskis, A., Lewis, S., Matese, J. C., Richardson, J. E., Ringwald, M., Rubin, G. M., & Sherlock, G. (2000). Gene Ontology: Tool for the unification of biology. *Nature Genetics*, *25*(1), 25–29. https://doi.org/10.1038/75556

Aso, Y., & Rubin, G. M. (2016). Dopaminergic neurons write and update memories with cell-type-specific rules. *eLife*, *5*, e16135. https://doi.org/10.7554/eLife.16135

Ayroles, J. F., Buchanan, S. M., O'Leary, C., Skutt-Kakaria, K., Grenier, J. K., Clark, A. G., Hartl, D. L., & De Bivort, B. L. (2015). Behavioral idiosyncrasy reveals genetic control of phenotypic variability. *Proceedings of the National Academy of Sciences*, *112*(21), 6706–6711. https://doi.org/10.1073/pnas.1503830112

Bader, R., Colomb, J., Pankratz, B., Schröck, A., Stocker, R. F., & Pankratz, M. J. (2007). Genetic dissection of neural circuit anatomy underlying feeding behavior in *Drosophila*: Distinct classes of *hugin* -expressing neurons. *Journal of Comparative Neurology*, *502*(5), 848–856. https://doi.org/10.1002/cne.21342

Baines, R. A., Uhler, J. P., Thompson, A., Sweeney, S. T., & Bate, M. (2001). Altered Electrical Properties in *Drosophila* Neurons Developing without Synaptic Transmission. *The Journal of Neuroscience*, *21*(5), 1523–1531. https://doi.org/10.1523/JNEUROSCI.21-05-01523.2001

Barnea, G., Strapps, W., Herrada, G., Berman, Y., Ong, J., Kloss, B., Axel, R., & Lee, K. J. (2008). The genetic design of signaling cascades to record receptor activation. *Proceedings of the National Academy of Sciences*, *105*(1), 64–69. https://doi.org/10.1073/pnas.0710487105

Barretto, R. P. J., Gillis-Smith, S., Chandrashekar, J., Yarmolinsky, D. A., Schnitzer, M. J., Ryba, N. J. P., & Zuker, C. S. (2015). The neural representation of taste quality at the periphery. *Nature*, *517*(7534), 373–376. https://doi.org/10.1038/nature13873

Bartholomew, N. R., Burdett, J. M., VandenBrooks, J. M., Quinlan, M. C., & Call, G. B. (2015). Impaired climbing and flight behaviour in Drosophila melanogaster following carbon dioxide anaesthesia. *Scientific Reports*, *5*(1), 15298. https://doi.org/10.1038/srep15298

Bates, A. S., Schlegel, P., Roberts, R. J. V., Drummond, N., Tamimi, I. F. M., Turnbull, R., Zhao, X., Marin, E. C., Popovici, P. D., Dhawan, S., Jamasb, A., Javier, A., Serratosa Capdevila, L., Li, F., Rubin, G. M., Waddell, S., Bock, D. D., Costa, M., & Jefferis, G. S. X. E. (2020). Complete Connectomic Reconstruction of Olfactory Projection Neurons in the Fly Brain. *Current Biology*, *30*(16), 3183-3199.e6. https://doi.org/10.1016/j.cub.2020.06.042

Bell, A. M. (2024). The evolution of decision-making mechanisms under competing demands. *Trends in Ecology & Evolution*, *39*(2), 141–151. https://doi.org/10.1016/j.tree.2023.09.007

Benton, R., Vannice, K. S., Gomez-Diaz, C., & Vosshall, L. B. (2009). Variant Ionotropic Glutamate Receptors as Chemosensory Receptors in Drosophila. *Cell*, *136*(1), 149–162. https://doi.org/10.1016/j.cell.2008.12.001

Bharucha, K. N., Tarr, P., & Zipursky, S. L. (2008). A glucagon-like endocrine pathway in *Drosophila* modulates both lipid and carbohydrate homeostasis. *Journal of Experimental Biology*, *211*(19), 3103–3110. https://doi.org/10.1242/jeb.016451

Bogovic, J. A., Otsuna, H., Heinrich, L., Ito, M., Jeter, J., Meissner, G., Nern, A., Colonell, J., Malkesman, O., Ito, K., & Saalfeld, S. (2020). An unbiased template of the Drosophila brain and ventral nerve cord. *PLOS ONE*, *15*(12), e0236495. https://doi.org/10.1371/journal.pone.0236495

Bohra, A. A., Kallman, B. R., Reichert, H., & VijayRaghavan, K. (2018). Identification of a Single Pair of Interneurons for Bitter Taste Processing in the Drosophila Brain. *Current Biology*, *28*(6), 847-858.e3. https://doi.org/10.1016/j.cub.2018.01.084

Bosch, J. A., Birchak, G., & Perrimon, N. (2021). Precise genome engineering in *Drosophila* using prime editing. *Proceedings of the National Academy of Sciences*, *118*(1), e2021996118. https://doi.org/10.1073/pnas.2021996118

Boto, T., Stahl, A., & Tomchik, S. M. (2020). Cellular and circuit mechanisms of olfactory associative learning in *Drosophila*. *Journal of Neurogenetics*, *34*(1), 36–46. https://doi.org/10.1080/01677063.2020.1715971

Brand, A. H., & Perrimon, N. (1993). Targeted gene expression as a means of altering cell fates and generating dominant phenotypes. *Development*, *118*(2), 401–415. https://doi.org/10.1242/dev.118.2.401

Branson, K., Robie, A. A., Bender, J., Perona, P., & Dickinson, M. H. (2009). High-throughput ethomics in large groups of Drosophila. *Nature Methods*, *6*(6), 451–457. https://doi.org/10.1038/nmeth.1328

Bray, S., & Amrein, H. (2003). A Putative Drosophila Pheromone Receptor Expressed in Male-Specific Taste Neurons Is Required for Efficient Courtship. *Neuron*, *39*(6), 1019–1029. https://doi.org/10.1016/S0896-6273(03)00542-7

Broughton, S. J., Piper, M. D. W., Ikeya, T., Bass, T. M., Jacobson, J., Driege, Y., Martinez, P., Hafen, E., Withers, D. J., Leevers, S. J., & Partridge, L. (2005). Longer lifespan, altered metabolism, and stress resistance in *Drosophila* from ablation of cells making insulin-like ligands. *Proceedings of the National Academy of Sciences*, *102*(8), 3105–3110. https://doi.org/10.1073/pnas.0405775102

Brown, E. B., Shah, K. D., Palermo, J., Dey, M., Dahanukar, A., & Keene, A. C. (2021). Ir56d-dependent fatty acid responses in Drosophila uncover taste discrimination between different classes of fatty acids. *eLife*, *10*, e67878. https://doi.org/10.7554/eLife.67878

Buchanan, S. M., Kain, J. S., & De Bivort, B. L. (2015). Neuronal control of locomotor handedness in *Drosophila*. *Proceedings of the National Academy of Sciences*, *112*(21), 6700–6705. https://doi.org/10.1073/pnas.1500804112

Cachero, S., Gkantia, M., Bates, A. S., Frechter, S., Blackie, L., McCarthy, A., Sutcliffe, B., Strano, A., Aso, Y., & Jefferis, G. S. X. E. (2020). BAcTrace, a tool for retrograde tracing of neuronal circuits in Drosophila. *Nature Methods*, *17*(12), 1254–1261. https://doi.org/10.1038/s41592-020-00989-1

Cameron, P., Hiroi, M., Ngai, J., & Scott, K. (2010). The molecular basis for water taste in Drosophila. *Nature*, *465*(7294), 91–95. https://doi.org/10.1038/nature09011

Cannell, E., Dornan, A. J., Halberg, K. A., Terhzaz, S., Dow, J. A. T., & Davies, S.-A. (2016). The corticotropin-releasing factor-like diuretic hormone 44 (DH 44) and kinin neuropeptides modulate desiccation and starvation tolerance in Drosophila melanogaster. *Peptides*, *80*, 96–107. https://doi.org/10.1016/j.peptides.2016.02.004

Card, G., & Dickinson, M. H. (2008). Visually Mediated Motor Planning in the Escape Response of Drosophila. *Current Biology*, *18*(17), 1300–1307. https://doi.org/10.1016/j.cub.2008.07.094

Carvalho-Santos, Z., Cardoso-Figueiredo, R., Elias, A. P., Tastekin, I., Baltazar, C., & Ribeiro, C. (2020). Cellular metabolic reprogramming controls sugar appetite in Drosophila. *Nature Metabolism*, *2*(9), 958–973. https://doi.org/10.1038/s42255-020-0266-x

Casillas, S., & Barbadilla, A. (2017). Molecular Population Genetics. *Genetics*, *205*(3), 1003–1035. https://doi.org/10.1534/genetics.116.196493

Cavey, M., Collins, B., Bertet, C., & Blau, J. (2016). Circadian rhythms in neuronal activity propagate through output circuits. *Nature Neuroscience*, *19*(4), 587–595. https://doi.org/10.1038/nn.4263

Charlu, S., Wisotsky, Z., Medina, A., & Dahanukar, A. (2013). Acid sensing by sweet and bitter taste neurons in Drosophila melanogaster. *Nature Communications*, *4*(1), 2042. https://doi.org/10.1038/ncomms3042

Chen, X., Gabitto, M., Peng, Y., Ryba, N. J. P., & Zuker, C. S. (2011). A Gustotopic Map of Taste Qualities in the Mammalian Brain. *Science*, *333*(6047), 1262–1266. https://doi.org/10.1126/science.1204076

Chen, Y.-C. D., & Dahanukar, A. (2017). Molecular and Cellular Organization of Taste Neurons in Adult Drosophila Pharynx. *Cell Reports*, *21*(10), 2978–2991. https://doi.org/10.1016/j.celrep.2017.11.041

Chen, Y.-C. D., & Dahanukar, A. (2020). Recent advances in the genetic basis of taste detection in Drosophila. *Cellular and Molecular Life Sciences*, *77*(6), 1087–1101. https://doi.org/10.1007/s00018-019-03320-0

Chen, Z., Wang, Q., & Wang, Z. (2010). The Amiloride-Sensitive Epithelial Na + Channel PPK28 Is Essential for *Drosophila* Gustatory Water Reception. *The Journal of Neuroscience*, *30*(18), 6247–6252. https://doi.org/10.1523/JNEUROSCI.0627-10.2010

Cheriyamkunnel, S. J., Rose, S., Jacob, P. F., Blackburn, L. A., Glasgow, S., Moorse, J., Winstanley, M., Moynihan, P. J., Waddell, S., & Rezaval, C. (2021). A neuronal mechanism controlling the choice between feeding and sexual behaviors in Drosophila. *Current Biology*, *31*(19), 4231-4245.e4. https://doi.org/10.1016/j.cub.2021.07.029

Cheung, S. K., & Scott, K. (2017). GABAA receptor-expressing neurons promote consumption in Drosophila melanogaster. *PLOS ONE*, *12*(3), e0175177. https://doi.org/10.1371/journal.pone.0175177

Chiang, A.-S., Lin, C.-Y., Chuang, C.-C., Chang, H.-M., Hsieh, C.-H., Yeh, C.-W., Shih, C.-T., Wu, J.-J., Wang, G.-T., Chen, Y.-C., Wu, C.-C., Chen, G.-Y., Ching, Y.-T., Lee, P.-C., Lin, C.-Y., Lin, H.-H., Wu, C.-C., Hsu, H.-W., Huang, Y.-A., … Hwang, J.-K. (2011). Three-Dimensional Reconstruction of Brain-wide Wiring Networks in Drosophila at Single-Cell Resolution. *Current Biology*, *21*(1), 1–11. https://doi.org/10.1016/j.cub.2010.11.056

Chu, B., Chui, V., Mann, K., & Gordon, M. D. (2014). Presynaptic Gain Control Drives Sweet and Bitter Taste Integration in Drosophila. *Current Biology*, *24*(17), 1978–1984. https://doi.org/10.1016/j.cub.2014.07.020

Clyne, P. J., Warr, C. G., & Carlson, J. R. (2000). Candidate Taste Receptors in *Drosophila*. *Science*, *287*(5459), 1830–1834. https://doi.org/10.1126/science.287.5459.1830

Corrales-Carvajal, V. M., Faisal, A. A., & Ribeiro, C. (2016). Internal states drive nutrient homeostasis by modulating exploration-exploitation trade-off. *eLife*, *5*, e19920. https://doi.org/10.7554/eLife.19920

Costa, M., Manton, J. D., Ostrovsky, A. D., Prohaska, S., & Jefferis, G. S. X. E. (2016). NBLAST: Rapid, Sensitive Comparison of Neuronal Structure and Construction of Neuron Family Databases. *Neuron*, *91*(2), 293–311. https://doi.org/10.1016/j.neuron.2016.06.012

Court, R., Costa, M., Pilgrim, C., Millburn, G., Holmes, A., McLachlan, A., Larkin, A., Matentzoglu, N., Kir, H., Parkinson, H., Brown, N. H., O'Kane, C. J., Armstrong, J. D., Jefferis, G. S. X. E., & Osumi-Sutherland, D. (2023). Virtual Fly Brain—An interactive atlas of the Drosophila nervous system. *Frontiers in Physiology*, *14*, 1076533. https://doi.org/10.3389/fphys.2023.1076533

Crickmore, M. A., & Vosshall, L. B. (2013). Opposing Dopaminergic and GABAergic Neurons Control the Duration and Persistence of Copulation in Drosophila. *Cell*, *155*(4), 881–893. https://doi.org/10.1016/j.cell.2013.09.055

Crocker, A., Shahidullah, M., Levitan, I. B., & Sehgal, A. (2010). Identification of a Neural Circuit that Underlies the Effects of Octopamine on Sleep:Wake Behavior. *Neuron*, *65*(5), 670–681. https://doi.org/10.1016/j.neuron.2010.01.032

Croset, V., Rytz, R., Cummins, S. F., Budd, A., Brawand, D., Kaessmann, H., Gibson, T. J., & Benton, R. (2010). Ancient Protostome Origin of Chemosensory Ionotropic Glutamate Receptors and the Evolution of Insect Taste and Olfaction. *PLoS Genetics*, *6*(8), e1001064. https://doi.org/10.1371/journal.pgen.1001064

Dahanukar, A., Lei, Y.-T., Kwon, J. Y., & Carlson, J. R. (2007). Two Gr Genes Underlie Sugar Reception in Drosophila. *Neuron*, *56*(3), 503–516. https://doi.org/10.1016/j.neuron.2007.10.024

de Haro, M., Al-Ramahi, I., Benito-Sipos, J., López-Arias, B., Dorado, B., Veenstra, J. A., & Herrero, P. (2010). Detailed analysis of leucokinin-expressing neurons and their

candidate functions in the Drosophila nervous system. *Cell and Tissue Research*, *339*(2), 321–336. https://doi.org/10.1007/s00441-009-0890-y

Deng, B., Li, Q., Liu, X., Cao, Y., Li, B., Qian, Y., Xu, R., Mao, R., Zhou, E., Zhang, W., Huang, J., & Rao, Y. (2019). Chemoconnectomics: Mapping Chemical Transmission in Drosophila. *Neuron*, *101*(5), 876-893.e4. https://doi.org/10.1016/j.neuron.2019.01.045

Dickinson, M. H., & Muijres, F. T. (2016). The aerodynamics and control of free flight manoeuvres in *Drosophila*. *Philosophical Transactions of the Royal Society B: Biological Sciences*, *371*(1704), 20150388. https://doi.org/10.1098/rstb.2015.0388

Dionne, H., Hibbard, K. L., Cavallaro, A., Jui-Chun Kao, & Rubin, G. M. (2018). *Supplement to Dionne et al., 2018* (p. 46327 Bytes) [dataset]. [object Object]. https://doi.org/10.25386/GENETICS.5987542

Dobin, A., Davis, C. A., Schlesinger, F., Drenkow, J., Zaleski, C., Jha, S., Batut, P., Chaisson, M., & Gingeras, T. R. (2013). STAR: Ultrafast universal RNA-seq aligner. *Bioinformatics*, *29*(1), 15–21. https://doi.org/10.1093/bioinformatics/bts635

Dorkenwald, S., McKellar, C. E., Macrina, T., Kemnitz, N., Lee, K., Lu, R., Wu, J., Popovych, S., Mitchell, E., Nehoran, B., Jia, Z., Bae, J. A., Mu, S., Ih, D., Castro, M., Ogedengbe, O., Halageri, A., Kuehner, K., Sterling, A. R., … Seung, H. S. (2022). FlyWire: Online community for whole-brain connectomics. *Nature Methods*, *19*(1), 119–128. https://doi.org/10.1038/s41592-021-01330-0

Dunipace, L., Meister, S., McNealy, C., & Amrein, H. (2001). Spatially restricted expression of candidate taste receptors in the Drosophila gustatory system. *Current Biology*, *11*(11), 822–835. https://doi.org/10.1016/S0960-9822(01)00258-5

Dweck, H. K. M., & Carlson, J. R. (2020). Molecular Logic and Evolution of Bitter Taste in Drosophila. *Current Biology*, *30*(1), 17-30.e3. https://doi.org/10.1016/j.cub.2019.11.005

Dweck, H. K. M., & Carlson, J. R. (2023). Diverse mechanisms of taste coding in *Drosophila*. *Science Advances*, *9*(46), eadj7032. https://doi.org/10.1126/sciadv.adj7032

Dweck, H. K. M., Talross, G. J. S., Luo, Y., Ebrahim, S. A. M., & Carlson, J. R. (2022). Ir56b is an atypical ionotropic receptor that underlies appetitive salt response in Drosophila. *Current Biology*, *32*(8), 1776-1787.e4. https://doi.org/10.1016/j.cub.2022.02.063

Eckstein, N., Bates, A. S., Champion, A., Du, M., Yin, Y., Schlegel, P., Lu, A. K.-Y., Rymer, T., Finley-May, S., Paterson, T., Parekh, R., Dorkenwald, S., Matsliah, A., Yu, S.-C., McKellar, C., Sterling, A., Eichler, K., Costa, M., Seung, S., … Funke, J. (2023). *Neurotransmitter Classification from Electron Microscopy Images at Synaptic Sites in Drosophila Melanogaster*. https://doi.org/10.1101/2020.06.12.148775

Engert, S., Sterne, G. R., Bock, D. D., & Scott, K. (2022). Drosophila gustatory projections are segregated by taste modality and connectivity. *eLife*, *11*, e78110. https://doi.org/10.7554/eLife.78110

Enjin, A., Zaharieva, E. E., Frank, D. D., Mansourian, S., Suh, G. S. B., Gallio, M., & Stensmyr, M. C. (2016). Humidity Sensing in Drosophila. *Current Biology*, *26*(10), 1352–1358. https://doi.org/10.1016/j.cub.2016.03.049

Erion, R., DiAngelo, J. R., Crocker, A., & Sehgal, A. (2012). Interaction between Sleep and Metabolism in Drosophila with Altered Octopamine Signaling. *Journal of Biological Chemistry*, *287*(39), 32406–32414. https://doi.org/10.1074/jbc.M112.360875

Feinberg, E. H., VanHoven, M. K., Bendesky, A., Wang, G., Fetter, R. D., Shen, K., & Bargmann, C. I. (2008). GFP Reconstitution Across Synaptic Partners (GRASP) Defines Cell

Contacts and Synapses in Living Nervous Systems. *Neuron*, *57*(3), 353–363. https://doi.org/10.1016/j.neuron.2007.11.030

Feng, K.-L., Weng, J.-Y., Chen, C.-C., Abubaker, M. B., Lin, H.-W., Charng, C.-C., Lo, C.-C., De Belle, J. S., Tully, T., Lien, C.-C., & Chiang, A.-S. (2021). Neuropeptide F inhibits dopamine neuron interference of long-term memory consolidation in Drosophila. *iScience*, *24*(12), 103506. https://doi.org/10.1016/j.isci.2021.103506

Fishilevich, E., & Vosshall, L. B. (2005). Genetic and Functional Subdivision of the Drosophila Antennal Lobe. *Current Biology*, *15*(17), 1548–1553. https://doi.org/10.1016/j.cub.2005.07.066

Flood, T. F., Iguchi, S., Gorczyca, M., White, B., Ito, K., & Yoshihara, M. (2013). A single pair of interneurons commands the Drosophila feeding motor program. *Nature*, *499*(7456), 83–87. https://doi.org/10.1038/nature12208

Freeman, E. G., & Dahanukar, A. (2015). Molecular neurobiology of Drosophila taste. *Current Opinion in Neurobiology*, *34*, 140–148. https://doi.org/10.1016/j.conb.2015.06.001

Freeman, E. G., Wisotsky, Z., & Dahanukar, A. (2014). Detection of sweet tastants by a conserved group of insect gustatory receptors. *Proceedings of the National Academy of Sciences*, *111*(4), 1598–1603. https://doi.org/10.1073/pnas.1311724111

French, A., Moutaz, A. A., Mitra, A., Yanagawa, A., Sellier, M.-J., & Marion-Poll, F. (2015). Drosophila Bitter Taste(s). *Frontiers in Integrative Neuroscience*, *9*. https://doi.org/10.3389/fnint.2015.00058

Fujii, S., Yavuz, A., Slone, J., Jagge, C., Song, X., & Amrein, H. (2015). Drosophila Sugar Receptors in Sweet Taste Perception, Olfaction, and Internal Nutrient Sensing. *Current Biology*, *25*(5), 621–627. https://doi.org/10.1016/j.cub.2014.12.058

Gáliková, M., Dircksen, H., & Nässel, D. R. (2018). The thirsty fly: Ion transport peptide (ITP) is a novel endocrine regulator of water homeostasis in Drosophila. *PLOS Genetics*, *14*(8), e1007618. https://doi.org/10.1371/journal.pgen.1007618

Gáliková, M., & Klepsatel, P. (2022). Ion transport peptide regulates energy intake, expenditure, and metabolic homeostasis in *Drosophila*. *Genetics*, *222*(4), iyac150. https://doi.org/10.1093/genetics/iyac150

Galili, D. S., Jefferis, G. S., & Costa, M. (2022). Connectomics and the neural basis of behaviour. *Current Opinion in Insect Science*, *54*, 100968. https://doi.org/10.1016/j.cois.2022.100968

Ganguly, A., Pang, L., Duong, V.-K., Lee, A., Schoniger, H., Varady, E., & Dahanukar, A. (2017). A Molecular and Cellular Context-Dependent Role for Ir76b in Detection of Amino Acid Taste. *Cell Reports*, *18*(3), 737–750. https://doi.org/10.1016/j.celrep.2016.12.071

The Gene Ontology Consortium. (2017). Expansion of the Gene Ontology knowledgebase and resources. *Nucleic Acids Research*, *45*(D1), D331–D338. https://doi.org/10.1093/nar/gkw1108

Gentleman, R. C., Carey, V. J., Bates, D. M., Bolstad, B., Dettling, M., Dudoit, S., Ellis, B., Gautier, L., Ge, Y., Gentry, J., Hornik, K., Hothorn, T., Huber, W., Iacus, S., Irizarry, R., Leisch, F., Li, C., Maechler, M., Rossini, A. J., … Zhang, J. (2004). Bioconductor: Open software development for computational biology and bioinformatics. *Genome Biology*.

González Segarra, A. J., Pontes, G., Jourjine, N., Del Toro, A., & Scott, K. (2023). Hunger- and thirst-sensing neurons modulate a neuroendocrine network to coordinate sugar and water ingestion. *eLife*, *12*, RP88143. https://doi.org/10.7554/eLife.88143

Gordon, M. D., & Scott, K. (2009). Motor Control in a Drosophila Taste Circuit. *Neuron*, *61*(3), 373–384. https://doi.org/10.1016/j.neuron.2008.12.033

Hakeda-Suzuki, S., Takechi, H., Kawamura, H., & Suzuki, T. (2017). Two receptor tyrosine phosphatases dictate the depth of axonal stabilizing layer in the visual system. *eLife*, *6*, e31812. https://doi.org/10.7554/eLife.31812

Hall, J. C. (1994). The Mating of a Fly. *Science*, *264*(5166), 1702–1714. https://doi.org/10.1126/science.8209251

Hamada, F. N., Rosenzweig, M., Kang, K., Pulver, S. R., Ghezzi, A., Jegla, T. J., & Garrity, P. A. (2008). An internal thermal sensor controlling temperature preference in Drosophila. *Nature*, *454*(7201), 217–220. https://doi.org/10.1038/nature07001

Harris, D. T., Kallman, B. R., Mullaney, B. C., & Scott, K. (2015). Representations of Taste Modality in the Drosophila Brain. *Neuron*, *86*(6), 1449–1460. https://doi.org/10.1016/j.neuron.2015.05.026

Harrison, N. J., Connolly, E., Gascón Gubieda, A., Yang, Z., Altenhein, B., Losada Perez, M., Moreira, M., Sun, J., & Hidalgo, A. (2021). Regenerative neurogenic response from glia requires insulin-driven neuron-glia communication. *eLife*, *10*, e58756. https://doi.org/10.7554/eLife.58756

Harzer, H., Berger, C., Conder, R., Schmauss, G., & Knoblich, J. A. (2013). FACS purification of Drosophila larval neuroblasts for next-generation sequencing. *Nature Protocols*, *8*(6), 1088–1099. https://doi.org/10.1038/nprot.2013.062

He, Z., Luo, Y., Shang, X., Sun, J. S., & Carlson, J. R. (2019). Chemosensory sensilla of the Drosophila wing express a candidate ionotropic pheromone receptor. *PLOS Biology*, *17*(5), e2006619. https://doi.org/10.1371/journal.pbio.2006619

Henriques, S. F., Dhakan, D. B., Serra, L., Francisco, A. P., Carvalho-Santos, Z., Baltazar, C., Elias, A. P., Anjos, M., Zhang, T., Maddocks, O. D. K., & Ribeiro, C. (2020). Metabolic cross-feeding in imbalanced diets allows gut microbes to improve reproduction and alter host behaviour. *Nature Communications*, *11*(1), 4236. https://doi.org/10.1038/s41467-020-18049-9

Hergarden, A. C., Tayler, T. D., & Anderson, D. J. (2012). Allatostatin-A neurons inhibit feeding behavior in adult *Drosophila*. *Proceedings of the National Academy of Sciences*, *109*(10), 3967–3972. https://doi.org/10.1073/pnas.1200778109

Hiroi, M., Marion-Poll, F., & Tanimura, T. (2002). Differentiated Response to Sugars among Labellar Chemosensilla in Drosophila. *Zoological Science*, *19*(9), 1009–1018. https://doi.org/10.2108/zsj.19.1009

Hiroi, M., Meunier, N., Marion-Poll, F., & Tanimura, T. (2004). Two antagonistic gustatory receptor neurons responding to sweet-salty and bitter taste in *Drosophila*. *Journal of Neurobiology*, *61*(3), 333–342. https://doi.org/10.1002/neu.20063

Honegger, K., & De Bivort, B. (2018). Stochasticity, individuality and behavior. *Current Biology*, *28*(1), R8–R12. https://doi.org/10.1016/j.cub.2017.11.058

Honegger, K. S., Smith, M. A.-Y., Churgin, M. A., Turner, G. C., & de Bivort, B. L. (2020). Idiosyncratic neural coding and neuromodulation of olfactory individuality in *Drosophila*. *Proceedings of the National Academy of Sciences*, *117*(38), 23292–23297. https://doi.org/10.1073/pnas.1901623116

Hu, Y., Comjean, A., Attrill, H., Antonazzo, G., Thurmond, J., Li, F., Mohr, S. E., Brown, N. H., & Perrimon, N. (2023). PANGEA: A New Gene Set Enrichment Tool for Drosophila and Common Research Organisms. *BioRxiv*. https://doi.org/10.1101/2023.02.20.529262.

Huang, T., Niesman, P., Arasu, D., Lee, D., De La Cruz, A. L., Callejas, A., Hong, E. J., & Lois, C. (2017). Tracing neuronal circuits in transgenic animals by transneuronal control of transcription (TRACT). *eLife*, *6*, e32027. https://doi.org/10.7554/eLife.32027

Huber, W., Carey, V. J., Gentleman, R., Anders, S., Carlson, M., Carvalho, B. S., Bravo, H. C., Davis, S., Gatto, L., Girke, T., Gottardo, R., Hahne, F., Hansen, K. D., Irizarry, R. A., Lawrence, M., Love, M. I., MacDonald, J., Obenchain, V., Oleś, A. K., … Morgan, M. (2015). Orchestrating high-throughput genomic analysis with Bioconductor. *Nature Methods*, *12*(2), 115–121. https://doi.org/10.1038/nmeth.3252

Hughson, B. N. (2021). The Glucagon-Like Adipokinetic Hormone in Drosophila melanogaster – Biosynthesis and Secretion. *Frontiers in Physiology*, *12*, 710652. https://doi.org/10.3389/fphys.2021.710652

Hussain, A., Zhang, M., Üçpunar, H. K., Svensson, T., Quillery, E., Gompel, N., Ignell, R., & Grunwald Kadow, I. C. (2016). Ionotropic Chemosensory Receptors Mediate the Taste and Smell of Polyamines. *PLOS Biology*, *14*(5), e1002454. https://doi.org/10.1371/journal.pbio.1002454

Inagaki, H. K., Ben-Tabou de-Leon, S., Wong, A. M., Jagadish, S., Ishimoto, H., Barnea, G., Kitamoto, T., Axel, R., & Anderson, D. J. (2012). Visualizing Neuromodulation In Vivo: TANGO-Mapping of Dopamine Signaling Reveals Appetite Control of Sugar Sensing. *Cell*, *148*(3), 583–595. https://doi.org/10.1016/j.cell.2011.12.022

Inagaki, H. K., Panse, K. M., & Anderson, D. J. (2014). Independent, Reciprocal Neuromodulatory Control of Sweet and Bitter Taste Sensitivity during Starvation in Drosophila. *Neuron*, *84*(4), 806–820. https://doi.org/10.1016/j.neuron.2014.09.032

Itskov, P. M., Moreira, J.-M., Vinnik, E., Lopes, G., Safarik, S., Dickinson, M. H., & Ribeiro, C. (2014). Automated monitoring and quantitative analysis of feeding behaviour in Drosophila. *Nature Communications*, *5*(1), 4560. https://doi.org/10.1038/ncomms5560

Itskov, P. M., & Ribeiro, C. (2013). The Dilemmas of the Gourmet Fly: The Molecular and Neuronal Mechanisms of Feeding and Nutrient Decision Making in Drosophila. *Frontiers in Neuroscience*, *7*. https://doi.org/10.3389/fnins.2013.00012

Jaeger, A. H., Stanley, M., Weiss, Z. F., Musso, P.-Y., Chan, R. C., Zhang, H., Feldman-Kiss, D., & Gordon, M. D. (2018). A complex peripheral code for salt taste in Drosophila. *eLife*, *7*, e37167. https://doi.org/10.7554/eLife.37167

Jeanne, J. M., Fişek, M., & Wilson, R. I. (2018). The Organization of Projections from Olfactory Glomeruli onto Higher-Order Neurons. *Neuron*, *98*(6), 1198-1213.e6. https://doi.org/10.1016/j.neuron.2018.05.011

Jenett, A., Rubin, G. M., Ngo, T.-T. B., Shepherd, D., Murphy, C., Dionne, H., Pfeiffer, B. D., Cavallaro, A., Hall, D., Jeter, J., Iyer, N., Fetter, D., Hausenfluck, J. H., Peng, H., Trautman, E. T., Svirskas, R. R., Myers, E. W., Iwinski, Z. R., Aso, Y., … Zugates, C. T. (2012). A GAL4-Driver Line Resource for Drosophila Neurobiology. *Cell Reports*, *2*(4), 991–1001. https://doi.org/10.1016/j.celrep.2012.09.011

Jeong, Y. T., Oh, S. M., Shim, J., Seo, J. T., Kwon, J. Y., & Moon, S. J. (2016). Mechanosensory neurons control sweet sensing in Drosophila. *Nature Communications*, *7*(1), 12872. https://doi.org/10.1038/ncomms12872

Jeong, Y. T., Shim, J., Oh, S. R., Yoon, H. I., Kim, C. H., Moon, S. J., & Montell, C. (2013). An Odorant-Binding Protein Required for Suppression of Sweet Taste by Bitter Chemicals. *Neuron*, *79*(4), 725–737. https://doi.org/10.1016/j.neuron.2013.06.025

Jiao, Y., Moon, S. J., & Montell, C. (2007). A *Drosophila* gustatory receptor required for the responses to sucrose, glucose, and maltose identified by mRNA tagging. *Proceedings of*

the National Academy of Sciences, *104*(35), 14110–14115. https://doi.org/10.1073/pnas.0702421104

Jiao, Y., Moon, S. J., Wang, X., Ren, Q., & Montell, C. (2008). Gr64f Is Required in Combination with Other Gustatory Receptors for Sugar Detection in Drosophila. *Current Biology*, *18*(22), 1797–1801. https://doi.org/10.1016/j.cub.2008.10.009

Jin, H., Fishman, Z. H., Ye, M., Wang, L., & Zuker, C. S. (2021). Top-Down Control of Sweet and Bitter Taste in the Mammalian Brain. *Cell*, *184*(1), 257-271.e16. https://doi.org/10.1016/j.cell.2020.12.014

Jourjine, N., Mullaney, B. C., Mann, K., & Scott, K. (2016). Coupled Sensing of Hunger and Thirst Signals Balances Sugar and Water Consumption. *Cell*, *166*(4), 855–866. https://doi.org/10.1016/j.cell.2016.06.046

Jovanic, T. (2020). Studying neural circuits of decision-making in *Drosophila* larva. *Journal of Neurogenetics*, *34*(1), 162–170. https://doi.org/10.1080/01677063.2020.1719407

Kahsai, L., Kapan, N., Dircksen, H., Winther, Å. M. E., & Nässel, D. R. (2010). Metabolic Stress Responses in Drosophila Are Modulated by Brain Neurosecretory Cells That Produce Multiple Neuropeptides. *PLoS ONE*, *5*(7), e11480. https://doi.org/10.1371/journal.pone.0011480

Kain, P., & Dahanukar, A. (2015). Secondary Taste Neurons that Convey Sweet Taste and Starvation in the Drosophila Brain. *Neuron*, *85*(4), 819–832. https://doi.org/10.1016/j.neuron.2015.01.005

Kang, K., Panzano, V. C., Chang, E. C., Ni, L., Dainis, A. M., Jenkins, A. M., Regna, K., Muskavitch, M. A. T., & Garrity, P. A. (2012). Modulation of TRPA1 thermal sensitivity enables sensory discrimination in Drosophila. *Nature*, *481*(7379), 76–80. https://doi.org/10.1038/nature10715

Kim, H., Kirkhart, C., & Scott, K. (2017). Long-range projection neurons in the taste circuit of Drosophila. *eLife*, *6*, e23386. https://doi.org/10.7554/eLife.23386

Kim, J., Bang, H., Ko, S., Jung, I., Hong, H., & Kim-Ha, J. (2008). Drosophila ia2 modulates secretion of insulin-like peptide. *Comparative Biochemistry and Physiology Part A: Molecular & Integrative Physiology*, *151*(2), 180–184. https://doi.org/10.1016/j.cbpa.2008.06.020

Kiral, F. R., Dutta, S. B., Linneweber, G. A., Hilgert, S., Poppa, C., Duch, C., von Kleist, M., Hassan, B. A., & Hiesinger, P. R. (2021). Brain connectivity inversely scales with developmental temperature in Drosophila. *Cell Reports*, *37*(12), 110145. https://doi.org/10.1016/j.celrep.2021.110145

Knecht, Z. A., Silbering, A. F., Ni, L., Klein, M., Budelli, G., Bell, R., Abuin, L., Ferrer, A. J., Samuel, A. D., Benton, R., & Garrity, P. A. (2016). Distinct combinations of variant ionotropic glutamate receptors mediate thermosensation and hygrosensation in Drosophila. *eLife*, *5*, e17879. https://doi.org/10.7554/eLife.17879

Koh, T.-W., He, Z., Gorur-Shandilya, S., Menuz, K., Larter, N. K., Stewart, S., & Carlson, J. R. (2014). The Drosophila IR20a Clade of Ionotropic Receptors Are Candidate Taste and Pheromone Receptors. *Neuron*, *83*(4), 850–865. https://doi.org/10.1016/j.neuron.2014.07.012

Koyama, M., & Pujala, A. (2018). Mutual inhibition of lateral inhibition: A network motif for an elementary computation in the brain. *Current Opinion in Neurobiology*, *49*, 69–74. https://doi.org/10.1016/j.conb.2017.12.019

Krashes, M. J., DasGupta, S., Vreede, A., White, B., Armstrong, J. D., & Waddell, S. (2009). A Neural Circuit Mechanism Integrating Motivational State with Memory Expression in Drosophila. *Cell*, *139*(2), 416–427. https://doi.org/10.1016/j.cell.2009.08.035

Kristan, W. B. (2008). Neuronal Decision-Making Circuits. *Current Biology*, *18*(19), R928–R932. https://doi.org/10.1016/j.cub.2008.07.081

Kubrak, O., Koyama, T., Ahrentløv, N., Jensen, L., Malita, A., Naseem, M. T., Lassen, M., Nagy, S., Texada, M. J., Halberg, K. V., & Rewitz, K. (2022). The gut hormone Allatostatin C/Somatostatin regulates food intake and metabolic homeostasis under nutrient stress. *Nature Communications*, *13*(1), 692. https://doi.org/10.1038/s41467-022-28268-x

LeDue, E. E., Chen, Y.-C., Jung, A. Y., Dahanukar, A., & Gordon, M. D. (2015). Pharyngeal sense organs drive robust sugar consumption in Drosophila. *Nature Communications*, *6*(1), 6667. https://doi.org/10.1038/ncomms7667

LeDue, E. E., Mann, K., Koch, E., Chu, B., Dakin, R., & Gordon, M. D. (2016). Starvation-Induced Depotentiation of Bitter Taste in Drosophila. *Current Biology*, *26*(21), 2854–2861. https://doi.org/10.1016/j.cub.2016.08.028

Lee, K.-S., You, K.-H., Choo, J.-K., Han, Y.-M., & Yu, K. (2004). Drosophila Short Neuropeptide F Regulates Food Intake and Body Size. *Journal of Biological Chemistry*, *279*(49), 50781–50789. https://doi.org/10.1074/jbc.M407842200

Lee, Y., Moon, S. J., & Montell, C. (2009). Multiple gustatory receptors required for the caffeine response in *Drosophila*. *Proceedings of the National Academy of Sciences*, *106*(11), 4495–4500. https://doi.org/10.1073/pnas.0811744106

Li, F., Lindsey, J. W., Marin, E. C., Otto, N., Dreher, M., Dempsey, G., Stark, I., Bates, A. S., Pleijzier, M. W., Schlegel, P., Nern, A., Takemura, S., Eckstein, N., Yang, T., Francis, A., Braun, A., Parekh, R., Costa, M., Scheffer, L. K., … Rubin, G. M. (2020). The connectome of the adult Drosophila mushroom body provides insights into function. *eLife*, *9*, e62576. https://doi.org/10.7554/eLife.62576

Li, H., Janssens, J., De Waegeneer, M., Kolluru, S. S., Davie, K., Gardeux, V., Saelens, W., David, F. P. A., Brbić, M., Spanier, K., Leskovec, J., McLaughlin, C. N., Xie, Q., Jones, R. C., Brueckner, K., Shim, J., Tattikota, S. G., Schnorrer, F., Rust, K., … Zinzen, R. P. (2022). Fly Cell Atlas: A single-nucleus transcriptomic atlas of the adult fruit fly. *Science*, *375*(6584), eabk2432. https://doi.org/10.1126/science.abk2432

Li, K., Tian, Y., Yuan, Y., Fan, X., Yang, M., He, Z., & Yang, D. (2019). Insights into the Functions of LncRNAs in Drosophila. *International Journal of Molecular Sciences*, *20*(18), 4646. https://doi.org/10.3390/ijms20184646

Li, S.-S., Li, A.-Q., Liu, Z.-Y., Zhao, X.-Y., Wang, G.-R., Deng, Y., & Wang, Q.-P. (2024). Glutamine enhances sucrose taste through a gut microbiota-gut-brain axis in Drosophila. *Life Sciences*, *339*, 122415. https://doi.org/10.1016/j.lfs.2024.122415

Lima, S. Q., & Miesenböck, G. (2005). Remote Control of Behavior through Genetically Targeted Photostimulation of Neurons. *Cell*, *121*(1), 141–152. https://doi.org/10.1016/j.cell.2005.02.004

Lin, S., Senapati, B., & Tsao, C.-H. (2019). Neural basis of hunger-driven behaviour in *Drosophila*. *Open Biology*, *9*(3), 180259. https://doi.org/10.1098/rsob.180259

Ling, F., Dahanukar, A., Weiss, L. A., Kwon, J. Y., & Carlson, J. R. (2014). The Molecular and Cellular Basis of Taste Coding in the Legs of *Drosophila*. *The Journal of Neuroscience*, *34*(21), 7148–7164. https://doi.org/10.1523/JNEUROSCI.0649-14.2014

Linneweber, G. A., Andriatsilavo, M., Dutta, S. B., Bengochea, M., Hellbruegge, L., Liu, G., Ejsmont, R. K., Straw, A. D., Wernet, M., Hiesinger, P. R., & Hassan, B. A. (2020). A neurodevelopmental origin of behavioral individuality in the *Drosophila* visual system. *Science*, *367*(6482), 1112–1119. https://doi.org/10.1126/science.aaw7182

Liu, T., Starostina, E., Vijayan, V., & Pikielny, C. W. (2012). Two *Drosophila* DEG/ENaC Channel Subunits Have Distinct Functions in Gustatory Neurons That Activate Male Courtship. *The Journal of Neuroscience*, *32*(34), 11879–11889. https://doi.org/10.1523/JNEUROSCI.1376-12.2012

Liu, W. W., & Wilson, R. I. (2013). Transient and Specific Inactivation of Drosophila Neurons In Vivo Using a Native Ligand-Gated Ion Channel. *Current Biology*, *23*(13), 1202–1208. https://doi.org/10.1016/j.cub.2013.05.016

Liu, Y., Luo, J., Carlsson, M. A., & Nässel, D. R. (2015). Serotonin and insulin-like peptides modulate leucokinin-producing neurons that affect feeding and water homeostasis in *Drosophila*. *Journal of Comparative Neurology*, *523*(12), 1840–1863. https://doi.org/10.1002/cne.23768

Love, M. I., Huber, W., & Anders, S. (2014). Moderated estimation of fold change and dispersion for RNA-seq data with DESeq2. *Genome Biology*, *15*(12), 550. https://doi.org/10.1186/s13059-014-0550-8

Ma, D., Hu, M., Yang, X., Liu, Q., Ye, F., Cai, W., Wang, Y., Xu, X., Chang, S., Wang, R., Yang, W., Ye, S., Su, N., Fan, M., Xu, H., & Guo, J. (2024). Structural basis for sugar perception by *Drosophila* gustatory receptors. *Science*, *383*(6685), eadj2609. https://doi.org/10.1126/science.adj2609

Ma, Y., Zhang, L., & Huang, X. (2014). Genome modification by CRISPR /Cas9. *The FEBS Journal*, *281*(23), 5186–5193. https://doi.org/10.1111/febs.13110

Mackay, T. F. C., Richards, S., Stone, E. A., Barbadilla, A., Ayroles, J. F., Zhu, D., Casillas, S., Han, Y., Magwire, M. M., Cridland, J. M., Richardson, M. F., Anholt, R. R. H., Barrón, M., Bess, C., Blankenburg, K. P., Carbone, M. A., Castellano, D., Chaboub, L., Duncan, L., … Gibbs, R. A. (2012). The Drosophila melanogaster Genetic Reference Panel. *Nature*, *482*(7384), 173–178. https://doi.org/10.1038/nature10811

Macpherson, L. J., Zaharieva, E. E., Kearney, P. J., Alpert, M. H., Lin, T.-Y., Turan, Z., Lee, C.-H., & Gallio, M. (2015). Dynamic labelling of neural connections in multiple colours by trans-synaptic fluorescence complementation. *Nature Communications*, *6*(1), 10024. https://doi.org/10.1038/ncomms10024

Malita, A., Kubrak, O., Koyama, T., Ahrentløv, N., Texada, M. J., Nagy, S., Halberg, K. V., & Rewitz, K. (2022). A gut-derived hormone suppresses sugar appetite and regulates food choice in Drosophila. *Nature Metabolism*, *4*(11), 1532–1550. https://doi.org/10.1038/s42255-022-00672-z

Mamiya, A., Gurung, P., & Tuthill, J. C. (2018). Neural Coding of Leg Proprioception in Drosophila. *Neuron*, *100*(3), 636-650.e6. https://doi.org/10.1016/j.neuron.2018.09.009

Marella, S., Fischler, W., Kong, P., Asgarian, S., Rueckert, E., & Scott, K. (2006). Imaging Taste Responses in the Fly Brain Reveals a Functional Map of Taste Category and Behavior. *Neuron*, *49*(2), 285–295. https://doi.org/10.1016/j.neuron.2005.11.037

Marella, S., Mann, K., & Scott, K. (2012). Dopaminergic Modulation of Sucrose Acceptance Behavior in Drosophila. *Neuron*, *73*(5), 941–950. https://doi.org/10.1016/j.neuron.2011.12.032

Masse, N. Y., Turner, G. C., & Jefferis, G. S. X. E. (2009). Olfactory Information Processing in Drosophila. *Current Biology*, *19*(16), R700–R713. https://doi.org/10.1016/j.cub.2009.06.026

McKellar, C. E., Siwanowicz, I., Dickson, B. J., & Simpson, J. H. (2020). Controlling motor neurons of every muscle for fly proboscis reaching. *eLife*, *9*, e54978. https://doi.org/10.7554/eLife.54978

Meissner, G. W., Nern, A., Dorman, Z., DePasquale, G. M., Forster, K., Gibney, T., Hausenfluck, J. H., He, Y., Iyer, N. A., Jeter, J., Johnson, L., Johnston, R. M., Lee, K., Melton, B., Yarbrough, B., Zugates, C. T., Clements, J., Goina, C., Otsuna, H., … FlyLight Project Team. (2023). A searchable image resource of Drosophila GAL4 driver expression patterns with single neuron resolution. *eLife*, *12*, e80660. https://doi.org/10.7554/eLife.80660

Melcher, C., & Pankratz, M. J. (2005). Candidate Gustatory Interneurons Modulating Feeding Behavior in the Drosophila Brain. *PLoS Biology*, *3*(9), e305. https://doi.org/10.1371/journal.pbio.0030305

Milyaev, N., Osumi-Sutherland, D., Reeve, S., Burton, N., Baldock, R. A., & Armstrong, J. D. (2012). The Virtual Fly Brain browser and query interface. *Bioinformatics*, *28*(3), 411–415. https://doi.org/10.1093/bioinformatics/btr677

Mollá-Albaladejo, R., & Sánchez-Alcañiz, J. A. (2021). Behavior Individuality: A Focus on Drosophila melanogaster. *Frontiers in Physiology*, *12*, 719038. https://doi.org/10.3389/fphys.2021.719038

Montell, C. (2009). A taste of the Drosophila gustatory receptors. *Current Opinion in Neurobiology*, *19*(4), 345–353. https://doi.org/10.1016/j.conb.2009.07.001

Montell, C. (2013). Gustatory Receptors: Not Just for Good Taste. *Current Biology*, *23*(20), R929–R932. https://doi.org/10.1016/j.cub.2013.09.026

Montell, C. (2021). *Drosophila* sensory receptors—A set of molecular Swiss Army Knives. *Genetics*, *217*(1), 1–34. https://doi.org/10.1093/genetics/iyaa011

Moon, S. J., Köttgen, M., Jiao, Y., Xu, H., & Montell, C. (2006). A Taste Receptor Required for the Caffeine Response In Vivo. *Current Biology*, *16*(18), 1812–1817. https://doi.org/10.1016/j.cub.2006.07.024

Moreira, J.-M., Itskov, P. M., Goldschmidt, D., Baltazar, C., Steck, K., Tastekin, I., Walker, S. J., & Ribeiro, C. (2019). optoPAD, a closed-loop optogenetics system to study the circuit basis of feeding behaviors. *eLife*, *8*, e43924. https://doi.org/10.7554/eLife.43924

Moutinho-Pereira, S., Stuurman, N., Afonso, O., Hornsveld, M., Aguiar, P., Goshima, G., Vale, R. D., & Maiato, H. (2013). Genes involved in centrosome-independent mitotic spindle assembly in *Drosophila* S2 cells. *Proceedings of the National Academy of Sciences*, *110*(49), 19808–19813. https://doi.org/10.1073/pnas.1320013110

Münch, D., Goldschmidt, D., & Ribeiro, C. (2022). The neuronal logic of how internal states control food choice. *Nature*, *607*(7920), 747–755. https://doi.org/10.1038/s41586-022-04909-5

Murakami, K., Yurgel, M. E., Stahl, B. A., Masek, P., Mehta, A., Heidker, R., Bollinger, W., Gingras, R. M., Kim, Y.-J., Ja, W. W., Suter, B., DiAngelo, J. R., & Keene, A. C. (2016). Translin Is Required for Metabolic Regulation of Sleep. *Current Biology*, *26*(7), 972–980. https://doi.org/10.1016/j.cub.2016.02.013

Murphy, K. R., Deshpande, S. A., Yurgel, M. E., Quinn, J. P., Weissbach, J. L., Keene, A. C., Dawson-Scully, K., Huber, R., Tomchik, S. M., & Ja, W. W. (2016). Postprandial sleep mechanics in Drosophila. *eLife*, *5*, e19334. https://doi.org/10.7554/eLife.19334

Nässel, D. R., & Broeck, J. V. (2016). Insulin/IGF signaling in Drosophila and other insects: Factors that regulate production, release and post-release action of the insulin-like peptides. *Cellular and Molecular Life Sciences*, *73*(2), 271–290. https://doi.org/10.1007/s00018-015-2063-3

Nässel, D. R., Kubrak, O. I., Liu, Y., Luo, J., & Lushchak, O. V. (2013). Factors that regulate insulin producing cells and their output in Drosophila. *Frontiers in Physiology*, *4*. https://doi.org/10.3389/fphys.2013.00252

Nässel, D. R., & Wu, S.-F. (2021). Leucokinins: Multifunctional Neuropeptides and Hormones in Insects and Other Invertebrates. *International Journal of Molecular Sciences*, *22*(4), 1531. https://doi.org/10.3390/ijms22041531

Nässel, D. R., & Zandawala, M. (2019). Recent advances in neuropeptide signaling in Drosophila, from genes to physiology and behavior. *Progress in Neurobiology*, *179*, 101607. https://doi.org/10.1016/j.pneurobio.2019.02.003

Nériec, N., & Desplan, C. (2016). From the Eye to the Brain. In *Current Topics in Developmental Biology* (Vol. 116, pp. 247–271). Elsevier. https://doi.org/10.1016/bs.ctdb.2015.11.032

Ni, L. (2021). Genetic Transsynaptic Techniques for Mapping Neural Circuits in Drosophila. *Frontiers in Neural Circuits*, *15*, 749586. https://doi.org/10.3389/fncir.2021.749586

Ni, L., Klein, M., Svec, K. V., Budelli, G., Chang, E. C., Ferrer, A. J., Benton, R., Samuel, A. D., & Garrity, P. A. (2016). The Ionotropic Receptors IR21a and IR25a mediate cool sensing in Drosophila. *eLife*, *5*, e13254. https://doi.org/10.7554/eLife.13254

Nicolaï, L. J. J., Ramaekers, A., Raemaekers, T., Drozdzecki, A., Mauss, A. S., Yan, J., Landgraf, M., Annaert, W., & Hassan, B. A. (2010). Genetically encoded dendritic marker sheds light on neuronal connectivity in *Drosophila*. *Proceedings of the National Academy of Sciences*, *107*(47), 20553–20558. https://doi.org/10.1073/pnas.1010198107

Oh, Y., Lai, J. S.-Y., Mills, H. J., Erdjument-Bromage, H., Giammarinaro, B., Saadipour, K., Wang, J. G., Abu, F., Neubert, T. A., & Suh, G. S. B. (2019). A glucose-sensing neuron pair regulates insulin and glucagon in Drosophila. *Nature*, *574*(7779), 559–564. https://doi.org/10.1038/s41586-019-1675-4

Oka, S., Mori, K., & Watanabe, Y. (1990). Mammalian telencephalic neurons express a segment-specific membrane glycoprotein, telencephalin. *Neuroscience*, *35*(1), 93–103. https://doi.org/10.1016/0306-4522(90)90124-M

Olsen, S. R., & Wilson, R. I. (2008). Lateral presynaptic inhibition mediates gain control in an olfactory circuit. *Nature*, *452*(7190), 956–960. https://doi.org/10.1038/nature06864

Palmer, C. R., & Kristan, W. B. (2011). Contextual modulation of behavioral choice. *Current Opinion in Neurobiology*, *21*(4), 520–526. https://doi.org/10.1016/j.conb.2011.05.003

Pearson, J. M., Watson, K. K., & Platt, M. L. (2014). Decision Making: The Neuroethological Turn. *Neuron*, *82*(5), 950–965. https://doi.org/10.1016/j.neuron.2014.04.037

Pfeiffer, B. D., Ngo, T.-T. B., Hibbard, K. L., Murphy, C., Jenett, A., Truman, J. W., & Rubin, G. M. (2010). Refinement of Tools for Targeted Gene Expression in Drosophila. *Genetics*, *186*(2), 735–755. https://doi.org/10.1534/genetics.110.119917

Pool, A.-H., Kvello, P., Mann, K., Cheung, S. K., Gordon, M. D., Wang, L., & Scott, K. (2014). Four GABAergic Interneurons Impose Feeding Restraint in Drosophila. *Neuron*, *83*(1), 164–177. https://doi.org/10.1016/j.neuron.2014.05.006

Potter, C. J., & Luo, L. (2011). Using the Q system in Drosophila melanogaster. *Nature Protocols*, *6*(8), 1105–1120. https://doi.org/10.1038/nprot.2011.347

Raad, H., Ferveur, J.-F., Ledger, N., Capovilla, M., & Robichon, A. (2016). Functional Gustatory Role of Chemoreceptors in Drosophila Wings. *Cell Reports*, *15*(7), 1442–1454. https://doi.org/10.1016/j.celrep.2016.04.040

Raji, J. I., & Potter, C. J. (2021). The number of neurons in Drosophila and mosquito brains. *PLOS ONE*, *16*(5), e0250381. https://doi.org/10.1371/journal.pone.0250381

Reiter, S., Campillo Rodriguez, C., Sun, K., & Stopfer, M. (2015). Spatiotemporal Coding of Individual Chemicals by the Gustatory System. *The Journal of Neuroscience*, *35*(35), 12309–12321. https://doi.org/10.1523/JNEUROSCI.3802-14.2015

Ribeiro, C., & Dickson, B. J. (2010). Sex Peptide Receptor and Neuronal TOR/S6K Signaling Modulate Nutrient Balancing in Drosophila. *Current Biology*, *20*(11), 1000–1005. https://doi.org/10.1016/j.cub.2010.03.061

Roberts, A., Trapnell, C., Donaghey, J., Rinn, J. L., & Pachter, L. (2011). Improving RNA-Seq expression estimates by correcting for fragment bias. *Genome Biology*, *12*(3), R22. https://doi.org/10.1186/gb-2011-12-3-r22

Robertson, H. M., Warr, C. G., & Carlson, J. R. (2003). Molecular evolution of the insect chemoreceptor gene superfamily in *Drosophila melanogaster*. *Proceedings of the National Academy of Sciences*, *100*(suppl_2), 14537–14542. https://doi.org/10.1073/pnas.2335847100

Romero-Ferrero, F., Bergomi, M. G., Hinz, R. C., Heras, F. J. H., & de Polavieja, G. G. (2019). idtracker.ai: Tracking all individuals in small or large collectives of unmarked animals. *Nature Methods*, *16*(2), 179–182. https://doi.org/10.1038/s41592-018-0295-5

Ruedi, E. A., & Hughes, K. A. (2008). Natural Genetic Variation in Complex Mating Behaviors of Male Drosophila melanogaster. *Behavior Genetics*, *38*(4), 424–436. https://doi.org/10.1007/s10519-008-9204-5

Rulifson, E. J., Kim, S. K., & Nusse, R. (2002). Ablation of Insulin-Producing Neurons in Flies: Growth and Diabetic Phenotypes. *Science*, *296*(5570), 1118–1120. https://doi.org/10.1126/science.1070058

S., S., S.-K., P., C., P., & R., S. (2001). Gustatory organs of Drosophila melanogaster: Fine structure and expression of the putative odorant-binding protein PBPRP2. *Cell and Tissue Research*, *304*(3), 423–437. https://doi.org/10.1007/s004410100388

Sánchez-Alcañiz, J. A., & Benton, R. (2017). Multisensory neural integration of chemical and mechanical signals. *BioEssays*, *39*(8), 1700060. https://doi.org/10.1002/bies.201700060

Sánchez-Alcañiz, J. A., Silbering, A. F., Croset, V., Zappia, G., Sivasubramaniam, A. K., Abuin, L., Sahai, S. Y., Münch, D., Steck, K., Auer, T. O., Cruchet, S., Neagu-Maier, G. L., Sprecher, S. G., Ribeiro, C., Yapici, N., & Benton, R. (2018). An expression atlas of variant ionotropic glutamate receptors identifies a molecular basis of carbonation sensing. *Nature Communications*, *9*(1), 4252. https://doi.org/10.1038/s41467-018-06453-1

Sánchez-Alcañiz, J. A., Zappia, G., Marion-Poll, F., & Benton, R. (2017). A mechanosensory receptor required for food texture detection in Drosophila. *Nature Communications*, *8*(1), 14192. https://doi.org/10.1038/ncomms14192

Scheffer, L. K., Xu, C. S., Januszewski, M., Lu, Z., Takemura, S., Hayworth, K. J., Huang, G. B., Shinomiya, K., Maitlin-Shepard, J., Berg, S., Clements, J., Hubbard, P. M., Katz, W. T., Umayam, L., Zhao, T., Ackerman, D., Blakely, T., Bogovic, J., Dolafi, T., … Plaza, S. M. (2020). A connectome and analysis of the adult Drosophila central brain. *eLife*, *9*, e57443. https://doi.org/10.7554/eLife.57443

Schindelin, J., Arganda-Carreras, I., Frise, E., Kaynig, V., Longair, M., Pietzsch, T., Preibisch, S., Rueden, C., Saalfeld, S., Schmid, B., Tinevez, J.-Y., White, D. J., Hartenstein, V., Eliceiri, K., Tomancak, P., & Cardona, A. (2012). Fiji: An open-source platform for biological-image analysis. *Nature Methods*, *9*(7), 676–682. https://doi.org/10.1038/nmeth.2019

Schlegel, P., Texada, M. J., Miroschnikow, A., Schoofs, A., Hückesfeld, S., Peters, M., Schneider-Mizell, C. M., Lacin, H., Li, F., Fetter, R. D., Truman, J. W., Cardona, A., & Pankratz, M. J. (2016). Synaptic transmission parallels neuromodulation in a central food-intake circuit. *eLife*, *5*, e16799. https://doi.org/10.7554/eLife.16799

Schlegel, P., Yin, Y., Bates, A. S., Dorkenwald, S., Eichler, K., Brooks, P., Han, D. S., Gkantia, M., Dos Santos, M., Munnelly, E. J., Badalamente, G., Capdevila, L. S., Sane, V. A., Pleijzier, M. W., Tamimi, I. F. M., Dunne, C. R., Salgarella, I., Javier, A., Fang, S., … Jefferis, G. S. X. E. (2023). *Whole-brain annotation and multi-connectome cell typing quantifies circuit stereotypy in* Drosophila [Preprint]. Neuroscience. https://doi.org/10.1101/2023.06.27.546055

Schultzhaus, J. N., Saleem, S., Iftikhar, H., & Carney, G. E. (2017). The role of the Drosophila lateral horn in olfactory information processing and behavioral response. *Journal of Insect Physiology*, *98*, 29–37. https://doi.org/10.1016/j.jinsphys.2016.11.007

Schwarz, O., Bohra, A. A., Liu, X., Reichert, H., VijayRaghavan, K., & Pielage, J. (2017). Motor control of Drosophila feeding behavior. *eLife*, *6*, e19892. https://doi.org/10.7554/eLife.19892

Scott, K. (2005). Taste Recognition: Food for Thought. *Neuron*, *48*(3), 455–464. https://doi.org/10.1016/j.neuron.2005.10.015

Scott, K. (2018). Gustatory Processing in *Drosophila melanogaster*. *Annual Review of Entomology*, *63*(1), 15–30. https://doi.org/10.1146/annurev-ento-020117-043331

Scott, K., Brady, R., Cravchik, A., Morozov, P., Rzhetsky, A., Zuker, C., & Axel, R. (2001). A Chemosensory Gene Family Encoding Candidate Gustatory and Olfactory Receptors in Drosophila. *Cell Press*, *104*, 661–673. https://doi.org/10.1016/s0092-8674(01)00263-x

Seeds, A. M., Ravbar, P., Chung, P., Hampel, S., Midgley, F. M., Mensh, B. D., & Simpson, J. H. (2014). A suppression hierarchy among competing motor programs drives sequential grooming in Drosophila. *eLife*, *3*, e02951. https://doi.org/10.7554/eLife.02951

Shao, L., Saver, M., Chung, P., Ren, Q., Lee, T., Kent, C. F., & Heberlein, U. (2017). Dissection of the *Drosophila* neuropeptide F circuit using a high-throughput two-choice assay. *Proceedings of the National Academy of Sciences*, *114*(38). https://doi.org/10.1073/pnas.1710552114

Shearin, H. K., Dvarishkis, A. R., Kozeluh, C. D., & Stowers, R. S. (2013). Expansion of the Gateway MultiSite Recombination Cloning Toolkit. *PLoS ONE*, *8*(10), e77724. https://doi.org/10.1371/journal.pone.0077724

Shim, J., Lee, Y., Jeong, Y. T., Kim, Y., Lee, M. G., Montell, C., & Moon, S. J. (2015). The full repertoire of Drosophila gustatory receptors for detecting an aversive compound. *Nature Communications*, *6*(1), 8867. https://doi.org/10.1038/ncomms9867

Shiraiwa, T., & Carlson, J. R. (2007). Proboscis Extension Response (PER) Assay in Drosophila. *Journal of Visualized Experiments*, *3*, 193. https://doi.org/10.3791/193

Shiu, P. K., Sterne, G. R., Engert, S., Dickson, B. J., & Scott, K. (2022). Taste quality and hunger interactions in a feeding sensorimotor circuit. *eLife*, *11*, e79887. https://doi.org/10.7554/eLife.79887

Snell, N. J., Fisher, J. D., Hartmann, G. G., Zolyomi, B., Talay, M., & Barnea, G. (2022). Complex representation of taste quality by second-order gustatory neurons in Drosophila. *Current Biology*, *32*(17), 3758-3772.e4. https://doi.org/10.1016/j.cub.2022.07.048

Sorkaç, A., Moşneanu, R. A., Crown, A. M., Savaş, D., Okoro, A. M., Memiş, E., Talay, M., & Barnea, G. (2023). Retro-Tango enables versatile retrograde circuit tracing in Drosophila. *eLife*, *12*, e85041. https://doi.org/10.7554/eLife.85041

Steck, K., Walker, S. J., Itskov, P. M., Baltazar, C., Moreira, J.-M., & Ribeiro, C. (2018). Internal amino acid state modulates yeast taste neurons to support protein homeostasis in Drosophila. *eLife*, *7*, e31625. https://doi.org/10.7554/eLife.31625

Stensmyr, M. C., Dweck, H. K. M., Farhan, A., Ibba, I., Strutz, A., Mukunda, L., Linz, J., Grabe, V., Steck, K., Lavista-Llanos, S., Wicher, D., Sachse, S., Knaden, M., Becher, P. G., Seki, Y., & Hansson, B. S. (2012). A Conserved Dedicated Olfactory Circuit for Detecting Harmful Microbes in Drosophila. *Cell*, *151*(6), 1345–1357. https://doi.org/10.1016/j.cell.2012.09.046

Stocker, R. F. (1994). The organization of the chemosensory system in Drosophila melanogaster: A rewiew. *Cell and Tissue Research*, *275*(1), 3–26. https://doi.org/10.1007/BF00305372

Streit, A. K., Fan, Y. N., Masullo, L., & Baines, R. A. (2016). Calcium Imaging of Neuronal Activity in Drosophila Can Identify Anticonvulsive Compounds. *PLOS ONE*, *11*(2), e0148461. https://doi.org/10.1371/journal.pone.0148461

Sugita, M., & Shiba, Y. (2005). Genetic Tracing Shows Segregation of Taste Neuronal Circuitries for Bitter and Sweet. *Science*, *309*(5735), 781–785. https://doi.org/10.1126/science.1110787

Sweeney, S. T., Broadie, K., Keane, J., Niemann, H., & O'Kane, C. J. (1995). Targeted expression of tetanus toxin light chain in Drosophila specifically eliminates synaptic transmission and causes behavioral defects. *Neuron*, *14*(2), 341–351. https://doi.org/10.1016/0896-6273(95)90290-2

Talay, M., Richman, E. B., Snell, N. J., Hartmann, G. G., Fisher, J. D., Sorkaç, A., Santoyo, J. F., Chou-Freed, C., Nair, N., Johnson, M., Szymanski, J. R., & Barnea, G. (2017). Transsynaptic Mapping of Second-Order Taste Neurons in Flies by trans-Tango. *Neuron*, *96*(4), 783-795.e4. https://doi.org/10.1016/j.neuron.2017.10.011

Tauber, J. M., Brown, E. B., Li, Y., Yurgel, M. E., Masek, P., & Keene, A. C. (2017). A subset of sweet-sensing neurons identified by IR56d are necessary and sufficient for fatty acid taste. *PLOS Genetics*, *13*(11), e1007059. https://doi.org/10.1371/journal.pgen.1007059

Thistle, R., Cameron, P., Ghorayshi, A., Dennison, L., & Scott, K. (2012). Contact Chemoreceptors Mediate Male-Male Repulsion and Male-Female Attraction during Drosophila Courtship. *Cell*, *149*(5), 1140–1151. https://doi.org/10.1016/j.cell.2012.03.045

Thorne, N., Chromey, C., Bray, S., & Amrein, H. (2004). Taste Perception and Coding in Drosophila. *Current Biology*, *14*(12), 1065–1079. https://doi.org/10.1016/j.cub.2004.05.019

Trisal, S., VijayRaghavan, K., & Ramaswami, M. (2023). Habituation of Sugar-Induced Proboscis Extension Reflex and Yeast-Induced Habituation Override in Drosophila melanogaster. *BIO-PROTOCOL*, *13*(23). https://doi.org/10.21769/BioProtoc.4891

Tsubouchi, A., Yano, T., Yokoyama, T. K., Murtin, C., Otsuna, H., & Ito, K. (2017). Topological and modality-specific representation of somatosensory information in the fly brain. *Science*, *358*(6363), 615–623. https://doi.org/10.1126/science.aan4428

Uchizono, S., Itoh, T. Q., Kim, H., Hamada, N., Kwon, J. Y., & Tanimura, T. (2017). Deciphering the Genes for Taste Receptors for Fructose in Drosophila. *Molecules and Cells*, *40*(10), 731–736. https://doi.org/10.14348/molcells.2017.0016

Venken, K. J. T., Schulze, K. L., Haelterman, N. A., Pan, H., He, Y., Evans-Holm, M., Carlson, J. W., Levis, R. W., Spradling, A. C., Hoskins, R. A., & Bellen, H. J. (2011). MiMIC: A highly versatile transposon insertion resource for engineering Drosophila melanogaster genes. *Nature Methods*, *8*(9), 737–743. https://doi.org/10.1038/nmeth.1662

Venken, K. J. T., Simpson, J. H., & Bellen, H. J. (2011). Genetic Manipulation of Genes and Cells in the Nervous System of the Fruit Fly. *Neuron*, *72*(2), 202–230. https://doi.org/10.1016/j.neuron.2011.09.021

Verspoor, R. L., Heys, C., & Price, T. A. R. (2015). Dyeing Insects for Behavioral Assays: The Mating Behavior of Anesthetized Drosophila. *Journal of Visualized Experiments*, *98*, 52645. https://doi.org/10.3791/52645

Verstreken, P., Ohyama, T., Haueter, C., Habets, R. L. P., Lin, Y. Q., Swan, L. E., Ly, C. V., Venken, K. J. T., De Camilli, P., & Bellen, H. J. (2009). Tweek, an Evolutionarily Conserved Protein, Is Required for Synaptic Vesicle Recycling. *Neuron*, *63*(2), 203–215. https://doi.org/10.1016/j.neuron.2009.06.017

Vosshall, L. B., & Stocker, R. F. (2007). Molecular Architecture of Smell and Taste in *Drosophila*. *Annual Review of Neuroscience*, *30*(1), 505–533. https://doi.org/10.1146/annurev.neuro.30.051606.094306

Wada-Katsumata, A., Silverman, J., & Schal, C. (2013). Changes in Taste Neurons Support the Emergence of an Adaptive Behavior in Cockroaches. *Science*, *340*(6135), 972–975. https://doi.org/10.1126/science.1234854

Wang, Q.-P., Lin, Y. Q., Lai, M.-L., Su, Z., Oyston, L. J., Clark, T., Park, S. J., Khuong, T. M., Lau, M.-T., Shenton, V., Shi, Y.-C., James, D. E., Ja, W. W., Herzog, H., Simpson, S. J., & Neely, G. G. (2020). PGC1α Controls Sucrose Taste Sensitization in Drosophila. *Cell Reports*, *31*(1), 107480. https://doi.org/10.1016/j.celrep.2020.03.044

Wang, Z., Singhvi, A., Kong, P., & Scott, K. (2004). Taste Representations in the Drosophila Brain. *Cell*, *117*(7), 981–991. https://doi.org/10.1016/j.cell.2004.06.011

Watanabe, K., Chiu, H., Pfeiffer, B. D., Wong, A. M., Hoopfer, E. D., Rubin, G. M., & Anderson, D. J. (2017). A Circuit Node that Integrates Convergent Input from Neuromodulatory and Social Behavior-Promoting Neurons to Control Aggression in Drosophila. *Neuron*, *95*(5), 1112-1128.e7. https://doi.org/10.1016/j.neuron.2017.08.017

Weiss, L. A., Dahanukar, A., Kwon, J. Y., Banerjee, D., & Carlson, J. R. (2011). The Molecular and Cellular Basis of Bitter Taste in Drosophila. *Neuron*, *69*(2), 258–272. https://doi.org/10.1016/j.neuron.2011.01.001

Winding, M., Pedigo, B. D., Barnes, C. L., Patsolic, H. G., Park, Y., Kazimiers, T., Fushiki, A., Andrade, I. V., Khandelwal, A., Valdes-Aleman, J., Li, F., Randel, N., Barsotti, E., Correia, A., Fetter, R. D., Hartenstein, V., Priebe, C. E., Vogelstein, J. T., Cardona, A., & Zlatic, M. (2023). The connectome of an insect brain. *Science*, *379*(6636), eadd9330. https://doi.org/10.1126/science.add9330

Winther, Å. M. E., Lundquist, C. T., & Nässel, D. R. (1996). Multiple Members of the Leucokinin Neuropeptide Family are Present in Cerebral and Abdominal Neurohemal Organs in the Cockroach *Leucophaea maderae*. *Journal of Neuroendocrinology*, *8*(10), 785–792. https://doi.org/10.1046/j.1365-2826.1996.05219.x

Wu, Q., Wen, T., Lee, G., Park, J. H., Cai, H. N., & Shen, P. (2003). Developmental Control of Foraging and Social Behavior by the Drosophila Neuropeptide Y-like System. *Neuron*, *39*(1), 147–161. https://doi.org/10.1016/S0896-6273(03)00396-9

Wu, S.-F., Ja, Y.-L., Zhang, Y., & Yang, C.-H. (2019). Sweet neurons inhibit texture discrimination by signaling TMC-expressing mechanosensitive neurons in Drosophila. *eLife*, *8*, e46165. https://doi.org/10.7554/eLife.46165

Yamaguchi, M., & Yoshida, H. (2018). Drosophila as a Model Organism. In M. Yamaguchi (Ed.), *Drosophila Models for Human Diseases* (Vol. 1076, pp. 1–10). Springer Singapore. https://doi.org/10.1007/978-981-13-0529-0_1

Yang, Z., Huang, R., Fu, X., Wang, G., Qi, W., Mao, D., Shi, Z., Shen, W. L., & Wang, L. (2018). A post-ingestive amino acid sensor promotes food consumption in Drosophila. *Cell Research*, *28*(10), 1013–1025. https://doi.org/10.1038/s41422-018-0084-9

Yang, Z., Yu, Y., Zhang, V., Tian, Y., Qi, W., & Wang, L. (2015). Octopamine mediates starvation-induced hyperactivity in adult *Drosophila*. *Proceedings of the National Academy of Sciences*, *112*(16), 5219–5224. https://doi.org/10.1073/pnas.1417838112

Yao, Z., Macara, A. M., Lelito, K. R., Minosyan, T. Y., & Shafer, O. T. (2012). Analysis of functional neuronal connectivity in the *Drosophila* brain. *Journal of Neurophysiology*, *108*(2), 684–696. https://doi.org/10.1152/jn.00110.2012

Yao, Z., & Scott, K. (2022). Serotonergic neurons translate taste detection into internal nutrient regulation. *Neuron*, *110*(6), 1036-1050.e7. https://doi.org/10.1016/j.neuron.2021.12.028

Yapici, N., Cohn, R., Schusterreiter, C., Ruta, V., & Vosshall, L. B. (2016). A Taste Circuit that Regulates Ingestion by Integrating Food and Hunger Signals. *Cell*, *165*(3), 715–729. https://doi.org/10.1016/j.cell.2016.02.061

Yarmolinsky, D. A., Zuker, C. S., & Ryba, N. J. P. (2009). Common Sense about Taste: From Mammals to Insects. *Cell*, *139*(2), 234–244. https://doi.org/10.1016/j.cell.2009.10.001

Yoshinari, Y., Kosakamoto, H., Kamiyama, T., Hoshino, R., Matsuoka, R., Kondo, S., Tanimoto, H., Nakamura, A., Obata, F., & Niwa, R. (2021). The sugar-responsive enteroendocrine neuropeptide F regulates lipid metabolism through glucagon-like and insulin-like hormones in Drosophila melanogaster. *Nature Communications*, *12*(1), 4818. https://doi.org/10.1038/s41467-021-25146-w

Yu, J., Guo, X., Zheng, S., & Zhang, W. (2023). A dedicate sensorimotor circuit enables fine texture discrimination by active touch. *PLOS Genetics*, *19*(1), e1010562. https://doi.org/10.1371/journal.pgen.1010562

Yu, Y., Huang, R., Ye, J., Zhang, V., Wu, C., Cheng, G., Jia, J., & Wang, L. (2016). Regulation of starvation-induced hyperactivity by insulin and glucagon signaling in adult Drosophila. *eLife*, *5*, e15693. https://doi.org/10.7554/eLife.15693

Yurgel, M. E., Kakad, P., Zandawala, M., Nässel, D. R., Godenschwege, T. A., & Keene, A. C. (2019). A single pair of leucokinin neurons are modulated by feeding state and regulate sleep–metabolism interactions. *PLOS Biology*, *17*(2), e2006409. https://doi.org/10.1371/journal.pbio.2006409

Zandawala, M., Marley, R., Davies, S. A., & Nässel, D. R. (2018). Characterization of a set of abdominal neuroendocrine cells that regulate stress physiology using colocalized diuretic peptides in Drosophila. *Cellular and Molecular Life Sciences*, *75*(6), 1099–1115. https://doi.org/10.1007/s00018-017-2682-y

Zandawala, M., Yurgel, M. E., Texada, M. J., Liao, S., Rewitz, K. F., Keene, A. C., & Nässel, D. R. (2018). Modulation of Drosophila post-feeding physiology and behavior by the

neuropeptide leucokinin. *PLOS Genetics*, *14*(11), e1007767. https://doi.org/10.1371/journal.pgen.1007767

Zhang, Y. V., Aikin, T. J., Li, Z., & Montell, C. (2016). The Basis of Food Texture Sensation in Drosophila. *Neuron*, *91*(4), 863–877. https://doi.org/10.1016/j.neuron.2016.07.013

Zhang, Y. V., Ni, J., & Montell, C. (2013). The Molecular Basis for Attractive Salt-Taste Coding in *Drosophila*. *Science*, *340*(6138), 1334–1338. https://doi.org/10.1126/science.1234133

Zhao, Y., Khallaf, M. A., Johansson, E., Dzaki, N., Bhat, S., Alfredsson, J., Duan, J., Hansson, B. S., Knaden, M., & Alenius, M. (2022). Hedgehog-mediated gut-taste neuron axis controls sweet perception in Drosophila. *Nature Communications*, *13*(1), 7810. https://doi.org/10.1038/s41467-022-35527-4

Zheng, Z., Lauritzen, J. S., Perlman, E., Robinson, C. G., Nichols, M., Milkie, D., Torrens, O., Price, J., Fisher, C. B., Sharifi, N., Calle-Schuler, S. A., Kmecova, L., Ali, I. J., Karsh, B., Trautman, E. T., Bogovic, J. A., Hanslovsky, P., Jefferis, G. S. X. E., Kazhdan, M., … Bock, D. D. (2018). A Complete Electron Microscopy Volume of the Brain of Adult Drosophila melanogaster. *Cell*, *174*(3), 730-743.e22. https://doi.org/10.1016/j.cell.2018.06.019

Zhou, Y., Cao, L.-H., Sui, X.-W., Guo, X.-Q., & Luo, D.-G. (2019). Mechanosensory circuits coordinate two opposing motor actions in *Drosophila* feeding. *Science Advances*, *5*(5), eaaw5141. https://doi.org/10.1126/sciadv.aaw5141

ANNEX 1: SUPPLEMENTARY FIGURES

A

Sample		Brains	Neurons
Sweet Gr64f^{GSON}	1	406	21017
	2	512	23782
	3	191	21428
Bitter Gr66a^{GSON}	1	519	21260
	2	531	21599
	3	594	21433
Mechanosensory NompC^{GSON}	1	247	21772
	2	269	21101
	3	305	21800

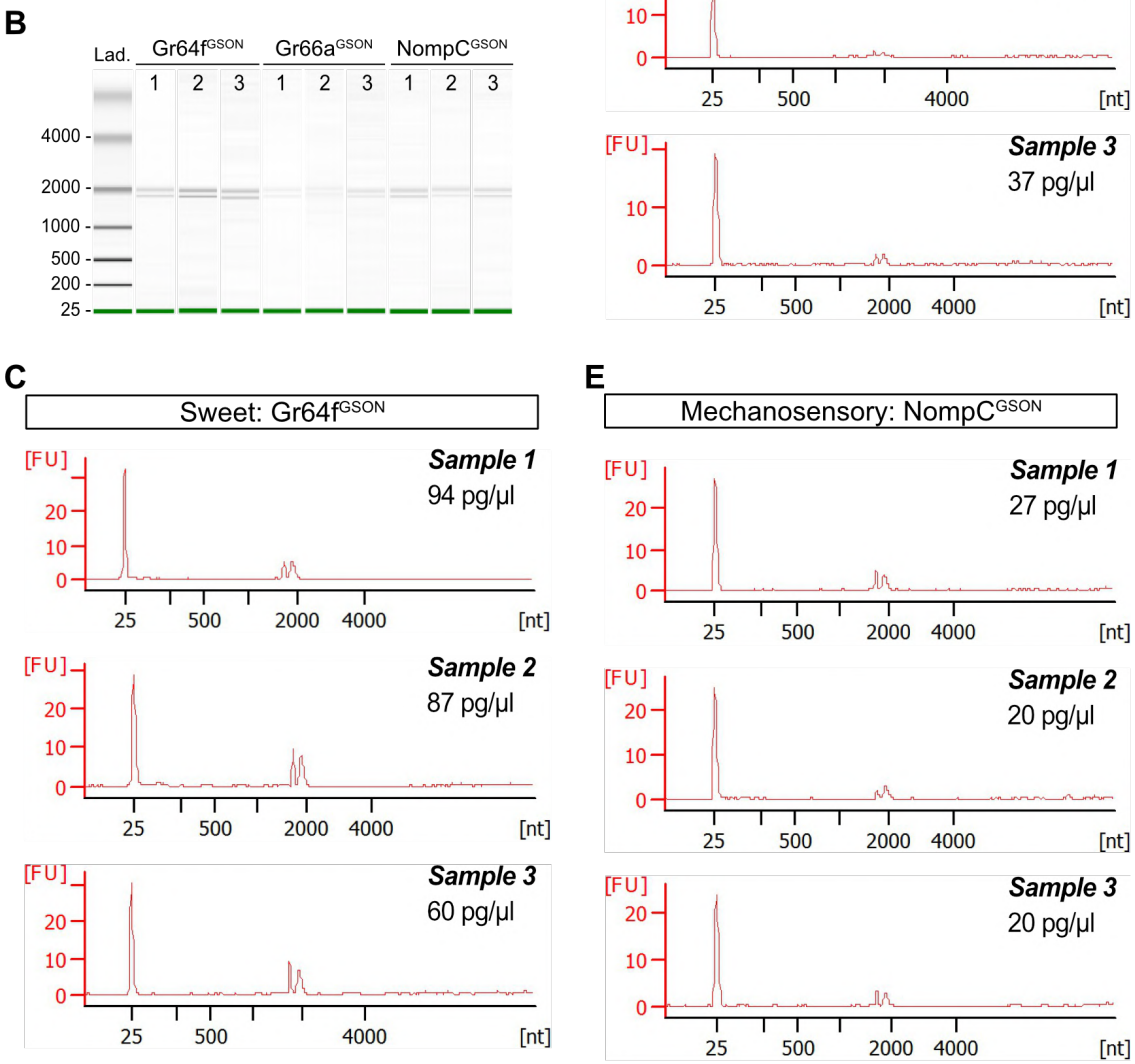

Figure S1: RNA quality and quantity evaluation of FACS sorted gustatory second-order neurons populations in fed conditions. (**A**) GSONs fed triplicate samples with the number of brains dissected and cells sorted for each of them. (**B**) RNA loading gel with the ladder and the different fed GSONs samples analyzed. (**C-E**) Representative electropherogram for each sweet (**C**), bitter (**D**) and mechanosensory (**E**) fed GSONs triplicate where the y-axis represent fluorescence intensity [FU] and the x-axis fragment size [nt], and the total RNA concentration in pg/µl.

A

Sample		Brains	Neurons
Sweet Gr64f^{GSON}	1	372	23126
	2	305	23387
	3	459	22675
Bitter Gr66a^{GSON}	1	657	27555
	2	718	27090
	3	636	26991
Mechanosensory NompC^{GSON}	1	410	26232
	2	362	26035
	3	411	25965

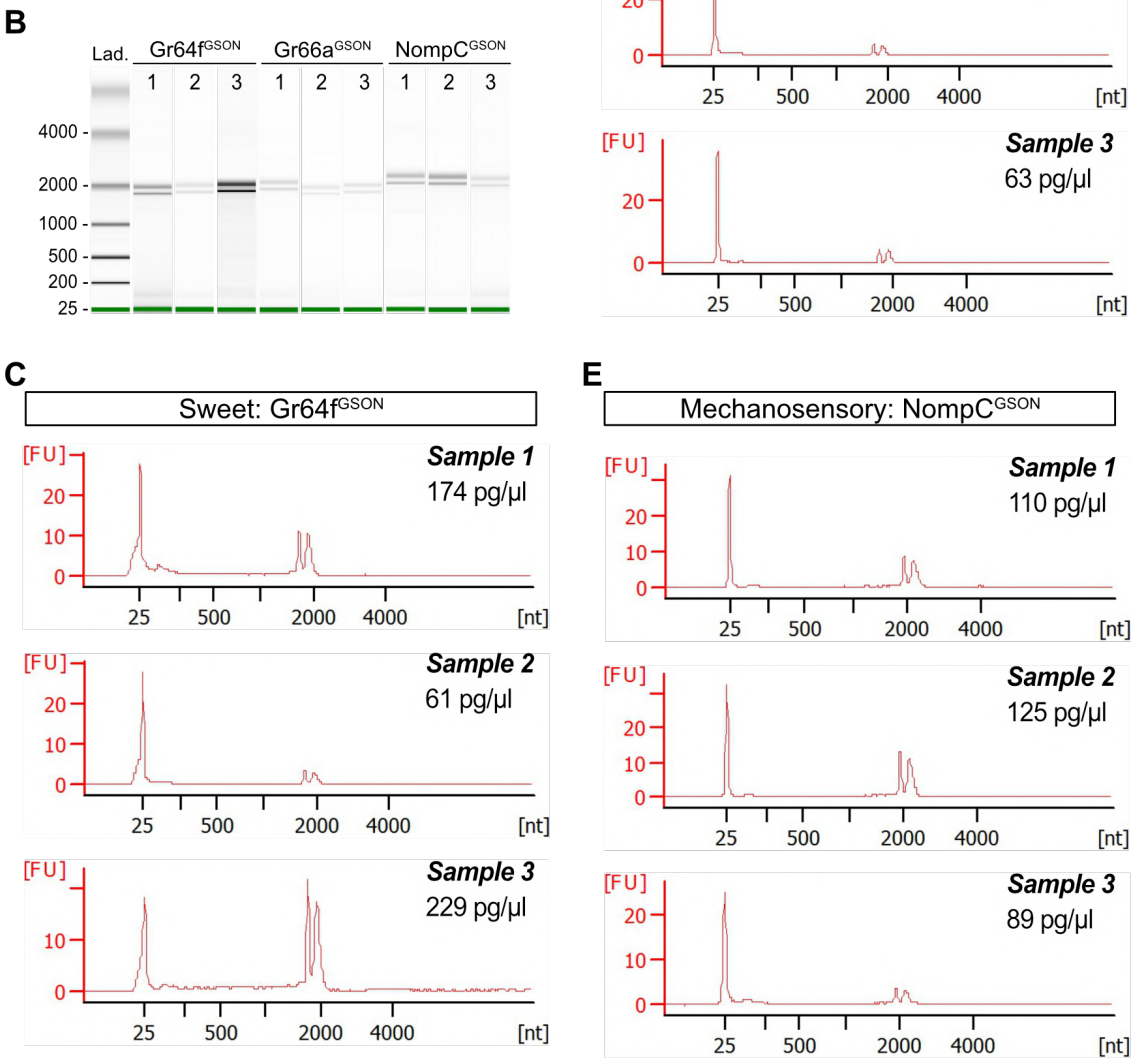

Figure S2: RNA quality and quantity evaluation of FACS sorted gustatory second-order neurons populations populations in starved conditions. (**A**) GSONs starved triplicate samples with the number of brains dissected and cells sorted for each of them. (**B**) RNA loading gel with the ladder and the different starved GSONs samples analyzed. (**C-E**) Representative electropherogram for each sweet (**C**), bitter (**D**) and mechanosensory (**E**) starved GSONs triplicate where the y-axis represent fluorescence intensity [FU] and the x-axis fragment size [nt], and the total RNA concentration in pg/µl.

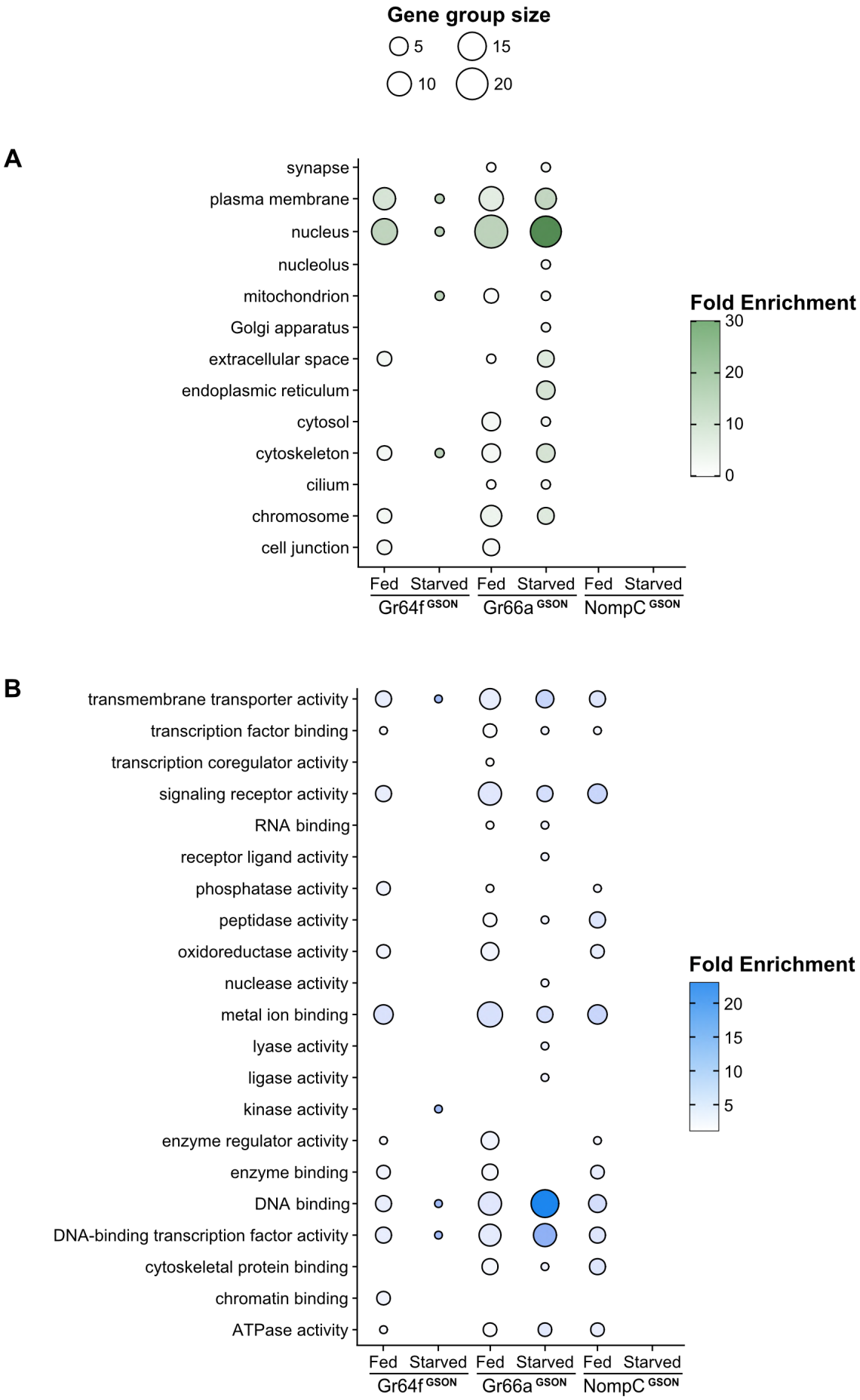
Gene group size
5
10
15
20
A
synapse
plasma membrane
nucleus
nucleolus
mitochondrion
Golgi apparatus
extracellular space
endoplasmic reticulum
cytosol
cytoskeleton
cilium
chromosome
cell junction
Fold Enrichment
30
20
10
0
Fed
Starved
Gr64f GSON
Gr66a GSON
NompC GSON
B
transmembrane transporter activity
transcription factor binding
transcription coregulator activity
signaling receptor activity
RNA binding
receptor ligand activity
phosphatase activity
peptidase activity
oxidoreductase activity
nuclease activity
metal ion binding
lyase activity
ligase activity
kinase activity
enzyme regulator activity
enzyme binding
DNA binding
DNA-binding transcription factor activity
cytoskeletal protein binding
chromatin binding
ATPase activity
Fold Enrichment
20
15
10
5

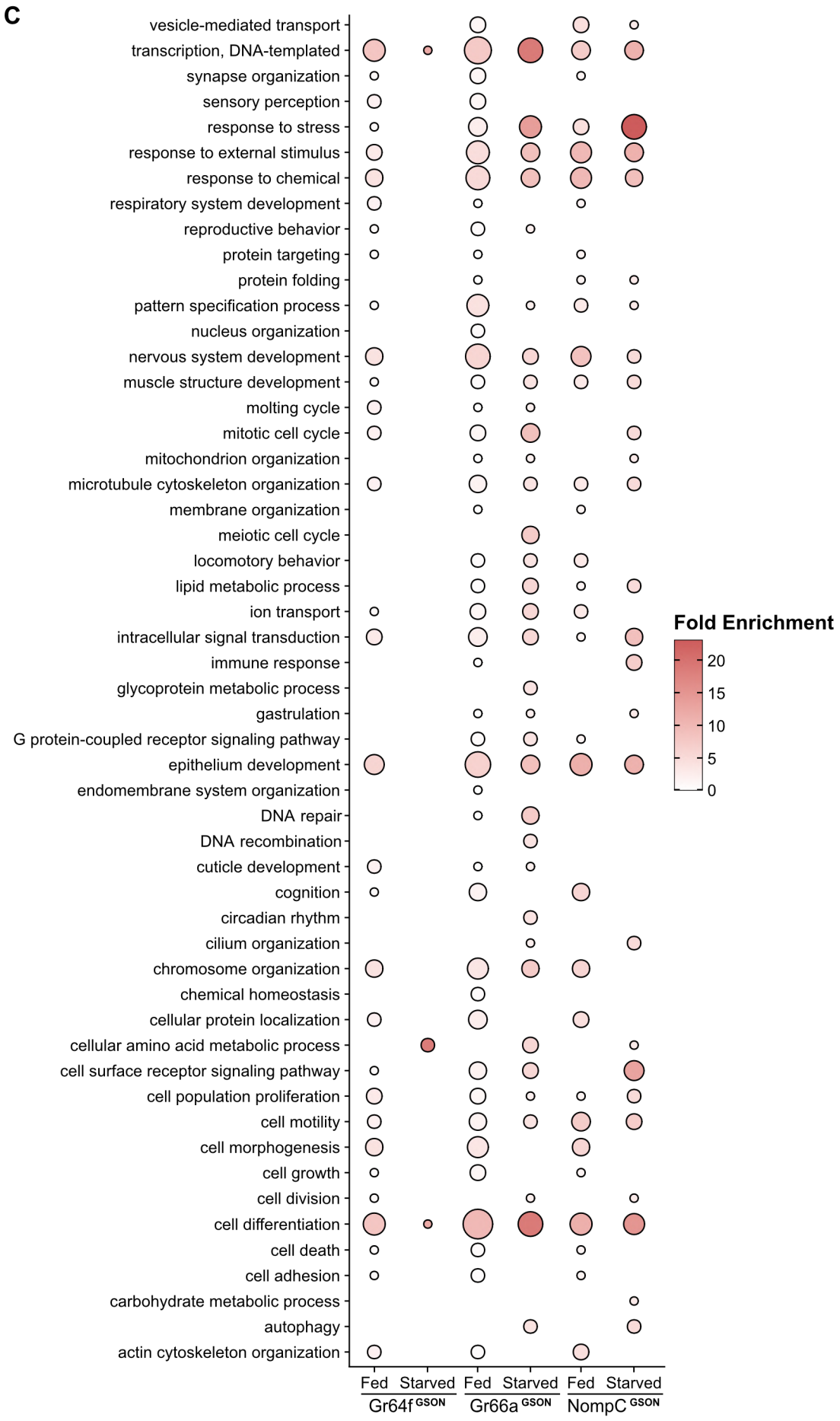
C
vesicle-mediated transport
transcription, DNA-templated
synapse organization
sensory perception
response to stress
response to external stimulus
response to chemical
respiratory system development
reproductive behavior
protein targeting
protein folding
pattern specification process
nucleus organization
nervous system development
muscle structure development
molting cycle
mitotic cell cycle
mitochondrion organization
microtubule cytoskeleton organization
membrane organization
meiotic cell cycle
locomotory behavior
lipid metabolic process
ion transport
intracellular signal transduction
immune response
glycoprotein metabolic process
gastrulation
G protein-coupled receptor signaling pathway
epithelium development
endomembrane system organization
DNA repair
DNA recombination
cuticle development
cognition
circadian rhythm
cilium organization
chromosome organization
chemical homeostasis
cellular protein localization
cellular amino acid metabolic process
cell surface receptor signaling pathway
cell population proliferation
cell motility
cell morphogenesis
cell growth
cell division
cell differentiation
cell death
cell adhesion
carbohydrate metabolic process
autophagy
actin cytoskeleton organization
Fold Enrichment
20
15
10
5
0
Fed
Starved
Fed
Starved
Fed
Starved
Gr64f GSON
Gr66a GSON
NompC GSON

Figure S3: Gene set enrichment analysis. Graphical representation of the GO terms obtained from the GSEA, grouped by the GO category: Cellular Compartment (**A**), Molecular Function (**B**) and Biological Process (**C**). The data represent the fold enrichment with a heatmap and the number of genes included in each GO term by size for all GSONs and metabolic states analyzed.

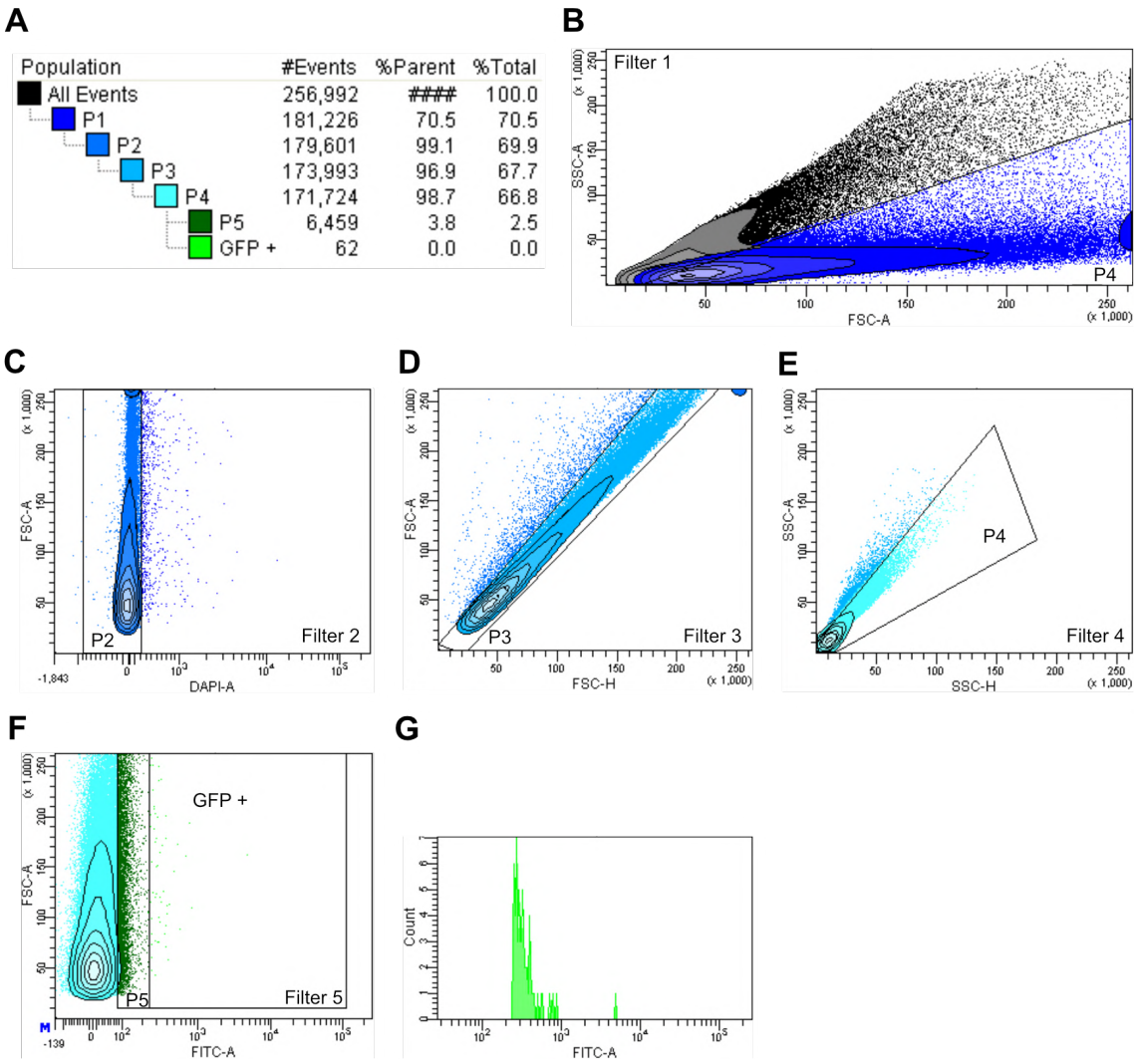

Figure S4: FACS sorting of leucokinin GFP positive neurons. *Lk-Gal4* promoter drove the expression of *UAS-CD8::GFP* in the Lk neurons. Filtering (**A**) of CB disaggregated cells from debris (**B**), dead cells using a DAPI labeling approach (**C**) and clustering single cells by morphology (**D**) and complexity (**E**) to finally separate the GFP$^+$ populations according to its green fluorescence (**F** and **G**).

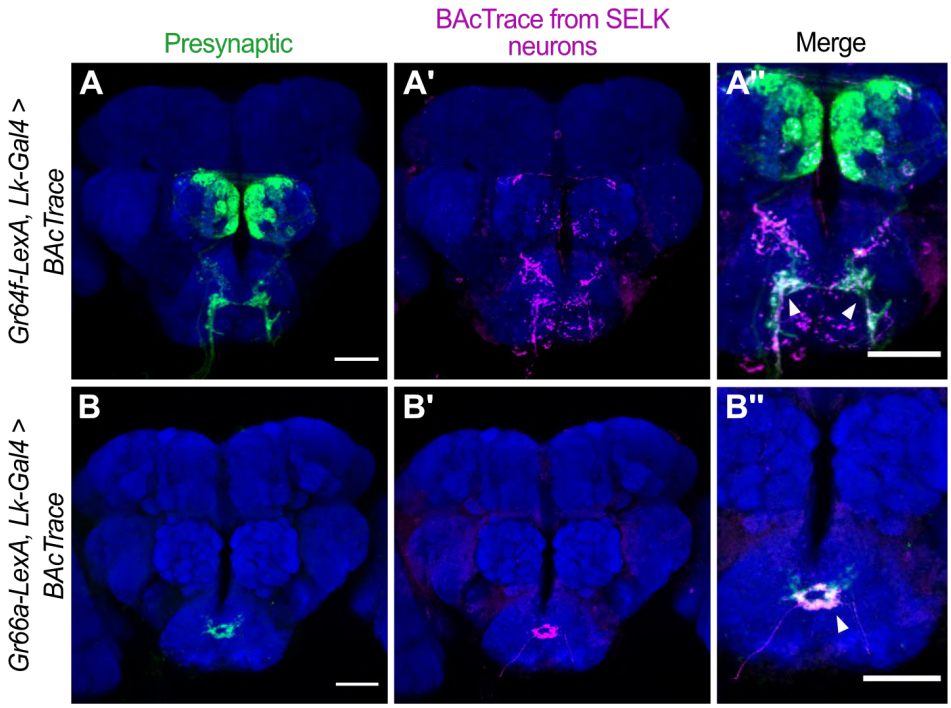

Figure S5: BAcTrace for the SELK neurons with the sweet and bitter gustatory receptor neurons. Sweet (**A**) and bitter (**B**) GRN axonal terminals (green, anti-GFP) innervating the SEZ and the BAcTrace signal (magenta, anti-mtdTomato) between from SELK neurons to sweet (**A'**) and bitter (**B'**) GRNs. Merge and *Zoom in* from both signals, GRNs axons and BAcTrace, and co-localization between them in white (white arrows) for sweet (**A''**) and bitter (**B''**) GRNs may indicate that SELK neurons are postsynaptic neurons to $Gr66a^{GRN}$ and $Gr64f^{GRN}$. Brain structure (blue) was labelled with anti-nc82. Scale bars: 50 µm.

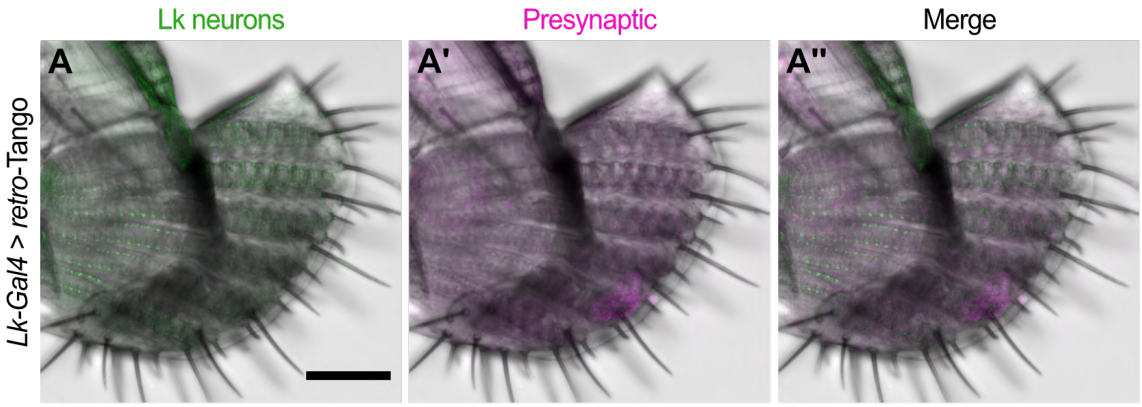

Figure S6: Presynaptic neurons to Lk neurons labelled with *retro*-Tango in the proboscis. Anatomy of the Lk neurons (**A**) located in the proboscis labeled with anti-GFP (green). mtdTomato (labeled with anti-RFP (magenta)) from *retro*-Tango transgene was expressed by using the *Lk-Gal4* driver transgenic lines to see the presence of presynaptic neurons in the proboscis (**B**). (**C**) Shows merge image. Scale bar: 50 µm.

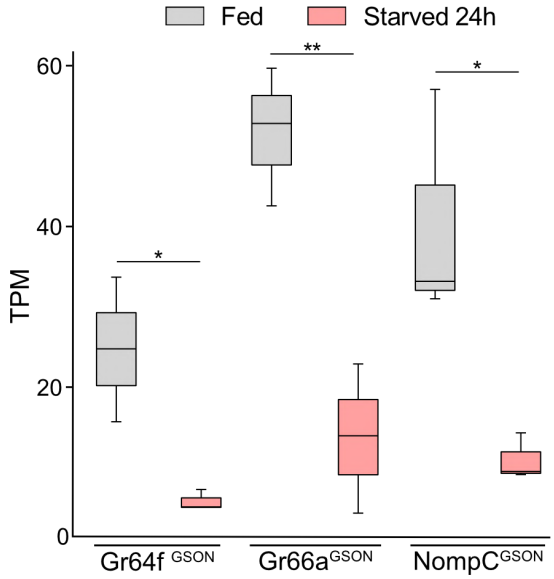

Figure S7: Expression levels for the *lncRNA:CR44834*. The lncRNA that match with the *Lk* gene sequence is overexpressed in fed conditions compared to starvation for all GSON populations. Boxplots represent total TPM taking into account the three replicates for each of the GSON populations and metabolic condition. Statistical analysis: *t*-test between fed and starved condition: **p<0.05, **p<0,01*.

ANNEX 2: PUBLICATION

frontiers in Physiology

REVIEW
published: 30 November 2021
doi: 10.3389/fphys.2021.719038

Behavior Individuality: A Focus on *Drosophila melanogaster*

*Rubén Mollá-Albaladejo and Juan A. Sánchez-Alcañiz**

Instituto de Neurociencias, UMH&CSIC, San Juan de Alicante, Spain

Among individuals, behavioral differences result from the well-known interplay of nature and nurture. Minute differences in the genetic code can lead to differential gene expression and function, dramatically affecting developmental processes and adult behavior. Environmental factors, epigenetic modifications, and gene expression and function are responsible for generating stochastic behaviors. In the last decade, the advent of high-throughput sequencing has facilitated studying the genetic basis of behavior and individuality. We can now study the genomes of multiple individuals and infer which genetic variations might be responsible for the observed behavior. In addition, the development of high-throughput behavioral paradigms, where multiple isogenic animals can be analyzed in various environmental conditions, has again facilitated the study of the influence of genetic and environmental variations in animal personality. Mainly, *Drosophila melanogaster* has been the focus of a great effort to understand how inter-individual behavioral differences emerge. The possibility of using large numbers of animals, isogenic populations, and the possibility of modifying neuronal function has made it an ideal model to search for the origins of individuality. In the present review, we will focus on the recent findings that try to shed light on the emergence of individuality with a particular interest in *D. melanogaster*.

Keywords: behavior individuality, *Drosophila melanogaster*, animal personality, neurobiology, stochasticity

OPEN ACCESS

Edited by:
Philippe Lucas,
Institut National de la Recherche Agronomique (INRA), France

Reviewed by:
Ralf Stanewsky,
University of Münster, Germany
Marko Brankatschk,
Technische Universität Dresden, Germany

****Correspondence:***
Juan A. Sánchez-Alcañiz
juan.sanchez@umh.es

Specialty section:
This article was submitted to Invertebrate Physiology, a section of the journal Frontiers in Physiology

Received: *01 June 2021*
Accepted: *11 October 2021*
Published: *30 November 2021*

Citation:
Mollá-Albaladejo R and Sánchez-Alcañiz JA (2021) Behavior Individuality: A Focus on Drosophila melanogaster. Front. Physiol. 12:719038. doi: 10.3389/fphys.2021.719038

1. INTRODUCTION

Individuality, temperament, behavioral syndromes, or animal personality are terms used to define the display of specific behavioral traits that are stable over time (Dall et al., 2004; Sih et al., 2004; Bell, 2007). At the population level, animals tend to show homogeneous behavior. However, if analyzed in more detail, it is clear that individuals within a group show behavioral patterns that differentiate them from the average. For example, in humans, food perception is highly personal, and it depends on the combination of both sociocultural experience and genetic polymorphisms that affect the function of gustatory (Kim et al., 2003) and olfactory receptors (Wysocki and Beauchamp, 1984; Kowalewski and Ray, 2020). This interindividual variation is not exclusive to humans and is generally observed in all living beings. For example, bacteria grown in the laboratory display variations in swimming behavior due to changes in gene expression, indicating that even in populations with the same genetic background and grown in similar conditions, heterogeneous behaviors can be observed (Davidson and Surette, 2008). Experiments with the clonal fish *Poecilia formosa* show that individuals grown in standardized conditions in isolation after birth display considerable differences in their behavior (Bierbach et al., 2017). Those results would suggest that stochastic developmental events lead to high variability in behavior. For example, variations in mushroom body size in *D. melanogaster*, affecting aggression, lifespan, and sleep, have been

linked with polymorphisms in more than 100 genes (Zwarts et al., 2015). It is important to remark that those variations in behavior are consistent over time. We are not referring to just an acute change in their behavioral pattern or the minor variations resulting from the "noise" in the system that might induce temporary changes in a particular behavior (Faisal et al., 2008). Other stochastic events, inherent to any biological system, such as changes in gene expression or development, will have a more profound impact on the outcome of the behavior, contributing to persistent variations in behavior and the emergence of individuality (Honegger and de Bivort, 2018).

The genetic background of the organism and the developmental history of an individual dramatically affect how the animal will express this individuality (Dall et al., 2004; Sih et al., 2004; Wolf and Weissing, 2010). Although animals of the same species share the same genome, subtle changes during development (i.e., axon guidance) can have severe effects on the final connectivity of the neurons due to stochastic events altering specific behaviors (Linneweber et al., 2020; Kiral et al., 2021). In addition, environmental factors during growth and epigenetic changes will modify gene expression. It is important to remark that although animal personality defines the animal and shows specific stability, it has certain levels of plasticity, as happens with foraging behaviors on a day-to-day basis (Anreiter and Sokolowski, 2019). Previous experiences, growth and developmental conditions, and epigenetic factors form a complex milieu where behavior and individual differences emerge.

D. melanogaster is an outstanding model to study behavior individuality for several reasons. For example, it is possible to dispose of a large number of individuals to analyze per experiment; there is an extensive collection of isogenic lines available with sequenced genomes, and we can manipulate flies at the genetic level (Casillas and Barbadilla, 2017). Moreover, with only 100,000 neurons in the central brain (Raji and Potter, 2021) and a large collection of tools to manipulate neural circuits, *D. melanogaster* is an excellent model system to understand the genetic and neural basis of behavior heterogeneity.

The present review presents the scientific advances in the study of behavior individuality in *D. melanogaster*. We will cover the knowledge gained in genetics, development, epigenetics, and the methods used to study individual behavior in flies.

2. GENETIC BASIS OF ANIMAL INDIVIDUALITY

Animal behavior and, ultimately, animal personality results from the interaction of genetic and non-genetic factors. Indeed, animals combine genetic and environmental traits to promote specific adaptation to available resources from the environment and their gene expression adapts to the circumstances (**Figure 1A**) (Honegger and de Bivort, 2018; Koyama et al., 2020). However, neither nature nor nurture in isolation can explain how and why animals behave the way they do, as each of the two components has its weight. Even more, the expression of specific genes is not constant over time but can change through the life course of the animal, causing modifications in the personality of an individual (Juneja et al., 2016; Lin et al., 2016). Hence, genes are in constant communication with non-genetic factors coupling complex and sensitive networks that will finally define the personality of an individual in response to natural pressure.

The advent of genomics during the last decades has revolutionized the field of behavioral neuroscience, providing evidence on how genes can face natural dynamic variation between individuals and affect different behavioral outputs contributing to population performance (Jin et al., 2001; Ueno and Takahashi, 2020). How, when, and where a gene or genes are expressed and modulate brain activity and processing, could explain why two individuals from the same species, similar genetic backgrounds, and raised in similar conditions behave differently. For example, in *D. melanogaster* genetic variation in olfactory receptors (*Or22a/Or22b, Or35a, and Or47a*) affect different odor guidance perceptions among individuals of the same population (Richgels and Rollmann, 2011). Also, variation in odor guidance to 2,3-butanedione showed genes associated with neural development and the later processing in the central nervous system which might be related to that behavioral variation (Brown et al., 2013). This genotypic variation is seen not only at the behavioral level but also, for example, in lifespan or morphological and anatomical traits as brain, wing, thorax, or eye size (Carreira et al., 2016; Buchberger et al., 2021).

In behavioral neuroscience (and neuroscience in general), the use of inbred lines can reduce phenotypic variability. However, even in highly controlled experimental conditions, high levels of variability can be observed both in mice and *D. melanogaster* (Honegger and de Bivort, 2018). Many animals available and short reproductive time made it possible to generate numerous collections of isogenic lines. The Drosophila Genetic Reference Panel (DGRP) are a set of fly populations derived from subsequent inbred generations producing lines with sequenced genomes and all its polymorphisms annotated (Mackay et al., 2012). As the genome of each of those fly lines is sequenced, it is possible to test the variations in behavior for each line to later search for the genetic basis responsible for such behavior. Also, studies in simple stereotyped behaviors have found complex genetic architectures involved in the final output performance of specific behaviors that differ between individuals. Thirteen genes are involved in the flight performance in *D. melanogaster* where the variation in the expression and regulation of these genes may reflect the variation in the flight performance among individuals. Among them, polymorphisms at the regulatory region of the transmembrane tyrosine kinase, Egfr, showed the largest behavioral variation affecting wing shape (Spierer et al., 2021). Other studies have used DGRP lines to search genetic variation in aggressive behavior, virgin egg retention, or immune response against pathogens (i.e., *Coxiella burnetii*) (Akhund-Zade et al., 2017; Guzman et al., 2021). Interestingly, interindividual variation can also be observed in *D. melanogaster* mating behavior. During courtship, male flies execute a series of stereotyped and progressive behaviors that culminate in mating (Hall, 1994). Even in behavior as stereotyped as courtship, which must avoid interspecies mating, studies made in natural

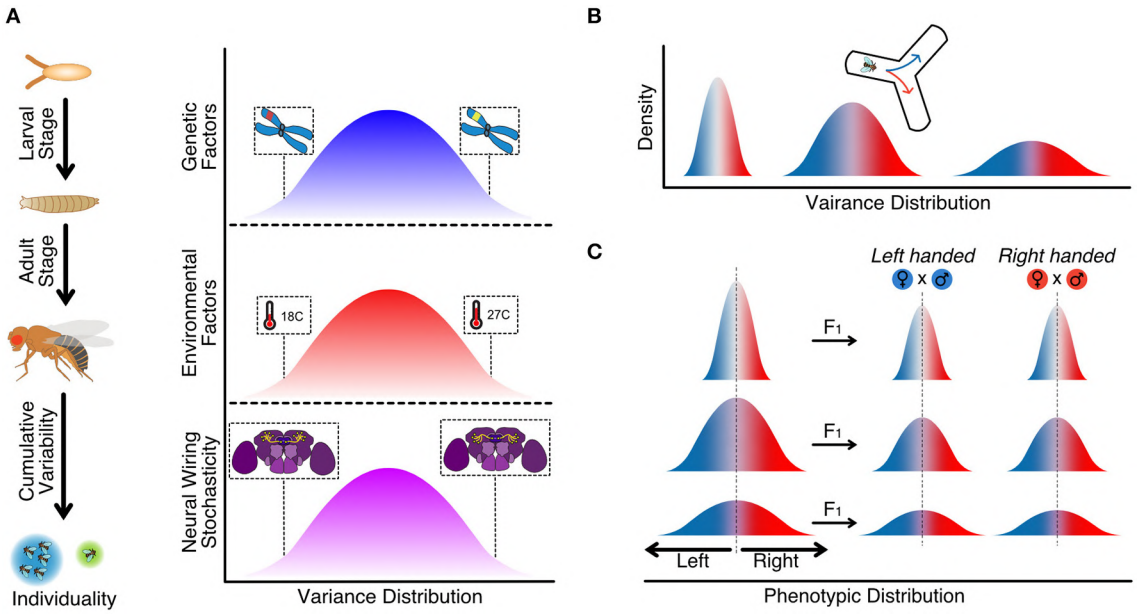

FIGURE 1 | (A) Cumulative and relative contribution of different sources of interindividual variability from early development stages to adult life experience. Individuality emerges from the combination of genetic factors, environmental factors, and stochastic factors. **(B)** Variance distribution for a given phenotypic trait evoking variability among individuals within a population (Buchanan et al., 2015). **(C)** Variance distribution of phenotypic handedness is inherited to next generations within a population (Ayroles et al., 2015).

populations have observed variability in male courtship behaviors toward mated females (Ruedi and Hughes, 2008). Genome-Wide Association Studies (GWAS) performed in the inbred collection of DGRP flies showed the influence of genetic variation in courtship variability. Particularly, the transition from copulation to no engagement was associated with SNPs in *Serrate* and *Furin-1* genes (Gaertner et al., 2015).

A key question in behavior individuality is why animals show this range of erratic behaviors. A possible explanation derives from the natural variability in the surrounding environment. A genetically uniform population might be desirable in a stable environment with no threats, as individuals diverting from the average might not be well-adapted. However, in an ever-changing environment, animals must develop strategies to survive. One option would be phenotypic plasticity, where individuals have developed the ability to change their behavior upon environmental requirements. For example, fruit flies adapt their diet to environmental temperature. *D. melanogaster* feeds primarily from yeast, but if the temperature drops below 15°C, flies change to a plant-based diet. Plants provide the flies with unsaturated fatty acids, increasing cell membrane fluidity and lifespan (Brankatschk et al., 2018). Phenotypic plasticity can also be observed in overwintering *Drosophila*, winter morphs, where flies display different phenotypic plasticity to adapt to low temperatures (Panel et al., 2020; Stockton et al., 2020).

Another possibility is to hedge their options or diversified bet-hedging. In this scenario, a single genotype produces a distribution of phenotypes, assuring that at least some individuals within the population will be well-adapted to cope with any environmental change (Honegger and de Bivort, 2018). Under those circumstances, individuals show heterogeneous natural behavior. This natural variability would be heritable, causing the behavioral individuality observed. Experiments using wild-type and inbreed lines exploring the animal idiosyncrasies have studied the mechanistic behind animal handedness or better performance using left or right hand. This behavior can be observed in *D. melanogaster* when it is forced to choose to go left or right in an arena with no other stimulus. In this paradigm, flies showed considerable variability in this particular trait, which relates to specific genotypes (Ayroles et al., 2015; Buchanan et al., 2015). The authors showed that although each population averaged a 50% chance of turning either right or left, some were more variable, with more individuals either turning left or right (**Figure 1B**). Thus, the turning bias of individual flies was not heritable but was the degree of variability of the population. Furthermore, crossing two "righty" or two "lefty" individuals did not produce hybrids all "righty" and "lefty," respectively, as the F1 progeny would show average turn vias of 50%. However, the variability of the particular line would be inherited (**Figure 1C**). A gene encoding an axon guidance molecule, *Tenascin-a*, has been proposed as a candidate involved in the observed behavior heterogeneity (refer to next section) (Ayroles et al., 2015; Buchanan et al., 2015). This distribution of phenotypes observed might be an evolutionary strategy, diversified bet-hedging, to guarantee that at least some individuals will be well-adapted when facing unpredictable environments. Bet-hedging could be the possible source of variation in the phototactic behavior of flies in two populations of flies from two different climates.

Flies from very stable tropical regions where day/light time is relatively stable would show less variability in a phototactic choice assay than the ones from a nordic region, where seasonal changes in light/dark are more dramatic. Serotonin variation among the populations could be the source of such variation as feeding flies with serotonin would decrease variability (Kain et al., 2012; Krams et al., 2021). To reinforce this idea, other studies focused on other species such as *Caenorhabditis elegans* show that in isogenic sibling individuals raised under the same conditions, serotonin might regulate behavioral variability. Complete depletion of serotonin (*tph-1*) or some of the G-protein coupled receptors (SER-1, SER-4, and SER-7) induce changes in the individual roaming behavior across development (Stern et al., 2017).

As we have seen, some of those genes affect the development of specific neural circuits. In contrast, others affect neuromodulatory networks, such as serotonin in locomotor behavior in *C. elegans*. In other cases, mutations in particular alleles affect particular gene regulatory networks, ultimately affecting neuronal function. For example, it is the case of the chaperone *heat shock protein 90* (HSP90), involved in the folding and maturation of other proteins. HSP90 mutants show high levels of interindividual morphology variation (Rutherford and Lindquist, 1998). In addition, recent studies have shown that HSP90 mutant flies display a high interindividual variation in circadian motor control (Hung et al., 2009). Daily cycles of light and darkness can entrain the circadian clock. Once established, a gene network can keep it oscillating without environmental cues (Williams and Sehgal, 2001). While wild-type flies showed low variations in their rhythmic activity, flies with decreased activity of the chaperone HSP90 showed variation between individuals, from rhythmic and arrhythmic to other complex behaviors. Those results indicated that HSP90 could be acting as a capacitor of behavior individuality, affecting the degree of variation in circadian behavioral activity (Hung et al., 2009).

All these studies support the idea that in flies from the same population, there is an accumulation of polymorphisms due to spontaneous mutations, natural pressure, or simple genomic diversification from the average of the population, conferring different behavioral personalities among them. Consistent individual differences can result from intra-genotypic variations among individuals and differences in the value of state variables such as metabolic rate, growth rate, or energetic reserves (Amat et al., 2018). Also, stochastic gene expression may underlie the phenomenon of partial penetrance of mutations and variability that may interfere in individual personality (Topalidou and Chalfie, 2011).

3. DEVELOPMENTAL AND GROWTH CONDITIONS SHAPE ANIMAL PERSONALITY

In the previous section, we have discussed the genetic basis for behavioral variability. However, we also mentioned the critical role of the developmental process and growth in individual behaviors. We refer to the variations of behavior that are non-genetic as intragenotypic variation. This variability derives from stochastic microenvironmental effects such as temperature, isolation, or food sources that force individuals to adapt phenotypically to the environment (Becher et al., 2010).

Temperature is a wide-ranging environmental factor that flies can experience and must manage to maintain their homeostasis. In *D. melanogaster*, the life cycle takes longer at low temperatures and accumulates more fat energy stores as a mechanism to cope with possible future starvation periods (Klepsatel et al., 2019, 2020). Previous studies have shown that there is gene expression variation in response to low temperatures in *D. melanogaster* due to plasticity phenomena (Fry, 2008). Whole-genome sequencing in fly populations evolved in different temperatures has revealed the role of different genes in the recombination rate divergence between populations (Winbush and Singh, 2021). The transcription factors *chimo* and *eve* show different levels of expression between flies reared at different temperatures (25 vs. 17°C). This variation modifies the arborization of sensory neurons inducing interindividual variability perceiving temperature (Alpert et al., 2020; Huang et al., 2020). Those temperature changes affect synaptic connectivity in the *D. melanogaster* visual system, as flies grown at low temperatures (19°C) have more synapse numbers than the ones grown at higher temperatures (25°C) (Kiral et al., 2021). Furthermore, phenotypic plasticity in front of temperature variation is not exclusive of drosophilids as other social insects as honey bees show different learning abilities related to labors within the colony depending on the larvae developmental temperature (Tautz et al., 2003; Jeanson, 2019). Those results indicate that temperature is a major source of phenotypic plasticity and interindividual variability within a population.

Environmental factors can dramatically influence the development of the animal and condition its growth, modifying its behavior. Flies raised in stimulating naturalistic environment vials vs. vials without any enrichment that could match natural environments showed significant differences in fitness. Enriched populations showed higher intragenotypic variability for most of the behavioral traits measured, concluding that enrichment stimuli environment is one of the central sources of variability for behavior traits crucial to surviving (Akhund-Zade et al., 2019). Also, gene expression noise varies depending on the specific gene function, suggesting that variance in gene expression noise in order to evoke phenotypic plasticity may be beneficial for survival to environmental changes (Blake et al., 2006; Newman et al., 2006; Viney and Reece, 2013).

Even in conditions where genetic background and environment are kept constant, similar individuals can develop non-heritable idiosyncratic behaviors, morphology, and gene expression profiles evoking variability that could be consistent with development and life. Stochastic development wiring or minute differences in growth conditions can contribute to the trait under study. Identical populations of pea aphids and flies grown in identical environmental conditions display heterogeneous behaviors, eliminating the role of any internal factor (Schuett et al., 2011; Kain et al., 2012; Ayroles et al., 2015). Therefore, the role of those non-heritable traits in brain development and, therefore, in individual behavior is

gaining importance in neuroscience. Studies carried on the visual orientation behavior in *D. melanogaster* showed that the Dorsal Cluster Neurons axonal projections within the medulla brain are a predictor of visual orientation, suggesting that stochastic variation in brain wiring evoke non-heritable behavioral variations (Linneweber et al., 2020). We mentioned in the previous section that different populations of flies showed variations in their handedness behavior. *Tenascin-a* encodes a cell surface protein involved in axon guidance and synaptogenesis. GWAS studies of the DGRP lines showed that this protein participates in the wiring of the neural circuits involved in locomotor behavior. Presumably, variations in the protein function might affect the synaptic connectivity of the neurons in the Central Complex of the fly brain, creating the high individual to individual variations, which ultimately will affect the apparent random choice, left or right, creating a bias in specific individuals (Ayroles et al., 2015; Buchanan et al., 2015). These studies indicate how intricate the relation between genes and environment is, showing that the genetic background of a population would determine the observed variability level, becoming heritable. However, the stochastic neuronal wiring in individuals can also be the source of particular behaviors.

These findings support the idea that stochastic variation in brain wiring and gene expression combined with different genetic traits are determinants of such behavior variability.

4. HOW EPIGENETICS INFLUENCE BEHAVIOR

Epigenetics involve any biological mechanisms that regulate the expression of genes without changing the DNA sequences, becoming the crossroad between the genetic and the environmental factors leading to a biological impact upon gene expression (Heard and Martienssen, 2014; Schuebel et al., 2016; Schiele and Domschke, 2018). Different factors influence epigenetic modifications such as diet, experience, characteristics of the ecosystem, lifestyle, and the physiological state of the individuals, impacting on disease outcome, social organization, and individual behavior, among others (Waterland and Jirtle, 2003; Cunliffe, 2016; Dawson et al., 2018; Baenas and Wagner, 2019).

Epigenetic modifications affect animals at the individual and social level, modifying the role of individuals inside specific social contexts (Anreiter et al., 2017; Sara et al., 2019). For example, honey bees display DNA methylation after intruders encounter, leading to aggressive behavior (Herb et al., 2018). Differential histone 3 (H3) acetylation (H3K27) affects morphologically and behaviorally *Camponotus floridanus* ant workers. Those modifications induce differences in foraging and scouting behaviors leading to high levels of task distribution (Simola et al., 2013, 2016; Yan et al., 2014). Epigenetic modifications also alter parasocial insects like the fruit fly behavioral, developmental, and physiological traits. For example, a low-protein diet induces H3K27 heterochromatin trimethylation shortening the lifespan of flies. In addition, acetylation of H3K27 by blocking the *Drosophila Polycomb* gene induces a dysregulation of the repression of homeotic genes (Tie et al., 2009, 2016). Furthermore, epigenetic regulation affects foraging behavior by histone methylation of the *for* (foraging) gene promoter *pr4* establishing a polymorphism between sitters and rovers behaviors in *D. melanogaster* (Anreiter et al., 2017). Other studies showed that euchromatin histone methyltransferase activity affects non-associative learning and courtship memory in *Drosophila* (Kramer et al., 2011).

5. INDIVIDUALITY IN COLLECTIVE BEHAVIOR

Animals coordinate their behavior with other individuals for benefits, including increased opportunities to mate, greater migratory and foraging efficiency, less chance of being attacked, and better energy costs (Handegard et al., 2012; Berdahl et al., 2013; Jolles et al., 2019). Several researchers have focused their research on the study of the neurogenetic bases of collective behavior in order to understand how individuals can form complex social networks among themselves, improving their survival as occurs in social animals like fishes, ducks, bees, or flies (Becher et al., 2010; Bialek et al., 2014; Ramdya et al., 2017).

Behavior individuality within a colony can emerge from self-organization and social interactions benefiting host hospitalization and decision-making processes (Jeanson, 2019). Individual roles within an animal social network can change over time as an evolutionary method to decrease disease transmission (Stroeymeyt et al., 2018). In other cases, biological roles can be persistent for each individual, such as birds taking turns as alarm-calling sentinels in the colony or the task distribution in ant colonies, respectively (Nagy et al., 2010; Yan et al., 2014; Ramdya et al., 2017; Friedman et al., 2020). Individuals in social networks experience social encounters to spread information from informed to uninformed to transmit beneficial information for survival and relevant future decision-making processes (Canright and Engø-Monsen, 2006). Different studies revealed that fruit flies coordinate their oviposition sites based on the information shared by experienced flies through social encounters. Those experiments suggest that highly clustered flies show a high potential to spread information among individuals (Pasquaretta et al., 2016). Besides, flies are aware of the number of individuals and adjust their interactive behavior to the group size (Rooke et al., 2020). Other studies have shown that collective aggregation depends on external stimuli. For example, the *Poxn* transcription factor and Orco co-receptor are involved in the chemical detection of fly cuticle hydrocarbon pheromones that may be involved in clustering mechanisms (Schneider et al., 2012b). In addition, the mechanoreceptor NompC is involved in collective behavior as *NompC* mutant flies only avoid noxious CO_2 when are clustered with wild-type flies compared with isolated *NompC* mutant ones. These results indicate that there is spread of information from wild type flies to *NompC* mutants (Ramdya et al., 2015). These studies, in addition to others, support the idea that fruit flies integrate sensory information in order to drive appropriate collective behavior and facilitate social learning and foraging decisions in larvae and adulthood to buffer

efficiently environmental stress (Tinette et al., 2004; Billen, 2006; Lihoreau et al., 2016; Dombrovski et al., 2017; Jolles et al., 2017; Jiang et al., 2020).

Despite all the benefits derived from the establishment of social networks within a group of individuals, *D. melanogaster* has a parasocial organization where collective and individual behavior remains cohesive. Each group member behaving differently could explain that the cascade of group motion likely emerges from specific individual patterns of behavior (Rosenthal et al., 2015). Nevertheless, there is no evidence that some individuals act as leaders beginning the clustering within groups of fruit flies. However, the aggregation process grows as more flies join the pioneer ones, affecting information spreading (Jiang et al., 2020).

Even if *D. melanogaster* organization does not fit in a eusocial pattern where there is specific and hierarchical task distribution, the presence of individual behavior heterogeneity may drive crucial collective behavior beneficial for both the individual and the conspecifics individuals. Thus, understanding the dynamics of collective behavior in the fruit fly may guide understanding the neurogenetic bases involved and how the behavioral patterns of animal societies arise.

6. METHODS TO STUDY BEHAVIOR INDIVIDUALITY

D. melanogaster has emerged as an excellent model to study behavior individuality for several reasons: the small size and short breeding time allow us to obtain large quantities of animals to test in small setups in short periods of time; there is a large number of inbred lines with sequenced and annotated genomes to search for the possible genetic basis of individuality, and; finally, the possibility to manipulate the genome and neurons of the flies allow us to test ultimately how the candidate genes (and neural circuits) affect the generation of behavioral variation (Venken et al., 2011). The number of behavioral paradigms developed to study *Drosophila* (and in general animal behavior) have blossomed in the last years due to an increase in computer capacity and the development of machine learning algorithms dedicated to it. In **Figure 2**, we describe some hardware (with custom associated software) used to study behavior in individual flies. For example, the classic Y-maze, where flies can choose between two paths, is scaled up to allow multiple simultaneous recordings of individual flies. With this high-throughput system, the behavior of 25,000 individuals was analyzed and permitted the study of the neural and genetic basis of handedness in flies, identifying candidate genes and neurons (Buchanan et al., 2015) (**Figure 2A**). As mentioned in previous sections, animals, and particularly *D. melanogaster* display idiosyncratic behavioral responses to odors. To study this behavior, Honegger et al. build a paradigm arena where individual flies could choose between two odors emanating from opposing ends of a corridor. By video tracking the fly behavior, it was possible to show how neuromodulation was involved in the preferential choice of individuals (**Figure 2B**) (Honegger et al., 2019). Other innate behaviors like object orientation responses can be analyzed in a high-throughput manner using multiple Buridian paradigm arenas and video tracking (**Figure 2C**). Using this set up, the authors demonstrated that stochastic developmental events were altering the Dorsal Cluster Neuron circuits of different individuals, leading to idiosyncratic behaviors in flies (Linneweber et al., 2020). Finally, it is also possible to study feeding in *D. melanogaster*. *FlyPad* is an automated high-throughput method to study fly ingestion in individual flies. This system would allow the analysis of behavior individuality in, for example, the ability of flies to choose between two types of foods (Itskov et al., 2014) (**Figure 2D**). Recently, an upgrade in *FlyPad* named *OptoPad* allows optogenetically modifying the activity of selected circuits in real-time by ectopically expressing channelrhodopsins in those neurons. With this method, it is possible to couple the feeding activity of the fly with the modification of the neural activity in a closed-loop manner (Moreira et al., 2019).

The previously described methods are focused on the analysis of individual flies. However, the social context is lost, and although flies are non-eusocial insects, flies can aggregate both *in vitro* (Jiang et al., 2020) and in the wild (Soto-Yéber et al., 2019). The formation of *Drosophila* clusters is motivated by the presence of mating partners or food, with pheromones like cis-Vaccenyl acetate (Bartelt et al., 1985) and neuromodulators like serotonin (Sun et al., 2020) playing an essential role. As shown in the previous section, individuality can affect collective behavior. For example, within a group, some individuals display "bold" or "shy" behaviors. Newer software, like *idtracker.ai*, can identify each individual unequivocally in large groups (i.e., up to 70 flies), track overtime their trajectory, and the interaction with other members of the group (Romero-Ferrero et al., 2019). Finally, it is essential to mention that all those methods require standardized procedures, which start with the breeding conditions. Different mediums to homogenize the growth of flies can decrease variability due to external conditions (Piper et al., 2014). **Table 1** contains a thorough description of many hardware and software developed in recent years that are applied or can be applied to study behavior individuality. Most of the software and hardware listed are open source and shared with any laboratory that requests its use. We indicate the species for which they were designed or most used. However, researchers can modify the published versions to adapt them to their model system of interest. We apologize in advance for the methods we forgot to mention or did not find, as many appear constantly.

After describing the behavior of interest, we need to understand such behavior's genetic and neural basis. The advancement of genomic tools like Next Generation Sequencing, QTL, and GWAS is helping to understand how genes relate to behavioral traits (Bengston et al., 2018) (Figure 1E). Furthermore, we have seen the advantage of working with already sequenced collections of isogenic lines (Mackay et al., 2012). In addition, now we can do experiments to study large natural populations of flies and sequence all individuals with excellent coverage depth at low cost.

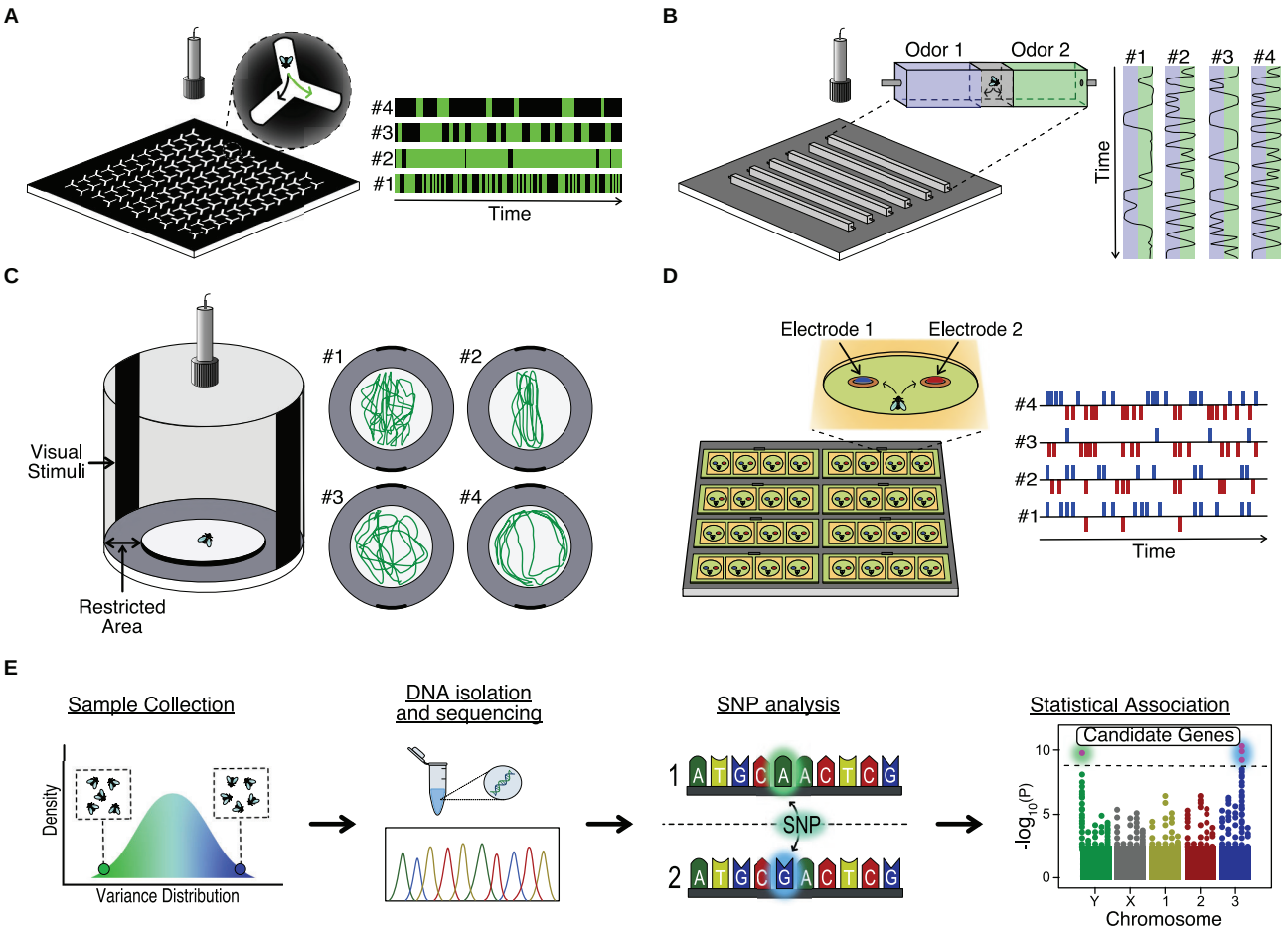

FIGURE 2 | High throughput analysis of behavior variance. **(A)** Schematic set up for study locomotor handedness variability by Y-maze (Ayroles et al., 2015; Buchanan et al., 2015). **(B)** Schematic setup for study olfactory guidance variability. Adapted from Honegger et al. (2019). **(C)** Schematic Buridian arena to study visual orientation variability (Colomb et al., 2012). **(D)** Schematic FlyPAD set-up to study feeding microstructure variability (Itskov et al., 2014). **(E)** Genome-Wide Association Studies (GWAS) workflow.

Finally, the study of the neural circuitry involved in behavior, *D. melanogaster*, is an excellent system as many different transgenic lines have been created to label, trace, and analyze complete neural circuits (Jenett et al., 2012). Similar to *C. elegans*, we aim to map all synaptic partners in the brain of *D. melanogaster* through electron microscopy (EM). Although we still need to map the whole brain, the connectome for the central brain already exists (Scheffer et al., 2020). So far, those data provide a standalone image of the *Drosophila* brain. However, it would be desirable to have a full EM reconstruction of each individual's brain analyzed, although this looks right now as an impossible effort. Even for smaller organisms, it is a daunting task, but it could be beneficial as a recent work where EM reconstruction of eight *C. elegans* brains showed variations in synaptic connectivity between them, making each brain unique (Witvliet et al., 2021). As we learn more about the circuitry involved in particular behaviors, it might be possible in the future to focus our EM reconstruction efforts on small regions of the brain known to control particular behaviors. We could then reconstruct those regions synaptically for multiple individuals, gaining excellent knowledge regarding neural circuit variability between individuals.

7. CONCLUSIONS

How do heritable (genetic) and non-heritable (stochastic events) factors interact to shape behavior? It could be possible that individuals carrying particular polymorphisms might be more susceptible to environmental changes, leading to enough variations among individuals to show specific individual persistent behaviors. It would not be easy to differentiate between the genetic and non-genetic basis of such behavior as there is a constant interplay in this particular case. To add more complexity to the problem epigenetic modifications, alter gene function. It means we cannot just focus our efforts on finding particular genetic sequences as the final goal, as we need to understand how genomes change along with the life of an individual. Finally, from a behavioral point of view, we are constantly talking about individuality. At the same time, animals modify their behaviors during their lifetime as they interact with other conspecifics. All

TABLE 1 | Overview of automated and high throughput software and hardware for animal behavior analysis.

Hardware/software	Utility	Software/ hardware	Programming language	Species*	References
AnTrax	Tracking software for color-tagged individuals of small species	Software	Matlab	*Ooceraea biroi*	Gal et al., 2020
Automated *Drosophila* Olfactory Conditioning System	Automated software and hardware system to study olfactory behavior coupled with learning and memory assessment	Software and Hardware	Arduino and Labview	*Drosophila melanogaster*	Jiang et al., 2016
BEEtag	Image tracking software to track labeled identified individual bees or anatomical markers	Software	Matlab	*Apis mellifera*	Crall et al., 2015
Buritrack	Tracking software either in the presence or in the absence of visual targets in a Buridian paradigm setup	Software and Hardware	R	Different species	Colomb et al., 2012
ClockLab	Analysis of circadian locomotor activity data collected using DAM system	Software	Matlab	*Drosophila melanogaster*	Pfeiffenberger et al., 2010
CTrax	Tracking software for automatically quantify individual and social behavior of fruit flies	Software	Matlab	*Drosophila melanogaster*	Branson et al., 2009
DAM	*Drosophila Activity Monitor* . System from Trikinetics for locomotion, sleep and circadian rhythms activity quantification	Hardware	None	*Drosophila melanogaster*	www.trikinetics.com
DART	*Drosophila Arousal Tracking*. Hardware and software that reports locomotor and positional activity data of individual flies in multiple chambers	Software and Hardware	Matlab	*Drosophila melanogaster*	Faville et al., 2015
DeepLabCut	Markerless pose estimation based on machine learning with deep neural networks that achieves excellent results with minimal training data to study behavior by tracking various body parts	Software	Python	*Mus musculus* and *Drosophila melanogaster*	Mathis et al., 2018
DeepPoseKit	Machine learning software for deep estimation of pose location to analyze specific behavior parameters	Software	Python	Different species	Graving et al., 2019
DIAS	*Dynamic Image Analysis System*. Tracking software to analyze locomotor behavior in the adult fruit fly as in other individuals	Software	Matlab	*Drosophila melanogaster*	Slawson et al., 2009
Drosophila Island	Algorithm that quantify locomotor and flight activity behavior from fruit flies on specific Island platforms	Software	Fiji and R	*Drosophila melanogaster*	Eidhof et al., 2017
Ethoscopes	Machine learning software to track and profile behavior in real time while trigger stimulus to flies in a feedback-loop mode	Software	R	*Drosophila melanogaster*	Geissmann et al., 2017
Expresso	Automated feeding hardware to measure individual meal-bouts with high temporal and volume resolution	Hardware	Matlab	*Drosophila melanogaster*	Yapici et al., 2016
FIM / FIMTrack	*FTIR-based Imaging Method*. Tracking hardware and software to study locomotion behavior based on internal reflection of infrared light (FTIR) operating at all wavelengths allowing *in vivo* detection of fluorescent proteins	Software and Hardware	C++	*Drosophila melanogaster*	Risse et al., 2013
FLIC	*Fly Liquid-Food Interaction Counter*. Automated hardware to detect and quantify physical contact with liquid food to study feeding behavior in fruit flies	Software and Hardware	Matlab	*Drosophila melanogaster*	Ro et al., 2014
Flyception	Retroreflective based tracking coupled with imaging brain activity on free walking fruit flies	Hardware	C++	*Drosophila melanogaster*	Grover et al., 2020
FlyGrAM	*Fly Group Activity Monitor*. Software for monitoring real-time group locomotion based on background subtraction	Software	Python	*Drosophila melanogaster*	Scaplen et al., 2019
FlyMAD	*Fly Mind-Altering Device*. Infrared laser targeting hardware for accurately thermogenetic silencing or activation on freely walking flies	Hardware	None	*Drosophila melanogaster*	Bath et al., 2014
FlyPAD	*Fly Proboscis and Activity Detector*. Detailed, automated and high-throughput quantification of feeding behavior based on capacitance data	Software and Hardware	Matlab	*Drosophila melanogaster*	Itskov et al., 2014

(Continued)

TABLE 1 | Continued

Hardware/software	Utility	Software/ hardware	Programming language	Species*	References
FlyPEZ	High-throughput hardware system to rapidly analyze individual fly behavior with tracking and controlled sensory or optogenetic stimulation	Hardware	Matlab	*Drosophila melanogaster*	Williamson et al., 2018
Flywalk	Automatic olfactory preference tracking hardware for screening individual flies	Hardware	Matlab	*Drosophila melanogaster*	Steck et al., 2012
Idtrackerai	Individual tracking of all trajectories from small and large collectives with high identification accuracy	Software	Python	Different species	Romero-Ferrero et al., 2019
Imaging system for zebrafish larvae behavior analyses	Three-camera imaging system hardware to image zebrafish larvae behavior in front of visual stimuli provided by specific slides in a high-throughput manner	Hardware	None	*Danio rerio*	Richendrfer and Créton, 2013
JAABA	Machine learning-based system for automatically quantify different animal behavior parameters	Software	Matlab	Different species	Kabra et al., 2013
Machine learning tracking software	Machine learning-based tracking software for individual trajectories inside a group	Software	None	Insects	Wario et al., 2017
pySOLO	Sleep and locomotor activity software analyzer of multiple isolated flies	Software	Python	*Drosophila melanogaster*	Gilestro, 2012
RFID	Radiofrequency identification based tracking hardware on individual ID infrared detection by antennas	Hardware	Matlab	Different species	Schneider et al., 2012a; Torquet et al., 2018; Reinert et al., 2019
RING	*Rapid Iterative Negative Geotaxis*. Digital photography based hardware to measure negative geotaxis in individual or collective animal groups simultaneously	Hardware	Scion Image - Pascal	*Drosophila melanogaster*	Gargano et al., 2005
The Tracked Program	Tracking of small movements at any location on a DAM set up to study sleep behavior and structure	Software	Java	*Drosophila melanogaster*	Donelson et al., 2012
WormFarm	Integrated microfluidic hardware to quantify different behaviors such as survival from images and videos	Hardware	None	*Caenorhabditis elegans*	Xian et al., 2013

**Species for which the hardware or software was initially designed. Nevertheless, most of them can be adapted to other species.*

this information indicates that the emergence of individuality or animal personality requires the study at different levels.

The latest advancements and development of high-throughput sequencing have finally opened the door to looking for the genetic basis of animal individuality and how the environment affects gene expression. We know individual animals show particular personalities, from flies to mice, monkeys to humans. However, at this very moment, we can start thinking to move from pure ethological studies to the molecular dissection of those behaviors. Neural circuitry tracing and reconstruction through electron microscopy are helping to build a map of the neural connections of the brain. So far, we do not have more than a few individuals. However, understanding and dissecting those circuits might help us finally understand how the expression of particular genes during a particular period or the subtle variations in connectivity could lead to a deeper understanding of individuality.

It is intriguing that nervous systems, like many other biological systems, are plastic within certain boundaries, so we can expect that personal individuality will be expressed deferentially over time or under certain environmental circumstances. *D. melanogaster* offers an excellent model system as we can test our hypothesis in large groups of animals in a short period of time (Buchanan et al., 2015). In addition, we can control to a large degree the genetic variation of our population by using inbred lines (Ayroles et al., 2015; Linneweber et al., 2020). The generation of the DGRP lines has helped advance this field, as controlling the genetic variation of the populations of interest can help us narrow down the candidate genetic variants, if any, or discard the genetic variation and ascribe it to stochastic developmental processes.

We have focused on the genetic and epigenetic changes that alter individual behavior. We have also studied how stochastic developmental processes alter neural connectivity leading to interindividual variation. However, another possible source of potential behavioral variability might come from the interaction of individuals with environmental microbes, from *Wolbachia* infections to changes in the gut microbiome. In this particular case, no genetic variation or neural circuit alteration would be responsible for the change in behavior. It is known that *Wolbachia* infection affects different *D. melanogaster* behaviors such as sleep (Bi et al., 2018), temperature preference (Truitt et al., 2019), or aggression (Rohrscheib et al., 2015). Alteration in the gut microbiome can affect aggression in *Drosophila* males (Jia et al., 2021) or sleep and memory (Silva et al., 2021). Those results point to the interaction of individuals with microorganisms as another potential source of interindividual behavior variability that must be taken into consideration.

Finally, from an evolutionary point of view, individuality might play an essential role in providing an adaptative advantage. For example, we have described that animals might use diversified bet-hedging as a mechanism to produce high levels of variation within a population to ensure that at least some individuals will be well-adapted when facing unpredictable environments. Although more experimental evidence accumulates to support this theory, without any doubt, we are in front of a growing field of knowledge that will evolve soon.

AUTHOR CONTRIBUTIONS

RM-A and JS-A conceived and wrote the manuscript. All authors contributed to the article and approved the submitted version.

FUNDING

This study was supported by grants from the Generalitat Valenciana, CIDEGENT program (CIDEGENT/2018/035), Spanish Ministry of Science and Innovation (PID2019-105839GA-I00) and Program Ramón y Cajal (RyC2019-026747-I).

ACKNOWLEDGMENTS

We thank the Generalitat Valenciana and Spanish Ministry of Science for financial support and José María Buil Gómez for critical discussions and comments on the manuscript.

REFERENCES

Akhund-Zade, J., Bergland, A. O., Crowe, S. O., and Unckless, R. L. (2017). The genetic basis of natural variation in Drosophila (Diptera: Drosophilidae) virgin egg retention. *J. Insect Sci.* 17. doi: 10.1093/jisesa/iew094

Akhund-Zade, J., Ho, S., O'Leary, C., and de Bivort, B. (2019). The effect of environmental enrichment on behavioral variability depends on genotype, behavior, and type of enrichment. *J. Exp. Biol.* 222. doi: 10.1242/jeb.202234

Alpert, M. H., Frank, D. D., Kaspi, E., Flourakis, M., Zaharieva, E. E., Allada, R., et al. (2020). A circuit encoding absolute cold temperature in Drosophila. *Curr. Biol.* 30, 2275.e5–2288.e5. doi: 10.1016/j.cub.2020.04.038

Amat, I., Desouhant, E., Gomes, E., Moreau, J., and Monceau, K. (2018). Insect personality: what can we learn from metamorphosis? *Curr. Opin. Insect Sci.* 27, 46–51. doi: 10.1016/j.cois.2018.02.014

Anreiter, I., Kramer, J. M., and Sokolowski, M. B. (2017). Epigenetic mechanisms modulate differences in Drosophila foraging behavior. *Proc. Natl. Acad. Sci. U.S.A.* 114, 12518–12523. doi: 10.1073/pnas.1710770114

Anreiter, I., and Sokolowski, M. B. (2019). The foraging gene and its behavioral effects: pleiotropy and plasticity. *Annu. Rev. Genet.* 53, 373–392. doi: 10.1146/annurev-genet-112618-043536

Ayroles, J. F., Buchanan, S. M., O'Leary, C., Skutt-Kakaria, K., Grenier, J. K., Clark, A. G., et al. (2015). Behavioral idiosyncrasy reveals genetic control of phenotypic variability. *Proc. Natl. Acad. Sci. U.S.A.* 112:6706. doi: 10.1073/pnas.1503830112

Baenas, N., and Wagner, A. E. (2019). *Drosophila melanogaster* as an alternative model organism in nutrigenomics. *Genes Nutr.* 14:14. doi: 10.1186/s12263-019-0641-y

Bartelt, R. J., Schaner, A. M., and Jackson, L. L. (1985). Cis-vaccenyl acetate as an aggregation pheromone inDrosophila *melanogaster*. *J. Chem. Ecol.* 11, 1747–1756. doi: 10.1007/BF01012124

Bath, D. E., Stowers, J. R., Hörmann, D., Poehlmann, A., Dickson, B. J., and Straw, A. D. (2014). FlyMAD: Rapid thermogenetic control of neuronal activity in freely walking Drosophila. *Nat. Methods* 11, 756–762. doi: 10.1038/nmeth.2973

Becher, M. A., Hildenbrandt, H., Hemelrijk, C. K., and Moritz, R. F. (2010). Brood temperature, task division and colony survival in honeybees: a model. *Ecol. Modell.* 221, 769–776. doi: 10.1016/j.ecolmodel.2009.11.016

Bell, A. M. (2007). Future directions in behavioural syndromes research. *Proc. R. Soc. B Biol. Sci.* 274, 755–761. doi: 10.1098/rspb.2006.0199

Bengston, S. E., Dahan, R. A., Donaldson, Z., Phelps, S. M., van Oers, K., Sih, A., et al. (2018). Genomic tools for behavioural ecologists to understand repeatable individual differences in behaviour. *Nat. Ecol. Evol.* 2, 944–955. doi: 10.1038/s41559-017-0411-4

Berdahl, A., Torney, C. J., Ioannou, C. C., Faria, J. J., and Couzin, I. D. (2013). Emergent sensing of complex environments by mobile animal groups. *Science* 339, 574–576. doi: 10.1126/science.1225883

Bi, J., Sehgal, A., Williams, J. A., and Wang, Y.-F. (2018). Wolbachia affects sleep behavior in *Drosophila melanogaster*. *J. Insect Physiol.* 107, 81–88. doi: 10.1016/j.jinsphys.2018.02.011

Bialek, W., Cavagna, A., Giardina, I., Mora, T., Pohl, O., Silvestri, E., et al. (2014). Social interactions dominate speed control in poising natural flocks near criticality. *Proc. Natl. Acad. Sci. U.S.A.* 111, 7212–7217. doi: 10.1073/pnas.1324045111

Bierbach, D., Laskowski, K. L., and Wolf, M. (2017). Behavioural individuality in clonal fish arises despite near-identical rearing conditions. *Nat. Commun.* 8:15361. doi: 10.1038/ncomms15361

Billen, J. (2006). Signal variety and communication in social insects. *Proc. Neth. Entomol. Soc. Meet* 17, 9–25.

Blake, W. J., Balázsi, G., Kohanski, M. A., Isaacs, F. J., Murphy, K. F., Kuang, Y., et al. (2006). Phenotypic consequences of promoter-mediated transcriptional noise. *Mol. Cell* 24, 853–865. doi: 10.1016/j.molcel.2006.11.003

Brankatschk, M., Gutmann, T., Knittelfelder, O., Palladini, A., Prince, E., Grzybek, M., et al. (2018). A temperature-dependent switch in feeding preference improves Drosophila development and survival in the cold. *Dev. Cell* 46, 781.e4–793.e4. doi: 10.1016/j.devcel.2018.05.028

Branson, K., Robie, A. A., Bender, J., Perona, P., and Dickinson, M. H. (2009). High-throughput ethomics in large groups of Drosophila. *Nat. Methods* 6, 451–457. doi: 10.1038/nmeth.1328

Brown, E. B., Layne, J. E., Zhu, C., Jegga, A. G., and Rollmann, S. M. (2013). Genome-wide association mapping of natural variation in odour-guided behaviour in Drosophila. *Genes Brain Behav.* 12, 503–515. doi: 10.1111/gbb.12048

Buchanan, S. M., Kain, J. S., and de Bivort, B. L. (2015). Neuronal control of locomotor handedness in Drosophila. *Proc. Natl. Acad. Sci. U.S.A.* 112:6700. doi: 10.1073/pnas.1500804112

Buchberger, E., Bilen, A., Ayaz, S., Salamanca, D., Matas de las Heras, C., Niksic, A., et al. (2021). Variation in pleiotropic hub gene expression is associated with interspecific differences in head shape and eye size in Drosophila. *Mol. Biol. Evol.* 38, 1924–1942. doi: 10.1093/molbev/msaa335

Canright, G. S., and Engø-Monsen, K. (2006). Spreading on networks: a topographic view. *Complexus* 3, 131–146. doi: 10.1159/000094195

Carreira, V. P., Mensch, J., Hasson, E., and Fanara, J. J. (2016). Natural genetic variation and candidate genes for morphological traits in *Drosophila melanogaster*. *PLoS ONE* 11:e0160069. doi: 10.1371/journal.pone.0160069

Casillas, S., and Barbadilla, A. (2017). Molecular population genetics. *Genetics* 205, 1003–1035. doi: 10.1534/genetics.116.196493

Colomb, J., Reiter, L., Blaszkiewicz, J., Wessnitzer, J., and Brembs, B. (2012). Open source tracking and analysis of adult Drosophila locomotion in Buridan's paradigm with and without visual targets. *PLoS ONE* 7:e42247. doi: 10.1371/journal.pone.0042247

Crall, J. D., Gravish, N., Mountcastle, A. M., and Combes, S. A. (2015). BEEtag: a low-cost, image-based tracking system for the study of animal behavior and locomotion. *PLoS ONE* 10:e0136487. doi: 10.1371/journal.pone.0136487

Cunliffe, V. T. (2016). The epigenetic impacts of social stress: how does social adversity become biologically embedded? *Epigenomics* 8, 1653–1669. doi: 10.2217/epi-2016-0075

Dall, S. R. X., Houston, A. I., and McNamara, J. M. (2004). The behavioural ecology of personality: consistent individual differences from an adaptive perspective. *Ecol. Lett*. 7, 734–739. doi: 10.1111/j.1461-0248.2004.00618.x

Davidson, C. J., and Surette, M. G. (2008). Individuality in bacteria. *Annu. Rev. Genet*. 42, 253–268. doi: 10.1146/annurev.genet.42.110807.091601

Dawson, E. H., Bailly, T. P. M., Dos Santos, J., Moreno, C., Devilliers, M., Maroni, B., et al. (2018). Social environment mediates cancer progression in Drosophila. *Nat. Commun*. 9:3574. doi: 10.1038/s41467-018-05737-w

Dombrovski, M., Poussard, L., Moalem, K., Kmecova, L., Hogan, N., Schott, E., et al. (2017). Cooperative behavior emerges among Drosophila larvae. *Curr. Biol*. 27, 2821.e2–2826.e2. doi: 10.1016/j.cub.2017.07.054

Donelson, N., Kim, E. Z., Slawson, J. B., Vecsey, C. G., Huber, R., and Griffith, L. C. (2012). High-resolution positional tracking for long-term analysis of Drosophila sleep and locomotion using the "tracker?? program. *PLoS ONE* 7:e37250. doi: 10.1371/journal.pone.0037250

Eidhof, I., Fenckova, M., Elurbe, D. M., van de Warrenburg, B., Nobau, A. C., and Schenck, A. (2017). High-throughput analysis of locomotor behavior in the Drosophila island assay. *J. Visual. Exp*. 2017, 1–11. doi: 10.3791/55892

Faisal, A. A., Selen, L. P. J., and Wolpert, D. M. (2008). Noise in the nervous system. *Nat. Rev. Neurosci*. 9, 292–303. doi: 10.1038/nrn2258

Faville, R., Kottler, B., Goodhill, G. J., Shaw, P. J., and Van Swinderen, B. (2015). How deeply does your mutant sleep? Probing arousal to better understand sleep defects in Drosophila. *Sci. Rep*. 5:8454. doi: 10.1038/srep08454

Friedman, D., Johnson, B., and Linksvayer, T. (2020). Distributed physiology and the molecular basis of social life in eusocial insects. *Hormones Behav*. 122:104757. doi: 10.1016/j.yhbeh.2020.104757

Fry, J. D. (2008). Genotype-environment interaction for total fitness in Drosophila. *J. Genet*. 87:355. doi: 10.1007/s12041-008-0058-7

Gaertner, B. E., Ruedi, E. A., McCoy, L. J., Moore, J. M., Wolfner, M. F., and Mackay, T. F. C. (2015). Heritable variation in courtship patterns in *Drosophila melanogaster*. *Genes Genomes Genet*. 5, 531–539. doi: 10.1534/g3.114.014811

Gal, A., Saragosti, J., and Kronauer, D. J. (2020). antrax, a software package for high-throughput video tracking of color-tagged insects. *eLife* 9:e58145. doi: 10.7554/eLife.58145

Gargano, J. W., Martin, I., Bhandari, P., and Grotewiel, M. S. (2005). Rapid iterative negative geotaxis (RING): a new method for assessing age-related locomotor decline in Drosophila. *Exp. Gerontol*. 40, 386–395. doi: 10.1016/j.exger.2005.02.005

Geissmann, Q., Garcia Rodriguez, L., Beckwith, E. J., French, A. S., Jamasb, A. R., and Gilestro, G. F. (2017). Ethoscopes: an open platform for high-throughput ethomics. *PLoS Biol*. 15:e2003026. doi: 10.1371/journal.pbio.2003026

Gilestro, G. F. (2012). Video tracking and analysis of sleep in *Drosophila melanogaster*. *Nat. Protoc*. 7, 995–1007. doi: 10.1038/nprot.2012.041

Graving, J. M., Chae, D., Naik, H., Li, L., Koger, B., Costelloe, B. R., et al. (2019). Deepposekit, a software toolkit for fast and robust animal pose estimation using deep learning. *eLife* 8, 1–42. doi: 10.7554/eLife.47994

Grover, D., Katsuki, T., Li, J., Dawkins, T. J., and Greenspan, R. J. (2020). Imaging brain activity during complex social behaviors in Drosophila with flyception2. *Nat. Commun*. 11:623. doi: 10.1038/s41467-020-14487-7

Guzman, R. M., Howard, Z. P., Liu, Z., Oliveira, R. D., Massa, A. T., Omsland, A., et al. (2021). Natural genetic variation in *Drosophila melanogaster* reveals genes associated with *Coxiella burnetii* infection. *Genetics* 217. doi: 10.1093/genetics/iyab005

Hall, J. C. (1994). The mating of a fly. *Science* 264, 1702–1714. doi: 10.1126/science.8209251

Handegard, N. O., Boswell, K. M., Ioannou, C. C., Leblanc, S. P., Tjøstheim, D. B., and Couzin, I. D. (2012). The dynamics of coordinated group hunting and collective information transfer among schooling prey. *Curr. Biol*. 22, 1213–1217. doi: 10.1016/j.cub.2012.04.050

Heard, E., and Martienssen, R. A. (2014). Transgenerational epigenetic inheritance: myths and mechanisms. *Cell* 157, 95–109. doi: 10.1016/j.cell.2014.02.045

Herb, B. R., Shook, M. S., Fields, C. J., and Robinson, G. E. (2018). Defense against territorial intrusion is associated with DNA methylation changes in the honey bee brain. *BMC Genomics* 19:216. doi: 10.1186/s12864-018-4594-0

Honegger, K., and de Bivort, B. (2018). Stochasticity, individuality and behavior. *Curr. Biol*. 28, R8-R12. doi: 10.1016/j.cub.2017.11.058

Honegger, K. S., Smith, M. A.-Y., Churgin, M. A., Turner, G. C., and de Bivort, B. L. (2019). Idiosyncratic neural coding and neuromodulation of olfactory individuality in Drosophila. *Proc. Natl. Acad. Sci. U.S.A*. doi: 10.1073/pnas.1901623116

Huang, W., Carbone, M. A., Lyman, R. F., Anholt, R. R. H., and Mackay, T. F. C. (2020). Genotype by environment interaction for gene expression in *Drosophila melanogaster*. *Nat. Commun*. 11:5451. doi: 10.1038/s41467-020-19131-y

Hung, H.-C., Kay, S. A., and Weber, F. (2009). Hsp90, a capacitor of behavioral variation. *J. Biol. Rhythms* 24, 183–192. doi: 10.1177/0748730409333171

Itskov, P. M., Moreira, J.-M., Vinnik, E., Lopes, G., Safarik, S., Dickinson, M. H., et al. (2014). Automated monitoring and quantitative analysis of feeding behaviour in Drosophila. *Nat. Commun*. 5:4560. doi: 10.1038/ncomms5560

Jeanson, R. (2019). Within-individual behavioural variability and division of labour in social insects. *J. Exp. Biol*. 222. doi: 10.1242/jeb.190868

Jenett, A., Rubin, G. M., Ngo, T.-T., Shepherd, D., Murphy, C., Dionne, H., et al. (2012). A gal4-driver line resource for Drosophila neurobiology. *Cell Rep*. 2, 991–1001. doi: 10.1016/j.celrep.2012.09.011

Jia, Y., Jin, S., Hu, K., Geng, L., Han, C., Kang, R., et al. (2021). Gut microbiome modulates Drosophila aggression through octopamine signaling. *Nat. Commun*. 12:2698. doi: 10.1038/s41467-021-23041-y

Jiang, H., Hanna, E., Gatto, C. L., Page, T. L., Bhuva, B., and Broadie, K. (2016). A fully automated Drosophila olfactory classical conditioning and testing system for behavioral learning and memory assessment. *J. Neurosci. Methods* 261, 62–74. doi: 10.1016/j.jneumeth.2015.11.030

Jiang, L., Cheng, Y., Gao, S., Zhong, Y., Ma, C., Wang, T., et al. (2020). Emergence of social cluster by collective pairwise encounters in *Drosophila*. *eLife* 9:e51921. doi: 10.7554/eLife.51921

Jin, W., Riley, R. M., Wolfinger, R. D., White, K. P., Passador-Gurgell, G., and Gibson, G. (2001). The contributions of sex, genotype and age to transcriptional variance in *Drosophila melanogaster*. *Nat. Genet*. 29, 389–395. doi: 10.1038/ng766

Jolles, J. W., Boogert, N. J., Sridhar, V. H., Couzin, I. D., and Manica, A. (2017). Consistent individual differences drive collective behavior and group functioning of schooling fish. *Curr. Biol*. 27, 2862.e7–2868.e7. doi: 10.1016/j.cub.2017.08.004

Jolles, J. W., King, A. J., and Killen, S. S. (2019). The role of individual heterogeneity in collective animal behaviour. *Trends Ecol. Evol*. doi: 10.1016/j.tree.2019.11.001

Juneja, P., Quinn, A., and Jiggins, F. M. (2016). Latitudinal clines in gene expression and cis-regulatory element variation in *Drosophila melanogaster*. *BMC Genomics* 17:981. doi: 10.1186/s12864-016-3333-7

Kabra, M., Robie, A. A., Rivera-Alba, M., Branson, S., and Branson, K. (2013). Jaaba: interactive machine learning for automatic annotation of animal behavior. *Nat. Methods* 10, 64–67. doi: 10.1038/nmeth.2281

Kain, J. S., Stokes, C., and de Bivort, B. L. (2012). Phototactic personality in fruit flies and its suppression by serotonin and white. *Proc. Natl. Acad. Sci. U.S.A*. 109, 19834–19839. doi: 10.1073/pnas.1211988109

Kim, U.-K., Jorgenson, E., Coon, H., Leppert, M., Risch, N., and Drayna, D. (2003). Positional cloning of the human quantitative trait locus underlying taste sensitivity to phenylthiocarbamide. *Science* 299, 1221–1225. doi: 10.1126/science.1080190

Kiral, F. R., Dutta, S. B., Linneweber, G. A., Poppa, C., von Kleist, M., Hassan, B. A., et al. (2021). Variable brain wiring through scalable and relative synapse formation in Drosophila. *bioRxiv*. doi: 10.1101/2021.05.12.443860

Klepsatel, P., Girish, T. N., and Gáliková, M. (2020). Acclimation temperature affects thermal reaction norms for energy reserves in Drosophila. *Sci. Rep*. 10:21681. doi: 10.1038/s41598-020-78726-z

Klepsatel, P., Wildridge, D., and Gáliková, M. (2019). Temperature induces changes in Drosophila energy stores. *Sci. Rep*. 9:5239. doi: 10.1038/s41598-019-41754-5

Kowalewski, J., and Ray, A. (2020). Predicting human olfactory perception from activities of odorant receptors. *iScience* 23. doi: 10.1016/j.isci.2020.101361

Koyama, T., Texada, M. J., Halberg, K. A., and Rewitz, K. (2020). Metabolism and growth adaptation to environmental conditions in Drosophila. *Cell. Mol. Life Sci*. 77, 4523–4551. doi: 10.1007/s00018-020-03547-2

Kramer, J. M., Kochinke, K., Oortveld, M. A. W., Marks, H., Kramer, D., de Jong, E. K., et al. (2011). Epigenetic regulation of learning and memory by Drosophila EHMT/G9a. *PLoS Biol*. 9:e1000569. doi: 10.1371/journal.pbio.1000569

Krams, I. A., Krama, T., Krams, R., Trakimas, G., Popovs, S., Jøers, P., et al. (2021). Serotoninergic modulation of phototactic variability underpins a bet-hedging strategy in *Drosophila melanogaster*. *Front. Behav. Neurosci*. 15:66. doi: 10.3389/fnbeh.2021.659331

Lihoreau, M., Clarke, I. M., Buhl, J., Sumpter, D. J. T., and Simpson, S. J. (2016). Collective selection of food patches in Drosophila. *J. Exp. Biol*. 219, 668–675. doi: 10.1242/jeb.127431

Lin, Y., Chen, Z. X., Oliver, B., and Harbison, S. T. (2016). Microenvironmental gene expression plasticity among individual *Drosophila melanogaster*. *Genes Genomes Genetics* 6, 4197–4210. doi: 10.1534/g3.116.035444

Linneweber, G. A., Andriatsilavo, M., Dutta, S. B., Bengochea, M., Hellbruegge, L., Liu, G., et al. (2020). A neurodevelopmental origin of behavioral individuality in the Drosophila visual system. *Science* 367, 1112–1119. doi: 10.1126/science.aaw7182

Mackay, T. F. C., Richards, S., Stone, E. A., Barbadilla, A., Ayroles, J. F., Zhu, D., et al. (2012). The *Drosophila melanogaster* genetic reference panel. *Nature* 482, 173–178. doi: 10.1038/nature10811

Mathis, A., Mamidanna, P., Cury, K. M., Abe, T., Murthy, V. N., Mathis, M. W., et al. (2018). DeepLabCut: markerless pose estimation of user-defined body parts with deep learning. *Nat. Neurosci*. 21, 1281–1289. doi: 10.1038/s41593-018-0209-y

Moreira, J.-M., Itskov, P. M., Goldschmidt, D., Baltazar, C., Steck, K., Tastekin, I., et al. (2019). optopad, a closed-loop optogenetics system to study the circuit basis of feeding behaviors. *eLife* 8:e43924. doi: 10.7554/eLife.43924

Nagy, M., Ákos, Z., Biro, D., and Vicsek, T. (2010). Hierarchical group dynamics in pigeon flocks. *Nature* 464, 890–893. doi: 10.1038/nature08891

Newman, J. R. S., Ghaemmaghami, S., Ihmels, J., Breslow, D. K., Noble, M., DeRisi, J. L., et al. (2006). Single-cell proteomic analysis of *S. cerevisiae* reveals the architecture of biological noise. *Nature* 441, 840–846. doi: 10.1038/nature04785

Panel, A. D. C., Pen, I., Pannebakker, B. A., Helsen, H. H. M., and Wertheim, B. (2020). Seasonal morphotypes of Drosophila suzukii differ in key life-history traits during and after a prolonged period of cold exposure. *Ecol. Evol*. 10, 9085–9099. doi: 10.1002/ece3.6517

Pasquaretta, C., Battesti, M., Klenschi, E., Bousquet, C. A. H., Sueur, C., and Mery, F. (2016). How social network structure affects decision-making in *Drosophila melanogaster*. *Proc. R. Soc. B Biol. Sci*. 283:20152954. doi: 10.1098/rspb.2015.2954

Pfeiffenberger, C., Lear, B. C., Keegan, K. P., and Allada, R. (2010). Processing circadian data collected from the Drosophila activity monitoring (DAM) system. *Cold Spring Harbor Protoc*. 2010:5519. doi: 10.1101/pdb.prot5519

Piper, M. D. W., Blanc, E., Leitão-Gonçalves, R., Yang, M., He, X., Linford, N. J., et al. (2014). A holidic medium for *Drosophila melanogaster*. *Nat. Methods* 11, 100–105. doi: 10.1038/nmeth.2731

Raji, J. I., and Potter, C. J. (2021). The number of neurons in Drosophila and mosquito brains. *PLoS ONE* 16:e0250381. doi: 10.1371/journal.pone.0250381

Ramdya, P., Lichocki, P., Cruchet, S., Frisch, L., Tse, W., Floreano, D., et al. (2015). Mechanosensory interactions drive collective behaviour in Drosophila. *Nature* 519, 233–236. doi: 10.1038/nature14024

Ramdya, P., Schneider, J., and Levine, J. D. (2017). The neurogenetics of group behavior in *Drosophila melanogaster*. *J. Exp. Biol*. 220, 35–41. doi: 10.1242/jeb.141457

Reinert, J. K., Schaefer, A. T., and Kuner, T. (2019). High-throughput automated olfactory phenotyping of group-housed mice. *Front. Behav. Neurosci*. 13:267. doi: 10.3389/fnbeh.2019.00267

Richendrfer, H., and Créton, R. (2013). Automated high-throughput behavioral analyses in zebrafish larvae. *J. Visual. Exp*. 7, 1–6. doi: 10.3791/50622

Richgels, P. K., and Rollmann, S. M. (2011). Genetic variation in odorant receptors contributes to variation in olfactory behavior in a natural population of *Drosophila melanogaster*. *Chem. Senses* 37, 229–240. doi: 10.1093/chemse/bjr097

Risse, B., Thomas, S., Otto, N., Löpmeier, T., Valkov, D., Jiang, X., et al. (2013). FIM, a novel FTIR-based imaging method for high throughput locomotion analysis. *PLoS ONE* 8:e53963. doi: 10.1371/journal.pone.0053963

Ro, J., Harvanek, Z. M., and Pletcher, S. D. (2014). FLIC: high-throughput, continuous analysis of feeding behaviors in Drosophila. *PLoS ONE* 9:e101107. doi: 10.1371/journal.pone.0101107

Rohrscheib, C. E., Bondy, E., Josh, P., Riegler, M., Eyles, D., van Swinderen, B., et al. (2015). Wolbachia influences the production of octopamine and affects Drosophila male aggression. *Appl. Environ. Microbiol*. 81, 4573–4580. doi: 10.1128/AEM.00573-15

Romero-Ferrero, F., Bergomi, M. G., Hinz, R. C., Heras, F. J. H., and de Polavieja, G. G. (2019). idtracker.ai: tracking all individuals in small or large collectives of unmarked animals. *Nat. Methods* 16, 179–182. doi: 10.1038/s41592-018-0295-5

Rooke, R., Rasool, A., Schneider, J., and Levine, J. D. (2020). *Drosophila melanogaster* behaviour changes in different social environments based on group size and density. *Commun. Biol*. 3:304. doi: 10.1038/s42003-020-1024-z

Rosenthal, S. B., Twomey, C. R., Hartnett, A. T., Wu, H. S., and Couzin, I. D. (2015). Revealing the hidden networks of interaction in mobile animal groups allows prediction of complex behavioral contagion. *Proc. Natl. Acad. Sci. U.S.A*. 112, 4690–4695. doi: 10.1073/pnas.1420068112

Ruedi, E. A., and Hughes, K. A. (2008). Natural genetic variation in complex mating behaviors of male *Drosophila melanogaster*. *Behav. Genet*. 38, 424–436. doi: 10.1007/s10519-008-9204-5

Rutherford, S. L., and Lindquist, S. (1998). Hsp90 as a capacitor for morphological evolution. *Nature* 396, 336–342. doi: 10.1038/24550

Sara, M., Merrill, N. G., and Kobor, M. S. (2019). Social environment and epigenetics. *Curr. Top. Behav. Neurosci*. 42, 289–320. doi: 10.1007/7854_2019_114

Scaplen, K. M., Mei, N. J., Bounds, H. A., Song, S. L., Azanchi, R., and Kaun, K. R. (2019). Automated real-time quantification of group locomotor activity in *Drosophila melanogaster*. *Sci. Rep*. 9, 1–16. doi: 10.1038/s41598-019-40952-5

Scheffer, L. K., Xu, C. S., Januszewski, M., Lu, Z., Takemura, S.-,y., Hayworth, K. J., et al. (2020). A connectome and analysis of the adult *Drosophila* central brain. *eLife* 9:e57443. doi: 10.7554/eLife.57443

Schiele, M. A., and Domschke, K. (2018). Epigenetics at the crossroads between genes, environment and resilience in anxiety disorders. *Genes Brain Behav*. 17:e12423. doi: 10.1111/gbb.12423

Schneider, C. W., Tautz, J., Grünewald, B., and Fuchs, S. (2012a). RFID tracking of sublethal effects of two neonicotinoid insecticides on the foraging behavior of *Apis mellifera*. *PLoS ONE* 7:e30023. doi: 10.1371/journal.pone.0030023

Schneider, J., Dickinson, M. H., and Levine, J. D. (2012b). Social structures depend on innate determinants and chemosensory processing in Drosophila. *Proc. Natl. Acad. Sci. U.S.A*. 109(Suppl 2), 17174–17179. doi: 10.1073/pnas.1121252109

Schuebel, K., Gitik, M., Domschke, K., and Goldman, D. (2016). Making sense of epigenetics. *Int. J. Neuropsychopharmacol*. 19:pyw058. doi: 10.1093/ijnp/pyw058

Schuett, W., Dall, S. R. X., Baeumer, J., Kloesener, M. H., Nakagawa, S., Beinlich, F., et al. (2011). Personality variation in a clonal insect: the pea aphid, acyrthosiphon pisum. *Dev. Psychobiol*. 53, 631–640. doi: 10.1002/dev.20538

Sih, A., Bell, A. M., Johnson, J. C., and Ziemba, R. E. (2004). Behavioral syndromes: an integrative overview. *Q. Rev. Biol*. 79, 241–277. doi: 10.1086/422893

Silva, V., Palacios-Munoz, A., Okray, Z., Adair, K. L., Waddell, S., Douglas, A. E., et al. (2021). The impact of the gut microbiome on memory and sleep in Drosophila. *J. Exp. Biol*. 224:jeb233619. doi: 10.1242/jeb.233619

Simola, D. F., Graham, R. J., Brady, C. M., Enzmann, B. L., Desplan, C., Ray, A., et al. (2016). Epigenetic (re)programming of caste-specific behavior in the ant camponotus floridanus. *Science* 351:6268. doi: 10.1126/science.aac6633

Simola, D. F., Wissler, L., Donahue, G., Waterhouse, R. M., Helmkampf, M., Roux, J., et al. (2013). Social insect genomes exhibit dramatic evolution in gene composition and regulation while preserving regulatory features linked to sociality. *Genome Res*. 23, 1235–1247. doi: 10.1101/gr.155408.113

Slawson, J. B., Kim, E. Z., and Griffith, L. C. (2009). High-resolution video tracking of locomotion in adult *Drosophila melanogaster*. *J. Visual. Exp*. 24, 1–3. doi: 10.3791/1096

Soto-Yéber, L., Soto-Ortiz, J., Godoy, P., and Godoy-Herrera, R. (2019). The behavior of adult Drosophila in the wild. *PLoS ONE* 13:e0209917. doi: 10.1371/journal.pone.0209917

Spierer, A. N., Mossman, J. A., Smith, S. P., Crawford, L., Ramachandran, S., and Rand, D. M. (2021). Natural variation in the regulation of neurodevelopmental

genes modifies flight performance in Drosophila. *PLoS Genet*. 17:e1008887. doi: 10.1371/journal.pgen.1008887

Steck, K., Veit, D., Grandy, R., Badia, S. B. I., Mathews, Z., Verschure, P., et al. (2012). A high-throughput behavioral paradigm for Drosophila olfaction - the Flywalk. *Sci. Rep*. 2, 1–9. doi: 10.1038/srep00361

Stern, S., Kirst, C., and Bargmann, C. I. (2017). Neuromodulatory control of long-term behavioral patterns and individuality across development. *Cell* 171, 1649.e10–1662.e10. doi: 10.1016/j.cell.2017.10.041

Stockton, D. G., Wallingford, A. K., Brind'amore, G., Diepenbrock, L., Burrack, H., Leach, H., et al. (2020). Seasonal polyphenism of spotted-wing Drosophila is affected by variation in local abiotic conditions within its invaded range, likely influencing survival and regional population dynamics. *Ecol. Evol*. 10, 7669–7685. doi: 10.1002/ece3.6491

Stroeymeyt, N., Grasse, A. V., Crespi, A., Mersch, D. P., Cremer, S., and Keller, L. (2018). Social network plasticity decreases disease transmission in a eusocial insect. *Science* 362, 941–945. doi: 10.1126/science.aat4793

Sun, Y., Qiu, R., Li, X., Cheng, Y., Gao, S., Kong, F., et al. (2020). Social attraction in Drosophila is regulated by the mushroom body and serotonergic system. *Nat. Commun*. 11:5350. doi: 10.1038/s41467-020-19102-3

Tautz, J., Maier, S., Groh, C., Rössler, W., and Brockmann, A. (2003). Behavioral performance in adult honey bees is influenced by the temperature experienced during their pupal development. *Proc. Natl. Acad. Sci. U.S.A*. 100, 7343–7347. doi: 10.1073/pnas.1232346100

Tie, F., Banerjee, R., Fu, C., Stratton, C. A., Fang, M., and Harte, P. J. (2016). Polycomb inhibits histone acetylation by CBP by binding directly to its catalytic domain. *Proc. Natl. Acad. Sci. U.S.A*. 113, E744-E753. doi: 10.1073/pnas.1515465113

Tie, F., Banerjee, R., Stratton, C. A., Prasad-Sinha, J., Stepanik, V., Zlobin, A., et al. (2009). Cbp-mediated acetylation of histone h3 lysine 27 antagonizes Drosophila polycomb silencing. *Development* 136, 3131–3141. doi: 10.1242/dev.037127

Tinette, S., Zhang, L., and Robichon, A. (2004). Cooperation between Drosophila flies in searching behavior. *Genes Brain Behav*. 3, 39–50. doi: 10.1046/j.1601-183x.2003.0046.x

Topalidou, I., and Chalfie, M. (2011). Shared gene expression in distinct neurons expressing common selector genes. *Proc. Natl. Acad. Sci. U.S.A*. 108, 19258–19263. doi: 10.1073/pnas.1111684108

Torquet, N., Marti, F., Campart, C., Tolu, S., Nguyen, C., Oberto, V., et al. (2018). Social interactions impact on the dopaminergic system and drive individuality. *Nat. Commun*. 9:3081. doi: 10.1038/s41467-018-05526-5

Truitt, A. M., Kapun, M., Kaur, R., and Miller, W. J. (2019). Wolbachia modifies thermal preference in *Drosophila melanogaster*. *Environ. Microbiol*. 21, 3259–3268. doi: 10.1111/1462-2920.14347

Ueno, T., and Takahashi, Y. (2020). Intrapopulation genetic variation in the level and rhythm of daily activity in Drosophila immigrans. *Ecol. Evol*. 10, 14388–14393. doi: 10.1002/ece3.7041

Venken, K. J. T., Simpson, J. H., and Bellen, H. J. (2011). Genetic manipulation of genes and cells in the nervous system of the fruit fly. *Neuron* 72, 202–230. doi: 10.1016/j.neuron.2011.09.021

Viney, M., and Reece, S. E. (2013). Adaptive noise. *Proc. R. Soc. B Biol. Sci*. 280:20131104. doi: 10.1098/rspb.2013.1104

Wario, F., Wild, B., Rojas, R., and Landgraf, T. (2017). Automatic detection and decoding of honey bee waggle dances. *PLoS ONE* 12:e0188626. doi: 10.1371/journal.pone.0188626

Waterland, R. A., and Jirtle, R. L. (2003). Transposable elements: targets for early nutritional effects on epigenetic gene regulation. *Mol. Cell. Biol*. 23, 5293–5300. doi: 10.1128/MCB.23.15.5293-5300.2003

Williams, J. A., and Sehgal, A. (2001). Molecular components of the circadian system in Drosophila. *Annu. Rev. Physiol*. 63, 729–755. doi: 10.1146/annurev.physiol.63.1.729

Williamson, W. R., Peek, M. Y., Breads, P., Coop, B., and Card, G. M. (2018). Tools for rapid high-resolution behavioral phenotyping of automatically isolated Drosophila. *Cell Rep*. 25, 1636.e5–1649.e5. doi: 10.1016/j.celrep.2018.10.048

Winbush, A., and Singh, N. D. (2021). Genomics of recombination rate variation in temperature-evolved *Drosophila melanogaster* Populations. *Genome Biol. Evol*. 13, 1–18. doi: 10.1093/gbe/evaa252

Witvliet, D., Mulcahy, B., Mitchell, J. K., Meirovitch, Y., Berger, D. R., Wu, Y., et al. (2021). Connectomes across development reveal principles of brain maturation. *Nature*. doi: 10.1038/s41586-021-03778-8

Wolf, M., and Weissing, F. J. (2010). An explanatory framework for adaptive personality differences. *Philos. Trans. R. Soc. B Biol. Sci*. 365, 3959–3968. doi: 10.1098/rstb.2010.0215

Wysocki, C. J., and Beauchamp, G. K. (1984). Ability to smell androstenone is genetically determined. *Proc. Natl. Acad. Sci. U.S.A*. 81, 4899–4902. doi: 10.1073/pnas.81.15.4899

Xian, B., Shen, J., Chen, W., Sun, N., Qiao, N., Jiang, D., et al. (2013). WormFarm: A quantitative control and measurement device toward automated *Caenorhabditis elegans* aging analysis. *Aging Cell* 12, 398–409. doi: 10.1111/acel.12063

Yan, H., Simola, D. F., Bonasio, R., Liebig, J., Berger, S. L., and Reinberg, D. (2014). Eusocial insects as emerging models for behavioural epigenetics. *Nat. Rev. Genet*. 15, 677–688. doi: 10.1038/nrg3787

Yapici, N., Cohn, R., Schusterreiter, C., Ruta, V., and Vosshall, L. B. (2016). A taste circuit that regulates ingestion by integrating food and hunger signals. *Cell* 165, 715–729. doi: 10.1016/j.cell.2016.02.061

Zwarts, L., Vanden Broeck, L., Cappuyns, E., Ayroles, J. F., Magwire, M. M., Vulsteke, V., et al. (2015). The genetic basis of natural variation in mushroom body size in *Drosophila melanogaster*. *Nat. Commun*. 6:10115. doi: 10.1038/ncomms10115

Conflict of Interest: The authors declare that the research was conducted in the absence of any commercial or financial relationships that could be construed as a potential conflict of interest.

Publisher's Note: All claims expressed in this article are solely those of the authors and do not necessarily represent those of their affiliated organizations, or those of the publisher, the editors and the reviewers. Any product that may be evaluated in this article, or claim that may be made by its manufacturer, is not guaranteed or endorsed by the publisher.